

INFORMATION TO USERS

This manuscript has been reproduced from the microfilm master. UMI films the text directly from the original or copy submitted. Thus, some thesis and dissertation copies are in typewriter face, while others may be from any type of computer printer.

The quality of this reproduction is dependent upon the quality of the copy submitted. Broken or indistinct print, colored or poor quality illustrations and photographs, print bleedthrough, substandard margins, and improper alignment can adversely affect reproduction.

In the unlikely event that the author did not send UMI a complete manuscript and there are missing pages, these will be noted. Also, if unauthorized copyright material had to be removed, a note will indicate the deletion.

Oversize materials (e.g., maps, drawings, charts) are reproduced by sectioning the original, beginning at the upper left-hand corner and continuing from left to right in equal sections with small overlaps.

Photographs included in the original manuscript have been reproduced xerographically in this copy. Higher quality 6" x 9" black and white photographic prints are available for any photographs or illustrations appearing in this copy for an additional charge. Contact UMI directly to order.

**Bell & Howell Information and Learning
300 North Zeeb Road, Ann Arbor, MI 48106-1346 USA
800-521-0600**

UMI[®]

**Trophic Feedback and Carrying Capacity of Pacific
Salmon (*Oncorhynchus* spp.) on the High Seas of the
Gulf of Alaska**

by

Kerim Yunus Aydin

**A dissertation submitted in partial
fulfillment of the requirements for the
degree of**

DOCTOR OF PHILOSOPHY

University of Washington

2000

Program Authorized to Offer Degree:

Aquatic and Fishery Sciences

UMI Number: 9995337

Copyright 2000 by
Aydin, Kerim Yunus

All rights reserved.

UMI[®]

UMI Microform 9995337

Copyright 2001 by Bell & Howell Information and Learning Company.

All rights reserved. This microform edition is protected against
unauthorized copying under Title 17, United States Code.

Bell & Howell Information and Learning Company
300 North Zeeb Road
P.O. Box 1346
Ann Arbor, MI 48106-1346

© Copyright 2000

Kerim Yunus Aydin

In presenting this dissertation in partial fulfillment of the requirements for the Doctoral degree at the University of Washington, I agree that the Library shall make its copies freely available for inspection. I further agree that extensive copying of the dissertation is allowable only for scholarly purposes, consistent with "fair use" as prescribed in the U.S. Copyright Law. Requests for copying or reproduction of this dissertation may be referred to Bell and Howell Information and Learning, 300 North Zeeb Road, Ann Arbor, MI 48106-1346, to whom the author has granted "the right to reproduce and sell (a) copies of the manuscript in microform and/or (b) printed copies of the manuscript made from microform."

Signature AL. J.

Date Dec 10, 2000

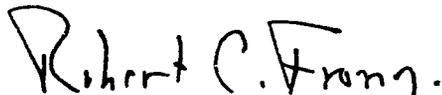
University of Washington
Graduate School

This is to certify that I have examined this copy of a doctoral dissertation by

Kerim Yunus Aydin

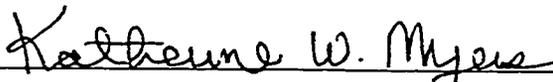
and have found that it is complete and satisfactory in all respects,
and that any and all revisions required by the final
examining committee have been made.

Chair of Supervisory Committee:



Dr. Robert C. Francis

Reading Committee:



Dr. Katherine W. Myers



Dr. Walton W. Dickhoff

Date:

Dec 10, 2000

University of Washington

Abstract

**Trophic Feedback and Carrying Capacity of Pacific
Salmon (*Oncorhynchus* spp.) on the High Seas of the
Gulf of Alaska**

by Kerim Yunus Aydin

Chairperson of the Supervisory Committee:
Professor Robert C. Francis
Department of Aquatic and Fishery Sciences

In this dissertation, I examine the ocean feeding patterns of several species of Pacific salmon (*Oncorhynchus* spp.) in the offshore waters of the Gulf of Alaska. My goal is to provide an appropriate context for comparing the relative effects of environmental variation and density-dependence on post-juvenile salmon "carrying capacity" in the northeastern Pacific Ocean. This will aid in assessing the role of inter- and intra-specific competition with increasing levels of artificial stock augmentation and climate change. I show how temporal and spatial variation in salmon food resources determines the variation in an individual salmon's growth in this region, and argue that interannual changes occur not only in the quantity of food available to salmon, but also in the structure of the food web itself.

My approach combines field sampling of salmon food habits with bioenergetics models, foraging models, climate data and historical records of salmon size from many North American salmon stocks. The results suggest that: (1) the winter prior to maturation is a critical time for salmon competitive interactions; (2) small differences in salmon body size observed immediately after this winter period may be magnified through trophic feedback, whereby the ability to capture large, energy-dense prey items is limited by slow growth rates; and (3) several of the previously-reported relationships between climate (especially sea surface temperature) and adult salmon growth may be traced to long-term biogeographic variation in micronektonic squid, especially *Beryteuthis anonychus*, a possible keystone species in the North Pacific Ocean.

Table of Contents

List of Figures		ii
List of Tables		v
Chapter 1	Dissertation outline and summary of results	
1.1	Introduction	1
1.2	Scales of the study	2
1.3	Outline and summary of results	6
Chapter 2	Physical and biological variability in the northeastern Pacific Ocean and the concept of carrying capacity	
2.1	Introduction	28
2.2	Long term variation in physical systems of the North Pacific	29
2.3	Biological processes	42
2.4	Salmon growth studies and carrying capacity in the northeastern Pacific	52
Chapter 3	Micronektonic squid in the diet of northeastern Pacific salmon	
3.1	Introduction	93
3.2	Calculating an index of squid abundance from salmon food habits data	107
3.3	Conclusions	124
Chapter 4	Trophic and oceanographic aspects of the summer distribution of salmon prey in the Gulf of Alaska and consequences for salmon growth rates	
4.1	Introduction	157
4.2	Variation in summer distribution of the prey of Pacific salmon in the offshore Gulf of Alaska in relation to oceanographic conditions, 1994-98	159
4.3	Bioenergetics models	179
4.3	Trends in potential squid/salmon overlap area, 1950-99, and relation to salmon body weights	200
Chapter 5	Trophic implications of seasonal prey supply and size-based ontogenetic diet shifts in adult Pacific salmon	
5.1	Introduction	297
5.2	Experiment 1: ocean area required for a fixed demand	301
5.3	Experiment 2: trophic feedback and seasonal growth	310
5.4	Experiment 3: mixed effects of density-dependence and water temperature	320
5.5	Conceptual model of salmon carrying capacity	324
Literature Cited		364
Appendix A	Calibrating the logistic response	379
Appendix B	Bioenergetics equations for salmon	383
Appendix C	Combining salmon foraging and bioenergetics models with density dependence	386

List of Figures

Number	Title.....	Page
1.1	Study area.....	16
1.2	Historical North Pacific salmon run sizes.....	17
1.3	Conceptual model of carrying capacity.....	18
1.4	A trophic triangle in the Gulf of Alaska.....	19
1.5	Logistic response of micronektonic squid in salmon diets.....	20
1.6	Sea surface temperature and squid distribution.....	21
1.7	Salmon growth in "high" and "low" growth regions.....	22
1.8	Salmon body size vs. squid overlap.....	23
1.9	Ocean surface area required for salmon growth.....	24
1.10	Growth trajectory of a pink salmon, April-September.....	25
1.11	Maximum instantaneous growth rate vs. water temperature.....	26
1.12	Conceptual model of salmon density dependence.....	27
2.1	Chapter 2 outline of carrying capacity.....	84
2.2	Oceanographic regions of the North Pacific.....	85
2.3	Oceanographic transect along 145°W.....	86
2.4	Oceanographic transect along 170°W.....	87
2.5	Oceanographic transect along 165°E.....	88
2.6	Oceanographic regions of the northeastern Pacific.....	89
2.7	July sea surface temperature transects.....	90
2.8	Seasonal cycle of the northeast Pacific water column.....	91
2.9	Winter and summer lower trophic level production.....	92
3.1	Chapter 3 outline of carrying capacity.....	137
3.2	Food web of salmon prey.....	138
3.3	Range of <i>Berryteuthis anonychus</i>	139
3.4	Sampling locations.....	140
3.5	Sea surface temperature by week.....	141
3.6	Seasonal trend in body weights.....	142
3.7	Fitted terms for response model.....	143
3.8	Body weight effect.....	146
3.9	Coho fitted response.....	147
3.10	Body weight response for three species.....	148
3.11	Squid index values by time period.....	149
3.12	Main transect lines.....	152
3.13	Squid index values along 145°W.....	153
3.14	Squid index values along 50°N.....	154
3.15	Squid index values along 55°N.....	155

Number	Title.....	Page
3.16	Squid index vs. sea surface temperature	156
4.1	Chapter 4 outline of carrying capacity	254
4.2	Transect line of T/S <i>Oshoro maru</i>	255
4.3	IGOSS SST fitting	256
4.4	Surface to 250 m water temperature	257
4.5	Buoyancy frequency	258
4.6	Salinity at 0 and 100 m depth	259
4.7	First principle component.....	260
4.8	Water temperature profiles	261
4.9	Oceanographic boundaries.....	262
4.10	Zooplankton densities	263
4.11	Phytoplankton densities	264
4.12	Squid index values by temperature and latitude.....	265
4.13	Squid index values by year and latitude	266
4.14	Latitude of north/south border.....	267
4.15	Squid index values by sample size	268
4.16	Relationship between measured variables	269
4.17	Salmon body weight trends	270
4.18	Diet composition of sockeye salmon	271
4.19	Diet composition of chum salmon	272
4.20	Diet composition of pink salmon	273
4.21	Diet composition of coho salmon	274
4.22	Simulated growth rates of salmon, low squid caloric density	275
4.23	Simulated growth rates of salmon, high squid caloric density	276
4.24	CV of growth rates	277
4.25	Change in growth rates with water column temperature	278
4.26	Change in growth rates with sea surface temperature	279
4.27	Long-term averaged July SST	280
4.28	Long-term July SST by transect	281
4.29	SST transect by month	282
4.30	SST vs. squid index values.....	283
4.31	Ocean surface area of salmon/squid overlap	284
4.32	Ocean surface area of overlap by region.....	285
4.33	Latitude of SST minimum.....	286
4.34	SST at minimum	287
4.35	Curvature of SST	288
4.36	Run sizes of pink and sockeye salmon.....	289
4.37	Time series of salmon size and oceanography	290

Number	Title.....	Page
4.38	Normalized time series	291
4.39	Large-cold vs. small-warm years	292
4.40	Normalized regression relationships.....	293
4.41	Slopes of pink salmon density dependence	294
4.42	Condition factor of pink and sockeye salmon	295
4.43	Hypothetical water temperature/density-dependent relationship.....	296
5.1	Chapter 5 outline of carrying capacity	338
5.2	Tagging releases and recoveries.....	339
5.3	Weekly sea surface temperatures	340
5.4	Salmon body weight by month at sea.....	341
5.5	Prey energy required per day	346
5.6	Zooplankton long-term mean by month	347
5.7	Surface area required to support one salmon	348
5.8	Sensitivity to zooplankton variation.....	349
5.9	Zooplankton density by season and year	350
5.10	Pink salmon diet under four scenarios.....	351
5.11	Pink salmon growth trajectories	352
5.12	Pink salmon growth trajectories	353
5.13	Growth as a function of body weight.....	354
5.14	Ecosystem effects of feeding –low/low	355
5.15	Ecosystem effects of feeding –low/high.....	356
5.16	Ecosystem effects of feeding –high/low.....	357
5.17	Ecosystem effects of feeding –high/high	358
5.18	Overall effects change	359
5.19	Density dependent feeding relationship.....	360
5.20	Swimming velocity vs. growth rate.....	361
5.21	Maximum growth rates.....	362
5.22	Final conceptual model of carrying capacity.....	363

List of Tables

Number	Title.....	Page
1.1	Relative effects of summer and winter salmon prey variation	15
2.1	North Pacific oceanographic definitions	80
2.2	Frequencies of natural variation	81
2.3	Carrying capacity modeling techniques	82
2.4	Salmon stocks in offshore waters	83
3.1	Foraging modes	129
3.2	Major salmon prey groups	130
3.3	Salmon prey by region	131
3.4	Data sources	132
3.5	Sample size	133
3.6	Analysis of deviance	134
3.7	Monthly trends of squid response	135
3.8	Squid index corrections by salmon species	136
4.1	Squid index correction summary	220
4.2	Oceanographic correlations	221
4.3	PCA of oceanographic data	222
4.4	PC1 vs. ocean region	223
4.5	Zooplankton vs. ocean region	224
4.6	Squid vs. ocean region	225
4.7	Relationship between squid and SST minimum	226
4.8	Best salmon CPUE models	227
4.9	Salmon body weight by region	228
4.10	Salmon prey caloric densities	229
4.11	Measured water temperature	230
4.12	Salmon catch by weight	231
4.13	Estimated daily ration	232
4.14	Physiological P-values	233
4.15	Prey caloric densities	234
4.16	Predicted salmon growth rates	235
4.17	Predicted conversion efficiency of energy	236
4.18	Predicted conversion efficiency of biomass	237
4.19	Growth rate change with body weight	238
4.20	Growth rate change with daily ration	239
4.21	Growth rate change with prey caloric density	240
4.22	Growth rate change with water temperature	241
4.23	Salmon body size time series	242

Number	Title.....	Page
4.24	Oceanographic time series	243
4.25	Correlations between overlap indices and oceanography	244
4.26	Correlations between oceanographic variables	245
4.27	Correlations between oceanography and run sizes	246
4.28	Correlations between salmon body sizes and other measures	247
4.29	Pre-1976 correlations.....	248
4.30	Post-1976 correlations	249
4.31	Fraser River body sizes vs. squid/salmon overlap area	250
4.32	Warm/small vs cold/large years and few/many fish	251
4.33	Correlations in years of "few" and "many" fish	252
4.34	Density dependence in warm/small and cold/large years	253
5.1	Experimental methods	327
5.2	Tagging locations and distance traveled	328
5.3	Age and maturity groups.....	329
5.4	Energy required for ocean salmon growth, by month	330
5.5	Sensitivity analysis of energy requirements.....	331
5.6	Mesozooplankton density by month, Ocean Station P	332
5.7	Ocean surface area required to support salmon growth	333
5.8	Growth results from changes in initial body weight	334
5.9	Changes in ecosystem consumption based on salmon body size	335
5.10	Density-dependent model parameters.....	336
5.11	Density-dependent/water temperature interactions	337

Acknowledgements

The author wishes to thank, first and foremost, the members of the High Seas Salmon Project at the University of Washington, Seattle: Katherine Myers, Robert (Trey) Walker, and Nancy Davis, without whose help and support this project would have been utterly impossible. I thank my committee members: Walt Dickhoff, Ray Hilborn, Glover Barnes, and my major advisor Robert Francis, whose continual commitment of time and energy has ensured the quality of this work and my education. A great deal of unpublished data was provided for the analyses in this dissertation: instrumental providers of data and advice were Bill Percy, Ric Brodeur, Peter Rand, Skip McKinnell, Dave Mackas, Brian Bigler, Steven Hare, Hiroji Onishi, Jim Murphy, Masahide Kaeriyama, and Jim Kitchell. I am also grateful to Pat Livingston for her support during the completion of this work. Finally, this dissertation depended heavily on the help and hospitality of the officers and crew of Hokkaido University's T.S. (Training Ship) *Oshoro maru*, particularly the captain of the vessel during my visits in 1995-98, Gen Anma. Finally, this work was greatly supported over the years by Mike Dahlberg, Jack Helle, and Dick Carlson, and was entirely funded by the Auke Bay Laboratory, Alaska Fisheries Science Center, U.S. National Marine Fisheries Service (NOAA Contract Nos. 50ABNF4001, 50ABNF700004, and 50ABNF000008).

Dedication

This work is dedicated to Dr. Carolyn E. Aydin, for first proving this endeavor to be possible (even with children!), and to Rebecca Vaux, for making the last six years worthwhile.

1 Dissertation outline and summary of results

1.1 Introduction

In this dissertation, I examine the ocean feeding patterns of several Pacific salmon species (*Oncorhynchus* spp.) in the offshore waters of the Gulf of Alaska (Figure 1.1). My goal is to provide an appropriate context for comparing the relative effects of environmental variation and density-dependence on post-juvenile salmon "carrying capacity" in the northeastern Pacific Ocean. I show how temporal and spatial variation in salmon food resources determines the variation in an individual salmon's growth in this region, and argue that interannual changes occur not only in the quantity of food available to salmon, but in the structure of the food web itself.

In the following chapters, I combine data on salmon food habits, physical oceanography, prey distribution and abundance, salmon abundance, body size, and growth rate, into a synthesis of salmon feeding opportunities across multiple trophic levels, environmental conditions, time, and space. My primary focus is on measuring and modeling actual mechanisms of predator/prey interaction, in order to determine the range of natural variation of each individual factor that contributes to salmon growth as a whole.

I confine my study to the four most abundant species of Pacific salmon in the North Pacific Ocean: sockeye salmon (*O. nerka*), chum salmon (*O. keta*), pink salmon (*O. gorbuscha*) and coho salmon (*O. kisutch*). The first three of these species made up 97% of total North Pacific salmon numbers in the 1990s (Rogers 1999), and as such have the greatest potential for affecting other species in the ecosystem. As coho salmon feed on a higher trophic level, they are included as a counterpoint to the other three more zooplanktivorous species. Chinook salmon (*O. tshawytscha*) and steelhead (*O. mykiss*) were not sampled in high enough numbers to be included in these analyses.

The total abundance of Pacific salmon has increased since the late 1970s, and current numbers are the highest in recorded history (Figure 1.2). The last twenty years have been a time of change, both for environmental factors such as climate, and for human interactions within the ecosystem such as fishing, hatchery releases, and the potential effects of global warming. The large-scale change in salmon populations, in combination with the increasing availability of environmental and experimental data, means that now is a good time to examine the carrying capacity of salmon with respect to its high seas environment.

This dissertation focuses on the post-juvenile body weight increase of individual salmon, from their first autumn and winter at sea through the spring and summer of their maturation year. Salmon begin their high seas life at a minimum body weight between 100-200 g, and end with body weights between 1000-5000 g or more, depending on species. For pink and coho salmon, this size range represents fish from the winter to the summer of their maturation year; for chum and sockeye salmon, it represents immature and maturing fish who have spent between one to five years in the ocean (ocean age .1+).

My approach is to examine the scales and variations in the structure and function of the northeast Pacific pelagic food web and their effects on the growth of salmon in offshore waters. I hope that the results lead to a clearer picture of variation in salmon carrying capacity in the North Pacific.

1.2 Scales of the study

Figure 1.3 shows a conceptual model of cause and effect underlying a individual salmon's body growth at sea. The "final" body weight of returning salmon (lower right box) is the direct result of cumulative day-to-day ("instantaneous") growth throughout its lifetime. Final body weight is connected to ocean conditions through a web of cause and effect which operates on multiple scales of time and space. There are four broad scales of interaction

which are considered in this dissertation: (1) local, or “instantaneous,” (2) seasonal, (3) annual, and (4) long-term, or “interannual.”

The instantaneous scale of interactions, the heart of the relationship between a salmon’s growth and its environment, is shown by the bold arrows in Figure 1.3. Two categories of “direct” factors are shown to be controlling instantaneous growth rates. Abiotic water conditions, such as temperature or circulation patterns, may influence salmon growth by creating habitat which is physiologically suited or unsuited to a particular salmon. Local prey abundance affects the amount of food a salmon may find in a given day, and the effort required to find that food. Additionally, prey distribution may be affected by local abiotic conditions. The relative importance of each possible pathway of cause and effect is the main theme of Chapter 4.

The seasonal scale is perhaps the most difficult to examine, as the scale is dominated by feedback loops, by which variation in instantaneous growth early in a salmon’s life may translate into a greater variation later in life. Feedback loops lie at the heart of density-dependence and carrying capacity: a feedback loop is a fundamental way of modeling an organism’s effect upon itself. A feedback loop may be either self-promoting (positive), leading to exponential growth, or self-regulating (negative), leading to a limit, or “carrying capacity.” Acting to modify rates of instantaneous growth, feedback loops make instantaneous growth into both a cause and an effect.

As I discuss in Section 2.4, the scale of the season is the scale on which carrying capacity matters for salmon. Seasonal scale interactions are shown by the solid lines in Figure 1.3, and three feedback loops, labeled A-C, are identified. The first loop, labeled A, is the connection between juvenile population size and mortality, and is thought to be the main factor in determining the population size (in numbers) of salmon stocks. I do not directly consider this feedback loop in the dissertation, although I review it in Chapter 2.

In general, salmon numbers, as determined by juvenile processes, are taken as external inputs to this dissertation's models of adult salmon growth.

The second feedback loop (B) is between salmon body weight and its diet ontogeny. Specifically, I focus on a "trophic triangle" in the offshore Gulf of Alaska (Figure 1.4) between salmon, zooplankton, and micronekton, primarily squid. The diet shift itself, as a function of body weight for each salmon species, is examined in Chapter 3 using a combination of new and historical data sources.

The importance of this trophic triangle lies not in its form, but in its variation. Due to the technical difficulty of sampling micronektonic species such as small squid, the geographic and temporal variation of this food web has been noted but not well-explored (LeBrasseur 1972; Pearcy et al. 1988). Conducting such an exploration, whether through sampling or modeling, yields information on the surprising and sometimes subtle dynamics of salmon growth both within and across seasons. One of my main conclusions is that existence and variation of an intermediate trophic level of micronektonic squid and, to a lesser extent, myctophids may be the single largest source of variability in maturing salmon feeding and growth in the northeastern Pacific.

As a prey item for and competitor with salmon, micronektonic squid have a tremendous potential for affecting salmon production. Yet technological difficulties have prevented any assessment of this important prey from being conducted. Micronekton are little understood, because of their lack of direct commercial value and the difficulty inherent in trying to sample organisms that are neither stationary enough to be caught in zooplankton nets nor large enough to be caught in commercial gear. Squid are especially hard to sample as their rapid swimming speed makes them difficult to catch in most trawls. But the combination of rapid growth and high food quality—the functional equivalent of anchovies in upwelling systems—doubly emphasizes their importance in

determining the carrying capacity of other species. Chapter 5 tackles the feedback loop between predator and prey abundance, labeled (C) in Figure 1.3. Food web control may be neither top-down nor bottom-up, but rather middle-out. The models presented in Chapter 5 attempt to focus on the rate-controlling elements within this loop.

The nature of salmon predation makes it important to count micronekton in general, and squid in particular, as a distinct prey group in the Gulf of Alaska. As they grow, they shift from being competitors with squid to being predators on squid (Figure 1.4). This single adjustment in the food web, creating a situation known in the literature as "intraguild" predation, creates a much more complicated model than does one with a single predator and prey (Rice 1995). In such a relationship, the biological feedback between small salmon and squid, squid and zooplankton, and large salmon and squid, may account for previous observations that suggest that in spite of the presence of an abundance of zooplankton in the open ocean, salmon show density-dependent growth, indicating substantial competition for food.

Most previous studies of salmon ocean growth have been conducted on the annual scale, between the three double-lined boxes in Figure 1.3: adult salmon body weight, salmon numbers, and specific abiotic conditions, especially sea surface temperature (SST). The yearly scale has been examined most often in past studies because the annual returns of salmon to coastal fisheries and freshwater spawning grounds has been the subject of the most intensive measurements and management efforts.

Negative correlations between body weight and annual salmon return numbers are considered to be evidence of density-dependence in salmon growth. Similarly, correlations between body weight and an index of environmental conditions are often considered to be evidence of that factor's direct importance in determining salmon growth. However, as Figure 1.3

shows, there are many mechanistic steps between the measured annual quantities and final salmon body weight. Correlations are useful as a method of predicting body weights or return numbers, providing the mechanisms determining the relationships are accurate, and do not vary from year to year.

However, density-dependent relationships may change with other environmental conditions. As discussed in Chapter 5, new models of instantaneous growth rate predict nonlinear changes in the relationship between salmon numbers and growth rates with changing water temperature.

On the largest scale, long-term changes in abiotic or biotic conditions such as climate change or species invasions, occur over multiple years. The connection between long-term changes and the rest of the ecosystem is shown by the dashed arrows on the left of Figure 1.3. The long-term changes, or "regime shifts," occur across entire ecosystems and affect annual abiotic conditions, local and annual prey abundance, and conditions which may determine the total growth of salmon from year to year.

1.3 Outline and summary of results

Chapter 2 is a review of previous studies of links between salmon growth, salmon numbers, and the environment. In Section 2.2, I review the oceanographic characteristics of the Gulf of Alaska, and discuss the circulation and physical driving forces which shape the pelagic ecosystem. I focus on factors that may control the biology of the surface layer, such as mixed-layer depth, eddies, and upwelling. I review the types and frequencies of variation occurring on interannual time scales, from decadal-scale regime shifts to El Niño/Southern Oscillation (ENSO) cycles and possible long term changes such as global warming. In Section 2.3, I review the seasonal cycle of primary, and secondary production in the region, and review the available data and extensive modeling efforts which have examined the mechanisms of production on lower trophic levels.

In Section 2.4.1, I review the history and formulations, both conceptual and mathematical, of carrying capacity in the context of a species or ecosystem. Specifically, I ask: under what conditions is it meaningful to discuss a species' carrying capacity, and under what conditions can it be measured? Is correlation between numbers and growth enough to show density-dependence? Will metrics of carrying capacity be based on historical trends or other indices, such as primary production? Are such measurements applicable to salmon in particular? I attempt to place the concept of a single species' carrying capacity in the context of ecosystem stability and evolution as a whole.

In Section 2.4.2, I review some of the historical trends in salmon production and the research that has made individual salmon growth an important management issue. I emphasize the previous correlations which have been used to explain measured variations in survival and growth in the juvenile and adult ocean phases of the salmon's life cycle. The aim is to review evidence linking salmon production to the biological and physical state of the pelagic ecosystem.

Chapters 3, 4, and 5 present the bulk of my original research. The focus of this research is on the mechanistic links that control adult salmon production in the northeastern Pacific. In particular, I try to bridge the gap between instantaneous interactions and annual salmon growth through models of predator/prey feedback loops on a seasonal scale. The chapters themselves focus on the data used in creating conceptual and mathematical models as well as on the models' results. Some of the more detailed mathematical derivations of the bioenergetics, foraging and trophic models used in Chapters 3-5 are found in the Appendices.

Chapter 3 begins by briefly describing salmon prey guilds in the Gulf of Alaska, and reviews the available biological data on the life histories of the micronektonic squid found in salmon stomachs. The species found in this

region are primarily a species of gonatid squid, *Berryteuthis anonychus*, and the biogeography of this species is reviewed in Section 3.3. In Section 3.4, I discuss the use of General Additive Models (GAMs) to measure squid species' abundance in the environment using data obtained from salmon stomachs. The models are calibrated using data from over 11,000 pink, sockeye and coho salmon stomachs collected between 1956 and the 1998. The results, presenting in Section 3.5, serve two purposes:

1. They provide a quantitative functional form for the change in diet of pink, sockeye and coho salmon as they grow (Figure 1.5). Most pink salmon in the Gulf of Alaska achieve the body weight to make this dietary transition during the spring of their maturation year (ocean age .1), while most sockeye make the transition during the spring of their ocean age .2 year. Making this transition greatly increases a salmon's potential for growth rate when micronektonic squid are present in the ocean environment.
2. The results remove this size- and species- dependent feeding response to find a formula for a "predator-independent" measure of squid density.

Chapter 4 describes the analysis of data from a series of July cruises conducted aboard the Japanese T.S. *Oshoro maru* between 1994-98. During these cruises, data collection included salmon stomachs, zooplankton, salmon catch rates and oceanographic conditions.

Section 4.2 examines the relationships between oceanographic conditions, zooplankton and squid abundance, and salmon feeding, distribution and body size. I discuss direct links with environmental factors such as sea surface temperature, eddies, and the position of regional oceanographic boundaries. Squid presence is correlated with a composite of oceanographic conditions, including lower sea surface temperatures and weaker seasonal thermoclines. An examination of squid densities measured from salmon

stomachs reveals a precipitous decline in squid density from south to north along 145° W. Interannual variation in the latitude at which this decline occurs is correlated with the latitudinal July sea surface temperature minimum, which may be associated with the center of the Alaskan Gyre (Figure 1.6).

South of the July sea surface temperature minimum, surface waters are influenced by the West Wind Drift and are generally cooler, less stratified, and contain a high abundance of squid in the diets of all salmon except chum. North of the minimum, surface waters are warmer and more stratified, and squid is replaced in salmon diets by less energy-dense zooplankton. Zooplankton net sampling indicates that summer zooplankton densities are higher in the north and lower in the south. The latitude of the temperature minimum varies from year.

In Section 4.3, the *Oshoro maru* data are used to perform a sensitivity analysis of a bioenergetics model of individual salmon growth. The purpose of this analysis is to determine, on a local scale, which of the bold arrows in Figure 1.3 is responsible for the most variation in growth: the direct link between the abiotic environment and salmon growth, or the indirect link through variation in prey.

I show that within the range of sampled variation, prey availability was the most significant factor influencing growth, while water temperature was the second. In regions of high squid density, south of the July SST minimum, growth is higher for the "squid-eating" species and size-classes of salmon (Figure 1.7). Feeding in this region may be rich enough that 1-2°C increases in SST may improve salmon growth locally, as increased metabolic activity is a boon if food is plentiful. This counterintuitive result may not hold as salmon migrate through poorer waters.

Previous studies of salmon growth found negative correlations between sea surface temperatures in the center of the Gulf of Alaska and the adult body

size of some salmon stocks. Furthermore, researchers have projected a substantial decrease in viable salmon habitat in some scenarios of future global warming. However, the link between squid and July SSTs suggests another explanation. It is possible that sea surface temperatures measured at a single geographical location are, in current and past oceanic regimes, partially correlated with changes in ocean circulation, and thus with changes in prey abundance.

As evidenced by the diets of other fish species, micronektonic squid distribution in the summer extends further south in the ocean than salmon distribution. Thus, there is a range of overlap between salmon and squid. Within the region of overlap, squid densities do not vary significantly from year to year. However, the total area of the overlap varies significantly.

If a 13°C SST is used as the limit to the southern distribution for sockeye salmon in the northeastern Pacific, the area of squid-salmon overlap can be computed as the area between the 13° isotherm in the south and the temperature minimum in the north (Figure 1.8). In Section 4.4, for the years 1954-98, I compute the total ocean area of squid/salmon overlap between these two boundaries and the eastern and western edges of the Alaska Gyre.

The total area of proposed dietary overlap varies between a high of 4.2 million square kilometers in 1971 and a low of 1.9 million square kilometers in 1997. It shows a strong negative correlation ($r=0.9$) with sea surface temperatures used in previous analyses of salmon body sizes. Moreover, a comparison with 41 time series of salmon body size in Section 5.4 suggests that there is a stronger relationship between the overlap area and body size than there is between temperature and body size. This relationship becomes especially strong in the 1980s, during the period of high salmon numbers and a low overlap area (Figure 1.8).

Further, my analyses suggest salmon body length has a stronger (negative) relationship with salmon numbers than with squid overlap area, while salmon body weight has a stronger relationship with overlap area. Since weight growth is greatest in the summer months immediately prior to maturation, this suggests that density-dependence may be a stronger force prior to summer, in the winter and early spring. During the summer on the open ocean, environmental variation in prey distribution is probably more important than density-dependence. Oceanographic conditions in the summer affect salmon growth both directly and indirectly.

Chapter 5 concludes the dissertation by combining the bioenergetics and trophic models from the preceding sections. Section 5.2 further emphasizes the importance of winter growth by comparing the quantitative differences in winter and summer food webs. Using historical zooplankton and salmon data, I suggest that the winter is the time of year during which salmon must forage more extensively for food, despite low growth rates during this period. This suggests that density-dependent effects are most likely to occur during winter months at sea (Figure 1.9).

In Section 5.3, I present bioenergetics models which follow salmon during their final season. The models are the first to include ontogenetic diet changes in North Pacific salmon growth. They show that the period immediately prior to this feeding transition, winter and early spring, is especially critical to salmon growth. As shown in Figure 1.10, a small difference in winter body weights resulting from limited forage may be amplified into large differences by the summer. A 10% difference in an individual salmon's body weight at the end of winter may translate into a 50% difference in its body weight at the end of summer, as the initial difference in body weights will delay the salmon from reaching a large enough size to catch squid.

Winter is a period of time when (1) salmon ocean ranges may be most limited, (2) mesozooplankton production is low, (3) both fish and micronekton are eating zooplankton and (4) the ranges of pink and sockeye from Russia, Bristol Bay, central Alaska, southeast Alaska, British Columbia and Washington State show the most overlap (Myers et al. 1996). Hence it is probably during this time that between-stock density-dependent prey limitation takes place.

In Section 5.3, I revisit the relationship between density-dependence and water temperature. Water temperature is an important physiological factor in determining salmon growth. However, rather than linearly increasing or decreasing growth rates, it may interact with foraging efficiency to change the nature of the density-dependent growth curve in a nonlinear manner (Figure 1.11).

Finally, in Section 5.4, I outline a conceptual model of factors that control maturing salmon growth in the NE Pacific. The model unites density-dependent growth (competition), direct environmental effects on growth (such as the link between physiological processes and water temperature), and environmental and geographic effects that control prey type and abundance (Figure 1.12). I discuss other recent research applicable to carrying capacity, such as life history modeling, behavioral and seasonal timing issues, and issues of physiological control of growth. I discuss the possibility that small squid are a "keystone" species—highly productive, and at times showing negative correlations with zooplankton densities and positive correlations with salmon growth.

The conceptual model of Figure 1.12 differs from previous models of salmon carrying capacity in that it suggests that the critical period of density-dependent growth occurs in the winter for pink and ocean age .2 sockeye salmon, rather than in the final weeks of their summer homeward migration. An

important component of this model is the quantification of the ontogenetic shift of pink and sockeye salmon diets from zooplankton to micronektonic squid.

Pink salmon will be most strongly affected by this density-dependence, due both to their high numbers and their need to obtain their final size during a single year at sea. Maturing ocean-age .2 sockeye would be affected as well, yet the timing of their maturation decision, if occurring in the late winter/spring or the previous fall (Thorpe et al. 1998), may mitigate density-dependence. Coho salmon and older sockeye salmon, which feed at a higher trophic level, may be limited by the abundance of squid as described below, but not as influenced by winter density-dependence. Chum salmon density-dependence has not been quantified, due to their high digestion rates, distinct feeding mode, and unidentifiable nature of some of their prey in samples.

While the trophic triangle of intraguild predation may be hard to untangle, I present some predictions from the combination of food web variation and climate in Section 5.4—these predictions are shown in Table 1.1. If squid and zooplankton densities are independent, the presence of squid will determine whether or not the ontogenetic feedback loop exists, and therefore whether density-dependence is strong or weak in the population. This loop is further modified by environmental temperature.

This research should be taken as an outline for further study, especially with respect to the importance of micronekton to the production of commercial fish. Any confirmation of this work beyond models cannot take place without further sampling. Further work should extend models of the squid and salmon overlap to examine its importance further to the west, especially as more data becomes available along 165°W and 180° transects. Moreover, to confirm these results, it is important to begin a sampling program for micronektonic squid in conjunction with salmon food habits studies.

The ocean growth of Pacific salmon varies substantially by stock, species, and region. However there are common factors affecting growth on the scale of multiple years across the entire North Pacific. My results suggest that the carrying capacity for salmonids, as expressed through lower growth during periods of high abundance, may arise through a complex array of abiotic and biotic factors occurring on multiple scales. Hopefully the models and analyses presented here will show how components of the pelagic food web affect the population ecology of Pacific salmon.

Table 1.1. Predicted differences in instantaneous ocean growth rates of maturing pink and ocean age .2 sockeye as the result of changing environmental conditions. "Low" and "High" represent the extremes of natural variation measured in the offshore Gulf of Alaska. This model assumes that squid densities, zooplankton densities, and ambient water temperatures vary independently (From Chapter 5).

		Summer squid density	
		Low	High
Winter-Spring zooplankton density	Low	Poor overall growth, density-dependence weak	Poor overall growth, density dependence strong
	High	Medium overall growth, density-dependence weak	High overall growth, density dependence strong
Effect of spring/ summer ambient water temperature (upper 50m)		A steeper density-dependent growth slope will occur at higher water temperatures. At low salmon densities, fish may be larger at higher water temperatures than at lower water temperatures, while at high salmon densities, fish may be smaller at higher water temperatures and larger at lower water temperatures.	

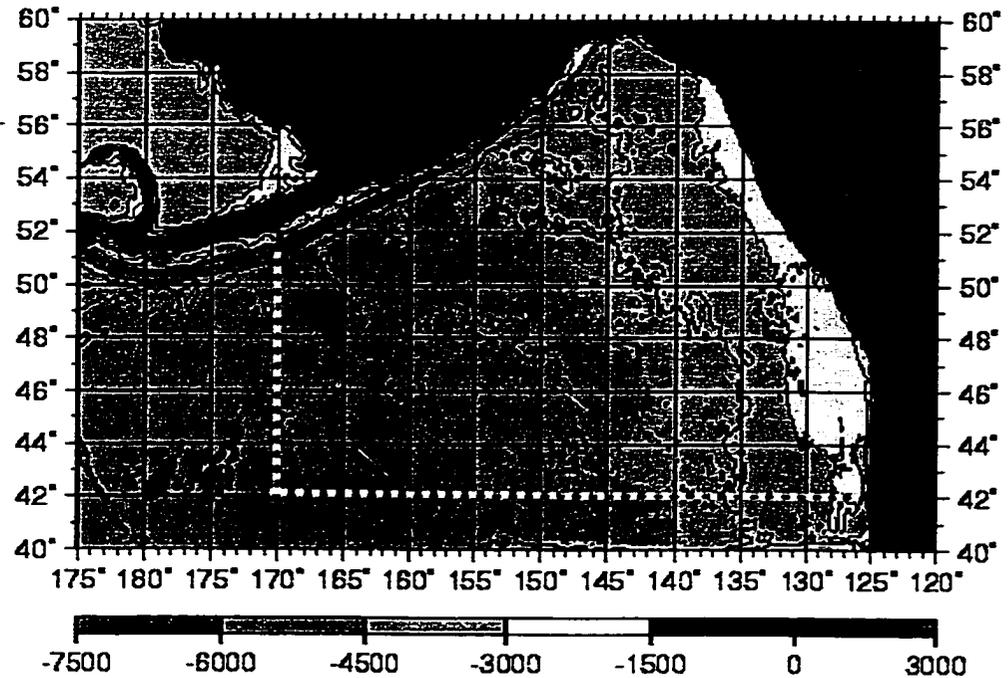


Figure 1.1. Study area in the "offshore" Gulf of Alaska. The portion of the northeastern Pacific Ocean covered in this study is defined by the continental shelf break (1500 m isobath). Shallower shelf areas are shown in black. This area hereafter shall be known as the *offshore* waters of the Gulf of Alaska. This geographic boundary lies closer to shore than the area defined by the legal definition of *high seas*, which covers any areas outside the 200-mile jurisdiction of a country. Contour lines and shading indicate bottom depth: white dashed lines indicate the southern and western borders of the study area.

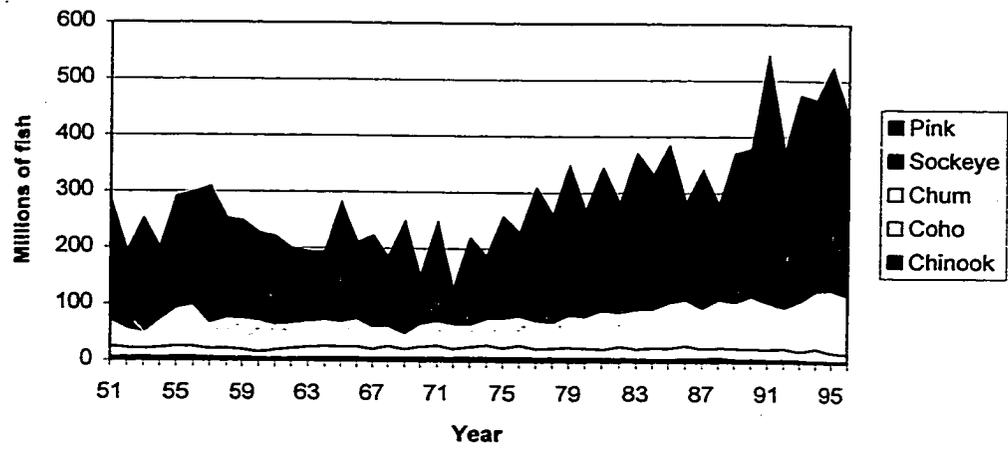


Figure 1.2. Number of salmon returning to North Pacific (Asian and North American) fisheries and spawning grounds between 1951-1997 (Rogers 1999).

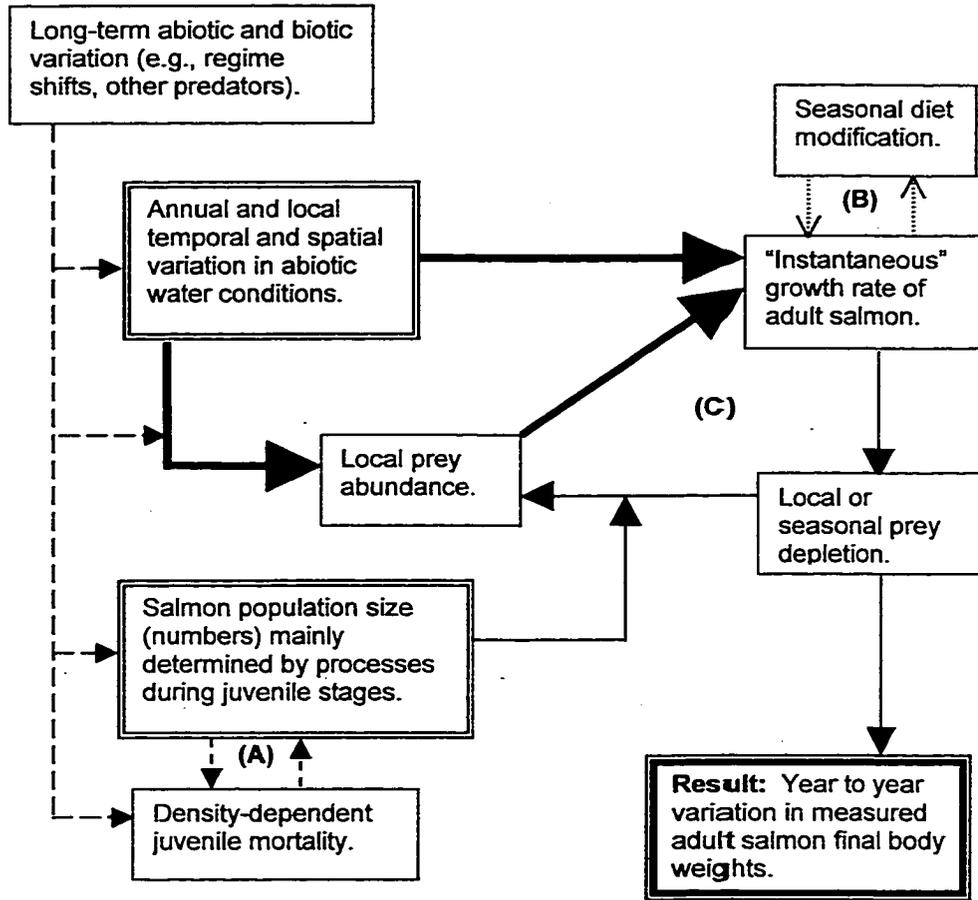


Figure 1.3. Conceptual model of cause and effect underlying relationships between salmon adult body size and ecosystem conditions. Arrows indicate the hypothesized directions from cause to effect. Letters indicate feedback loops. Arrow and box patterns differentiate chapters in the dissertation as follows: Chapter 2, dashed arrows and loop 'A'; Chapter 3, dotted arrows and loop 'B'; Chapter 4, bold arrows; Chapter 5, solid arrows and loop 'C'.

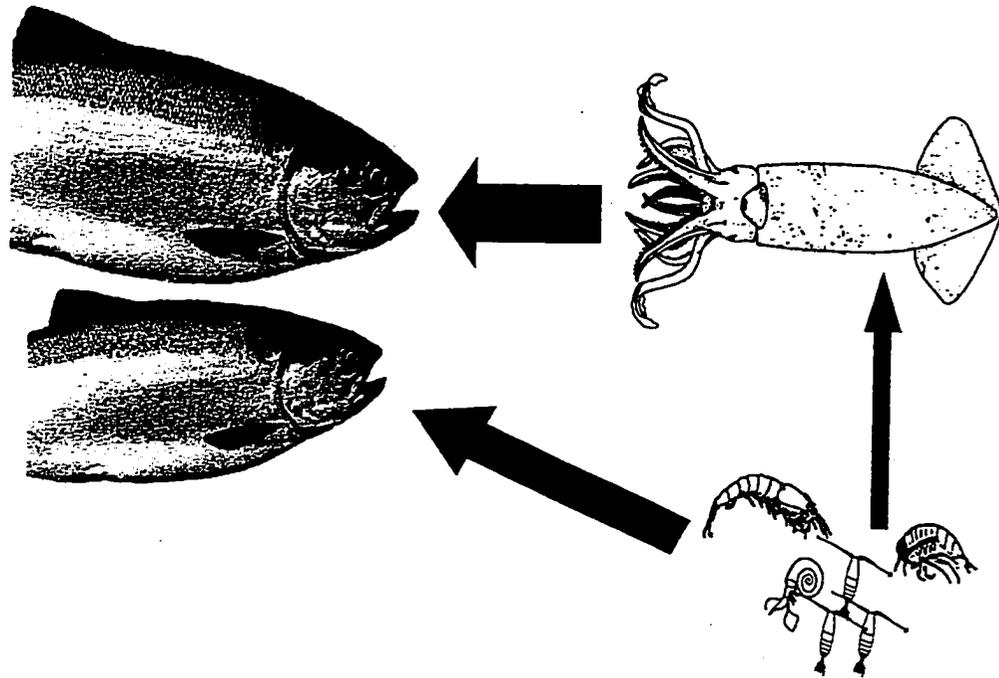


Figure 1.4. An important trophic triangle in the offshore Gulf of Alaska. Coho salmon feed at the higher trophic position in this triangle, feeding primarily on squid. Pink and sockeye salmon occupy a middle ground, feeding on zooplankton at smaller sizes (<1000g), and increasingly on squid as they grow larger. Chum salmon feed on zooplankton, and also find a major prey resource in gelatinous species. (From Chapter 3).

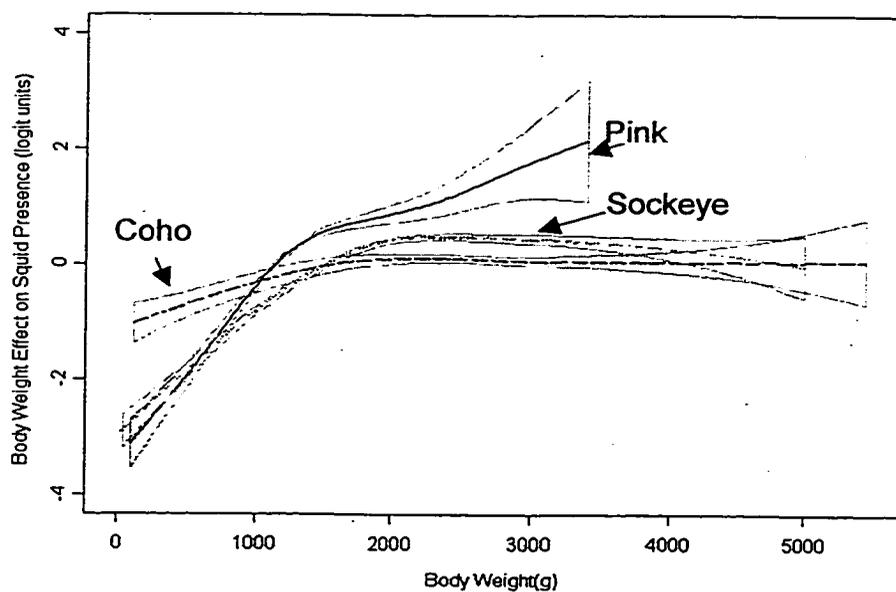


Figure 1.5. Adjusted logistic response of micronektonic squid in salmon diets as a function of the body weight of pink salmon (solid line), sockeye salmon (dotted line) and coho salmon (dashed line). An increasing logistic response indicates an increasing probability that a salmon feeds on squid. Grey boxed areas show pointwise standard errors. Results are from a general additive model and compensate for environmental factors. While the body weight dependence is similar for all available months of data, most pink salmon make the transition to squid feeding in the spring of their maturing year, while most sockeye make the transition in the spring of their ocean age .2 year (From Chapter 3).

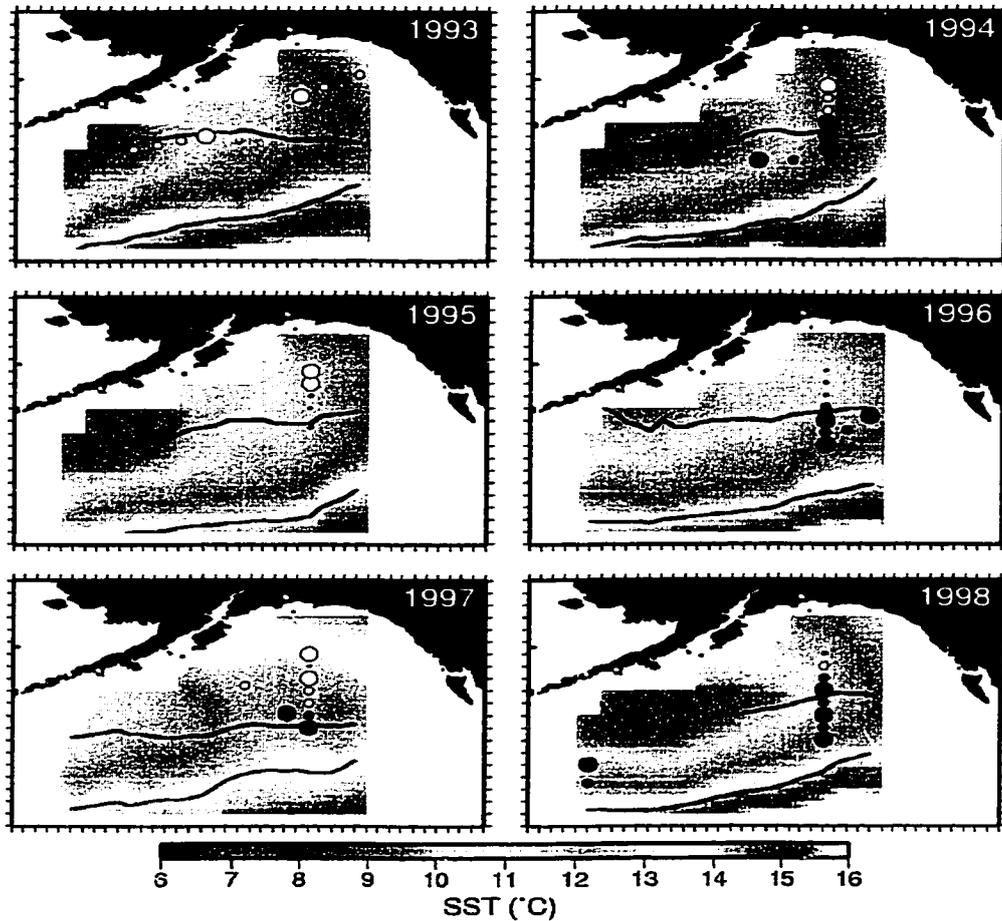


Figure 1.6. Sea surface temperature and squid distribution. Sea surface temperatures for July are shown with squid densities as measured from salmon stomachs, 1993-1998. Sea surface temperatures are colors, squid densities are circles. Large black circles indicate squid densities significantly higher than average, and large white circles indicate squid densities significantly lower than average. The northern solid line shows the July latitudinal temperature minimum in the Alaskan Gyre, which has a high correlation with the latitude at which squid densities switch from above average to below average. The southern solid line shows the 13°C isotherm which has been proposed as the southern temperature maximum for sockeye salmon in July (From Chapter 4).

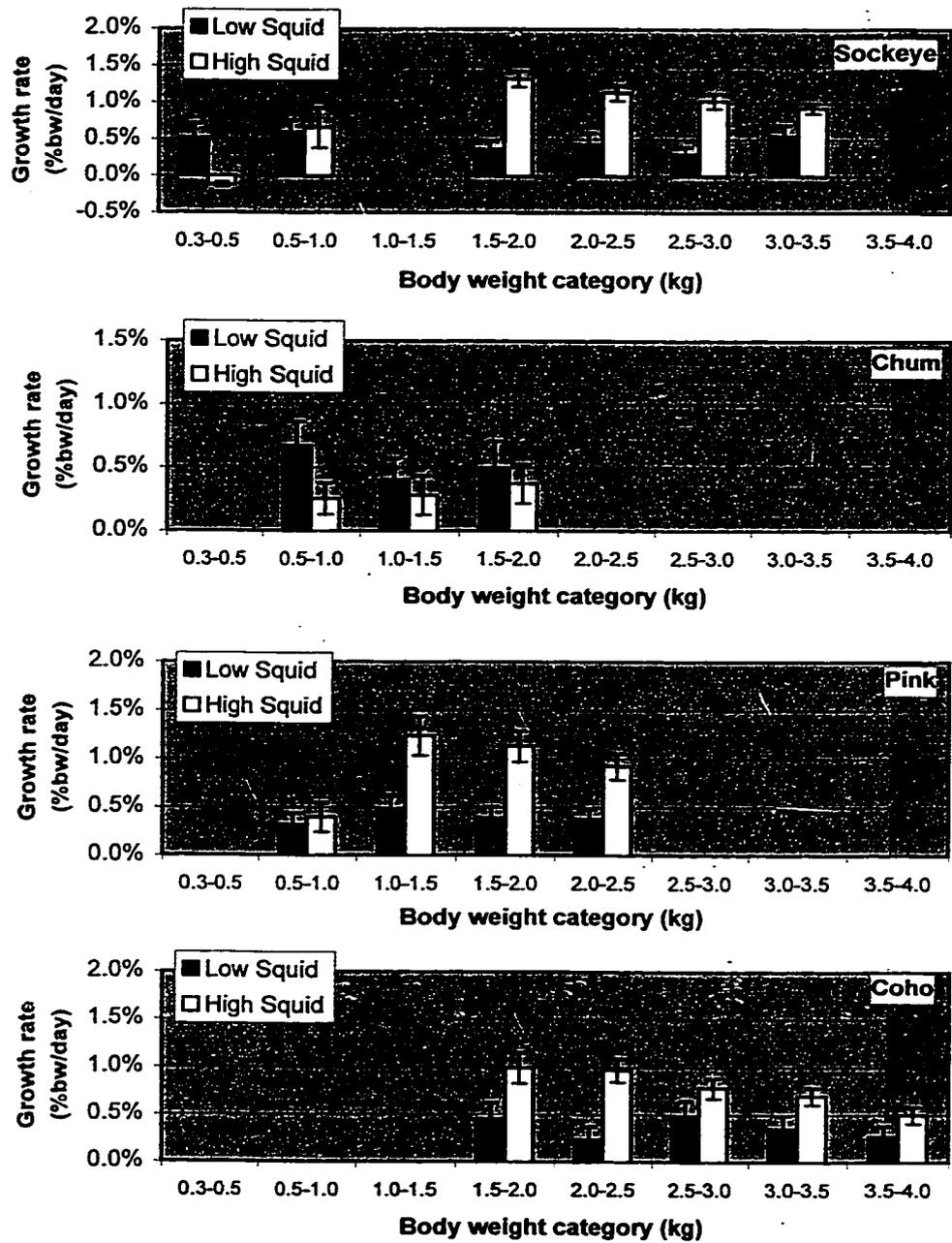


Figure 1.7. Difference in modeled growth rates for salmon, as a function of body weight, in "high" squid and "low" squid regions, 1994-98 (From Chapter 4).

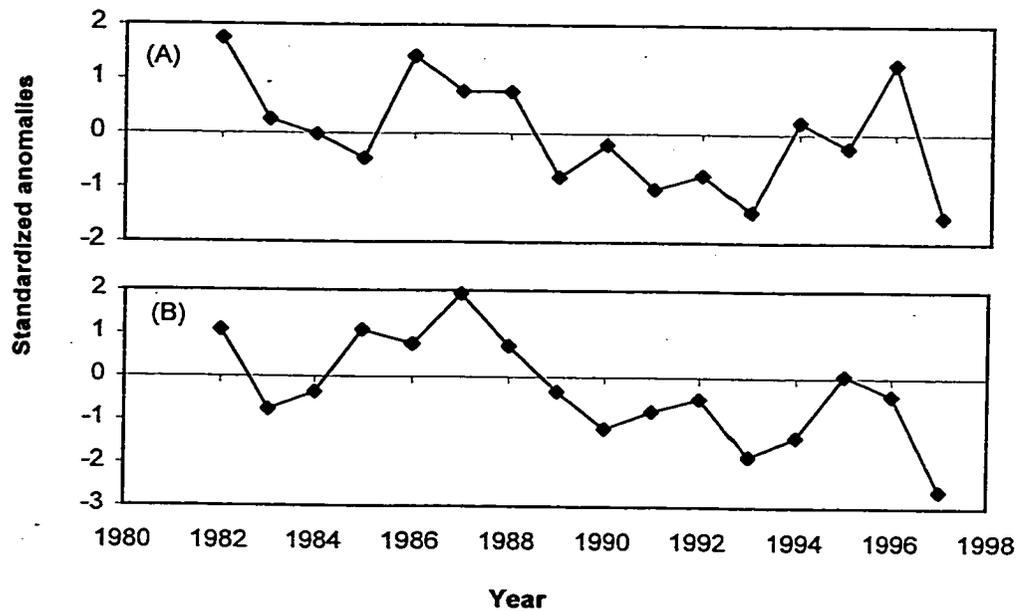


Figure 1.8. Salmon size vs. overlap with squid, 1982-97. (A) Standardized anomalies of body weights for seined-caught sockeye salmon in three British Columbia statistical areas which predominantly catch Fraser River fish. (B) Standard anomalies of area of overlapping distribution of squid and salmon, as calculated by the distance enclosed each year by 141°W-163°W on the east and west, the Alaska Gyre sea surface temperature minimum on the north, and the 13°C sea surface temperature isotherm on the south. Correlations between the area of overlap and body weights are between $R=0.63-0.65$ for all body weights shown (From Chapter 4).

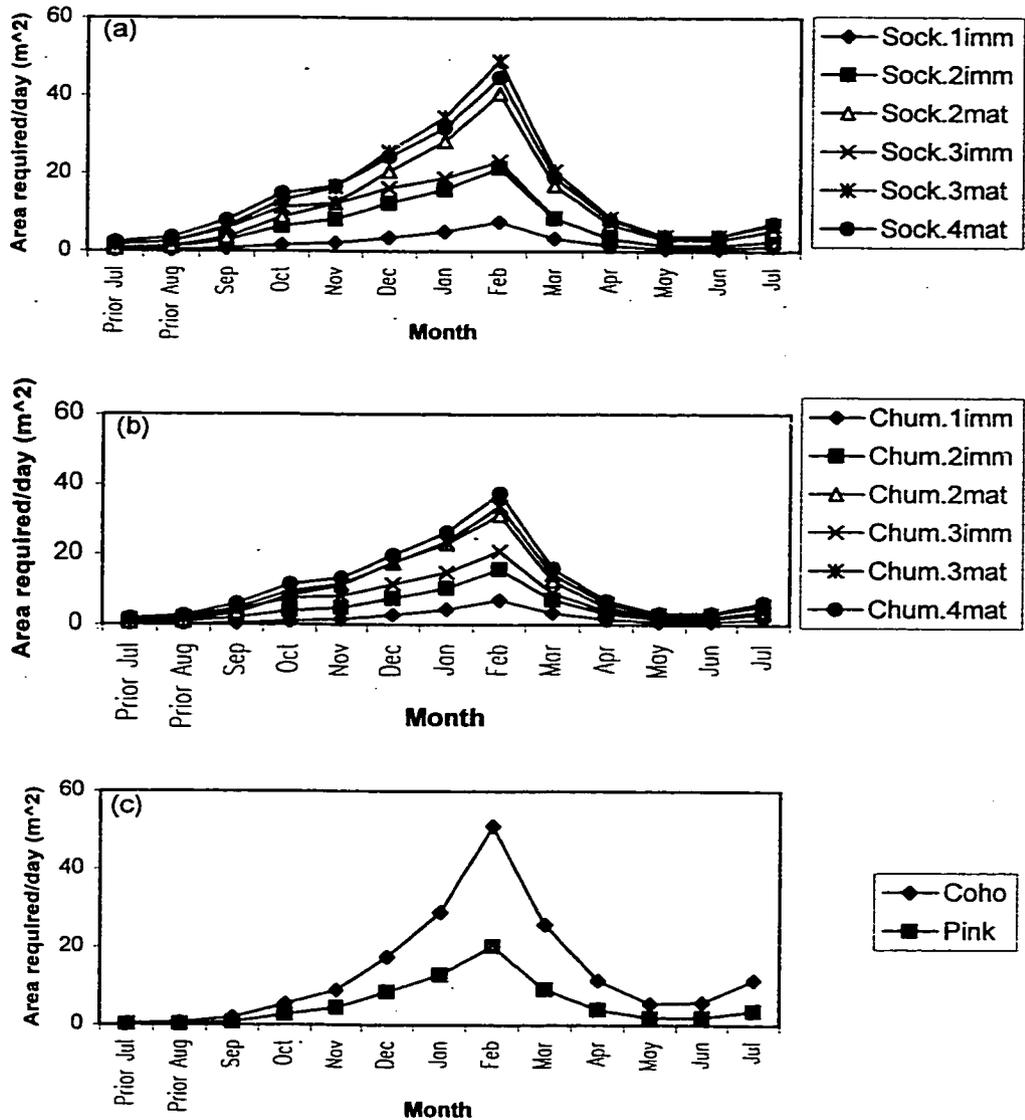


Figure 1.9. Total surface area of ocean at Ocean Station P (50°N, 145°W) which must be emptied of mesozooplankton to support the average growth of a single salmon, based on historical monthly mean values of zooplankton densities and salmon body weights. Ocean age and maturity status (mat or imm) are indicated for the salmon in the final (rightmost) July (From Chapter 5).

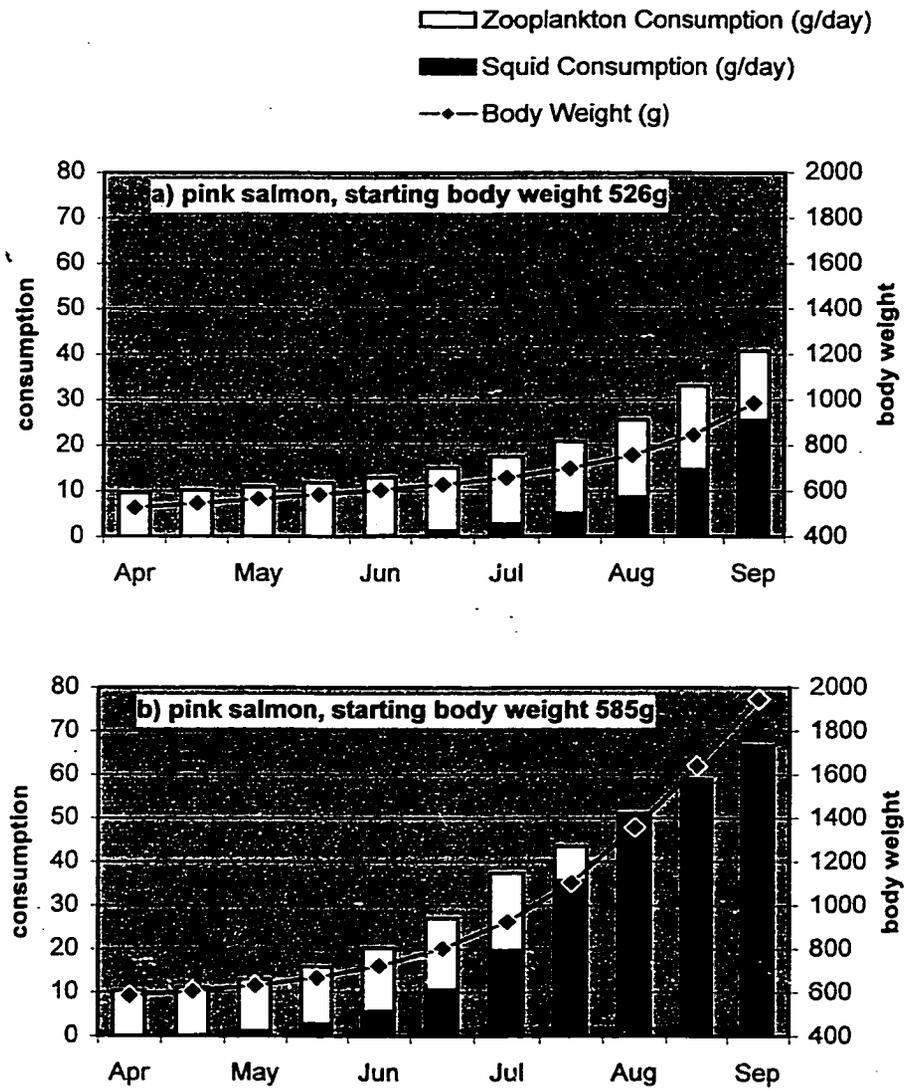


Figure 1.10. Predicted consumption rate and growth trajectory for maturing pink salmon, April-September, assuming a body-weight dependent foraging rate for squid as suggested in Figure 1.6. The only difference between the two runs is a 10% difference in April body weight (From Chapter 5).

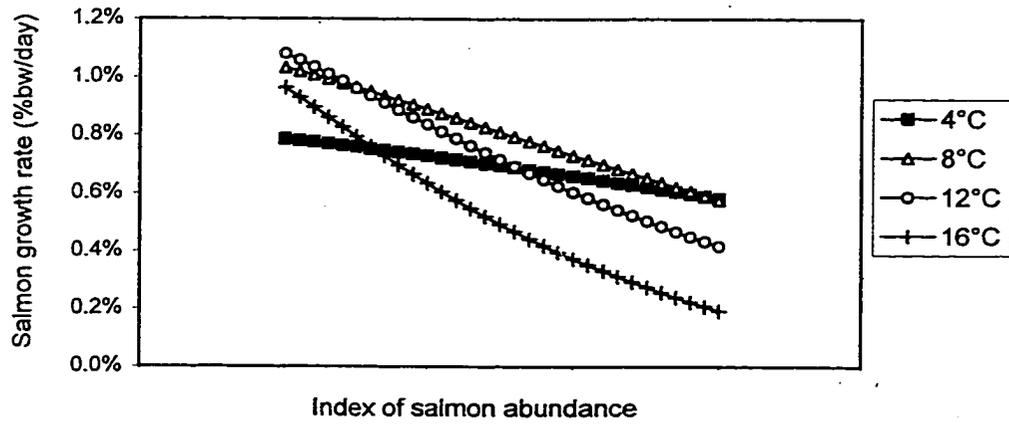


Figure 1.11. The maximum instantaneous (daily) growth rate of a 1500g pink salmon as a function of increasing competition for food, as calculated by bioenergetics modeling for a range of ambient water temperatures. "Competition" is proportional to (predator density/prey density). The caloric value of the prey is assumed to be fixed (From Chapter 5).

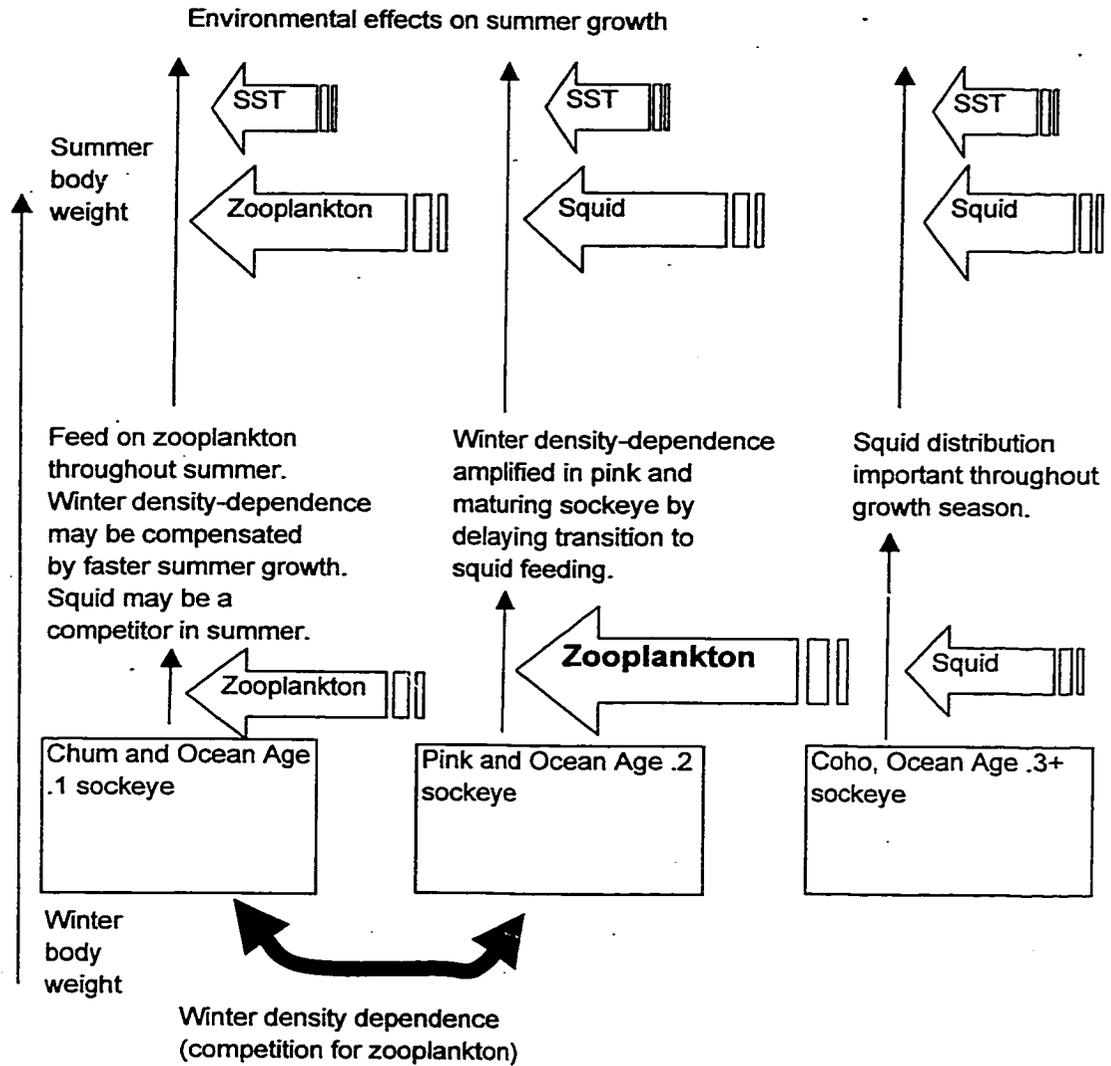


Figure 1.12. A conceptual model of density-dependence vs. environmental control of growth for salmon from winter to summer. For pink and some sockeye salmon, density dependence (food competition) may be strongest in the winter, although sockeye may respond to density dependence by delaying maturation. Block arrows indicate influences on salmon growth, with size of arrows proportional to the importance of each influence in determining final body weight (From Chapter 5).

2 Physical and biological variability in the northeastern Pacific Ocean and the concept of carrying capacity

2.1 Introduction

Chapter 2 reviews the physical properties of the northeastern subarctic Pacific Ocean, its planktonic food web, long term climate variation and its effects on Pacific salmon prey, and previously-reported relationships between climate, salmon population size, salmon survival, and adult salmon body weights (Figure 2.1). The discussion aims to pinpoint the proper scales of time and space on which to examine the possible density-dependent growth of adult salmon in the open ocean.

Section 2.2 reviews the oceanographic features, frontal zones, and seasonal cycle of the subarctic Pacific, and briefly describes the atmospheric driving forces which determine many of its physical properties. I also summarize current research on the longer time scale changes in Pacific physical conditions.

Section 2.3 reviews the biogeography of the Gulf of Alaska's pelagic ecosystem by describing (1) the seasonal cycle of major lower trophic level fauna which characterize the oceanographic region, and (2) some of the hypotheses linking long-term physical changes to observed variation in the planktonic food web. The purpose of this summary is to set the stage for examining the mechanisms that link long-term physical and planktonic variation to variation in the production of Pacific salmon throughout the region.

Section 2.4 reviews studies of the long-term trends of salmon production in the region, and discusses past studies in terms of the idea of ocean carrying capacity. The goal is to narrow the broad concept of "carrying capacity" into the study of specific processes accounting for variation in salmon growth and

survival, and to determine if "carrying capacity" is a meaningful quantitative term in the detailed study of a species or ecosystem.

2.2 Long term variation in physical systems of the North Pacific

Atmospheric circulation divides the North Pacific into two major latitudinal regions: a subtropical domain dominated by the clockwise-rotating Central Subtropical Gyre (shaded southern region in Figure 2.2), and a subarctic domain dominated by the counterclockwise-rotating Subarctic Gyre (shaded northern region in Figure 2.2). Between the subtropical and subarctic domains lies a broad band of eastwardly-moving waters known as the Transition Zone. Within the Transition Zone, the Subarctic Boundary separates subtropical and subarctic waters (Table 2.1; Dodimead et al. 1963; Uda 1963; Favorite et al. 1976).

The Subarctic Gyre is pinched at its longitudinal center by the Aleutian Islands, which causes recirculation of its waters into two sub-gyres: the Western Subarctic Gyre ('A' in Figure 2.2) and the Alaska Gyre ('B' in Figure 2.2). Eastern and western circulation is further divided by the Emperor Seamount Chain, extending north-south along 170° E for 2500 km (Favorite et al. 1976). The two subarctic gyres are biologically distinct, supporting different species and production patterns from plankton through salmon (Beamish 1999). The majority of the work in this dissertation concerns biological production in the Alaska Gyre and its boundary regions.

The characteristics of the transition between subtropical and subarctic waters can be seen in temperature and salinity profiles along the three north/south transects shown in Figure 2.2 (Figures 2.3-5). In the subtropical domain, low precipitation, evaporation, and high thermal input create a temperature-stratified surface layer (mixed layer), in which the higher

temperature of the surface layer allows more saline water to sit on top of less saline water (shown as dark gray surface waters above 35.0‰ salinity on the southern end of the transects in Figures 2.3c-2.5c). The thermocline exists year-round, shallowing to its minimum depth in the summer and deepening to its maximum depth in the winter (Figures 2.3a,b-2.5a,b; Longhurst 1998).

In the subarctic domain, on the other hand, lower thermal input and large freshwater input gives the water column a salinity-stratified surface layer, in which low salinity at the surface allows colder water to sit on top of warmer water (shown as dark gray surface waters below 33.0‰ salinity on the northern end of the transects in Figures 2.3c-2.5c). While a shallow (30-60m) thermocline appears in the water column in the summer, winter mixing is permanently limited by a salinity gradient (halocline) at 100-300 meters depth (Figure 2.3a,b-2.5a,b). A comparison of Figures 2.3c and 2.5c shows that the north/south extent of the Alaska Gyre is greater than that of the Western Subarctic Gyre, due to the geography of the basins.

The limitation of deep mixing creates productive conditions in the Alaska and western Subarctic Gyres, and they have been likened to year-round estuaries, in which organic nutrients are held at the surface by the salinity-induced density gradient (Tully 1965). In addition, a combination of upwelling at the center of the gyre and deep water moving upward as it hits the continental shelf brings cold, nutrient-rich waters from below 1000m to the surface in winter, and to just below the seasonal thermocline in summer (shown as the rising of the shaded 4°C isotherm in Figures 2.3a,b-2.5a,b; Van Scoy 1991). This "plateau" of shallow cold water stretches across the subarctic region and is called the Ridge Domain (Favorite et al. 1976). As seen by comparing Figures 2.3a,b and 2.5a,b, the Ridge Domain feature is stronger and shallower in the western Pacific and weaker in the east.

The transition between subtropical and subarctic water types is not constant in time and space. Rather, the Transition Zone consists of a series of horizontal temperature and salinity fronts, visible in the upward tilting isolines of temperature or salinity (Table 2.1 and unshaded areas between 33.8-34.6‰ salinity in Figures 2.3c-2.5c). A salinity front between 34.6-35.0‰ salinity stretches across the Pacific and forms the Subtropical Frontal Zone, separating subtropical waters from the Transition Zone (southern shaded areas in Figures 2.3c-2.5c). A second front between 33.0-33.8‰ salinity defines the Subarctic Frontal Zone (Roden 1991).

Frontal structures are generally stronger in the western North Pacific, at the confluence of the warm Kuroshio Current and the cold Oyashio Current. The movement of these waters from west to east propagates the fronts across the Pacific (Roden 1991; Zhang and Hanawa 1993; Yuan and Talley 1996; Dinniman and Rienecker 1999). Within these frontal zones, convoluted individual fronts exist which vary, meander and shed eddies (Roden 1991). The width and latitudinal position of the main fronts may be also be subject to substantial variation (Yuan and Talley 1996).

The broad band of easterly-moving waters which feed the northeast Pacific have variously been called the Subarctic Current, the North Pacific Current, or the West Wind Drift. At times, multiple names are used, typically with the North Pacific Current applied to the subtropical waters, and the Subarctic Current applying to the subarctic waters, although the name North Pacific Current has also been applied to all easterly moving waters entering the Gulf of Alaska. As the region of the Alaska Gyre studied in this dissertation is north of the Transition Zone boundary, the term Subarctic Current is used to refer to waters moving east or northeast along the southern boundary of the Gyre.

For subarctic species such as Pacific salmon, the succession of frontal zones may represent borders and concentration areas between ecosystems, and migratory fish may concentrate at fronts to feed (Brandt 1993; Murphy 1995; Bakun 1996). Fronts may propagate across the Pacific to different extents from year to year, and may be a source of variation in water input into the Alaska Gyre. As such, the long time-scale changes in the position or dynamics of these fronts should be considered as an important source of biological variation.

2.2.1 Northeastern subarctic oceanographic structure

The Alaska Gyre is the largest oceanographic feature in the Gulf of Alaska in terms of surface area. It is bounded on the south by the Subarctic Current, on the northeast by the Alaska Current, and on the northwest by the Alaska Stream (Figure 2.6). The Alaska Gyre is centered near 150° W, 52-54° N, although the center may vary in position from year to year (Royer and Emory 1987).

The origin of the Subarctic Current is at the confluence of the Oyashio Current with smaller cold currents from the Bering and Okhotsk Seas, near 45°N, 155°E (Favorite et al. 1976). The flow crosses the Pacific into the Gulf of Alaska, where the Subarctic Current diverges as it approaches the North American coast, forming two currents along the continental shelf: the California Current to the south, and the Alaska Current to the north.

The Alaska Current is a combination of waters from both the Subarctic Current and the northward-moving coastal currents which become the Alaska Stream as they move to the west. Processes in the Alaska Current may generate anticyclonic eddies of coastal water on the eastern border of the Gyre which may last from weeks to months and move westward into the Gyre itself (Tabata 1982; Musgrave et al. 1992; Meyers et al. 1998).

The divergence and weakening of the Subarctic Current at its eastern end, in combination with the westward extension of dilute plumes from the Columbia River, Strait of Juan de Fuca, Queen Charlotte Sound and Dixon Entrance, forms a surface region known as the Dilute Domain. The Dilute Domain may extend westward from North America as far as 160° W, although it is a surface feature only, mainly visible at 100m or less of depth (Dodimead et al. 1963).

The strong onshore transport of surface currents, coupled with Ekman transport of water from the center of the gyre, creates intense downwelling along the coast, and further downwelling occurs around the Alaska Gyre between the Alaska Current and the Alaskan shore. To replace this water in the surface layer, cold, saline, nutrient-rich but oxygen-poor water rises to the surface in the center of the Alaska Gyre creating the Ridge Domain (Royer 1981; Bakun 1996). Studies of tracers such as tritium in the Alaska Gyre have indicated that the center of the Gyre may be a substantial source of deep (intermediate, or sub-halocline) water into the surface waters of the Gyre (Van Scoy et al. 1991; Aydin et al. 1998).

In the summer, a zonal temperature minimum occurs within the Ridge Domain on the sea surface. This surface temperature minimum can be seen in the both the western Subarctic and Alaska Gyres, although not in the area of the Ridge Domain between the two gyres (Figure 2.7). The temperature minimum has been suggested by Aydin et al. (1998) to be a boundary between waters entering from the west (south of the minimum) and the recirculating outcroppings of the gyre itself (north of the minimum). They call the waters between the Ridge Domain/Subarctic Current boundary and the temperature minimum the Western Subpolar Waters (WSW) (Table 2.1).

Measurements of CFC concentrations distinguish the water properties of the WSW from those of the Subarctic Current to the south or the central gyre to

the north (Aydin et al. 1998). Some surveys from the 1950s identify WSW water properties as those of Oyashio Current waters extending into the Alaska Gyre (Dodimead et al. 1963). The possible importance of the WSW to salmon and their prey is discussed in Chapter 4.

2.2.2 Variation in northeastern Pacific physical systems

The major sources of water moving into and out of the Alaska Gyre are connected to the air circulation patterns. The primary driver of horizontal surface circulation within the Subarctic Domain is the Aleutian Low Pressure System, a deep, extensive low pressure atmospheric feature that develops in the autumn over the Bering Sea, increases and moves southeastward to the Gulf of Alaska by December, then shifts back to the west before weakening in the summer. A secondary driving force, an eastern Pacific high pressure system, arises in the spring in the northeast portions of the domain, and reaches its maximum intensity between June and August, covering most of the Gulf of Alaska (Favorite et al. 1976).

The resulting seasonal pattern of water flow is an intensification of circulation around the Subarctic Domain during the autumn and winter and a relaxation in the spring and summer. Direct heat input via sunlight provides a second major structuring force in the ocean. Sunlight drives the seasonal cycle in the vertical water column structure that is critical to the ocean's biological productivity. Seasonal variation due to solar heating dominates the vertical structure of the upper 100m of the water column (Tully 1965).

During the winter, temperature throughout the water column is relatively uniform, and the mixed-layer depth (MLD) is determined by the permanent halocline (Figures 2.3 and 2.8). During the spring and summer, solar input causes the surface water to warm up, forming a seasonal thermocline above 50m depth, thereby raising the mixed-layer depth from the halocline to the upper 50m. There is little seasonal variation found in water properties in depths

below the halocline. While a seasonal warming causes the creation of a thermocline and a shallowing of the mixed layer depth in the spring and summer, the temperature gradient disappears entirely from the surface waters in the winter.

While the amplitude of atmospheric variation is greatest over an annual period, the horizontal circulation of the Gyre varies most strongly on an interannual scale. Royer (1981) found that while the range of variation in the annual cycle of wind stress in the Gulf was 100% of the annual average, the range of annual variation in the flow of the Alaska Stream was only 13% of the mean annual value, while the interannual variation in the flow was 30%.

This shift of scales occurs as a result of the "white noise" of the atmosphere being transformed into "red noise" typical of ocean circulation (Steele 1991). The Pacific Ocean is particularly prone to fluctuations on multi-year scales: it is so large that it is not as tightly coupled to seasonal continental atmospheric forcing as smaller oceans are (Bakun 1996). Determining links between multiple temporal and spatial scales of physical forcing and ecosystem variability is the crux of understanding ecosystem dynamics (Allen and Hoekstra 1992; Francis et al. 1998).

2.2.3 Long-term variation

Beginning in the 1980s, advanced technology and a globally increasing availability of historical fisheries and climate data sets have enabled scientists to examine marine ecosystems as never before, over increasingly large scales of time and space. For example, the reconstruction of fish populations from anoxic sediment cores has revealed population fluctuations on the scale of decades continuing throughout the last few thousand years (c.f. Baumgartner et al. 1996). Satellites can provide information on patterns of primary production and other variables across an entire ocean. Such information is often available in near-real time.

Studies correlating fluctuations in fish populations with both decadal and longer scale cycles in the physical properties of climate and oceans strongly suggest that the two are related. Multiple symposia and related published volumes such as Beamish (1995) demonstrate the rising recognition of the role of historical analysis in addressing the role of climate in fisheries research and management (Francis and Hare 1994). One important aspect of coupled biological/ physical systems is that physical and biological processes may remain relatively constant for long periods of time, and then change rapidly to another state—such a rapid change has been dubbed a “regime shift.”

Variables used for oceanographic time series analyses generally fall into three categories: (1) the measurement of a single variable, such as sea-surface temperature, at a single site, (2) the measurement of a proxy, or index value, such as tree rings as a proxy for air temperature, or (3) the analysis of multiple variables over a large spatial scale, which are resolved into modes of variation that may be summarized by an index of combined conditions. Correlation between individual analysis of disparate records may reveal changes occurring over large spatial scales.

Atmospheric pressure and surface ocean conditions, such as sea surface temperature and altimetry, are readily adaptable to the third type of analysis. For example, to describe interannual variation in the atmospheric driving forces of the northeastern Pacific, Trenberth (1990) constructed an index of circulation of the Aleutian Low known as the North Pacific Pressure Index (NPI or NPPI) from a weighted mean of sea level pressure over 30°-60°N, 160°E-140°W. An examination of this index from 1925-1995 indicates prolonged (20+ year) periods of strong or weak Aleutian Lows with rapid switches between the two states occurring in the late 1940s and the late 1970s (Trenberth and Hurrell 1995).

In the ocean, long time-scale trends in surface conditions have been found to correspond with atmospheric anomalies. Of primary interest is the Pacific Decadal Oscillation (PDO) which describes alternating modes of sea surface temperature (SST) anomalies occurring on a 20+ year time scale (Mantua et al. 1997). It is generally agreed that a regime shift in the PDO occurred in the winter of 1976-77, and this shift is visible in many indices of northeastern Pacific conditions. Mantua et al. (1997) also identified previous shifts that occurred in 1947 and 1925, identical to shifts occurring in the NPI. The correlation coefficient between the NPI and PDO, adjusted for autocorrelation, is -0.50.

The correlation between the NPI and the PDO describes a relationship between atmospheric and SST patterns in the northeastern Pacific; however, it has been more difficult to associate these patterns with variations in frontal structure and surface currents in the region. Direct observations of horizontal water movement and subsurface water conditions, especially salinity, have been taken relatively infrequently over the years. However, horizontal movement and salinity define many of the subarctic fronts that may be critical to biological productivity (Table 2.1). Thus, the link between climate and biology has relied on large-scale correlative studies or developed conceptual models.

One of the more influential conceptual models of flow variation in the Gulf of Alaska was based on the analysis of sea surface heights from tide gauges along the Pacific coast (Chelton and Davis 1982). They noted an out-of-phase relationship between sea surface heights in the Alaska and California Current and interannual variations in the strength of the Aleutian Low. This model, elaborated in Hollowed and Wooster (1992), suggested that variation in the wind system caused the Subarctic Current water to alternately push more water into the Alaska Current or the California Current.

A wind-driven Ocean Surface Current model, OSCURS, confirms this atmosphere/ocean connection, and suggests that the Subarctic Current varies at its bifurcation point as it splits to create the Dilute Domain (Ingraham et al. 1998). During periods of strong Aleutian Lows, such as those seen 1976-98, OSCURS predicts that surface waters of the Subarctic Current would have a greater tendency to circulate northward into the Alaska Current. During periods of weak Aleutian Lows, drifters would have a tendency to move southward and enter the California Current.

In addition, measurements of surface altimetry patterns coupled with 3D ocean circulation modeling suggest that during the post-1976 period, high cyclonic winds increased the water exiting the gyre to the northeast via the Ekman drift (Bhaskaran et al. 1993; Lagerloef 1995; Wu and Hsieh 1999). Water circulation in the Alaska Gyre weakened on the northeast side of the gyre, as increased cyclonic winds pushed more surface waters onshore to the northeast, rather than into the Alaska Stream.

Combining these results, during periods of intense Aleutian Lows, more water enters the gyre from the southwest via the Subarctic Current, and more water exits the gyre onto the continental shelf in the northeast. The overall pattern brings warmer southern waters to the north during intense Aleutian Lows, and suggests that the PDO is driven by alternating periods of intensification and weakening of the winds of the Aleutian Low pressure system causing alternately a slowing down or "spinning-up" of the Alaska Gyre (Schwing 1998).

The physical consequences of this change in horizontal circulation around the Gyre may include stronger horizontal gradients at frontal structures. In addition, the increased circulation would increase the Ekman pumping at the center of the Gyre and the resulting Ekman drift of intermediate-layer water out of the Gyre—such changes have been noted in recent years (Schwing 1998).

The flow of Subarctic Current waters into the Gulf of Alaska may also be influenced by the location of the center of the Alaska Gyre. Lagerloef's (1995) analysis of surface altimetry data suggested that the Gyre weakened and shifted more to the east, rather than intensified, as a result of the climate shift.

Finally, shoaling (shallowing) of the winter halocline in the central Gulf of Alaska has been noted in recent years and it has been attributed to this increase in upwelling (Polovina et al. 1995). However, Freeland et al. (1998) report that the shoaling trend in the halocline may have been uniform since the 1960s, and a result of increased precipitation and heating of ocean surface layers, possibly as a response to global warming.

The 20+ year PDO is not the only large-scale climate frequency which has been detected (Table 2.1). The most famous is the El Niño-Southern Oscillation (ENSO), a Pacific-wide oscillation of conditions on the time scale of 3-5 years. ENSO effects have been noted as having strong effects on the biology of the NE Pacific. Additionally, a Quasi-Biennial Oscillation (QBO) has been detected in several climatic variables on a frequency of 2-3 years. The movement of the Gyre center from east to west may occur on time scales shorter than a few years (Royer and Emory 1987; Kelly et al. 1993).

Most hypotheses linking climate indices and biological production have resulted from correlation or frequency analysis. For example, zooplankton production has been shown to share some of the frequencies of climate indices (Table 2.1): the theories linking climate with lower trophic level production and fisheries production are summarized below in Section 2.3. It is worth noting that while hypothesized mechanistic links may be intriguing, they must be confirmed with experimentation conducted on proper temporal and spatial scales. None of the mechanistic hypotheses connecting climate indices to biological productivity have been traced to direct interactions between physics and biology, except in the most general sense. The distinction between correlation and mechanism is

important to make, as it affects our understanding of the models we use to understand the system (Francis and Hare 1994).

Scale is critical. For example, as described below, the shoaling mixed layer is used by Polovina et al. (1995) to predict increases in zooplankton production based on the increased concentration of nutrients within the mixed layer. However, as Freeland et al. (1998) point out, while the mixed layer may concentrate nutrients during the spring growth of zooplankton, it may also limit resupply of nutrients later in the season. Recent surveys have shown that nutrient concentration in the Gulf of Alaska may have decreased in recent years (Whitney et al. 1998). Thus, while the overall quantity of zooplankton production averaged annually may increase, the extent of the bloom throughout a season, and the resulting zooplankton community structure and transfer of energy to other portions of the food web, may increase for some species but decrease for others.

Choosing the scale of measurements is thus a necessary step in constructing comparisons, either experimental or hypothetical. As one example, one effect of ENSO interannual variation in the Gulf of Alaska may be a change of the frequency of mesoscale (100-200 km) downwelling eddies occurring in the Alaska Current, with eddies occurring more frequently during El Nino extremes of the ENSO cycle (Meyers et al. 1998). Determining mechanisms linking ENSO with biological production might require the resolution of measurements to be on the mesoscale within a single year rather than at the ENSO scale over multiple years.

In another example, a great deal of the time series analyses and models of zooplankton depend on data from the long-term continuous Canadian weather ship coverage of a single point in the ocean, Ocean Weather Station P (OSP, 50°N, 145°W) between the 1950s and 1980. But seasonal cycles may vary tremendously on a spatial scale, especially if viewed with respect to

distances from shifting oceanographic fronts. Station P is a geographic, not oceanographic fixed point. Station P may at times be influenced by waters of the Ridge Domain, Dilute Domain, or the Subarctic Current. Thus, it will not always be clear whether long-term variations in data at that single point are due to spatial or temporal variability.

Finally, the individual processes leading to ecosystem changes must be linked to driving variables through direct causation. For example, as mentioned above, the Subarctic Current entering the NE Pacific is formed near Japan, at the confluence of the warm Kuroshio Current and the cold Oyashio Current. The confluence of the currents into the Subarctic Current may result in internal structures separating water masses which may propagate across the Pacific, and may vary on annual and interannual time scales. A comparison of NE Pacific water types between two years, 1956 and 1959, showed that in 1956, Oyashio-influenced Subarctic Current waters did not enter the Gulf of Alaska, stopping at 170°W, while in 1959 the waters extended eastward past 145°W (Favorite and Hebard 1961).

Changes in the Subarctic Current frontal structures, and the input of differing water masses, may occur on a decadal scale. Measurements have not been conducted over a long enough time scale to determine the variation in this particular frontal structure. The relative volume of the Oyashio/Kuroshio water input may be correlated with changes in zooplankton, if both are affected by the NPI independently of each other. Increases in upper trophic levels biomasses may be a response to changing zooplankton or changing frontal structure, and the correlation between upper trophic levels and the NPI would remain the same.

It is important to distinguish correlations from mechanism to give a model predictive power. Correlations which have been used for prediction have been known to break down rapidly when the conditions which underlie them change.

This is especially worth considering in light of recent concerns over anthropogenic, unidirectional change, i.e., global warming. The changes in the mixed-layer depth mentioned above may be due to the PDO, or global warming, or both. Unidirectional change may break down correlations in unexpected ways—with an understanding of the distinct scales and properties of mechanisms linking climate to biological production, we may at least be able to explore the risk that pelagic marine ecosystems may be facing.

2.3 Biological processes

2.3.1 Seasonal cycle of phytoplankton and zooplankton

The stable, salinity-stratified water column of the subarctic Pacific, in combination with the upwelling of nutrients at the centers of the gyres, creates an environment in the subarctic Pacific suitable for phytoplankton growth. Overall, the long-term average phytoplankton concentration in the Subarctic Domain may be two orders of magnitude greater than in the Subtropical Domain. The seasonal plankton cycle within this highly productive region is important to understand in order to study the growth of larger fish.

One of the most characteristic biological traits of the Alaska Gyre is the year-round standing stock of phytoplankton. Yet in spite of the overall high phytoplankton concentration, and in spite of a mixed layer which concentrates nutrients in the photic zone during the spring and summer, the surface layer of the Alaska Gyre shows no spring phytoplankton bloom. This is contrary to other ecosystems, such as the North Atlantic, which possess similar physical changes in their mixed layer structures during the spring. In addition, contrary to other ecosystems, the phytoplankton seemingly do not limit their growth by depleting the macronutrients in the surface layer (nitrates, phosphates, and silicates) as the summer progresses.

The relationship between physical conditions and plankton seasonal cycles in the Alaska Gyre is considered by Longhurst (1998) to represent one of "the great enigmas in biological oceanography today" (p. 256). While the primary production peaks in the spring, the actual increase in system biomass appears in zooplankton, rather than in phytoplankton. Nitrate supply, which classically limits summer phytoplankton growth, remains high year round. This non-depletion of summer nitrate has led the area to be dubbed a "High Nitrate Low Chlorophyll" (HNLC) system.

Why, in spite of the presence of relatively high year-round standing stocks of phytoplankton, does the Gyre show no spring increase in phytoplankton standing stock, as is evident in other ecosystems? And why doesn't the existing primary production increase until it depletes the available mixed-layer nitrate? Answering this question is important in comparing year-to-year variation in fish populations with environmental variables, as the probable link between fish and the environment is through the plankton population.

Because we cannot experiment directly with changing environments, the only method of investigating mechanisms of linkage is through models. The most frequently-used family of models is the three-compartment differential equation model of seasonal interactions called the Nutrient-Phytoplankton-Zooplankton (NPZ) models. These models, calibrated with laboratory and ship-measured production data, have been used extensively to test hypotheses about the factors which control the seasonal dynamics of plankton.

The classic model, published by Evans and Parslow (1985), represents the growth rate of the lowest trophic level, phytoplankton, as a function of nutrient concentration in the water column and light input throughout the year. The model includes a self-limiting factor for phytoplankton, as the increased biomass of phytoplankton decreases the light penetration through the water column, thus decreasing production rate. Nutrient concentration is depleted by

phytoplankton, and refreshed by the changing mixed layer depth. The seasonal shoaling of the mixed layer in spring also concentrates phytoplankton and zooplankton near the surface.

An analysis of the model using mixed-layer depths corresponding to the north Atlantic and northeast Pacific showed that the difference in mixed-layer depth between the two systems was enough to account for the difference in the bloom (Evans and Parslow 1985). The model suggests that primary production in the Alaska Gyre is essentially light limited rather than nutrient limited. Additionally, control of phytoplankton by zooplankton was required to prevent the spring bloom. For this to occur, zooplankton could not drop to overly low levels during the winter, or they would not respond to changing spring phytoplankton growth rates fast enough to prevent a bloom.

For many years, the data used for zooplankton in the North Pacific was Station P watershipe data, which was collected with vertical zooplankton net tows from 150m depth to the surface. The nets favored mesozooplankton, primarily calanoid copepods. Initial assignment to the role of controlling grazer thus fell to these copepods. However, a series of research cruises in the 1980s, combined with new models, showed that heterotrophic bacteria and microzooplankton were the most important consumers of primary production (Frost 1987; Miller et al. 1991; Miller 1993).

This is especially true during the winter, when mesozooplankton standing stock is a fraction of that of smaller heterotrophs (Boyd et al. 1995a; Boyd et al. 1995b). Indeed, models suggested that the larger species of zooplankton could not respond rapidly enough to phytoplankton growth to control the spring bloom (McClain et al. 1996). Additional hypotheses for the control of primary production in the NE Pacific include micronutrient control (iron limitation; Martin et al. 1989), and the importance of the microbial loop and NH_4 recycling in inhibiting NO_3 uptake (Wheeler and Kokkinakis 1990).

The addition of microzooplankton as a controlling factor in oceanic production lengthens the food chain, but also changes the interpretations of mechanisms responsible for long-term change of fisheries production. Because energy supply for fisheries primarily comes from mesozooplankton, it is important that models which describe the link between NPZ models and fisheries accurately capture the dynamics of these multiple trophic levels.

2.3.2 Long-term changes in zooplankton production

Current estimates of long-term changes in the quantity of summer mesozooplankton production are almost entirely based on the analysis of copepod biomass. The only consistent long-term sampling of northeastern Pacific zooplankton has used nets which favor these animals. Further, estimates of changes in annual total production or annual average biomass of mesozooplankton are dominated by the spring peaks of copepod standing stock.

It is true that these species do represent a basis of the food web for many pelagic fish species; however, it is worth keeping this bias in mind, especially if historical trends of zooplankton biomass are to be compared with salmon growth occurring over an entire year.

The measurements of mesozooplankton biomass in the Gulf of Alaska do show a correspondence with indices of climate change. A time series analysis of the Station P data showed that the dominant frequencies of zooplankton fluctuations matched the dominant frequencies of the NPI (Table 2.1; Hameed and Conversi 1995; Conversi and Hameed 1997, 1998). This data series did not extend for long enough to examine changes on the regime time scale.

A comparison of summer zooplankton samples over a wider range of the northeastern Pacific in two time periods, 1956-62 and 1980-98, showed that the

standing stock across the Gulf averaged 2 times higher during latter period (226 g/1000m³ in 1980-89 vs. 94 g/1000m³ in 1956-62). In addition, the pattern of zooplankton distribution had changed. During 1956-62, the highest zooplankton concentrations were found near the center of the Alaska Gyre, whereas during 1980-89, the highest concentrations were in an extended band circling the central gyre, from the Transition Zone, around the Alaska Current and into the Alaska Stream (Brodeur and Ware 1992). Rand and Hinch (1998) examined the same data series by dividing the sample into years of high and low wind stress rather than between two time periods. Further, they examined both the spring and summer patterns of zooplankton density. Their findings showed that after a winter of high wind stress, zooplankton biomass was 100% higher in the spring and 50% higher in the summer than after a winter of low wind stress.

The mechanisms linking the NPI to Alaska Gyre zooplankton are not clear. Francis and Hare (1994) show that the correlation between the NPI and zooplankton biomass changed from positive in 1956-62 to negative in 1980-89, and the correlation was significant in both time periods. High winter wind stress may deepen the seasonal mixed-layer, which could retard zooplankton growth by diluting microzooplankton in the spring, according to a model by Frost (1993). However, the 1-D model fitted to Station P data found little change in primary production for any of the years 1956-80 (McClain et al. 1996). Conversely, a model by Polovina et al. (1995), using the shallowing of the permanent halocline in the last 20 years as a driver, predicted increases in primary productivity and microzooplankton production.

Further, it is possible that changes in primary production, filtered through complex layers of microzooplankton, are not the primary determinant of mesozooplankton growth rates. During winter months, heterotrophs and microzooplankton stay at relatively high biomass levels, and demand larger nutrient input than mesozooplankton (Figure 2.9; Boyd et al. 1995a). Miller et al. (1992) found that individual body lengths of *Neocalanus plumchrus* were

negatively correlated with an index of primary production minus microbial respiration for a number of years. If *N. plumchrus* body size is used in place of zooplankton biomass as an index of growth conditions for copepods, this relationship indicates that the interannual variation in energy lost via the microbial food web is more important than variation in primary productivity in determining mesozooplankton growth variation. Thus, it is possible that changes in the mixed-layer depth and primary production may be coincidentally or counterintuitively related to changes in mesozooplankton.

One clue to the link between the NPI and zooplankton lies in the fact that zooplankton standing stock in the Alaska Gyre is negatively correlated with zooplankton standing stock in the California Current (Brodeur et al. 1996). Given the alternating circulation patterns first noted by Chelton and Davis (1982), it is possible that a high biomass of zooplankton in the Transition Zone is advected into the Gulf of Alaska during periods of strong Aleutian Lows, and into the California Current during periods of weak Aleutian Lows.

An additional possibility is that similar large scale changes may affect zooplankton conversely in the two regions (Francis et al. 1998). For example, a warming of the surface layer may increase zooplankton production in the Alaska Gyre, while at the same time decreasing concentrations in the California Current by deepening and diluting the mixed layer (Brodeur et al. 1996). Finally, Gargett (1997) postulates on the existence of an "Optimal Stability Window" for phytoplankton, and thus zooplankton growth. In this model, phytoplankton growth is light-limited in overly turbulent water column regimes, and nutrient-limited in overly stable regimes. Between is a zone of "optimal stability" which varies in its geographical location between the Alaska Gyre and the California Current.

Regardless of the mechanism resulting in this measured increased standing stock, it is important to realize that seasonal patterns of zooplankton

production may shift as a result of climate change. If a single climate change shifts the timing of the zooplankton as well as its peak biomass density, a high level of zooplankton may not be beneficial to all predators.

It is worth noting, for example, that Brodeur et al. (1996) did not find significant correlations between spring/summer and fall or winter zooplankton biomass in the Gulf of Alaska. If the relative “badness” of a winter is more important to determining fish health than the relative “goodness” of a summer, the increase of summer zooplankton may not translate to increased production in fish. Mackas et al. (1998) found significant changes in the timing of peak copepod production between 1957 and the present. In the late 1950s, copepod production peaked in late May—this peak moved to its latest time in July during the 1970s, and since then has moved back to mid-May in the 1990s. This pattern shows coherence with the PDO and NPI time series.

Mackas et al. (1998) suggest that this timing change is related to the temperature of upper water column, with warmer water in recent years leading to faster copepod production. Taken with the possibility of depleted late summer nutrients due to shallowing MLD, suggested in Freeland et al. (1998) and evidenced by recent measurements (D. Mackas, Institute of Ocean Sciences, Fisheries and Oceans Canada, Sidney, British Columbia, pers. comm.), the combined effects may be detrimental to fish populations in spite of measurements of increased copepod production.

In order to determine the actual effects of these plankton changes on specific fish species in the Gulf of Alaska, it is necessary to sample and model fish feeding and growth throughout the entire season. I attempt to use this approach with Pacific salmon in Chapter 5.

2.3.3 Fisheries fluctuations in the Gulf of Alaska

It is clear that the environmental forcing patterns on multi-year scales described by the PDO, ENSO, and the QBO have an effect on the biology of higher trophic levels in multiple marine ecosystems (Beamish 1993; Brodeur and Ware 1995; Hollowed et al. 1998; Francis et al. 1998; Beamish et al. 1999). The effects of climate, however, are not limited to the direct increase or decrease of the biomass of the entire system. Animals with longer than annual life histories integrate short term changes, and their biomass may not respond immediately to changes in ocean conditions.

Instead, long-term ocean variation may affect specific critical periods of a species' life history, for example, by giving rise to high recruitment events, or by slowing, or speeding somatic growth or egg production. Each species may have a different sensitivity and respond in a different direction to climate change, not necessarily responding to increases in primary productivity by increasing their own biomass.

In one example, Hollowed et al. (1998) compared ENSO and PDO indices with time series of salmonid biomass and with recruitment time series of 23 groundfish and 5 non-salmonid pelagic species in the Gulf of Alaska, the California Current, and the Bering Sea. Their results showed complicated patterns of succession and climate interaction, with some stocks increasing and some stocks decreasing after 1976. In addition, while the long-lived species did not show a direct biomass response to ENSO, several of the species showed either high or low recruitment events during El Niño years.

The case of the Pacific salmon is the most well-known example of a long term climate/biological interaction in the Pacific Northwest. The numbers of salmon returning each year have reached record highs in the 1980s and 1990s across the Alaska and northern Asia (Mantua et al. 1997; Francis et al. 1998; Beamish et al. 1999). However, the pattern is more complicated than a simple

increase of all salmon stocks in concert with the strong Aleutian Lows. Time series analysis indicates that periods of high production of salmon in Alaska are correlated with the PDO, and alternate out of phase with periods of high production in the Pacific Northwest (Hare et al. 1999).

During the 1980s and 1990s, Pacific salmon production across the entire North Pacific reached record levels, with Alaska being a major source of the boom, while stock abundance in the Pacific Northwest has declined. This inverse relationship between the two regions extended back to the 1920s with alternating periods of high production in Alaska vs. the Pacific Northwest (Mantua et al. 1997).

Salmon ocean survival may be affected by growth rates during early coastal juvenile phases (Burgner 1991; Pearcy 1992; Francis and Hare 1994), so this increase in salmon numbers may be due to the changes in availability of zooplankton at the edges of the Gyre. The alternating pattern of zooplankton production in the Alaska Gyre and the California Current, mentioned above, may translate into alternating areas of good survival for salmonids. Conversely, alternating abiotic ocean conditions such as temperature may affect salmon and zooplankton independently. On shorter time scales, evidence for ENSO effects differs between stocks and is discussed later in this dissertation. One time series of sockeye catch showed frequencies matching the QBO (Table 2.2) at 2.3 years (Mysak et al. 1982). It is not clear if these matching frequencies reflect local or global conditions.

From the perspective of marine biogeography, the mechanistic link between changing physical conditions and changing productivity of a single species may take on many forms. These can be divided into two broad classes: direct physical effects, and food web effects. Direct physical effects are situations in which a changing physical property of the water directly influences the production of a species. For example, a change in ambient water

temperature may change the physiological rates of digestion of a fish, changing its efficiency of conversion of prey into body mass.

Food web effects, in their purest sense, are situations in which the production of a population changes solely due to the changing of prey supply (bottom-up forcing) or predator-induced mortality (top-down forcing). In pelagic ecosystems, the conventional wisdom holds that for fish populations, bottom-up forcing, or variation in plankton supply, is the most important component of ecosystem variation (Steele 1998). Therefore, many mechanistic studies have focused on the mechanism linking physical variation with plankton growth, assuming that fish will take advantage of available food in a predictable manner.

In a sense, the difference between food web effects and direct effects is a convenience to make a problem tractable. Food web effects must always be traceable to direct effects at some level: often, in the link between climate variation and phytoplankton. In the same way, direct effects become food web effects for neighboring trophic levels. For example, if changing water temperature limits the migration range of a species due to physiological concerns of temperature regulation, a predator/prey overlap in space and time may cease to exist.

Trophic (food web) variation and direct physiological variation may arise from changing food availability to a particular species, regardless of the amount of food measured in the ecosystem. For salmon and other actively foraging creatures, the presence/absence of oceanic fronts and concentrating/diluting factors such as eddies may greatly increase/decrease food supply (Brandt 1993, Murphy 1995). Further, changes in habitat suitability may increase or decrease the overlap between predator and prey in either time or space.

In summary, the link between climate forcing and fish stocks may occur through several pathways, either as climate applies direct physiological effects on fish, or as climate affects food supply and thus causes changes in the food

web (Francis et al. 1998). Direct links have been shown between climate forcing and primary and secondary production on PDO, ENSO and QBO scales in the Gulf of Alaska. Further, links have been shown between these scales and fluctuations in some fish stocks, specifically Pacific salmon.

This dissertation focuses on a single property of Pacific salmon: the "carrying capacity." As discussed in Section 2.4 below, this intuitive idea of a limit on total salmon production, which may change as a response to climate forcing, is greatly complicated by the wide range of effects which climate may have on fish. Without taking into account long-term changes in seasonal cycles and biogeography, using indices of primary or secondary production alone will not provide enough information. In order to give the question of carrying capacity meaning, it is necessary to carefully define its application in a manner specific to the ocean habitat of Pacific salmon.

2.4 Salmon growth studies and carrying capacity in the northeastern Pacific

2.4.1 Carrying capacity in theory and practice

The existence of an upper limit for the production (growth) rate of any element in an ecosystem is a fundamental thermodynamic principle of any defined system. This is true if the element under consideration is an individual, a species, a trophic level, or an ecosystem as a whole. Energy can neither be created nor destroyed, and a system can only assimilate as much energy as enters into it. In addition, the Second Law of Thermodynamics requires that any system which is not in "complete" thermodynamic equilibrium with its surroundings must expend a certain amount of energy from outside itself to maintain its basic structure. This is true even if the system does not grow, export material, or change internally.

Systems in complete thermodynamic equilibrium are not only what might be called "cold and dead" but are also utterly uniform. Almost any real physical system of practical interest or use to humanity falls into the category of needing to expend energy to remain the same. For many simple systems, a very small amount of energy is required, and the time scale of change is beyond the human scale of thought. For example, a glass jar, left on a shelf, will take longer than many human lifetimes for its molecules to lose their form, unless of course it is dropped. However, the time scale of energetic processes occurring in living organisms or populations is very much on the scale of human interest and thought.

At its heart, carrying capacity is a simple idea: you can't take more out of a box than you put into it, even if items change their form while in the box. It is a useful intuitive concept for considering human interaction with nature—the wishes of people notwithstanding, you can't take more out of nature than is put in, and expect to be able to take the same amount again year after year.

However, moving from this intuition into a quantitative statement about any living element in system: "the carrying capacity of fish in the lake is x tons," is fraught with peril, as care must be taken that the method of quantification used is meaningful.

A fundamental part of the human thought process is the use of models. Models of reality lie at the heart of all forms of language and communication. A model may be mathematical or conceptual: it is simply the creation of an analogy of nature (Francis et al. 1999). But as any analogy used in communication, the terms used to describe the model must be relevant to the questions asked.

2.4.1.1 The definition of carrying capacity in population ecology

A time-dynamic model, in a mathematical sense, describes the behavior of one or more "state variables" of interest by describing rules for the state variable's change over time. In population biology, the most often-used state variable is either numbers (N) of animals or the biomass (B) of a population at a given instant in time. In a 0-dimensional time-dynamic model, the state variable changes only with time (By convention, time is not counted as a dimension). Adding spatial variables such as depth or spatial location may make the model 1- 2- or 3-dimensional. All of the models considered in this dissertation are 0-dimensional, with changes in spatial structure being examined by the use of multiple 0-dimensional models.

A *static* model would simply present the level of the state variable without giving rules for change. The statement "Today, there are 200,000 tons of fish in this population" is a static model of biomass, as it does not describe how biomass might change over time. A single description of a food web is a static model of biomass for many species in an ecosystem. The state variable here is in *static equilibrium*, as there are no conceptions or rules allowing the variable to change.

In contrast, a *dynamic* model contains both a static description of a state variable at a starting time, or *initial conditions*, and rules for change from the initial conditions. A simple but complete dynamic model might be "Today, there are 200,000 tons of fish in this population, and that number will double every year." A dynamic model can be used to predict the level of the state variable at any time t after the initial conditions. It may be discrete (a *difference* equation), describing the state variable at set time intervals or continuous (a *differential* equation) describing the state variable for any value of t .

A state variable is in *dynamic equilibrium* if the dynamic model predicts that it will maintain the same value for all future times. The value of the state

variable when the model is in such an equilibrium is a *dynamic equilibrium point*. The model does not have to be in dynamic equilibrium initially for an equilibrium point to exist, as long as the model predicts that once the state variable reaches that value, it will not change afterwards.

In population ecology, the predicted quantity of the state variable of N or B of a population, at a stable dynamic equilibrium above zero, is known as the population's *carrying capacity*. By convention, if this quantity appears explicitly in the formulation of a model, it is usually designated by the letter K . Adding a carrying capacity to the simple model above might include the statement "Today, there are 200,000 tons of fish in this population. That number will double every year until there are 800,000 tons of fish, after which the population will not change." 800,000 tons is thus the carrying capacity K of the population.

The final concept required for exploring carrying capacity is *stability* of a dynamic equilibrium point. In the strictest sense, *stability* refers to tendency of change of the state variable "near" the equilibrium point. If an equilibrium point is stable, the state variable would return to that point after a small change (*perturbation*) of the state variable near the equilibrium point. Conversely, if a state variable is at an *unstable* equilibrium point, a perturbation would cause the state variable to leave the equilibrium. Making an equilibrium point in the above model stable would require the statement "If the population at any time is within 100,000 tons of 800,000, it will become 800,000 in the next year." Conversely, an unstable equilibrium point could state "If, at any time, the population dips under 800,000 tons, it will lose biomass until it reaches zero."

2.4.1.2 Applying carrying capacity to real-world populations

The reason for describing carrying capacity in terms of the simple dynamic models above is to discuss the difficulties which arise when attempting to apply the above intuitive concepts to real-world data. Some of the difficulties are practical. For example, Solow and Steele (1990) estimate that calibrating

well-known mathematical models of carrying capacity to actual data may require longer data series than are currently available for most species.

On a conceptual level, there is the confusion of definitions, especially with regard to the concept of stability. Grimm and Wissel (1997), in a survey of literature, note 163 definitions of 70 different stability concepts applying to species or ecosystems. Terms include resilience, persistence, constancy, or elasticity, all with slightly differing connotations. This wealth of definitions partially lies in the necessary oversimplifications that mathematical models must make in order to be tractable from either a mathematical or data-collection standpoint. However, on a fundamental level, the confusion arises from the conceptual difficulty of defining meaningful points of stasis in (1) a living, changing system, and (2) a hierarchical system.

A biological system changes and evolves in response to external forcing. Since the links between the elements in an ecosystem incorporate delays in time and space, a single component of a system will be affected by feedback. It is feedback in the dynamics of the most basic relationship in an ecosystem, the link between predator and prey, which determines if and when a species is controlled by bottom-up or top-down forcing.

Time delays in a negative feedback loop may create situations in which top-down forcing, usually not considered a force in structuring marine populations (Steele 1998), may be important in understanding the long-term dynamics of a species. Positive feedback may accelerate population or individual growth so that small differences in initial growth rates may create large observed differences at a later time. Small changes in external conditions, such as the change in timing of a plankton production peak may disrupt feedback and cause a regime shift in a biological system (Mackas et al. 1998).

If ecosystem forcing functions, such as primary production or heat input, were constant in an ecosystem, every element would eventually reach a stable equilibrium. In such a system, a definition of carrying capacity would not be necessary. If the system did not change, the most simple explanation, "There are x tons of species y ," would be sufficient. No dynamic equations with stable points would be required. In other words, carrying capacity is a kind of paradox: it is a description of a stable equilibrium point in a system that is only meaningful if the system is not able to reach that stable equilibrium (Levins and Schultz 1996).

On the other hand, a living and changing system makes carrying capacity a useful concept, but only if the functions determining the system vary with time—in other words, if the "stable" carrying capacity is a moving target, and varies with time. But if carrying capacity of a species is a state variable rather than a constant parameter, it cannot be considered as a stable point for a species' biomass. So why do models or ideas of ecosystems include carrying capacity as a concept at all?

Part of the answer lies in the incomplete nature of model descriptions, which may create a simple structure. Processes affecting state variables outside of the model structure are considered "stochastic" or unpredictable. Carrying capacity in this case is the value which the system returns to after such a perturbation.

The natural time scale and relative amplitude of perturbation may differ for different species, giving rise to the concept of 'r-selected' or 'K-selected' species. 'r-selected' species are adapted to undergo large fluctuations away from carrying capacity and subsequent rapid recovery, while 'K-selected' species are adapted to minimize the effect of fluctuations in forcing and remain near their stable equilibrium.

In 1993, the North Pacific Marine Science Organization (PICES) and Global Ocean Ecosystem Dynamics (GLOBEC) formed a Climate Change and Carrying Capacity working group (CCCC), with the goal of increasing understanding of the mechanisms that control the carrying capacity of fish species. The group took a broad view of carrying capacity as a working definition:

“Carrying capacity is a measure of the biomass of a given population that can be supported by the ecosystem. The carrying capacity changes over time with the abundance of predators and resources (food and habitat). Resources are a function of the productivity of the prey populations and competition. Changes in the physical and biotic environment affect the distributions and productivity of all populations involved.” (U.S. GLOBEC 1996)

While the term “supported” in this definition is unclear, it probably refers to the biomass of the population at the aforementioned stable equilibrium. A more interesting feature of this definition is the implicit notion of the time scale of change. The definition implies that while carrying capacity may change over time, its change is on a time scale which allows the population to track it. Without a definition of the time scale, it is not possible to tell how much a population is affected by the existence of a maximum limit to production. In order to understand the nature of the carrying capacity of a species, a modeler must provide a description of the mechanism which returns the species to carrying capacity when the species is perturbed from its equilibrium.

When the value of state variable in a system influences its rate of change, such a mechanism is known as a *feedback loop*. In a positive feedback loop, a variable's rate of change increases as the variable itself increases: exponential growth is an example of positive feedback. On the other hand, a rate which slows as the state variable increases is a negative feedback

loop. In population ecology, a feedback loop affecting the population numbers or biomass is known as a density dependent mechanism. Density-dependent biological mechanisms are required for carrying capacity to exist.

One critical aspect of this description is its time scale relative to the change of system parameters: if the carrying capacity of a system changes faster than a species can track it, the density dependent mechanism does not have a strong influence on biology, and density-independent processes will be more important to measure. Further, as implied by the use of the two terms "food and habitat" in the definition above, there may be multiple density dependent mechanisms affecting the rate of change of a population. There may be multiple *bottlenecks* which act to determine a "final" carrying capacity.

Each negative feedback loop may represent competition within a species for non-renewable resources (such as habitat) and renewable resources (such as prey). This split is defined specifically in the GLOBEC definition of carrying capacity, and the two types of resources require different modeling techniques (Berryman et al. 1995).

Again, the time scale of change is important, especially if different bottlenecks occur at different levels of the biological hierarchy. It is the hierarchy inherent in ecological systems which define the nature and time scale of both positive and negative feedback. A fundamental aspect of a living hierarchy is the existence of feedback—both positive and negative—across scales. The hierarchy of a living system begins with chemical and cellular processes, which are first grouped into individuals, and then on into populations, species, and ultimately ecosystems (Allen and Starr 1982). The structure of any given feedback loop depends on the interplay of hierarchical elements.

A prime example is seen in the case of density dependent foraging. A population of fish in a single area will consume zooplankton to grow, which will

decrease the population of zooplankton, thus slowing the growth rate of the fish when there are more of them. This simple idea can be modeled by a single negative feedback loop for the biomass of the fish. However, the actual decrease of prey occurs on a smaller level of the hierarchy, with an individual fish consuming one or more zooplankton.

What are the implications of a feedback loop which acts through multiple levels on a hierarchical structure? If there are multiple bottlenecks, the time scale of each one may determine which one is dominant in determining carrying capacity. Moreover, the interacting elements of feedback loops occurring on different hierarchical levels may create a situation in which *internal reorganization* of the system might occur on a scale between the shorter time scale of "fast" density dependent feedback loops and "slow" changes in abiotic forcing functions which makes the calculation of a meaningful carrying capacity difficult.

For example, if the prey of a fish population remains stable for a long period of time, then suddenly drops, the "instantaneous" result may be an increase in the mortality rate of fish due to starvation, leading to a lower carrying capacity as determined by the density dependent predator/prey interaction. If the prey remains low for a long period of time, however, secondary changes may occur—the fish may grow more slowly, reproducing later, or they may decrease egg production overall, which might mitigate the effects of survival.

Such internal reorganizations, which might be represented by a change in the efficiency of egg production or growth, could not be measured by knowing the biomass, density, or prey population alone. It is necessary to know either the frequency and variance structure of the prey biomass relative to the dynamics of the predator, or to measure the carrying capacity by describing each density dependent process individually and on the appropriate scale. In

the latter case, carrying capacity is not an absolute quantity but simply a framing concept for the total effect of each process.

Biomass, as a state variable of a population, provides an example. The biomass of a population at any given time, in most general terms, can be considered to be the sum of all individuals in the population, times the weight of each individual. In general terms, this can be written as:

$$\mathbf{Biomass} = \sum_{I=1}^n \mathbf{w}_{IND I}$$

where n is the number of individuals, and w_i the weight of each individual. Because it is not possible to measure the weight of each individual, frequently the population is divided into a number of cohorts, often distinguished by the age of the individual. If there are k cohorts in the entire population, with the number of individuals in each cohort being n_i , and the average weight of an individual in cohort i being $w_{avg i}$, the total biomass may be written as:

$$\mathbf{Biomass} = \sum_{I=1}^{kk} n_i w_{avg i}$$

Due to the chain rule, differentiating both sides with respect to time gives us the following:

$$\frac{d}{dt} \mathbf{Biomass} = \sum_{I=1}^k n_i \cdot (dw_{avg i} / dt) + \sum_{I=1}^k (dn_i / dt) \cdot w_{avg i}$$

Carrying capacity, as a stable equilibrium point, implies that the change in biomass over time is equal to zero. Examining the above equation shows that this will occur whenever both the sum of $(dw_{avg i}/dt)$ and (dn_i/dt) are equal to 0, or when the sums are of equal magnitude but opposite sign. But each of these rates may depend either on itself or on the other term. The change in numbers may depend on egg production which depends on individual adult

weight, and the change of weight may depend on competition for food which in turn depends on numbers.

2.4.1.3 Carrying capacity for differing life-history strategies

For tractability, many models of carrying capacity have focused on density dependent mortality ($dn/dt = f(n)$). This approach is most appropriate for r-selected species such as anchovies, for whom numerical fluctuations in birth and death rates may fluctuate more than the weight of an individual. K-selected species, consisting of smaller numbers of larger, longer-lived species, have been modeled by life-history tables which take into account both weight and numbers as functions of each other. This requires the collection of data for individual animals—this approach has been used most frequently for marine mammals.

However, recent analyses of the life-history parameters of large numbers of fish species have led some researchers to suggest a third life history strategy which is unique to the ocean (Winemiller and Rose 1992; McCann and Shuter 1997). This strategy, dubbed “periodic,” is a response to environments such as the northeastern Pacific, which are characterized by large-scale cyclic or spatial variation as discussed in Section 2.2.

Under the periodic strategy, fish may concentrate on relatively large rates of somatic growth during poor conditions in order to maximize reproductive output during “bursts” of good conditions. The reproductive bursts may be seasonal, occurring at the single best time of the year, or interannual, if good and bad conditions may be expected to cycle within the lifetime of a single individual. The periodic strategy is predominant among worldwide commercial fish stocks (Winemiller and Rose 1992) including groundfish and salmon, although the semelparous nature of salmon modifies their life history strategy somewhat (McCann and Shuter 1997).

The mathematical models of carrying capacity which have been developed for r-selected and K-selected species may not be appropriate for periodic species—models appropriate to each life history strategy are summarized in Table 2.3 (see Kashiwai (1995) for a review of mathematical models of carrying capacity). If the bursts occur on a regular, seasonal cycle, it is meaningless to average or sum the total growth of the species and call it carrying capacity—it will vary predictably depending on the point of the cycle. Rather, each bottleneck between birth and reproductive burst must be quantified separately. In this case, carrying capacity is not a stable point representing supportable biomass, but the *maximum total production* of a species between its birth and its burst of reproduction.

If the level of production during one cycle affects the level in the next cycle (i.e., a spawner/recruit relationship), carrying capacity in the more traditional sense may be meaningful. However, this carrying capacity represents a summary measure of a *stable periodic cycle* rather than a single stable point. A stable periodic cycle of this type is called a *quasi-equilibrium state*.

No single value in this stable cycle could be considered “carrying capacity” if carrying capacity is defined as an equilibrium point in a dynamic model. However, an intuitive version of carrying capacity can be divined from a quasi-equilibrium state; for example, by defining carrying capacity as the average biomass over some set period of the cycle (such as a year), or defining it as the maximum biomass “exported” from an equilibrium cycle over that time period, such as with salmon returning to spawn.

However, it is important to note that such averaging makes it meaningless to compare directly the carrying capacities of two species, or the carrying capacity of one species with respect to its level of prey. In a cyclical system, the annual average of two processes occurring on different time scales

may be weakly connected if connected, at all: the frequency or phase of the two cycles with respect to each other may be the factor controlling a given seasonal bottleneck. Additionally, if two species competing for the same resource have different cyclical dynamics, quantifying their competition as it occurs through the prey may be next to impossible.

Finally, it should be noted that difference in time scales between species means that more global concepts, such as the carrying capacity of an entire ecosystem given its primary production, are probably not meaningful unless the definition of carrying capacity is so constrained as to be practically useless.

Thus, in order to examine the "carrying capacity" of a periodic species, each feedback loop must be untangled in terms of its time scale, hierarchy, and controlling variables. The data-intensive nature of this operation makes the dynamics of such fish populations difficult to predict, especially if sampling is difficult at critical points in its cycle (such as during winter in the North Pacific).

If there are multiple bottlenecks in the cycle which are represented by multiple feedback loops, the interplay between one and the other may be extremely complex. If positive feedback loops are incorporated, such as accelerating growth due to changing prey, the dynamics may be chaotic and difficult to predict (Rice 1995). In this case, it is worth asking: what form of correlation implies density-dependent competition in the food web?

For periodic species, there may be a correlation between body weight and numbers of fish, implying competition for growth resources. However, correlation with prey resources may be positive, negative, or non-existent, depending on the structure of the food chain. Conversely, it is possible that negative correlation could exist between predator and prey, even in the absence of food competition among predators (Levins and Schultz 1996). This situation is discussed in depth in Chapter 5 for the case of the food web of salmon in the Gulf of Alaska.

2.4.1.4 Summary

In summary, the intuitive concept of carrying capacity has most often been translated in models into a stable point for the state variables of numbers or biomass in a dynamic population equation. A stable point must be maintained by negative feedback in the equation: both negative and positive feedback lie at the heart of the evolution of living systems. Two aspects are important: the time scale of the feedback, and the levels of the hierarchy on which the feedback occurs. The hierarchical nature allows multiple, nested changes, which must be untangled to determine carrying capacity.

However, salmon and other commercial fish species possess a periodic life history strategy which is more suited to defining a stable cycle rather than an equilibrium value. While the term "carrying capacity" is useful in its intuitive sense, the more appropriate question for salmon is "what is the maximum amount of biomass that a salmon cohort may accumulate between birth and reproduction?"

To answer this question, it is not enough to correlate the production of prey and salmon averaged over a set time period. Annual rates of primary or secondary production will not wholly determine a salmon population's growth. The temporal scale of each density-dependent feedback loop must be examined separately and in concert. The concept of carrying capacity is extendable to ecosystems or trophic levels only if the state variables are tightly constrained and the relative frequencies of external and internal variation are examined carefully.

Pacific salmon may be the perfect species for which to explore the concept of carrying capacity as it applies to a periodic species. Their semelparous nature makes their periodicity absolute: a single quantity of salmon enter and leave the ocean each year. Moreover, the land-based nature of data collection for both input (number of smolts entering the ocean) and

output (number of adult salmon returning to spawn) has enabled researchers to collect more data on both ends of their ocean life than exists for most other species.

Careful collection and analysis of salmon during their ocean life therefore gives us the best chance to examine the dynamics in individual feedback loops in this species. Below, I discuss three feedback loops which have been identified as controlling factors in salmon production. This dissertation focuses on attempting to partially integrate these loops into a broader picture of ocean production.

2.4.2 Ocean density dependent processes in salmonids

In the most general models of migration for Gulf of Alaska juvenile salmon, fish enter the ocean each spring and migrate along the North American continental shelf, into the Alaska Current, and westward along the Alaskan coast to the Aleutian Islands before moving south into offshore waters for the winter (Groot and Margolis 1991). During this juvenile coastal-ocean phase, ocean mortality of salmon is thought to be the highest of their ocean life (Hartt and Dell 1986). Environmental variations during the juvenile stage may have the greatest effect on determining the number of salmon which return to spawn each year. These processes may "set" the number of salmon returning each year (Pearcy 1992; Groot and Margolis 1991), given the number of smolts which enter the ocean, although juvenile freshwater processes may be the ultimate arbiter of stock size (e.g., Myers et al. 1998b).

The total ocean area over which salmon spread after leaving the coastal areas will vary by species, stock, and oceanographic conditions. Until their return migrations 1-5 years later, stocks from North America and Asia mix substantially. During this period, when mortality is considered to be relatively low, salmon put on 90-98% of their body weight (Ishida et al. 1998). Variation in

conditions during this latter period will probably affect individual growth weights and final body weights more than in the earlier period.

The appropriateness of a conceptual split between an early high-mortality phase and a later high-growth phase in salmon life history is suggested in a study of sockeye salmon by Peterman et al. (1999), who found that sockeye salmon survival rates were correlated between neighboring stocks but not between distant stocks. This indicates that the factors determining survival were strongest when stocks were relatively segregated, either in the freshwater or in the juvenile stages of their ocean life. On the other hand, a strong correlation in body weight was found between distant stocks, indicating that factors determining adult growth were important later in their life cycle, when stocks were mixed on the high seas.

This partitioning of survival and growth into different phases of the salmon's ocean life results in two bottlenecks which may determine the total production of salmon in a given year. The first, "coastal" bottleneck, may be the result of density-dependent processes that affect salmon survival, while the second, "oceanic" bottleneck, could arise through competition for growth opportunities.

This model is a simplification, as adult mortality may have density-dependent aspects, and the transition between the juvenile and adult phase will differ for many stocks. However, making this distinction between the two phases will make the subsequent analysis tractable.

The two feedback loops are shown in Figure 1.3, labeled with the letter **a** (density dependent juvenile mortality) and **c** (density dependent adult growth). A third feedback loop, labeled **c**, is a positive feedback loop, which is the result of an ontogenetic shift in prey. The body of the original research in this dissertation is a discussion of feedback loops **b** and **c**, which are first reviewed in Section 2.4.3 below and then examined fully in Chapters 3-5. Loop **a**,

representing density-dependent juvenile mortality, is not examined in detail in this dissertation, although it is worth presenting some of its details here, as the outcome of loop *a* is a driving input for loops *b* and *c*, and there have been decadal changes which have affected this density dependent relationship.

Since the 1976 regime shift, the survival rates of Alaskan and Asian stocks of salmon have increased dramatically, while the survival rates of stocks from British Columbia, Washington, and Oregon have gone down significantly. The total number of salmon surviving to return to fisheries and spawning grounds was higher in the 1980s and 1990s than at any other time in recorded history (Rogers 1999). This pattern of survival is similar to that of the zooplankton, which have increased in the Gulf and decreased in the California Current (Francis et al. 1998).

It seems likely, then, that the density-dependent aspect of juvenile survival may result from competition for food. One study of juvenile sockeye salmon suggests that a 50% increase in juvenile body length results in a 400% increase in survival (Burgner 1991). Therefore, the more salmon that exist to consume the food, the smaller they may grow, and the lower their survival may be. It is also possible that independent processes, such as freshwater output, affect juvenile survival (e.g., Cooney 1993; Cooney et al. 1995; Kaeriyama 1996b).

There are two hypotheses for why juvenile growth and survival are linked. First of all, predators take a huge toll on juvenile salmonids, and it is possible that the primary evolutionary pressure on juvenile salmon arises from the need to sustain a rapid rate of growth in order to escape predation—larger juveniles may be more difficult for predators to eat. Secondly, it is possible that salmon must reach a certain “critical size” before the winter period, in order to avoid starvation (Beamish and Mahnken 1999). The study of the juvenile phase

is ongoing in the Ocean Carrying Capacity Program at the Auke Bay Laboratory, National Marine Fisheries Service, Juneau, Alaska.

2.4.3 Adult ocean growth of salmon

Understanding the mechanisms of Pacific salmonid growth in the open ocean is a research priority, as historical studies have shown long-term changes in the final length and body weight of fish in many salmon stocks. Specifically, the body weights of salmon have been shown to be falling in recent decades, in some cases since the 1970s, and in some cases since the 1950s (Ricker 1981; Ishida et al. 1993; Ricker 1995; Bigler et al. 1996).

Falling salmon sizes cause concern both commercially and ecologically. Pound for pound, smaller fish are worth less to humans, both economically and culturally. Moreover, high salmon body weight is strongly linked to high salmon fecundity and spawning success, and thus to the health of salmon populations as a whole (Healey and Heard 1984; Beacham and Murray 1987; Healey 1987; Kaeriyama et al. 1995).

The evidence for density dependence in salmon growth is stronger than evidence for density dependence in salmon survival (Pearcy 1992). Negative correlations between numbers of fish and final adult return size have been found in many stocks in both North America and Asia. This inverse relationship between numbers of salmon and individual body weight, and the positive correlation between numbers and average age-at-maturity, has been shown over long and short time scales. The correlations have been noted mostly in within-species comparisons of pink salmon, sockeye salmon, and chum salmon, the three species that account for over 90% of total salmon production in the North Pacific (Rogers 1999).

Most of the studies have been conducted for individual stocks, so it is not clear if this inverse relationship represents a relationship between or among

stocks. Negative correlations between salmon body weight and population size have been reported since the 1930s for Asian and North American pink salmon (Ishida 1966), and since 1954 for Japanese chum salmon (Kaeriyama 1996a,c). The relationship between numbers and size of Japanese chum has been noted in relation to the extreme increases in Japanese hatchery production during the 1980s (Kaeriyama 1996c).

Rogers (1980) reports similar within stock correlations for Bristol Bay sockeye salmon and chum salmon. Further, Rogers and Ruggerone (1993) report a relationship between numbers and body size of four age classes of Bristol Bay sockeye salmon over the time period 1957-91, and suggest that the slope of the relationship, and thus the carrying capacity of the stock, changed after 1976.

Fewer between-stock comparisons of a single salmon species have been reported. Ishida et al. (1993) analyzed several Russian and Japanese chum salmon stocks and suggested that within-species competition explained 35% of the variation in growth, with the rest explainable by stock-specific or environmental effects. The other exception is North American sockeye. Peterman (1987) found a significant negative correlation between numbers of Bristol Bay sockeye and the size of Fraser River sockeye. McKinnell (1994) and Pyper and Peterman (1999) found significant covariation in body size between the two stocks.

Conversely, several reports prior to the 1980s found positive correlations between salmon numbers and body size (Pearcy 1992 pg. 103). If salmon survival and growth both increase in response to food supply when salmon numbers are low, it is possible that, prior to the 1980s, an increase in food leading to greater juvenile survival would also lead to increased adult body sizes, masking any density-dependent effects.

Sweeping, concurrent body size decreases in many stocks occurred during the 1980s. One survey found evidence of concurrent body weight decreases from 1970 to 1995 in 43 of 45 surveyed salmon stocks (Bigler et al. 1996). In addition, chum and sockeye salmon, with variable ages of maturity, have been coming back older in recent years, suggesting that poorer growth conditions or greater competition require fish to stay at sea longer (Ishida et al. 1993; Kaeriyama 1996c; Pyper et al. 1999). Therefore, the issue has become of greater concern in the last two decades, even as total numbers and biomass of salmon have reached all time highs.

The reason this has been a concern to resource managers is that never before have human actions had the potential for influencing salmon production on such a large scale. Hatchery salmon production has increased dramatically in recent years at the same time that the size-at-age of many salmon species has been declining. In Alaska, Japan, and Russia, hatchery output has increased exponentially since the 1970s (Kaeriyama 1996c; Cooney and Brodeur 1998; Pearcy 1992).

In addition, there has been considerable concern that large-scale environmental changes, most notably global warming, may adversely affect the health of salmon stocks, as warmer waters may limit the range over which salmon can successfully grow, and changes in ocean circulation may affect the supply of salmon prey. In order to place the magnitude of long time-scale global change in context, it is important to understand mechanisms of growth as well as correlations between growth and physical ocean conditions (Hinch et al. 1995; Cox and Hinch 1997; Welch et al. 1998).

It is clear that the climatic changes in 1976 had far-reaching effects in the Gulf of Alaska. The higher survival of salmon between 1976-1998 may exacerbate density dependence later in life; however there is evidence that

density-dependent relationships in salmon growth also change (Rogers 1984). Further, many stocks did not show a body size decrease until the 1980s.

However, some decreasing trends have been reported since the 1950s, independent of increases in population (Ricker 1995; Cox and Hinch 1997). Further, there is evidence of long-term periods of increasing and decreasing fish sizes running back to the 1920s (Ricker 1981). However, as these latter records are taken from fisheries, they may be confounded by the tendency of fisheries to target different sizes of fish over time. Multiple changes since 1976—including increased hatchery production, changes in fishing, and changes in temperature—may confound the analysis of a change in the carrying capacity of a given stock.

Several major hypotheses have been suggested for the decline in salmon sizes in recent years: eight possibilities combining fisheries and environment are discussed by Ricker (1981). The hypotheses concerning size selective fishing may be true for some stocks, but would not be relevant to the general trend of decrease across many North American stocks since the 1980s. Two remaining hypotheses: (1) increased density-dependence due to increases in salmon numbers; and (2) direct environmental changes affecting growth and foraging rates, must be considered to determine when and how growth limitation may be taking place in the open ocean.

2.4.3.1 Are adult salmon food-limited in the ocean? The role of food vs. environment .

Given the large body of evidence for negative correlations between numbers and body weights of salmon, food competition is a likely suspect. Most stocks of North American Pacific salmon, and many Asian stocks, spend part of their life feeding in offshore Gulf of Alaska waters (Table 2.3). The three most numerous Pacific salmon species—pink salmon, sockeye salmon and chum salmon—as well as the less-numerous stocks of coho salmon, chinook

salmon and steelhead feed in this area. Some stocks, such as central Alaskan pink salmon and Fraser River sockeye salmon, put on up to 90% of their body weight in this region while other stocks, for example Bristol Bay sockeye and Asian chum salmon, depend on food from the region for a lesser but still substantial amount of their growth (Myers et al. 1996; Ishida et al. 1998; see Rogers 1986 for an overall review of salmon in the Gulf of Alaska).

Because food overlap is intense in this area, any competition between populations will be most likely to occur in these waters. Because the relatively brief spring and summer maturation portion of the salmon's life cycle accounts for such a large proportion of a salmon's growth, researchers searching for the mechanisms that determine year-to-year variation in salmon body weights have focused on ocean conditions in the final stages of the salmon's life cycle.

However, any attempt to quantify potential between-stock food competition reveals a fundamental paradox in current models of Pacific salmon carrying capacity. The offshore region of the Gulf of Alaska is a highly productive pelagic ecosystem. Calculations of zooplankton biomass and production, when compared to demands made by foraging salmon, invariably indicated a surplus of available food. As a result of models constructed in the 1970s, Favorite and Levaestu (1979) concluded that the North Pacific could sustain ten times the 1970s standing stock of salmon.

Yet during the 1980s and 90s, when the system contained only twice the total biomass examined by Favorite and Levaestu, salmon sizes declined. Conservative production estimates, using observed 1980s and 1990s zooplankton and salmon biomass, indicate that adult salmon consume between 0.04% and 0.10% of available annual zooplankton production (Brodeur et al. 1999). Since salmon are the dominant pelagic nekton in the region, it seems unlikely that this level of consumption would lead to competition for prey and thus density dependent growth.

Studies relating zooplankton biomass or production to growth are mixed. Cooney and Brodeur (1998) found no relationship between zooplankton and body size in Prince William Sound pink salmon, while Peterman (1987) found that, if the total number of Fraser River pink salmon were divided by the annual cumulative available zooplankton measured at Station P, the relationship between fish per zooplankton and fish body weight was significantly negative with an r^2 of 0.74 between the years 1957-77.

Indirect evidence suggests that between-species competition for food occurs in the open ocean. Studies of the diets of pink and chum salmon in the Bering Sea show that during years of high pink abundance, chum salmon switch diets from energetic zooplankton (favored by pink) to less-energetic gelatinous material (Tadokoro et al. 1996). The fact that this adaptation exists, and that chum salmon have evolved a gut specialized to digesting this lower-energy food, suggests that between-species competition has been a major evolutionary consideration for salmonids (Welch 1997).

To reconcile this lack of direct evidence of prey limitation with the observed lower salmon growth during periods of high salmon numbers, several hypotheses have been put forth:

- First, it is possible that density-dependence is only a factor in the last few weeks of ocean growth, as salmon are once again entering coastal waters (Rogers and Ruggerone 1993). However, this does not explain the correlation in body size seen between widely separated stocks (Peterman et al. 1999).
- Second, competition for food in the winter may be a limiting factor to overall growth. Information on the winter feeding of salmon is limited, and zooplankton standing stock decreases substantially in the winter (Boyd et al. 1995a). Competition between salmon may be most intense during this time.

- Third, it is possible that physical factors such as water temperature, which vary between climatic regimes, may directly affect growth rates by influencing salmon physiology (c.f. Murphy 1995). If this last theory is true, the apparent density-dependence is not a direct cause and effect, but rather two independent aspects of climate change affecting fish production at different times.

This third hypothesis has garnered attention in recent years, especially in light of the threat of global warming. Sea surface temperatures in the Gulf of Alaska have increased since the 1980s, at the same time that salmon numbers have increased and salmon body weights have gone down. Some multiple regression analyses have found that salmon numbers and sea surface temperatures are independently and negatively correlated with salmon body size. Significant multiple regressions have been reported in chum salmon (Ishida et al. 1993) and Bristol Bay/Fraser River sockeye salmon (Rogers and Ruggerone 1993; Hinch et al. 1995; Adkison et al 1996; Cox and Hinch 1997; Pyper and Peterman 1999).

These multiple regressions bring up interesting possibilities in terms of carrying capacity. The physiological connection between salmon growth and water temperature is complex and nonlinear. While temperature may not have a large direct effect on instantaneous growth rates, it may change the profitability of foraging under different levels of competition. The direct physiological connection between water temperature and salmon feeding may cause density-dependent relationships to change in unpredictable ways with each regime shift.

To assess this possibility, the physiological effects of water temperature on salmon must be compared to the range of natural variability of food resources. A type of model used in this dissertation, bioenergetics, predicts growth rates based on the temperature and the amount of food eaten by a fish,

calibrated by laboratory experiments (Hewett and Johnson 1992). Salmon growth is a complex, nonlinear function of the type and amount of food eaten, energy expended to catch the food, and water temperature. In some cases, warmer temperatures may be better or worse, depending on the amount of food available and the effort required to obtain such food.

Finally, it is necessary to consider the food web as a whole. All food webs contain simplifications and aggregations of multiple trophic levels. Simplifications are necessary in order to make food web analysis tractable. Salmon diet (reviewed in the next chapter) may involve complex interactions between multiple prey types: before drawing conclusions with correlation between zooplankton and salmon, it is important to consider if the correlations capture the behavior of all of the important prey types. If salmon shift their feeding from one trophic guild to another as they grow, relatively minor and subtle density-dependent growth effects in early life history may magnify to large differences in adult body size.

2.4.4 Summary

Is there an overall limit, or carrying capacity to the amount of salmon that the Gulf of Alaska can produce? If so, is the ecosystem near that limit, and are hatchery-produced fish depleting Alaska Gyre food supplies, and thus having adverse effects on the overall ecosystem? And how do cycles in climate control affect carrying capacity from year to year?

It is important, in answering these questions, not just to find correlations between environmental conditions and biological responses, but to understand the mechanisms behind them. The fundamental nature of fluctuations in the ocean has been characterized as being consistent with a type of variation known as "red noise" wherein the amplitude of variation is inversely proportional to its frequency (Steele 1991). In other words, the longer time period over which you look for change, the greater the changes you observe. One

consequence of this is that a correlation between, for example, sea surface temperature, or a test fishery, and actual fish biomass may suddenly and dramatically change: such a change may have led to the failure of managers and scientists to predict low runs of Bristol Bay sockeye salmon in 1997 and 1998 (Kruse 1998).

Without understanding the mechanisms behind such a change, there is little hope of predicting or even recognizing it once it occurs, especially if the unexplained mechanisms between the environment and fish are moderated or amplified by the presence of feedback.

Synthetic correlative models suggest that both water temperature and density dependence are important factors for salmon growth. Both may have had a role in the decreasing size of salmon in the 1980s and 1990s. Repeated reports of negative correlation between the population size (in numbers of fish) and individual body size of specific salmon stocks imply that density-dependent adult growth occurs in the open ocean. However, attempts to pinpoint density-dependent mechanisms based on resource limitation have turned up mixed results. Specifically, comparisons of available forage in ocean waters with the metabolic demands of growing salmon have generally implied that there is "plenty" of food available for salmon, and that density-dependent observations must either be coincidental, inverse correlates of climate variation, or the results of near-shore processes occurring during the final weeks of salmon migration.

Ocean carrying capacity, as an intuitive concept, is an important management issue. Salmon management policies should be reviewed in light of this limitation especially as hatchery fish, and smaller fish in general, are seen as less valuable both commercially, ecologically, and culturally to the peoples of the North Pacific rim.

The "carrying capacity" of salmon, as measured by the total biomass returning to spawning grounds and fisheries each year, must be considered not

only in terms of the number of fish, but also in terms of the size and health of individual fish. In addition, if smaller stocks are harmed at the expense of larger stocks, a "total carrying capacity" based management approach might not make sense (Moberg et al. 1997). The consideration of ocean conditions in salmon management may require a more flexible style of thought (Bisbal and McConaha 1998).

High hatchery production, which pumps tremendous numbers of juvenile fish into the ocean, may result in larger numbers of smaller, less healthy and less commercially valuable fish, even during times when the ocean generally favors salmon growth. As salmon stocks have increased in number, salmon adult body sizes have generally decreased, and the age-at-return in many stocks has risen. This may be a contentious issue in terms of hatchery production, as an increasing proportion of overall salmon stocks has been made up of lower commercial value hatchery fish.

Correlations have also been drawn between water temperature and salmon size and distribution. While these relationships may have some predictive strength, it is important to understand the mechanisms through which environmental variation affects fish, so as to be able to understand the ecosystem's potential for change.

Studies of salmon growth on the open ocean have, to date, generally lacked the data to model the complexity of variation in the food web in the open ocean. In one sense, the generalist nature of salmon, feeding as omnivores on multiple trophic levels, has been taken to be a stabilizing influence on salmon growth. However, if the trophic levels differ substantially in nutritive content, distribution, or trophic linkages, variation in salmon prey relationships across time and space could play a large role in determining salmon growth.

The overall increase in North Pacific salmon production since 1976 raises some serious concerns. First, the prospect of a reverse regime shift, and

return to lower salmon production, is both likely and important to predict. Second, if long-term cycles between good and bad ocean years are predictable and independent of fisheries limits or freshwater enhancement efforts, these cycles should be incorporated into the philosophy of salmon management.

Table 2.1. North Pacific oceanographic domains and boundary definitions.

MAJOR DOMAINS	REGIONS WITHIN DOMAINS	BORDER DEFINITIONS
SUBTROPICAL DOMAIN	STG: Subtropical Gyre	STG / STTD: 35.0psu isohaline reaches surface
	STTD: Subtropical Transition Domain	STTD / TZ: 34.6psu isohaline reaches surface
TRANSITION ZONE	<i>Subarctic Boundary (SB) occurs in TZ where 34.0psu isohaline reaches surface</i>	
SUBARCTIC DOMAIN	SATD: Subarctic Transition Domain	TZ / SATD: 33.8psu isohaline reaches surface
	SAG: Subarctic Gyre	SATD / SAG: 33.0psu isohaline reaches surface
WHITHIN NORTH-EASTERN SUBARCTIC DOMAIN	SC: Subarctic Current	SC/R: 4°C isotherm rises from below 300m in the SC (south) to above 100m in Ridge
	Ridge/WSW: Ridge Domain influenced by western subpolar waters	Tmin: Latitudinal sea surface temperature minimum (summer)
	Ridge/Gyre Ridge Domain influenced by central gyre waters	R/AS: 4°C isotherm descends from above 100m in Ridge (south) to below 300m
	AS/C: Alaska Stream or Current	

Table 2.2. Frequencies of variation found in time series analyses of climatic and biological variables.

- (a) From Ware (1995) analysis of Gulf of Alaska wind speed, British Columbia air and sea temperatures, and sea level pressure in the Gulf of Alaska. Columns indicate four modes of oscillation—quasi biennial (QBO), El-Nino Southern (ENSO), Bidecadal (BDO) and very low frequency (VLF). Numbers indicate period of detected cycles in years.

	QBO	ENSO	BDO	VLF
WIND	2	5.5	21	50
BC Air Temp	2-3	5-7	25	50
BC Sea Temp	3	5	22	72
SLP at 55, 155	2.6	6,7	13.3	

- (b) From Conversi and Hameed (1997) analysis of zooplankton density at Station P and the North Pacific Index. Percentage indicates percent of variation explained by each frequency. The time series was not long enough to detect BDO or longer period cycles.

1956-1980 years)	(24 ANNUAL & Harmonics	Pole (1.1 years)	Tide	QBO (2.4 years)	"ENSO" detected
Zooplankton	57%	5.9%		1.1%	
NPI	60%	2.3%		0.67%	

Table 2.3. Carrying capacity modeling techniques for r-selected, K-selected, and periodic species.

Property	r-selected	K-selected	Periodic
Growth rate	Rapid, emphasizes numerical growth	Slow, emphasized individual development	Slow development followed by "bursts" of numerical growth (spawning)
Modeling techniques	Biomass-dynamics models with varying carrying capacity (dynamic habitats)	Life-history tables, tracking of individuals	Seasonal processes—stock/recruitment and density-dependent growth
Marine examples	Anchovies, sardines	Sharks, marine mammals	Gadidae, salmon

Table 2.4. Stocks of salmon in the offshore Gulf of Alaska waters. *Oncorhynchus* species tagged in the region shown in Figure 1.1 have returned to fisheries in the areas indicated below. Winter data is poor due to low tagging effort, while fish from Asian areas such as Russia may be underrepresented due to low tag recovery rates. Data is from Myers et al. (1996). * indicates presence, ** indicates hypothesized primary distribution area the majority of species and stocks.

	Prior to spring of maturation	Spring of maturation year	Summer of maturation year
Western Alaska (Bristol Bay)	*	**	*
Central Alaska	**	**	**
Southeast Alaska	**	**	**
British Columbia	**	**	**
Washington	*	*	*
Oregon, California	*	-	-
Japan	*	*	-
Russia	*	*	-

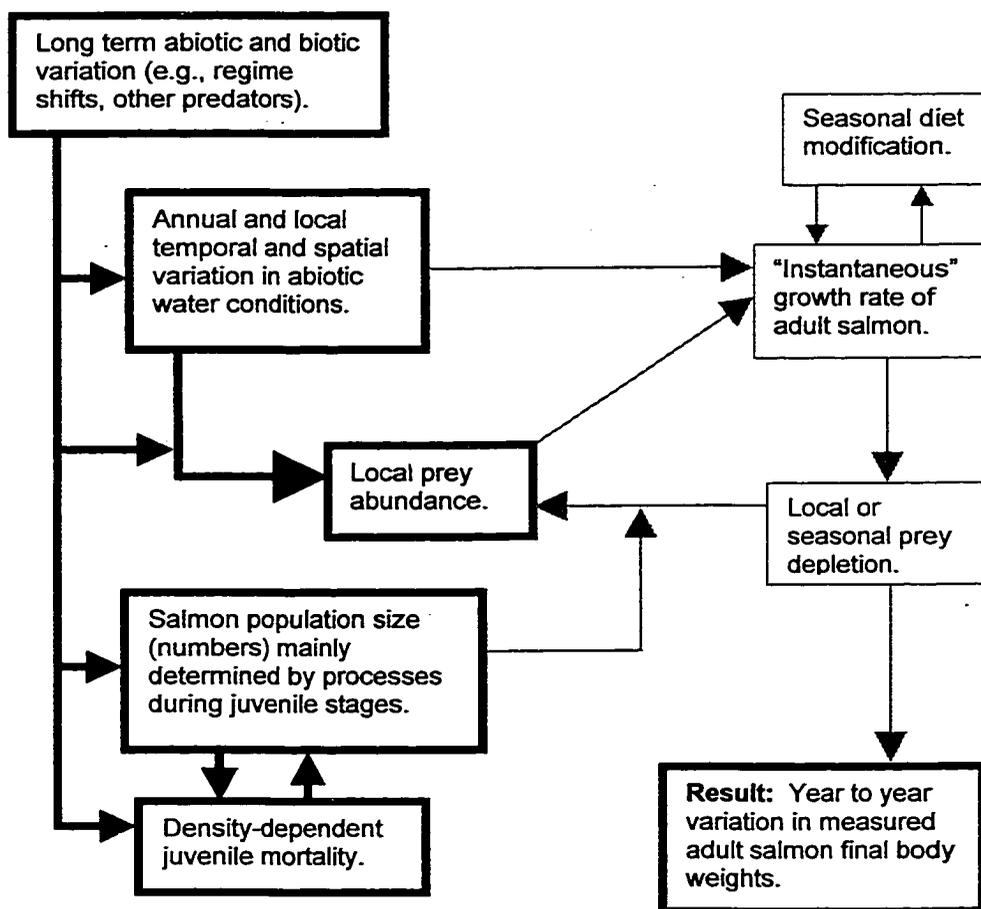


Figure 2.1. Aspects of salmon carrying capacity reviewed in Chapter 2 are shown by bold lines. See Chapter 1 for an explanation of this conceptual model of salmon carrying capacity.

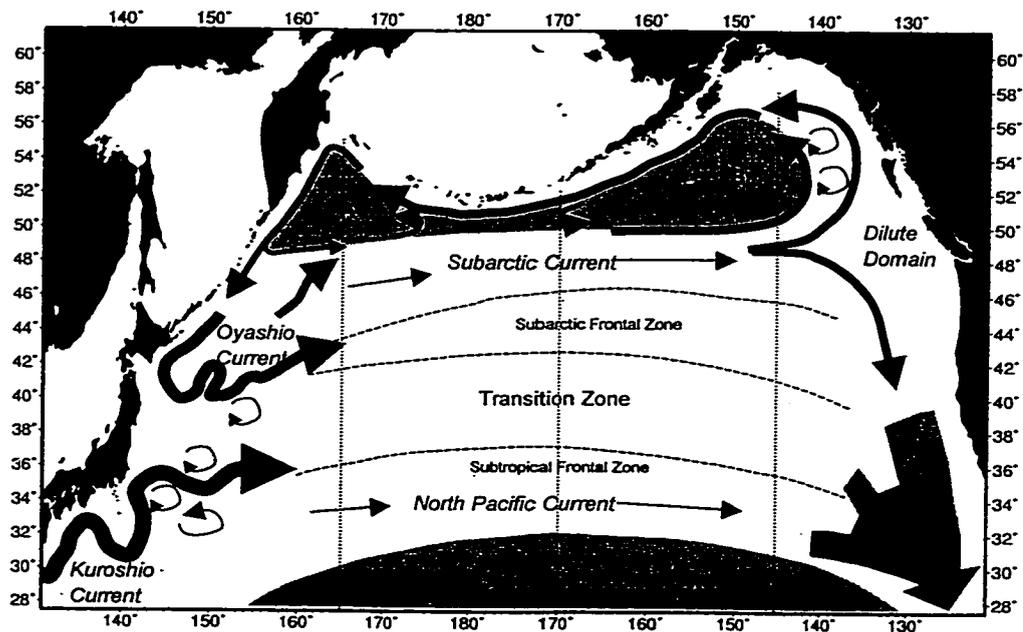


Figure 2.2. Oceanographic regions of the North Pacific. Arrows indicate current flow: the width of arrows shows the surface extent of currents rather than the volume of flow. The names of some currents and the circulation in marginal seas is omitted for clarity. (A) and (B) refer to the Western and Eastern (Alaska) Subarctic Gyres, respectively. Dashed lines suggest the approximate locations of transitional fronts. The three north/south dotted lines indicate the 145°W, 170°W, and 165°E transect lines shown in Figures 2.3-2.5.

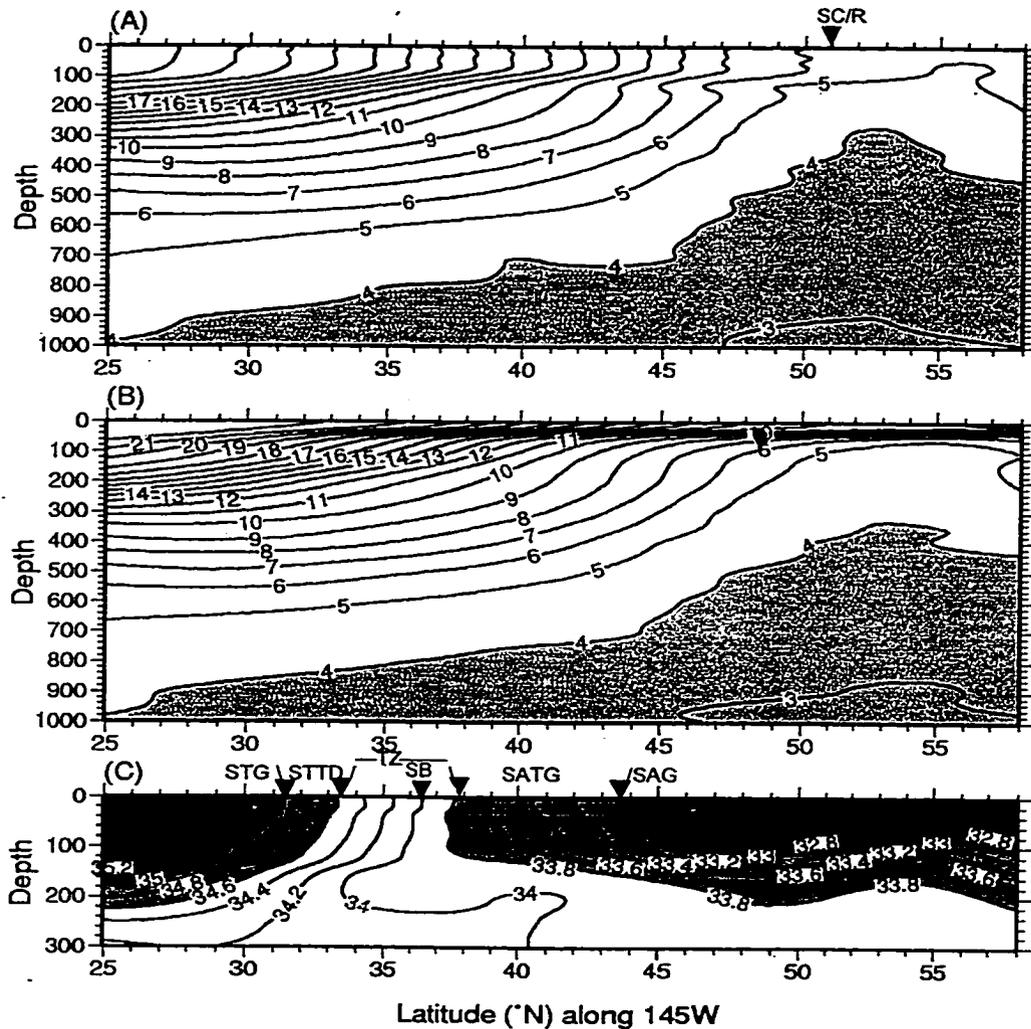


Figure 2.3. A transect along 145°W of the upper 1000m. (A) water temperature (°C) in December; (B) water temperature (°C) in July; (C) year-round upper 300m salinity (practical salinity units). Conditions represent long-term averages (World Ocean Atlas 1994). Shaded regions in (A) and (B) show water colder than 4°C. Dark shaded areas in (C) are the subtropical (south) and subarctic (north) gyre regions, while light shaded areas show subtropical and subarctic transition (frontal) domains. White area in (C) indicates the Transition Zone. Specific boundaries are shown between selected regions listed in Table 2.1.

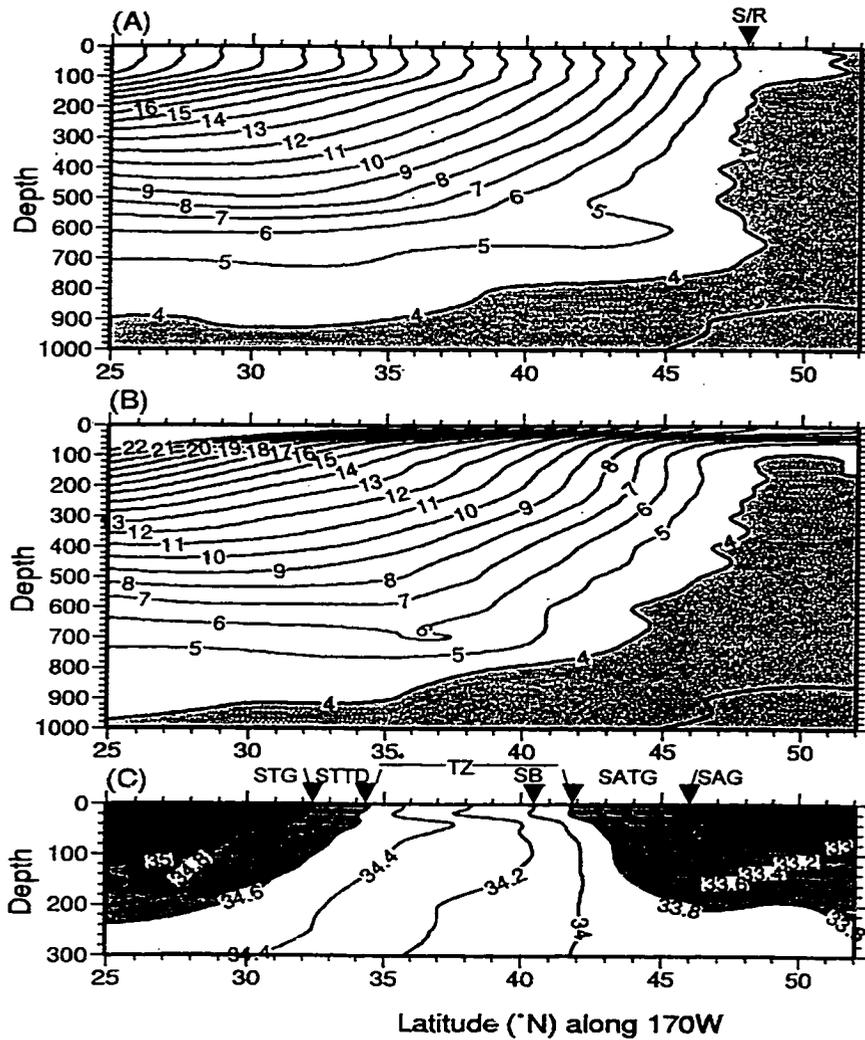


Figure 2.4. A transect along 170°W of the upper 1000m. (A) water temperature (°C) in December; (B) water temperature (°C) in July; (C) year-round upper 300m salinity (practical salinity units). Conditions represent long-term averages (World Ocean Atlas 1994). Shaded regions in (A) and (B) show water colder than 4°C. Dark shaded areas in (C) are the subtropical (south) and subarctic (north) gyre regions, while light shaded areas show subtropical and subarctic transition (frontal) domains. White area in (C) indicates the Transition Zone. Specific boundaries are shown between selected regions listed in Table 2.1.

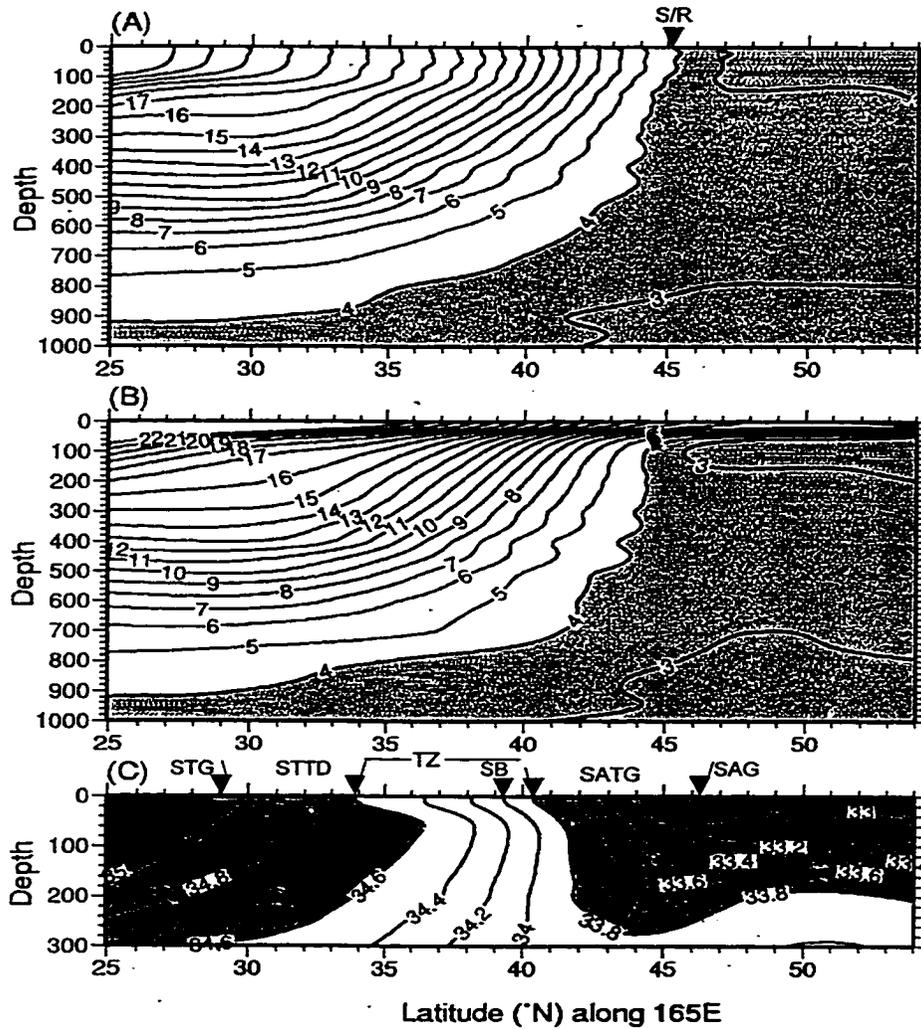


Figure 2.5. A transect along 165°E of the upper 1000m. (A) water temperature (°C) in December; (B) water temperature (°C) in July; (C) year-round upper 300m salinity (practical salinity units). Conditions represent long-term averages (World Ocean Atlas 1994). Shaded regions in (A) and (B) show water colder than 4°C. Dark shaded areas in (C) are the subtropical (south) and subarctic (north) gyre regions, while light shaded areas show subtropical and subarctic transition (frontal) domains. White area in (C) indicates the Transition Zone. Specific boundaries are shown between selected regions listed in Table 2.1.

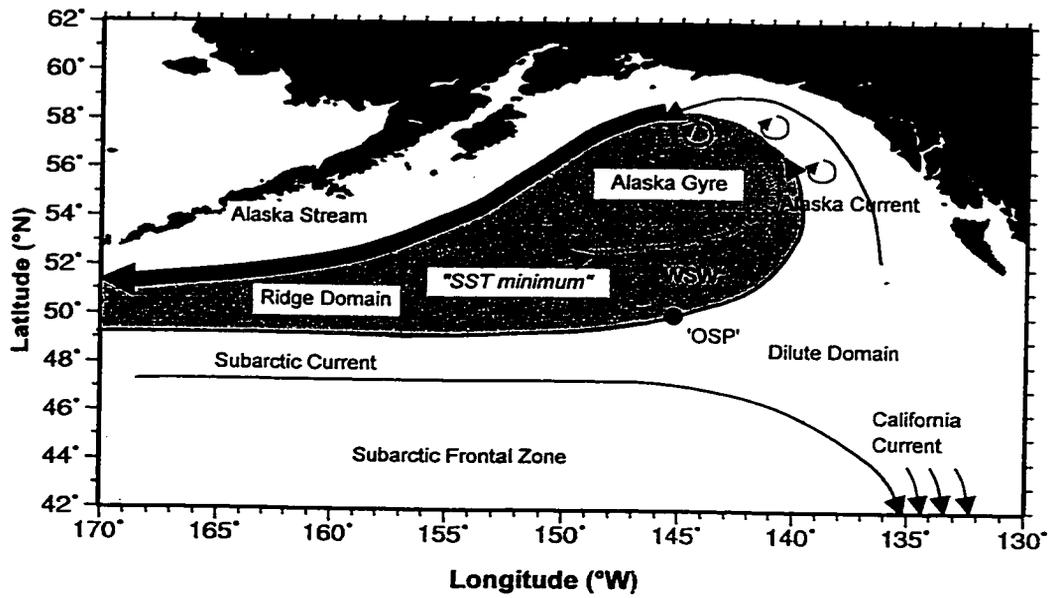


Figure 2.6. Oceanographic regions in the northeastern Pacific. Arrows show current movement while shaded areas show oceanographic regions. Boundaries between regions are general and not specific to the locations shown on the map. See text for defining characteristics of the regions.

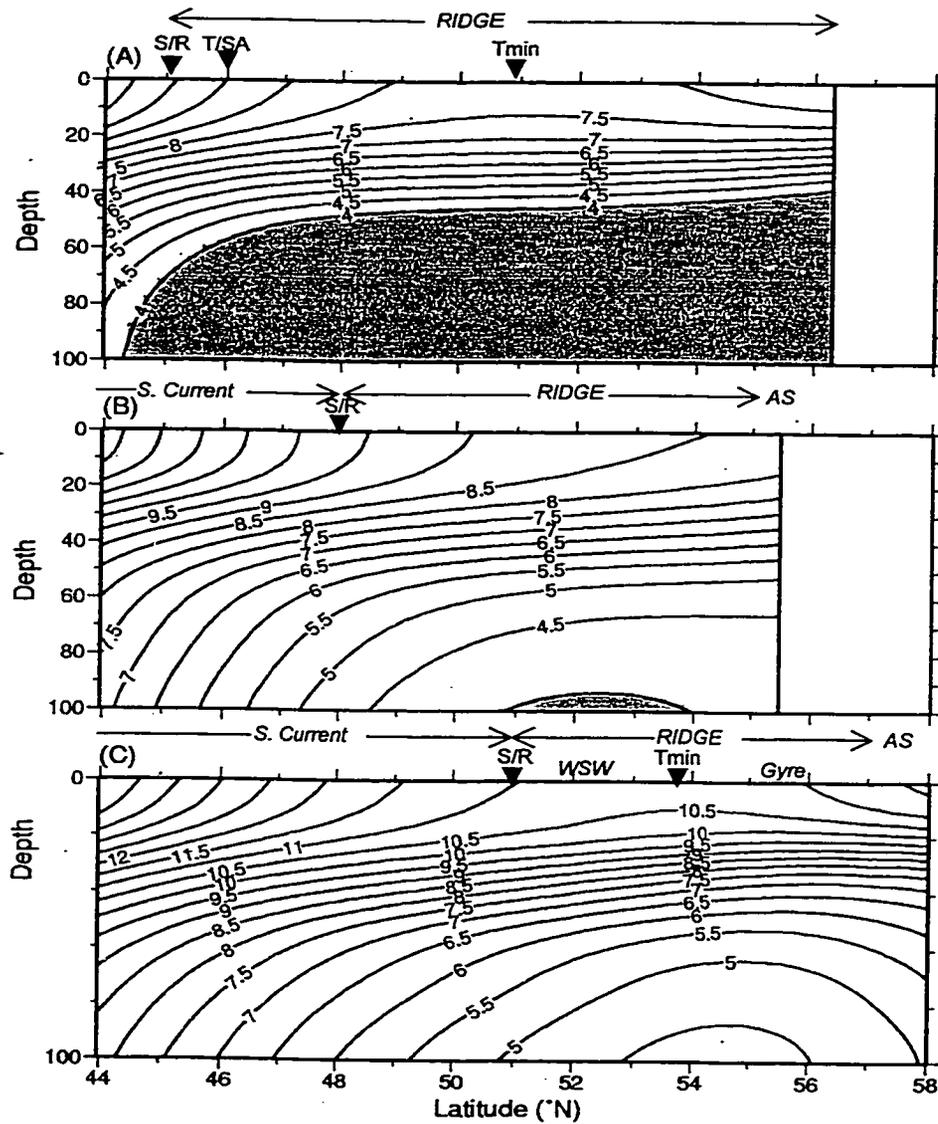


Figure 2.7. An enlargement of July sea surface temperatures from Figures 2.3-2.5 from 44°-58°N latitude, for (A) 165°W; (B) 170°W; (C) 145°W. Specific boundaries are shown between selected regions listed in Table 2.1.

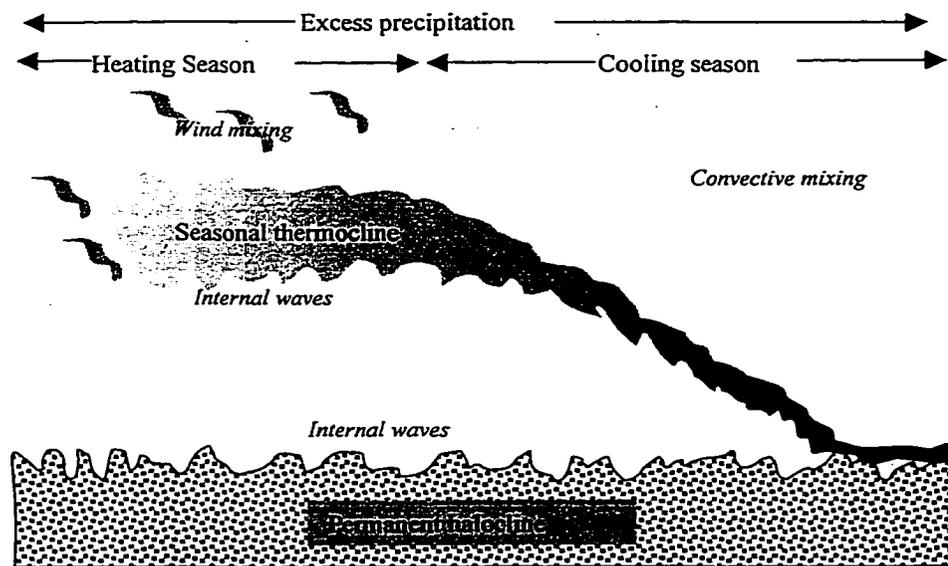


Figure 2.8. The seasonal cycle of the northeast Pacific water column near Ocean Station P, showing changes in the seasonal mixed layer. After Tully (1965).

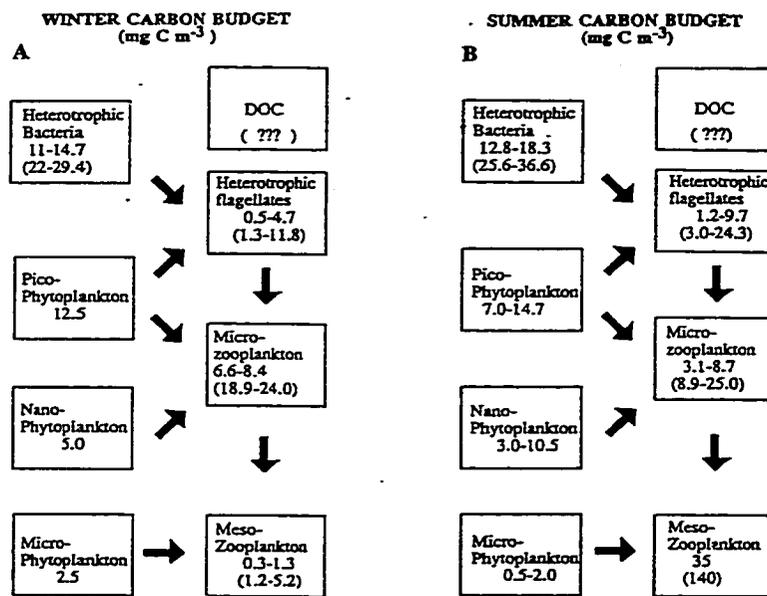


Figure 2.9. Autotrophic and heterotrophic production in the Alaska Gyre food web leading to mesozooplankton, in (A) winter and (B) summer, from sampling near Ocean Station P. Values in boxes represent 0-80m standing stock, while numbers in parentheses show the relative carbon requirements for each stock (assuming identical turnover times). Modified from Boyd et al. (1995a).

3 Micronektonic squid in the diet of northeastern Pacific salmon

3.1 Introduction

Many stocks of Pacific salmon returning to North American and Asian fisheries and spawning grounds put on a large proportion of their body weight in the offshore, or oceanic region of the Gulf of Alaska (Figure 1.1). In this broad area, between April and August during their final year at sea, an individual North American salmon may put on 1000-1500 g of somatic and gonadal growth, or 50-70% of its final adult weight (Ishida et al. 1998). Therefore, variation in the food web dynamics of this region may have a profound effect on salmon growth and migration patterns.

In this chapter, I re-analyze data from food habits studies conducted in the 1950s, 1960s, 1980s and 1990s in order to bring more detail to the geographic and seasonal changes of squid in the salmon's diet, and to elucidate the relative importance of salmon body size for determining foraging response and different densities of squid in the surface waters. I analyze micronektonic squid abundance through the re-examination of stomach contents data from over 11,000 pink, sockeye and coho salmon caught in the offshore Gulf of Alaska. This analysis is structured around two issues:

1. I consider the foraging behavior and trophic position of oceanic pink, sockeye, and coho salmon as a function of body size, especially for maturing fish between April and August. My goal is to describe the changing functional response between salmon and squid, given salmon species and body weight (Figure 3.1).
2. After correcting for the body weight and salmon species biases, I use the binary presence/absence data for squid to provide an index of squid

density at each sampled location. In considering the statistical design, my hope is to develop an index that, for a reasonable range of squid abundance, represents a catch-per-unit-effort which is proportional to actual squid density.

These analyses set the stage for later chapters, in which I describe and present data on the local interactions between mesozooplankton, squid and salmon in the Gulf of Alaska (Chapter 4), and on the implications of squid variation on the bioenergetic growth potential of salmon in the ocean (Chapter 5). The results from both of these modeling exercises lead to predictions of ecosystem and salmon carrying capacity changes in response to climate changes at the population level.

3.1.1 The food habits of adult salmon in the northeastern Pacific ocean

Pink salmon (*O. gorbuscha*), sockeye salmon (*O. nerka*), chum salmon (*O. keta*) and coho salmon (*O. kisutch*) are the most abundant salmon in the oceanic waters of the Gulf of Alaska. These four species are the most numerous Pacific salmon overall, making up over 99% by numbers of the estimated 1991-97 North Pacific salmon catch and escapement (Rogers 1999). In Gulf of Alaska research gillnet fishing between 1993-98, these four species represented 97% of salmonids caught during surface operations (0-10 meter depth). Chinook salmon (*O. tshawtscha*) and steelhead trout (*O. mykiss*) made up the remaining 3% of salmonids caught during this time period (Myers et al. 1998a).

Previous studies of the food habits of post-juvenile salmon (ocean age .1 or older) in the offshore waters emphasize that salmon are generalists, feeding on multiple trophic levels of mesozooplankton and micronektonic fish and squid (Figure 3.2; Allen and Aron 1957; Ito 1964; LeBrasseur 1966, 1972; Pearcy et

al. 1988). However, the relative magnitude of the flows represented by each arrow in Figure 3.2 may vary substantially in time, space, and with the species and body weight of the salmon.

Zooplankton and micronekton communities are patchy and may vary substantially from region to region. It is not practical or necessary to track the variation in each genus of prey when considering the effect of variation on salmon growth. However, oversimplification is not desirable if variation in the food web will create differing opportunities for salmon. The degree of food web complexity used in analysis should reflect differences in the cost and benefits of foraging and digestion and the flow of energy in the food web as a whole. This suggests dividing prey into differing guilds based on both nutrition and trophic level.

3.1.1.1 Defining prey guilds by foraging modes

Salmon foraging modes, trophic level, and nutrition are tightly linked. Experiments and models of fish foraging behavior consistently define two types of feeding modes in fish: planktivorous and piscivorous. Piscivorous animals in the open ocean are more appropriately called "nektivorous," as piscivory may include the consumption of squid and other nekton.

The difference in foraging behavior, rates, and strategies required for catching drifting plankton versus catching free-swimming nekton have been shown repeatedly, especially for predators in lakes (see Breck (1993) for a review). One critical difference between the two foraging modes is the importance of predator gape in determining foraging success (Table 3.1). Piscivorous fish swallow large prey whole, and therefore are limited to a maximum prey size by their gape.

A third mode of foraging, on gelatinous zooplankton such as salps and ctenophores, is little explored. Gelatinous prey are extremely low in caloric

content, and may digest extremely quickly in the gut, thus making their presence difficult to detect. The size of gelatinous species may make gape limitation and contrast important in determining consumption rates, but their free-swimming nature would make search rates for gelatinous zooplankton more like other plankton.

Based on this difference in foraging modes, salmon prey in this dissertation are first divided into 3 categories: nekton, zooplankton, and gelatinous zooplankton. Further, nekton are divided into fish and squid, due to their differential geographic distribution. While fish are extremely important prey items for salmon in coastal waters, they are less numerous in salmonid diets off of the continental shelf (LeBrasseur 1966).

It is difficult to decide how mesozooplankton should be subdivided for analysis. Zooplankton found in salmon stomachs in the Gulf of Alaska include copepods, euphausiids, pteropods, amphipods, decapods, polychaetes, and chaetognaths (Pearcy et al. 1988). Based on size and energy content, copepods and pteropods are the smallest and least energy-dense, while polychaetes and chaetognaths are the largest; therefore these have been placed in separate categories.

Euphausiids and amphipods, however, may vary in size and energy content between the two groups. This variation may be by species or maturity status. Based on visual observations of dominant prey sizes during the 1990s, I placed these species with the smaller mesozooplankton. While Pearcy et al. (1988) emphasize the importance of adult euphausiids (krill) in salmon diet, there is not enough distinct data to consider them separately from the other plankton.

The five categories of prey in the offshore Gulf of Alaska distinguished in this dissertation are shown in Table 3.2 and are as follows:

1. Mesozooplanktonic species of crustacea, mollusca, and larval fish. This includes copepods, pteropods, juvenile and adult euphausiids, amphipods, larval fish, larval decapods, and larval cephalopods. Their defining characteristic is their size of <2 cm total length, although some euphausiids and amphipods found in salmon stomachs may occasionally exceed this length. Traditionally, smaller mesozooplankton are called "herbivorous" although they are primarily feeders on microzooplankton in the Gulf of Alaska.
2. Gelatinous zooplankton, primarily salps.
3. Micronektonic (non-larval) fish. Threespine sticklebacks (*Gasterosteus aculeatus*) and myctophids are the two most common taxonomic groups found, with a size range of 2-10 cm.
4. Micronektonic squid of the family Gonatidae. In the offshore Gulf, the most abundant of the squid species is *Beryteuthis anonychus*, making up over 90% of non-larval squid found in salmon stomachs.
5. A tiny percentage of the remaining salmon food in this region includes the larger "carnivorous" zooplankton such as polychaetes, pinnaed shrimp, and chaetognaths. These species do not occur in salmon stomachs in high enough quantities in the Gulf of Alaska to be included in analyses in this dissertation.

Salmon may be either planktivorous or piscivorous. Their foraging strategy will vary by salmon species, body size, geography, season, and prey abundance.

The trophic triangle between salmon, squid, and zooplankton may be a key structuring element of the ecosystem with respect to salmon growth and carrying capacity. Squid are potentially both a competitor to and a food source for salmon. Adult squid are generally higher in caloric density than are zooplankton (Table 3.2), while at the same time consuming lower trophic level

resources. Therefore, squid in salmon foraging areas may compete with smaller salmon which are unable to consume squid, and at the same time provide a high energy food source for larger salmon. The type of species interaction is known as intraguild predation (Rice 1995), and may lead to complex interactions between species.

Several food web models have been constructed to compare zooplankton production to salmon production for the Gulf of Alaska (e.g., Favorite and Levasteau 1979; Sanger 1972). More recently, individual-based models which attempt to link zooplankton density directly to salmon growth have also been constructed (Rand et al. 1997). Due to paucity of information on squid abundance, none of the quantitative approaches have closely examined the interaction between the two distinct trophic levels of salmon prey.

3.1.2 Qualitative description of variation in salmon prey across the subarctic North Pacific

3.1.2.1 Variation in diet between salmon species

Ito (1964) and LeBrasseur (1966) summarize some of the between-species differences in summer salmon prey in the northeastern and northwestern Pacific Ocean. They found that pink salmon and sockeye salmon are the most opportunistic species with regard to trophic level, feeding on squid, fish, and several families of mesozooplankton shown in Figure 3.2. Coho salmon specialize on squid. Steelhead and chinook also feed on this higher trophic level. Fish, while present in coho, chinook, and steelhead stomachs, or in greater quantities near the continental shelf, are less common in salmon diets in the Gulf of Alaska. This general food web has been confirmed by studies in the 1980s (Pearcy et al. 1988) and the 1990s (Myers et al. 1998a).

Chum salmon possess a radically different feeding ecology, consuming very little squid while feeding on gelatinous zooplankton and mesozooplankton.

It has been suggested that the chum's specialized gut is adapted to feed on the lower-energy gelatinous material, and it is possible that competition for food between salmon species has led to this adaptation (Tadokoro et al. 1996, Welch 1997). A stable isotope analysis conducted on fish and prey from this area generally agrees with this trophic partitioning (Welch and Parsons 1993).

3.1.2.2 Geographic variation in summer salmon diet from west to east

Salmon prey varies from west to east across the Pacific, and also by the oceanic domains described in Chapter 2 (Table 3.3). In the northwestern Pacific Gyre, pink and sockeye consume similar quantities of fish, squid and euphausiids; coho diet is predominantly squid, and chum diet is mostly pteropods and euphausiids (Ito 1964). Allen and Aron (1957) report that copepods made up over 50% of sockeye and pink salmon diets in this area.

Myers et al. (1998a), describe food habits in the central North Pacific, along 180° longitude, for the months of June and July, from 1991 to 1998. They subdivide analyses into Transition Zone, Transition Domain, Subarctic Current, Ridge Domain, Alaska Stream and central Bering Sea waters (Table 2.1). Only coho and chum were captured in the Transition Zone; in the Transition Domain, steelhead and pink were also captured; in the Subarctic Current, all species of salmon except sockeye were plentiful. In the Ridge Domain and Alaska Stream, coho, chinook and steelhead were less common, but sockeye, chum and pink were plentiful. In contrast, in the Bering Sea, sockeye, chum, pink and chinook salmon were found, whilst coho and steelhead were rare.

In the Transition Zone, coho fed entirely on fish, while chum fed mostly on gelatinous materials, with some fish in their diets. In the Transition Domain, chum fed on gelatinous zooplankton and chaetognaths, coho salmon diet was almost entirely squid, with some fish and crustaceous zooplankton included. Pink salmon have a very diverse diet here, feeding on mesozooplankton, chaetognaths, squid and fish. In the Subarctic Current, the rarer sockeye fed

almost entirely on squid, as did pink, coho, chinook and steelhead, although steelhead also fed on fish and pinks also fed on mesozooplankton. Chum continued to feed almost entirely on gelatinous material and chaetognaths.

In the Ridge Domain, sockeye, chum and pink feed largely on the mesozooplankton groups of euphausiids, copepods, amphipods and pteropods, although some squid were present in sockeye and pink diets. In the Alaska Stream, the diets of sockeye, pink and chum were also diverse among mesozooplankton, squid and fish. Finally, in the central Bering Sea, sockeye and pink fed on mesozooplankton, squid and fish in similar quantities, while chum additionally fed on gelatinous material. Euphausiids were the dominant mesozooplankton. Chinook diets were similar portions of euphausiids, squid and fish. It should be noted that squid in the Bering Sea and northwestern Pacific Ocean were probably not the monoculture of *Berryteuthis anonychus* observed in the northeastern Pacific.

LeBrasseur (1966) divides the Gulf of Alaska into the following sections: coastal, Alaska Stream, offshore sub-arctic and transitional waters. In the coastal Gulf of Alaska, fish and euphausiids were principal prey items of all sampled salmon species. However, in the Alaska Stream, fish were predominant, although chum were also reported to consume pteropods, while in subarctic waters, all species except chum consumed squid as their primary diet. In transitional waters, by contrast, feeding was poorer, and consisted primarily of euphausiids and amphipods for pink and sockeye, and squid for coho. In these studies, material from chum stomachs was mostly unidentifiable.

Pearcy et al. (1988) further subdivide the Subarctic Region, as defined by LeBrasseur, into the Ridge Domain and the Subarctic Current. They describe the food habits of pink, sockeye and coho in the Subarctic Current as being rich in squid, while pink and sockeye diets in regions north of approximately 53° N are dominated by zooplankton. Myers et al. (1998a)

confirm this general pattern of squid being plentiful in the area between 49-52° North. The distinction between Ridge Domain and Subarctic Current feeding habits is further explored in Chapter 4.

It should be noted that Percy et al. (1984) and Davis et al. (in press) found that time of day was an important factor in determining salmon prey type in the Gulf of Alaska and the Bering Sea. This, along with the general patchy nature of zooplankton, may add complexity to the description above.

3.1.2.3 Variation in diet based on salmon size, age, and season: implications of the triangle

Seasonal variation in salmon prey is considerable, but few studies have been conducted in the winter and early spring in the North Pacific. LeBrasseur (1972) described a seasonal pattern in the Gulf of Alaska whereby copepods were dominant in pink, sockeye and chum diets in the spring, being progressively replaced with higher trophic levels in the summer. The paper further reported the importance of salmon body size in determining squid consumption, mentioning the qualitative observation that larger salmon ate more squid, especially in sockeye and pink salmon. Percy et al. (1988) also note this difference in pink and sockeye diets by body size. As multiple ocean age classes of sockeye and chum are of different sizes, the diet partitioning may occur by ocean age class as well.

Because salmon increase in size throughout the spring and summer, it is not clear from this earlier work whether the seasonal increase in squid consumption is due to (1) higher squid abundance in the ecosystem in the summer, (2) the lower abundance of other prey items during this time, or (3), a salmon's increasing ability to catch squid as its body weight increases during the season. In order to construct models that connect variation in salmon growth to salmon foraging response at varying prey densities, it is important to determine the relative importance of each of these hypotheses.

Energetics and digestion are important considerations in terms of the foraging success of salmonids. As shown in Figure 2.3, the maximum growth rate of a salmon depends on the caloric content of the prey and the effort it expends in foraging. A salmonid's gape limits its ability to catch larger squid and fish (Mason et al. 1998). Furthermore, its efficiency and ideal swimming speed varies with body size (Ware 1978; Dunback and Ware 1987). As shown in Figure 3.2 and Table 3.2, nekton tend to be on a higher trophic level, and more energetically dense (measured in calories/gram wet weight of prey). It is not clear whether nekton or zooplankton digest more quickly (see LeBrasseur (1966) and Jobling (1987) for conflicting accounts).

As a salmon grows larger, it may become more able to consume the more valuable prey species, which in turn enables it to grow even more quickly and capture still more valuable prey. Positive feedback of this nature may be extremely sensitive to the initial conditions in determining the final adult body weight. In other words, a slight variation in salmon growth during April may translate into a much larger variation in later summer growth and therefore in the final adult body weight. This is especially true for the more omnivorous species of pink and sockeye salmon. If a trophic jump in salmon diets occurs between zooplankton and squid, it is important to know if this is a function of season or body weight. In this chapter, I re-analyze salmon feeding on squid by body weight to address this question.

Foraging models define a functional response between prey density and predator feeding rate. In order to calibrate models, estimates of prey density or biomass are required. Some previous models have correlated salmon feeding rates with zooplankton abundance in the Gulf of Alaska. However, standard methods for independently sampling salmon are poor with respect to many species of prey such as euphausiids or micronektonic squid (W. Pearcy, College of Oceanic and Atmospheric Sciences, Oregon State University, Corvallis, pers. comm.).

The need for reformulating models of salmon foraging to include multiple trophic levels is especially acute if connections are to be made between climate change (such as global warming or regime shifts), salmon distribution, and carrying capacity. Welch et al. (1998) report a strong correlation between sea surface temperature and salmon distribution, and suggest that a warming sea surface would restrict salmon to a fraction of their current distribution. As Murphy (1995) points out, however, salmon habitat quality in the open ocean is a combined function of the direct physiological aspects of water temperature on salmon and prey density. If the prey densities are high enough, salmon will congregate around oceanographic fronts where prey congregate, such as near the Emperor Seamounts, regardless of the sea surface temperature.

If there is a link between water temperature and salmon distribution in the Gulf of Alaska, it is possible that the link is indirect, acting through changing spatial or temporal patterns in prey abundance or composition across these fronts.

Prey may have cycles which influence salmon, as well. Ito (1964) reports on an oscillation of squid abundance in salmon stomachs between even- and odd-numbered years: it is interesting to speculate on the nature of this cycle with respect to pink salmon and other species.

The relationship between climate cycles, oceanographic fronts, and micronektonic squid abundance and distribution is not well known. A first step in this direction might be to quantitatively analyze the change in squid in salmon diets over time and space, in order to gain an insight into the fluctuations of squid populations.

3.1.3 Gonatid squid in the northeastern Pacific

The great majority of squid identified in salmon stomachs in the offshore Gulf of Alaska are species of the family Gonatidae, a dominant planktivorous

squid family in the North Pacific. Information on the distribution and abundance of gonatid squid in subarctic waters is limited, but their importance in the ecosystem should not be underestimated. Jefferts (1988) lists 16 subarctic species endemic to the subarctic North Pacific, and Nesis (1997) places the total biomass of gonatid squids across the North Pacific at 15-20 million tons, with a yearly food consumption of 100-200 million tons. They have a shorter life cycle and a much higher Production/Biomass (P/B) ratio than mesopelagic fishes—Nesis estimates that while gonatid squid biomass is less than 10% of the total mesopelagic fish and squid population, they account for 58-67% of the total annual production of this combined group.

Gonatids play an important role in the diets of fish, seabirds, whales, seals, and other marine mammals. A Russian commercial fishery exists for one of these species, *Beryteuthis magister*, with an annual catch of between 22 and 70 thousand tons. The other North Pacific gonatids are not fished commercially, although there was a substantial gonatid bycatch in the Japanese high seas salmon and flying squid fisheries (Nesis 1997; Kubodera et al. 1983). Gonatids as a whole are highly eurybathic, living in depths from the surface to 1500m (Nesis 1997).

Midwater trawls in northeast subarctic waters (45-55°N, 130-150°W) show that seven gonatid species make up 89% by numbers of the squid population of this area. Four species are dominant: *Beryteuthis anonychus* (32% of total squid catch by numbers), *Gonatus onyx* (21%), *Gonatopsis borealis* (10%) and *Beryteuthis magister* (9.5%) (Jefferts 1988). Of these, the most highly abundant, *B. anonychus*, has the smallest adult size, and is the only species for which the maximum adult mantle length (ML) is small enough to be consumed by salmon. *B. anonychus* is a epipelagic, lipid-rich squid with a maximum ML of 150 mm (Roper et al. 1984). *G. onyx*, found occasionally in salmon stomachs, has a maximum ML of 260mm, while the other species are

larger still. There are few recorded instances of whole squid with MLs greater than 150mm being found in salmon stomachs (Aydin unpublished data).

The previously reported range of *B. anonychus* agrees overlaps with locations in which they are most abundant in salmon stomachs. They extend westward from North American continent to 160-180°W, between approximately 40 and 53°N; they occur in the open ocean but are most common over slope and eastern seamounts (Figure 3.3). Concentrations were observed during the 1980s between 48-53°N at 130-145°W, and the stock assessment conducted during these surveys placed the biomass in this area at 200-250 thousand t (Didenko 1990, reviewed in Nesis 1997). The adult *B. anonychus* are always epipelagic, found in waters of 0-200m depth (Nesis 1997). They undergo diel vertical migrations, moving from 50-200m in the daytime to 0-150m at night. This is a similar pattern of vertical movement to that hypothesized for salmon in the open ocean (Walker et al. in press).

During the month of July at Ocean Station 'P' (50°N, 145°W), *B. anonychus* made up 90-100% of a maturing coho salmon's diet, with this percentage decreasing farther to the north (Pearcy et al. 1988). It was not uncommon to find a single salmon stomach containing 100-200 g of this squid species, up to 3% of the salmon's body weight. During the summer, very few non-larval squid of less than ML 60 mm are found in salmon stomachs. Pearcy et al. (1988) list the size range found in salmon stomachs as being between ML 75-105mm, although during the 1990s July sampling, the size range extended to ML 140mm with many squid between 100-120mm.

During winter, the *B. anonychus* caught in trawls and found in salmon stomachs are smaller, with MLs between 40-60mm (Mori 1995). Year-round, in the offshore waters of the northeast Pacific it is the only regularly observed (in >5% of stomachs) food source with individual body lengths greater than 20 mm.

Therefore, for salmon, the squid represent a discrete jump from zooplankton in terms of prey size, caloric density, and trophic level.

The spawning habitat of *B. anonychus* is unknown, but spawning seems to be year-round with two peaks in February-April and June-September. Maturation occurs at 60-70mm mantle length (ML)—assuming a growth rate of 10mm per month, their life cycle may be approximately 1 year (Kubodera and Shimazaki 1989).

A summer study of 56 stomachs of adult *B. anonychus* (size range: ML 75-127mm, weight 12-64g) identified sixteen prey types, which included copepods, amphipods, euphausiids, ostracods, pteropods, siphonophores, and chaetognaths. Copepods were in 56% of the stomachs, amphipods in 52%, pteropods in 40%, and euphausiids in 28%. The species of zooplankton overlap considerably with those consumed by salmon during the same season. The prey weight found in squid stomachs was 0.043-4.21% of squid body weight (Lapshina 1988, reviewed in Nesis 1997).

As well as being consumed by salmon, *B. anonychus* have been found in the stomachs of many species, including Pacific pomfrets (*Brama japonica*), thick-billed murre (*Uria lomvia*), short-tailed shearwaters (*Puffinus tenuirostris*), neon flying squid (*Ommastrephes bartramii*), albacore (*Thunnus alalunga*), lancetfish (*Alepisaurus ferox*), Dall's porpoise (*Phocoenoides dalli*), fur seals (*Callorhinus ursinus*), and fin whales (*Balaenoptera physalis*). Further, there is evidence that the species is cannibalistic (Nesis 1997).

The interannual variation of *B. anonychus* distribution in relation to oceanographic properties such as sea surface temperature is not known. They congregate in rings and vortices associated with fronts and seamounts, and this last property is an important aspect of their biogeography, in terms of salmon feeding. As fronts may shift from year to year, determining the correlation

between these fronts and the squid distribution is important in establishing changes in salmon habitat potential.

3.2 *Calculating an index of squid abundance from salmon food habits data*

3.2.1 Methods

Part of the problem in conducting squid studies is technological—most direct sampling methods used in fisheries research today are notoriously poor or are biased at catching micronektonic prey such as small squids. As larger fish have specifically evolved to catch their prey, it would be extremely useful to be able to use the stomach contents of catchable predators as a catch-per-unit-effort (CPUE) index of prey abundance, especially if few prior estimates of prey biomass exist. Such a technique may provide more information than a human fishing-based estimation method would provide, as diet studies measure increases and decreases in prey as it directly affects the predator.

This chapter uses an index of abundance for gonatid squid based on salmon stomach contents and foraging theory to measure annual and decadal fluctuations in the summer gonatid squid abundance in the Gulf of Alaska. Data is combined from three sources covering the periods 1956-63, 1980-84, and 1993-98.

3.2.1.1 Preliminary data collection and preparation

Salmon food habits data from pink, coho and sockeye salmon were combined from studies conducted in the Gulf of Alaska between December and September during the years 1956-60, 1962-64, 1980-84, and 1993-98. Data sources, and references to collection methods are listed in Table 3.4. Data from 1956-64 is summarized in LeBrasseur (1966) and was provided in electronic format by P. Rand. The original data for 1980s operations,

summarized in Pearcy et al. (1988), were provided by W. Pearcy, while data from the 1990s were collected by K Myers, R. Walker, and the author, and are summarized in Myers et al (1998a).

The majority of the salmon were collected by nighttime surface (shallower than 10m) gillnet operations. The primary exceptions are between 1962-64, when samples were collected primarily by daytime longline operations, and for winter and spring sampling in the 1990s, when were collected by both daytime and nighttime trawling operations. A few longline-caught fish were included in 1956-60 data. All fishing operations conducted below 10m depth were removed from the sample.

The study area was restricted to the north and to the east by the edge of the continental shelf (Figure 1.1). The shelf break was taken to be at 1500m bottom depth; all samples collected at shallower depths were discarded. The selection of 1500m as the depth cutoff was based on a visual examination of ocean depths and chosen so as to leave abyssal seamount areas in the analysis.

At the southern edge, most data was collected north of 44°N, although fish caught as far south as 42°N in May 1998 are included. The southern limit is due both to lack of fishing effort and lack of salmon catch at southern stations. While sampling occurred as far west as 180°, very few samples were collected west of 170° W, and this latter longitude was chosen as the western limit.

The total number of salmon used was 11,654 fish caught during 604 fishing operations. Of these, 5,831 were sockeye salmon, 4,088 were pink salmon and 1,735 were coho salmon. The spread of operations by sampling period, latitude and longitude is shown Figure 3.4, and the number of salmon caught be week and year is listed in Table 3.5. Sampling effort differed in time and space for each of the studies. Data was collected from May-August from

1956-60, January and April-July for 1962-64, and June-July for the 1980s-90s. In addition, a lesser number of fish were collected during December, January, and May in the 1990s. Spring and summer sampling during the 1950s and 60s was generally spread throughout the Gulf, while sampling during the 1980s and 90s was restricted to specific transect lines, in particular a line along 145° W between 50° N and 56° N.

For each fish, the following information was recorded: Operation, gear type (gillnet, longline, or trawl), time of day (divided into 'night' and 'day'), week during year, year, longitude and latitude of gear retrieval (to the nearest minute), sea surface temperature (°C), salmon species, salmon body weight (to nearest 10g), and presence/absence of non-larval squid in each salmon's stomach. Stomach contents data on other prey species are not included in this analysis.

No body weights were available for salmon caught during 1980, and body weights were missing from approximately 5% of fish collected in other years. Fish without recorded body weights were excluded from the analysis of body weight dependency on feeding, but were used to calculate overall squid abundance. A by-species quantile-quantile plot of all body weight vs. a normal distribution showed a nearly normal distribution with a small number of larger outliers in all three species. For the body weight dependency analysis, an upper cutoff of 5500g for coho and sockeye and 3500g for pink was chosen by visual inspection.

All pink and coho salmon were considered to be ocean age .1 (ocean age .0 in December). Sockeye salmon showed a bimodal distribution in body weights, representing ocean age .1 and ocean age .2+ fish. During the spring and summer, sockeye of less than 500g body weight were probably ocean age .1 (Ishida et al. 1998).

3.2.1.2 Statistical analysis

The binary (Bernoulli) response variable of squid presence/absence in a salmon's stomach was chosen as the variable for analysis, as the probability of a salmon capturing its first squid during a feeding period is the best reflection of a salmon foraging at its maximum (most hungry) rate.

In contrast, use of the total weight of squid in a salmon's stomach would be prone to saturation at high squid densities and thus not be able to resolve high squid densities. In regions in which salmon captured the most squid, stomachs were observed as being filled to capacity with additional squid filling the esophagus and mouth of the salmon, indicating that prey saturation is an issue at these locations. Also, digestion rates which differ by species and temperature would affect prey weight more than presence/absence. See Appendix A for a discussion of the theoretical relationship between the binary response variable and squid density.

The most common method of analyzing binary data is through the use of logistic regression. For example, this method has been used in fisheries research to examine salmon distribution through the analysis of bycatch in the Japanese high seas squid driftnet fishery (Murphy 1995).

Logistic regression transforms a binomial or Bernoulli-distributed variable with mean p (where p , ranging from 0 to 1, represents the probability of at least one successful squid encounter visible in a salmon's stomach) into a variable γ ranging from $-\infty$ to $+\infty$ using the transformation $\gamma = \ln \left[\frac{p}{1-p} \right]$ (Cox and Snell 1989).

A logistic variable may be related to explanatory variables using several modern regression techniques. If responses are expected to be nonlinear with respect to explanatory variables, one of the more useful methods is the General

Additive Model (GAM) (Hastie and Tibshirani 1990). The model uses a general function for each explanatory variable as follows:

$$\gamma = \ln \left[\frac{p}{1-p} \right] = \alpha + f(X_1) + f(X_2) + \dots + f(X_k) + \text{error}$$

Each function $f(X_{1..k})$ can incorporate a linear or nonlinear function between the k explanatory variables and the response γ . The GAM algorithm contained in the S Plus® software package estimates each additive function so as to minimize an overall error statistic (Hastie 1993).

The GAM is constructed by examining all possible additive interactions to determine the model which best relates the explanatory variables to the response for the entire data set. This can be performed on the entire data set as well as on subsets (such as by month).

The best model is determined by the stepwise model selection algorithm contained in the S Plus® software package (Hastie 1993). The algorithm adds terms representing explanatory variables to the model one at a time and computes the trade-off between variance reduction and added degrees of freedom using the Cp statistic (Hastie 1993, pg. 282). Cp is a statistic that balances degrees of freedom lost with the amount of deviance gained by the inclusion of a term.

For any given model, the approximate significance of each term may be determined by dropping the term from the model and re-fitting the model excluding the term in question. A χ^2 -test is then used to determine the significance of the change in model variance for each such operation.

To use the GAM, two assumptions must be made. First, all non-linear terms in the model are assumed to be additive with respect to the response variable. While linear terms may be modeled as multiplicative, 2-way, or higher-order interactions, nonlinear combinations of explanatory variables cannot be

accurately modeled by smoothed terms, except by modeling subsets of data. Fortunately, the relationship of the logistic variable to foraging theory described in Appendix A suggests that the explanatory terms in this model may be considered additive, although care must be taken so that that nonlinear interactions are not missed. The second assumption is that covariance between the explanatory variables is minimal, which may not true in this case: sea surface temperature (for example) is dependent on time of year. To solve this second problem, once initial models are created using all the data, subsets of the data may be chosen to model.

One final problem with the GAM method is that, while it takes into account the differences between each individual salmon, it creates functions which show *relative* response of variables rather than absolute response. If the desire is to find an easily calculated quantity which, in future sampling, may be used as a measure of squid CPUE at a site, the GAM would require re-fitting of all of the previous data.

A second type of logistic analysis, which allows the calculation of an *absolute* logistic response for a single group of individuals, utilizes the empirical logistic transform described by Cox and Snell (1989). If all salmon are considered to be behaviorally identical, an estimate of the logistic variable γ , and thus of the density of squid, could be determined at each individual sampling station from an estimator \hat{p} of p . The empirical, or directly-calculated logistic transform would be equal to $\hat{\gamma} = \ln \left[\frac{\hat{p}}{1 - \hat{p}} \right]$.

Unfortunately if the logistic transformation is used, the estimator \hat{p} cannot be either 0 or 1, as the resulting estimator $\hat{\gamma}$ would be undefined. If the standard maximum likelihood estimator is used for \hat{p} , $\hat{p} = \left[\frac{N_{squid}}{N_{total}} \right]$ (where N_{squid} is the number of salmon with squid, and N_{total} is the total number of

salmon in a sample), samples in which either all sampled salmon or no sampled salmon caught squid would have to be discarded, biasing the sampling process: the fact that 0 out of 50 salmon caught squid is useful information!

To counter this, γ is estimated by using a bias-corrected empirical logistic transform derived in Cox and Snell (1989) pg. 32:

$$\hat{\gamma} = \ln \left[\frac{N_{squid} + \frac{1}{2}}{N_{total} - N_{squid} + \frac{1}{2}} \right]$$

The variable is part of a general family which is approximately normal: the variance of this estimator can be estimated as:

$$\hat{V}ar(\gamma) = \left[\frac{(N_{total} + 1)(N_{total} + 2)}{N_{total} (N_{squid} + 1)(N_{total} - N_{squid} + 1)} \right]$$

This procedure is a special case of estimating the mean of a binomial distribution using a Bayesian estimator as a prior distribution (Casella and Berger 1990, pg. 305). In this special case, the parameters for the prior are chosen for each sample so as to eliminate the bias from the estimate of logistic variable.

In this study, both the GAM and the empirical logistic method are used. Modeling of the data is conducted in four steps:

1. All the data is fit to a single GAM. The best model of explanatory variables for the complete data set is determined. The relative shapes are reported of all smooth functions of explanatory variables.
2. The same procedure is used to find the best GAM for each species (sockeye, pink and coho).
3. GAMs are constructed for each month of the year in which sufficient sampling exists. These are used to determine if responses of squid consumption to body weight and SST remain constant over the season.

4. To determine the bias in the empirical logistic transformation, corrections based on body weight and species are calculated from the GAM to determine a formula for calculating an independent Squid Density Index for each site.

3.2.1.3 Explanatory variables in GAM analysis

The explanatory terms for γ considered in this study are:

- Salmon species
- Salmon body weight
- Latitude and longitude
- Year
- Week of year
- Sea surface temperature

Of these explanatory variables, the important distinction to make is between those which predict an individual salmon's response to squid (catchability and effort) and those which describe the pattern of squid abundance itself. In this model, I use salmon species and body weight as the variables which control the foraging effort and success of each individual salmon within a sample, and latitude, longitude, year (or decade), and week of year to describe squid abundance. Ambient water temperature, as indexed by sea surface temperature, may affect both foraging effort/success and squid abundance, and thus requires special attention.

Water temperature may affect foraging rate in three ways. First of all, predator swimming speed in salmonids is known to increase with increasing temperature (Stewart and Ibarra 1991), and a predator's search volume per-unit time is dependent on swimming speed (Ware 1978). Secondly, a salmon's digestion rate increases with increasing temperature (see Chapter 2 in this

dissertation for a review). Thus, an increase in water temperature would simultaneously increase the amount of food a salmon may ingest per day, while at the same time decreasing the likelihood of a single prey item being detected in a salmon's stomach. Further, salmon foraging behavior, which maximizes the difference between energy obtained and energy expended, will change with water temperature. Finally, the temperature experienced by a salmon may vary significantly from the sea surface temperature, due to vertical migrations during feeding and digestion (Walker et al. in press).

For this model, I assume that the water temperature on predator foraging effort is small compared to the effect of temperature on squid abundance, and is linear with respect to the logistic transformation (see Appendix A). Furthermore, it may be predicted, as shown in Appendix A, that the slope will be decreasing with increasing water temperature at a rate between 0.05-0.10 logit units per °C. This digestion-rate correction is based on digestion rate which is calibrated identically for pink, sockeye, and coho salmon (Davis et al. 1998a). Any nonlinear response with respect to sea surface temperature, or any linear response with a slope differing significantly from the value above, shall be taken as being due to the relationship between temperature and squid density itself.

Other factors which would change the catchability of squid as viewed from salmon stomachs includes the time of day of sampling and gear type, if different gears sample different groupings of fish. In terms of fishing gear, the results from this study should be considered to be a reflection of squid predation by gillnet-caught fish, as gillnet sets dominate the data. There are not enough locations in which multiple types of gear were used to test for gear-dependent effects.

Salmon show a diel migration pattern: surface catch-per-unit-effort of salmon increases during nighttime hours, and recent tagging studies confirm that salmon migrate to the surface at night and into deeper waters (below 20

meters) in the daytime (Walker et al. in press). Two studies of diel patterns in salmon feeding (Pearcy et al 1984; Davis et al. 1998a) show that salmon prey may change substantially depending on the time of day. The squid found in salmon stomachs were associated with night feeding by Pearcy et al. (1984). Because it is when more salmon are in surface waters, night probably represents the most important foraging period for salmon on squid. During the 1960s, night gillnet sets did not take place. Therefore if the index of squid density in the 1960s is significantly different from other years, time of day may be a partial explanation. Finally, the influence of light levels, turbidity, and other oceanographic influences other than sea surface temperature, which may have an effect on salmon feeding, are not considered.

3.2.2 Results

3.2.2.1 Patterns in explanatory variables

Due to seasonal dynamics of the northeast Pacific, covariation between both salmon body weights and sea surface temperature occurs with season, as both variables increase significantly from December through August.

Figure 3.5 shows the trend in SST averaged by week over all geographic locations. Interannual and geographic variation is significant, although coverage of latitude and longitude was not uniform enough between years to examine temperature trends fully using this data set. However, it is worth noting that the years of sampling covered multiple phases of both the PDO and ENSO oscillations described in Chapter 1.

The average body weights for each sampling period, grouped by week of sampling period, are shown in Figure 3.6. The seasonal body weight trends for pink and coho salmon do not differ significantly between sampling periods, except for the occurrence of some larger pink salmon collected in May during 1956-60 (weeks 20-25). However, these fish were collected over a relatively

limited area during a single year, and thus cannot be considered significant over the Alaskan Gyre. Differences between sampling periods in sockeye body weights were probably due to variation in the age composition of the catches rather than differential growth within a cohort.

While the average body weight of sampled salmon increased from winter to summer, the variance increase of summer samples was such that smaller fish were caught throughout the year. Winter-caught coho were an exception, with coho caught between December-February being from a size range absent in later months. Sockeye salmon showed the greatest range of body weights for any given month, mostly due to multiple age classes and maturation states present ocean sockeye populations.

Size selectivity of fishing gear between sampling periods may also account for some of the observed variability. An examination of the multiple effects of latitude, longitude, sampling period, and week on both salmon body weight and SST, using a Generalized Linear Model (GLM), showed significant variation in some combinations of the factors (latitude)x(longitude)x(year), although data was too sparse to fully describe the variation over all times and areas.

3.2.2.2 Full GAM of squid consumption

All the data, pooled for all species, years, and seasons, were combined and subjected to the stepwise model selection procedure described above. Table 3.6 shows all the explanatory terms ranked from most significant to least significant factors, as judged by the reduction of the model's Cp value which occurs when each term is added. Total degrees of freedom are less than the total number of fish, as fish with missing values for body weight or sea surface temperature were removed from the model.

The final model selected assigned significant explanatory power to all of the variables examined. The smoothed terms were selected over linear terms for all of the continuous variables. Overall, the full model accounted for 22% of the variance in the null model. The discrete yearly term was the first selected and accounted for 50% of the deviance accounted for in the full model, followed by body weight (22%) and latitude (16%). Longitude, species, SST, and finally week of year accounted for decreasing percentages of the deviance, although all terms were significant. The terms varied in the magnitude of each effect. Magnitude is shown in Table 3.6 as the difference between the minimum and maximum of each fitted curve on the logit scale. The yearly term had the highest magnitude while the species term had the lowest.

Figure 3.7a-g shows the shape and relative magnitude of each additive effect. Of the individual behavioral terms, body weight was the most important factor, with squid consumption increasing roughly linearly from -3 to 0.6 logits between 0 and 1500-2000g body weight, then remaining constant for larger fish (Figure 3.7a). The effect of species was significant but of lesser magnitude, with coho consuming more squid than sockeye or pink (Figure 3.7b).

Of the spatial variables, latitude was the most significant term, although longitude had a greater magnitude (Figure 3.7c-d). Squid consumption was highest between 46-52°N latitude, decreasing greatly at higher latitudes. Consumption was fairly constant at longitudes between 140-170° W, and decreased rapidly towards the eastern continental shelf. Sampling at these eastern longitudes, however, was limited to 1956-64, and it is not clear if this is due to decreases in squid abundance or increases in other micronekton such as fish in the salmon diet. Sea surface temperature was also highest in these slope waters.

The yearly term (Figure 3.7e) shows a large change between the 1950s and the 1990s. The response decreases between 1956-1960 and between

1962-64. The response is much higher in the 1980s and 1990s. In addition, the 1990s show a possible alternating pattern with squid being more present in even years than in odd years.

The weekly term (Figure 3.7f) is the weakest in magnitude and the least significant, and shows a decreasing trend as the season progresses from winter to summer. However, there is little data available for February-April: in addition, some of this may be due to interaction with the body weight effect, as salmon are at their smallest sizes earlier in the season. Finally, the sea surface temperature effect (Figure 3.7g) shows the greatest squid consumption occurring between 6-10°C, decreasing at both high and low temperatures: data at lower temperatures is limited, however. Much of the decreasing response at higher temperature is probably dominated by July trends.

3.2.2.3 Species- and month- specific effects

To examine the changing shape of functional responses as the season progresses, the balance between sample size and seasonal variation is reached by stratifying each species by month. Data from each month was fit separately to the model $\gamma = s(\text{latitude}) + s(\text{longitude}) + s(\text{BW}) + s(\text{SST})$. The yearly term was removed as sampling did not occur in all months x years: May sampling, for example, was only conducted in one year since 1980. Sampling between December and February was combined into one pool due to lack of data for winter months.

Rather than selecting the best model through stepwise model selection, all terms were fitted for each month, and the significance of each term was determined by dropping a term, refitting the model, and comparing the resulting 3-term model with the 4-term model, using a χ^2 -test (Venables and Ripley, 1997 pg. 226). This was repeated for each of the four terms for each month and species. (Table 3.7).

In general, more terms were significant for sockeye than for any other species, probably due to higher sample sizes. All terms in July were significant with the exception of coho body weight. Coho body weight was never significant-coho of all sampled sizes fed on squid equally. The significance of latitude, longitude, and SST terms varied outside of the July models.

Figure 3.8 shows the shape of all of the body weight terms, both significant and non-significant, for all three species. While the offset (constant value) is different for each curve, the overall shape for pink and sockeye does not vary with month. Pink salmon squid consumption increases rapidly between 300 and 1000g body weight, while sockeye consumption increases more slowly, not reaching a maximum value until 2000g body weight. Coho, on the other hand, show almost no response between squid consumption and body weight, even in July. The curves shown for coho in the other months represent poor fits obtained for the smoothing curve.

The latitude, longitude and sea surface trends which were significant at each month showed a similar shape to the trends in the full GAM of Figure 3.7. The exception is for coho in winter, for which squid consumption increased in the south and west and was high at the coolest temperatures between 5-7°C.

The difference in the relationship between explanatory variables and squid consumption in winter coho is shown more fully in Figure 3.9, in which the logit response is modeled as a combined function of week and coho body weight (Figure 3.9a) and SST and body weight (Figure 3.9b). Consumption of squid by coho is high in the winter months compared with other months—sockeye and pink do not show this pattern, perhaps due to smaller body sizes. In addition, the squid in winter months are considerably smaller than those in summer months, and the feeding relationship between the species in the winter may be considerably different, involving a smaller size range or different species of squid.

3.2.2.4 Corrections to the empirical logistic response

As the shape of the body weight response curve was robust for all months for each species, one curve was assumed to be accurate for each species for the entire year—the curves for each species are shown in Figure 3.10. Monte-Carlo simulations in which fish were selected randomly from the data set to create replicate samples confirmed that this relationship with body weight was independent of other environmental factors.

As discussed earlier in this chapter, one of the purposes of this analysis is to find an index of squid density which may be calculated from salmon stomachs collected from a single site. Ideally, this index would be simple to calculate and proportional to squid density. While logistic modeling using a GAM, as described in the previous results, shows trends over time, it does not lend itself to the calculation of future values, as future data would need to be refitted to all data used in this study to determine relative responses.

Instead, if all fish are assumed to be identical, all fish from a single sample or region may be combined into a single, empirical logistic response estimate. However, as shown in the previous section, each species shows a distinct response with respect to squid catchability with body weight. An empirical logistic transformation must be calibrated for each species in order to include all species in a single index.

Due to the nonlinear nature of the feeding response at lower body weights, and the relatively constant feeding rate at higher body weights, the best way to measure squid density, using salmon stomach data, is probably to discard body weights below a cutoff value at which squid feeding falls off rapidly, and assume that body weight has no effect on foraging for salmon above the cutoff weight. If smaller fish are discarded before calculating the empirical transformation, the resulting value represents the squid density as capturable by the larger salmon, with smaller salmon feeding on squid at a

lower rate. The body weight cutoff used was chosen by visual inspection of Figure 3.10 and is shown in Table 3.8.

To place the index on the same scale for each fish species, a constant was subtracted for each species. The final squid index is thus:

$$\hat{y}_{species} = \ln \left[\frac{N_{squid,species} + \frac{1}{2}}{N_{total,species} - N_{squid,species} + \frac{1}{2}} \right] - \alpha_{species}$$

where species is one of pink, sockeye, or coho, N_{total} is the number fish of that species examined above the cutoff weight in Table 3.7, N_{squid} is the number of those fish containing squid, and $\alpha_{species}$ is the intercept value from Table 3.8. The intercept used was the species offset shown in Figure 3.7b, corrected for the discarding of the smaller fish.

The resulting values, one from each of the three species, may be averaged at each site to obtain an index of squid density, calibrated so that index=0 implies a 50% chance of a "large" salmon consuming a squid. The "large salmon" in this case is a statistical hybrid of coho, pink and sockeye. Conversely, the three values may be examined separately if a particular salmon species is of interest. The correlation coefficients between the values calculated for each species at each site are high (Table 3.8), indicating that the common factor of squid density outweighs any biological differences between the species used in this corrected index. This may not be true for winter months in which most fish are below the body weight cutoff.

Each index value, either for the species separately or combined, is approximately normally distributed with the variance calculated using the formula in 3.2.1.2. As discussed in Appendix A, if foraging is taken to be a Poisson process, the index is linearly proportional to $\ln(\text{squid density})$ for values less than 0 or linearly proportional to squid density for values greater than 0. The squid density index may be used to measure squid fluctuations in time and space.

3.2.2.5 Changing squid distribution in July, 1956-98

In this study, July is the only month for which relatively complete sampling is available over time and space and for which enough salmon above the body weight cutoff have been sampled.

Figure 3.11 shows the index averaged over all July sampling locations for each of the four sampling periods. In Figure 3.11, the squid index value is calculated for each species at each station shown by the circles. The values obtained at each station were averaged, and a smooth latitude x longitude surface was extrapolated between sample points. Blank areas are those in which no sampling occurred within 1° of latitude or longitude.

While sampling is scattered, some trends are apparent. In the 1950s and 1960s, squid density is in the central portions of the gyre between 140-150°W and around 54°N (Figure 3.11a,b). In the 1980s, higher densities are seen farther to the south, while in the 1990s, densities south of 52°N are extremely high, falling off to the north (Figure 3.11c,d). If the 1990s are separated into even and odd years (Figure 3.11e,f), the even years are seen to have the highest densities of squid between 40-52°N. In odd years, high densities are found further to the south. Due to sampling limitations it is not clear if this represents a north/south shift of salmon or fluctuations in squid density throughout the region. Also, the even/odd split may be a coincidental result of oceanographic patterns described in Chapter 4.

As sampling generally extended further south in the 1990s than in the earlier time periods, it is not clear from Figure 3.11 whether the lower squid densities in the earlier time are due changes in squid abundance or limitations in sampling area. However, an examination of squid index values along three transects shown in Figure 3.12 provides a clearer picture of the changes.

Figures 3.13-3.15 shows squid index values for each species along 145°W, 50°N, and 55°N, the most heavily-sampled transects in this study.

Each individual data point along 145°W represents the average of yearly squid index values calculated from fish pooled within a 1°latitude by 5°longitude square from the location of the point. Each point along the 50°N, and 55°N transects represents pooling in a 4°latitude by 2° longitude square.

North of approximately 54°N along 145°W, little change occurs between sampling periods. South of 54°N, squid density is higher in the period since 1980 (Figure 3.13). The transect line along 50°N (Figure 3.14) shows a similar result between 145°W and 160°W, with higher squid index values after 1980. Sampling East of 145°W was not conducted during this later period. Along 55°N there is little change between time periods (Figure 3.14).

Figure 3.16 plots all July squid index values for all species vs. SST, with 1950s and 1960s combined into a single pool. The low values at the higher temperatures during the earlier time period are mostly along the shelf. At temperatures between 7-9°C, even and odd years during the 1990s show a different relationship between the squid index and sea surface temperature, with even years having high index values at these temperatures, and odd years have low index values. Finally, a drop can be seen in squid index values at around 12.5°C, although the appearance of this drop may be due to high index values in odd years being associated with warmer temperatures. A more detailed analysis of the relationship between sea surface temperature and these index values for the 1990s can be found in the next chapter.

3.3 Conclusions

The data presented in this analysis agree with earlier studies in showing that, in the Gulf of Alaska, coho salmon consume more squid overall than pink or sockeye salmon. However, the change in squid consumption in pink and sockeye with increasing body weight is of a greater magnitude and statistical significance than the differences which occur between these three salmon species (Table 3.6). The empirical responses derived here show that pink and

sockeye increase their squid consumption between 100 and 1000 g body weight, while coho do not change their consumption over a wide range of body weights.

The squid density index, as calculated using the corrections for each of the three salmon species indicated in Table 3.8, provides a method for determining squid density at a single sampling location. The index is scaled so that a value of the index of 0 indicates a squid density at which 50% of the salmon have squid in their stomachs. Values of the index calculated separately for each of the salmon species at a single site showed that the values obtained for each species were highly correlated with each other ($R \approx 0.7$). This indicates that the between-salmon species behavioral differences in foraging modes may be less important than squid density in determining salmon foraging rates on squid.

If this method is used to measure squid densities at future sampling locations, it will be most accurate if calculated using surface-caught (0-10m) fish collected during nighttime or overnight sampling. In order to reconstruct actual squid densities, it would be useful to conduct such a study concurrently with net sampling of squid. Using three species of salmon may increase the useful range of the index, as the different salmon species may be more sensitive in their feeding responses over different ranges of squid density.

It is clear from the data presented in this chapter that, from the salmon's perspective, micronektonic squid populations in the Alaskan Gyre have fluctuated greatly. The yearly trends in Figure 3.7 and Figure 3.11 show overall increases between the earlier sampling period 1956-64 and the later periods of the 1980s and 1990s. However, due to the limited scope of the sampling, it is not possible to tell whether the population fluctuations occur on an annual scale or a decadal scale, or whether the changes represent changes in seasonal timing or spatial distribution.

Previous studies of decadal variation in the Gulf of Alaska indicate that both the overall level of production and the geographic pattern of production may change on a decadal scale. For example, Brodeur and Ware (1992) report that between the 1950s and 1980s, peak zooplankton production shifted from the center of the gyre to its edges, possibly due to changes in wind stress patterns. While a comparison of Figure 3.11a with Figure 3.11d may suggest a similar trend, there is not enough data to determine if this trend is real.

Some locations, however, showed clear changes between the sampling periods. For example, near Ocean Station 'P' in July, the squid density index, as calculated for sockeye salmon, increased between the 1950s and the 1990s from approximately -2 to 2 (Figures 3.12 and 3.13). That change is equivalent to a jump in the percentage of sockeye(>1000g body weight) eating squid from 12% to 88%. The change represents both an increase in the overall amount of food consumed, and a partial replacement of zooplankton with squid in the larger salmon's diets. As this change represents a substantial difference in the trophic level of salmon feeding, the effect on the efficiency of salmon growth may be large.

Seasonal variation in squid consumption by salmon is even more unclear, because of a lack of winter and spring sampling. One interesting aspect to the seasonal change is that specimens of squid found in salmon stomachs in winter are considerably smaller, possibly indicating matched seasonal cycles of growth. Coho salmon especially may change their feeding strategy substantially as the season progresses, and seasonal changes in feeding strategy may be an important aspect of a salmon's feeding response to changes in food availability.

The difference in body weights between squid consumers and non-squid consumers, occurs between age classes in sockeye, but within a single age class in pink. The flexibility in maturation timing of sockeye may be partially

controlled by squid abundance, while for pink and coho, squid abundance may be a larger controlling factor with respect to movement and foraging rates, as both species are required to grow to their largest sizes in a single year.

Because salmon increase in size throughout the spring and summer, it is not clear whether the overall seasonal change in squid consumption is due to (1) changes in squid abundance in the ecosystem in the summer, (2) the lower abundance of other prey items during this time, or (3), a salmon's changing ability to catch squid as its body weight increases during the season. In order to construct models that connect variation in salmon growth to salmon foraging response at varying prey densities, it is important to determine the relative importance of each of these hypotheses.

Complex interactions are likely between salmon body weight and squid consumption when considered over the range of an entire year of growth. For example, if stations which, in a single month, have salmon with higher than average body weights are also found to correspond with stations with high presence of squid, it will not be clear whether a high squid abundance leads to higher salmon body weights, or salmon with higher body weights are better able to consume squid—covariation between the two variables is probably caused by a combination of both effects. The detailed patterns of variation in body weights observed during the most heavily-sampled period, July 1993-98, are described more fully in the next chapter in an effort to determine causative factors of variation in salmon growth. Another important aspect is the balance between the food supply of zooplankton and squid: this is also explored more fully in the next chapter.

The relationship between water (sea surface) temperature and squid density is of specific interest, especially due to recent speculation concerning global warming and salmon habitat. In this study, data is only existent to calculate squid index values reliably for July. As can be seen in Figures 3.10

and 3.15, in many years/sampling periods there is a negative correlation between the squid index and sea surface temperature. Part of this correlation is due to the physiological change in digestion rates and squid detectability discussed in Appendix A, but the correlation is greater than would be expected from this effect alone.

In the western North Pacific, salmon are known to congregate around the Emperor Seamounts where the production of lower trophic levels is concentrated by the ocean circulation around the Seamounts (Murphy 1995). In the eastern North Pacific, in the range of temperatures reported, the sea surface temperatures may be an indication of the position of fronts in which food such as squid may congregate. If salmon congregate around these higher density food sources, a correlation between salmon density and sea surface temperature may arise independent of a direct physiological cause.

As a final note, during the 1990s, the squid observed in the majority of salmon stomachs in this study area was *Beryteuthis anonychus*: it is possible that other species of squid were more prevalent in salmon stomachs during previous periods.

Table 3.1. Differences between planktivory and piscivory ("nektivory") based on foraging behavior and energetic considerations. Foraging elements are from Breck (1993). The contrasting effect of digestion rates compares LeBrasseur (1966) with Jobling (1987).

Factor	Piscivory	Planktivory
Fish gape	Critical	Important for small fish
Number of prey consumed per day	Few large prey	Many small prey
Capture success	Lower	Higher
Limit to vision	Contrast	Visual acuity
Reactive distance	Similar for all prey	Increases with prey size
Trophic Level	High	Low
Digestion rate	Faster due to more digestible body parts, may be slow due to low surface/volume ratio.	Slow due to hard body parts, may be fast due to high surface/volume ratio.
Caloric density	High	Low

Table 3.2. Major salmon prey groups in the offshore northeast Pacific. Representative species and energy densities salmon prey groups. Prey are grouped by hypothesized similarities in trophic level and size. For a list broken down to the species-level, see Pearcy et al. 1988. Caloric values represent the ranges of means reported in the following sources: Davis et al. (1998); Higgs et al. (1995); Nishiyama (1977), and Ikeda (1972).

Prey Group	Representative taxa	Prey energy density (calories/g wet weight)	
1. Mesozooplankton (<2cm body length)	Calanoid copepods, e.g., <i>Neocalanus cristatus</i>	627-910	
	Euphausiacea <i>Thysanoessa</i> spp. <i>Euphausia pacifica</i>	743-1130	
	Hyperiid amphipods	589-975	
	Gastropoda <i>Limacina helicina</i> <i>Clione limacina</i>	520-636	
2. Gelatinous zooplankton	<i>Aglantha</i> spp. <i>Salpa</i> spp. <i>Doliolum</i> spp.	50-200	
	3. Micronektonic fish	<i>Gasterosteus aculeatus</i>	1166-1533
		<i>Lampanyctus</i> spp.	
4. Micronektonic squid	<i>Beryteuthis anonychus</i>		
	Small (28-38mm mantle l.)	978	
	Large (66-100mm mantle l.)	1550	
	Other Gonatid spp.	1125-1877	
5. Large zooplankton	Polychaeta, e.g., Alciopidae, <i>Tomopteris</i> spp. Chaetognaths Larvaceans Decapoda	800-1200	

Table 3.3. Salmon prey items in the subarctic and transitional North Pacific in the summer (see text for references). (-) indicates not present or captured in low numbers. The "small zooplankton" group consists of copepods, pteropods, small euphausiids, and small amphipods.

Area	Sockeye	Chum	Pink	Coho
Northwestern Subarctic Gyre	Fish, squid, euphausiids	Pteropods, euphausiids	Fish, squid, euphausiids	Squid
Central North Pacific				
Transition Zone	-	Gelatinous	-	Fish
Transition Domain	-	Gelatinous, cheatognaths	Sm. Zoop, squid, fish, cheatognaths	Squid, fish
Subarctic Current	Squid	Gelatinous, cheatognaths	Squid	Squid
Ridge Domain	Sm. Zoop.	Sm. Zoop	Sm. Zoop	-
Alaska Stream	Sm. Zoop, squid, fish	Sm. Zoop, squid, fish	Sm. Zoop, squid, fish	-
Central Bering Sea	euphausiids, squid, fish	Gelatinous	euphausiids, squid, fish	-
Eastern North Pacific				
Subarctic Current	Squid	Gelatinous	Squid	Squid
Ridge Domain	Sm. Zoop	Sm. Zoop.	Sm. Zoop.	Squid
Alaska Stream	Fish	Pteropods, fish	Fish	Fish
Coastal Domain	Fish, euphausiids	Fish, euphausiids	Fish, euphausiids	Fish, euphausiids

Table 3.4. Data sources. Data used in this analysis grouped by gear type and time period. Total stations are fishing operations in which salmon were caught, while total fish are the total sockeye, pink, and coho salmon caught. Descriptions of fishing operations may be found in: Chapter 4 in this dissertation and Myers et al. (1998) for *Oshoro maru* 1993-98; Percy et al. (1988) for *Oshoro maru* 1980-84; Ueno et al. (1997) for *Kaiyo maru* 1992, 96; Carlson et al. (1998) for *Great Pacific* 1998; and LeBrasseur (1966) for gillnet and longline sets 1956-64.

Ship and/or study period	Total stations and fish sampled	Gear used	Set time	Time of year covered	Analysis notes
<i>Oshoro maru</i> 1993-98	55 sets 2688 fish	Non size-selective gillnet	Overnight	Late June- Early July	
<i>Oshoro maru</i> , 1980, 1982-84	29 sets 2145 fish	Non size-selective gillnet	Overnight	Late June- Early July	Missing body weights in 1980
<i>Kaiyo maru</i> 1992, 1996	18 sets 445 fish	Trawl	Mixed day and night	Dec 1992, Jan 1996	Difficulty in identifying species of smaller salmon.
<i>Great Pacific</i> , 1998	26 sets 161 fish	Trawl	Mixed day and night	May	
Gillnet sets, 1956-60	108 sets 3540 fish	Gillnet	Mainly night	Most April-August, some Jan-Feb.	
Longline sets, 1962-64	367 sets 2675 fish	Longline	Mainly dawn and day.	Most April-August, some earlier.	Small numbers of fish at each station.

Table 3.5. Number of sockeye, pink and coho salmon sampled by week and year. Negative weeks refer to December sampling during the previous year (i.e., weeks -2 to -1 of 1993 represents December 1992. Dotted lines indicate the four major separate study periods.

Month	Week	Year																	Total	
		1956	1957	1958	1959	1960	1962	1963	1964	1980	1982	1983	1984	1993	1994	1995	1996	1997		1998
December	-2													161						161
	-1													97						97
January	3							14								115				129
February	4							39	7							72				118
	5							76	57											133
	6								24											24
April	15						30	140												170
	16						30	88												118
	17						34	90												124
	18						22	226											13	261
May	19						18	15												46
	20			4	26		72	203											49	354
	21			6	70	277	21	18	107										53	552
	22	22	2	137	162		64	226												613
June	23	6	97	274		98	191	11												677
	24		162	70	232	28	113													605
	25	3	17	185	74		147													426
	26	12	93	59	246		287								71				65	833
July	27		151		205	5	134				82		160	136	136	223	132	219		1583
	28	141	104		17	11	145		236		374		123	273	104	264	414	368		2574
	29	167	106	3	25	2	46		210	75	508									1142
	30		6	1	32	1				519	141									700
August	31		32	1	11															44
	32		6	23	8															37
	33			22																22
	34	53	25																	78
Total		404	811	871	1289	166	1351	1221	102	446	594	456	649	541	409	311	674	546	813	11654

Table 3.6. Analysis of deviance table from the full model (all salmon species and locations). Terms are listed in order of selection (most to least explanative) by the stepwise model selection algorithm. s(variable) indicates a smoothed function of a continuous variable with approximately 4 degrees of freedom. The magnitude of each effect is the difference, in the logit scale, between the maximum and minimum values calculated for that effect. The percentage shown under deviance reduced is the percentage of the total deviance difference between the full and null models accounted for by each term.

Term Added	Magni- tude	Df (residual)	Deviance (residual)	DF added	Deviance Reduced	Cp
Total Deviance (null model)		10877	12106	-	-	12108
+Year	5.0	10861	10743	16	1363 (11%)	10777
+s(BW)	3.6	10857	10159	4	585 (5%)	10201
+s(Lat)	1.6	10853	9727	4	432 (4%)	9777
+s(Lon)	2.5	10848	9560	4	167 (1%)	9620
+Species	0.7	10846	9478	2	82 (0.7%)	9542
+s(SST)	1.1	10842	9423	4	55 (0.4%)	9495
+s(Week)	1.2	10838	9401	4	22 (0.2%)	9481

Table 3.7. Significance of monthly trends of squid response. Number of fish, offset value, and significance of each fitted effect for each of four explanatory variables for the model $\text{logit}(\text{Squid}) = \text{offset} + s(\text{body weight}) + s(\text{latitude}) + s(\text{longitude}) + s(\text{sea surface temperature})$ fit for each species and each month over all years. Significance for a term is measured by dropping the term from the model, refitting the model to the remaining three variables, and comparing the deviance between the models using an X^2 -test (Venables and Ripley pg. 226). December-February were combined due to low sample sizes. Bold values indicate P-Values < 0.10.

Month	Species	Count	Offset	s(BW)	s(Lat.)	s(Lon.)	S(SST)
December-February	Sockeye	313	-1.58	.056	.37	.0046	.0018
	Pink	228	-3.77	.53	.99	.99	.99
	Coho	119	-0.125	.29	.00081	.0035	.061
April	Sockeye	383	-1.12	<.0001	.38	<.0001	.00098
	Pink	258	-3.69	.34	.37	.064	.32
	Coho	32	-1.32	.050	.21	.28	.58
May	Sockeye	1013	-1.61	<.0001	<.0001	.00077	.018
	Pink	481	-2.89	.054	.74	.028	.068
	Coho	103	-0.457	.82	.11	.12	.36
June	Sockeye	1464	-1.74	<.0001	<.0001	<.0001	<.0001
	Pink	884	-2.13	.022	.011	<.0001	.017
	Coho	186	-0.271	.35	.17	.65	.14
July	Sockeye	2232	-0.859	<.0001	<.0001	<.0001	<.0001
	Pink	2002	-0.944	<.0001	<.0001	<.0001	<.0001
	Coho	1167	-0.0922	.66	<.0001	<.0001	<.0001

Table 3.8. Estimated corrections to empirical logistic equation for each salmon species.

Species	N	Nsquid	Body weight cutoff (g)	Alpha offset (intercept)	Correlation coefficients		
					Sockeye	Pink	Coho
Sockeye	5831	1318	1000	-0.03	1		
Pink	4088	747	1000	-0.41	0.703	1	
Coho	1735	791	500	+0.60	0.752	0.718	1

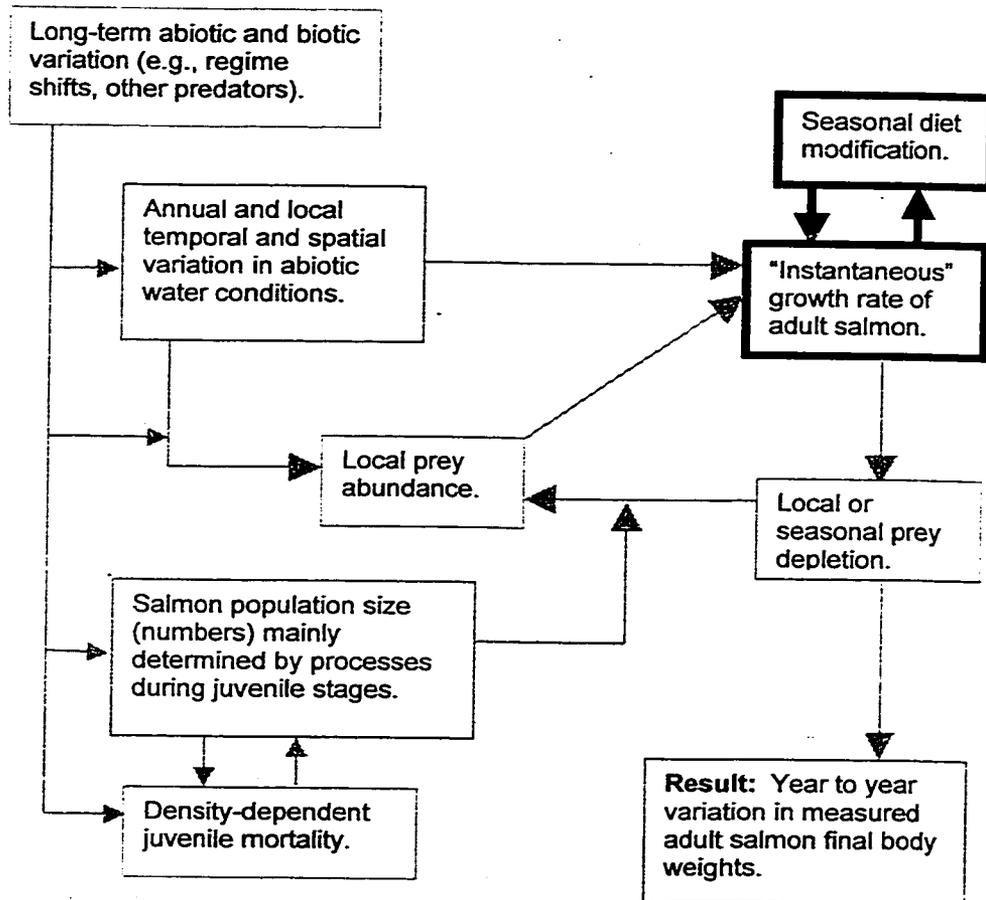


Figure 3.1. Aspects of salmon carrying capacity reviewed in Chapter 3 are shown by bold lines. See Chapter 1 for an explanation of this conceptual model of salmon carrying capacity.

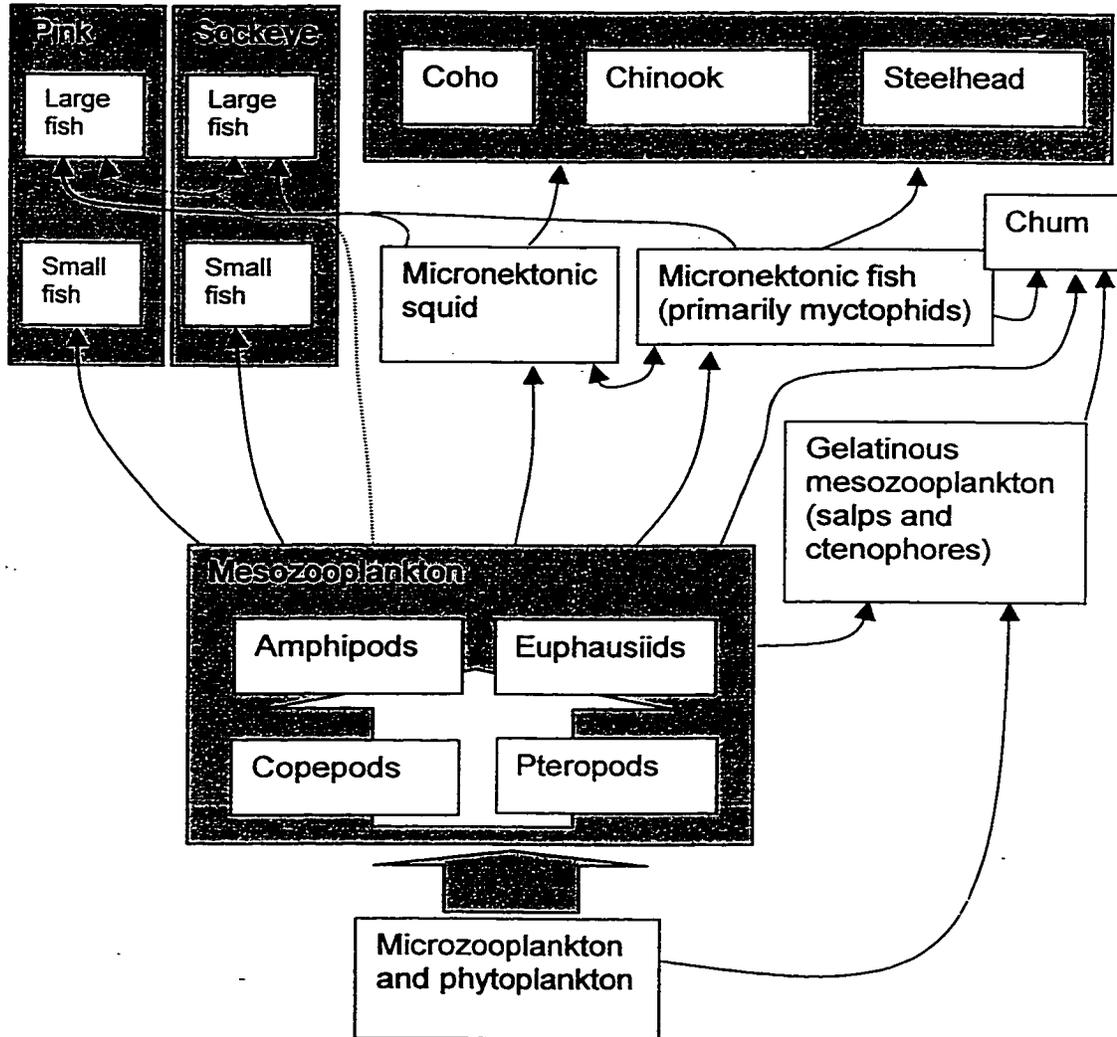


Figure 3.2. A generalized food web of post-juvenile (ocean age .1 or older) salmon prey in the northeastern Pacific Ocean (Alaska Gyre and Subarctic Current). Competitors and predators of salmon are not shown. Large block arrows indicate general flows for which pathways are not well-defined. Some lesser flows, such as plankton to coho, chinook, and steelhead, are not shown. Food webs containing salmon predators and competitors are found in Brodeur et al. 19xx and Pauly and Christensen (1996).

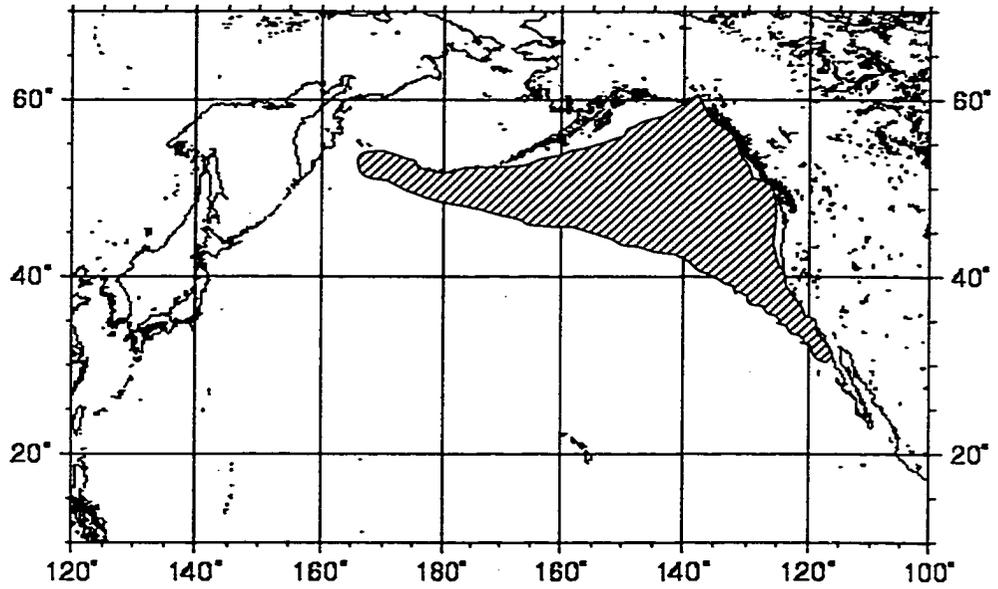


Figure 3.3. Reported range of *Berryteuthis anonychus*. Adapted from Nesis (1997).

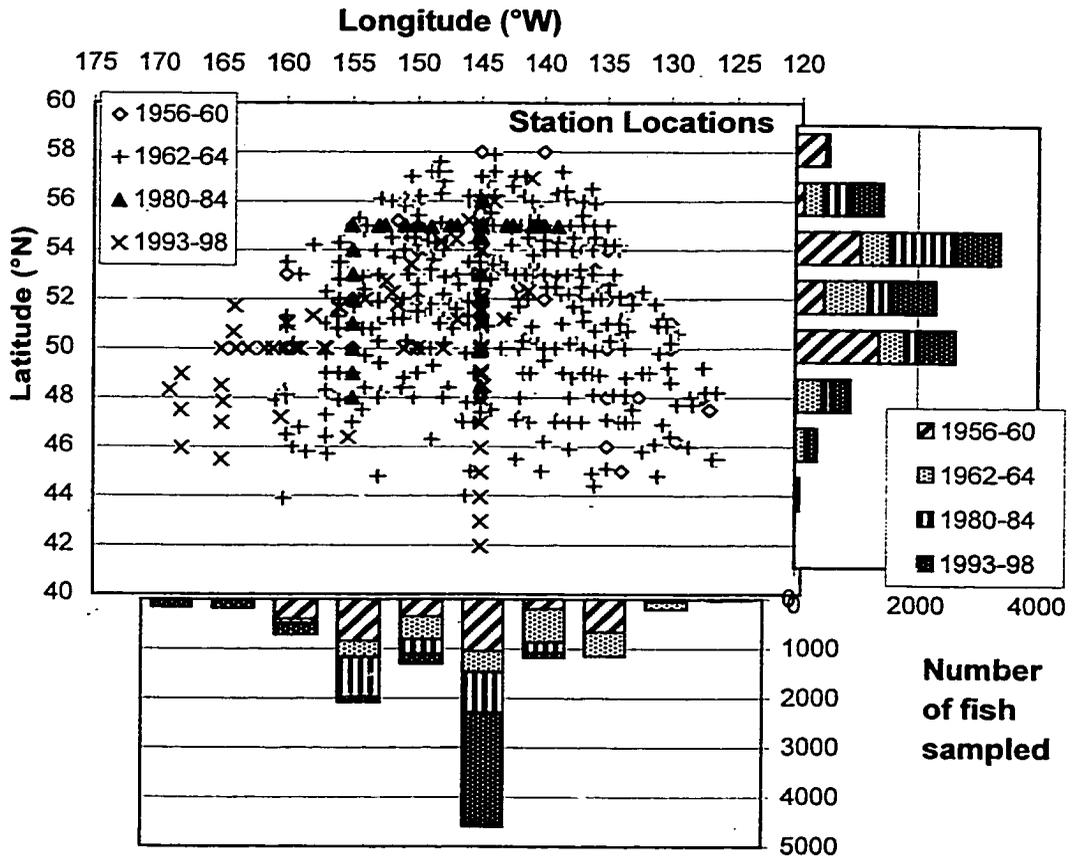


Figure 3.4. Sampling locations by latitude, longitude, and sampling period. Station locations and number of sockeye, pink and coho salmon sampled by latitude and longitude for each sampling period, all months. Histograms show number of fish caught by 2° latitude or 5° longitude blocks.

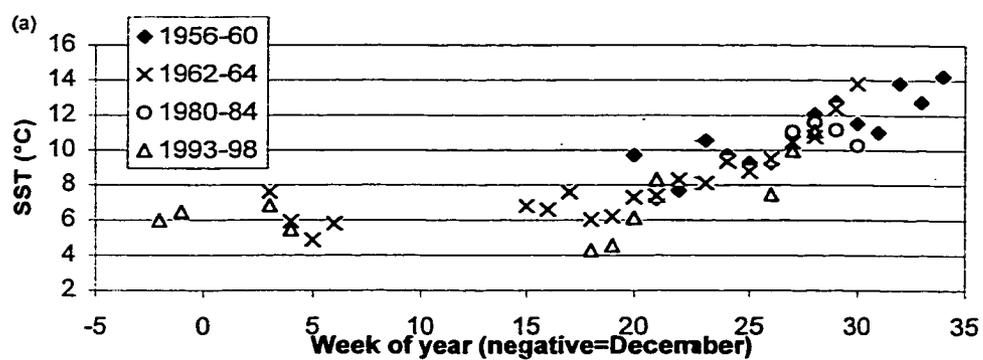


Figure 3.5. Sea surface temperature by week for each sampling period. Average sea surface temperature at all sampling locations by week and sampling period. Variation between sampling periods may be due to interannual variability or differences in latitude and longitude of sampling. Negative weeks=December.

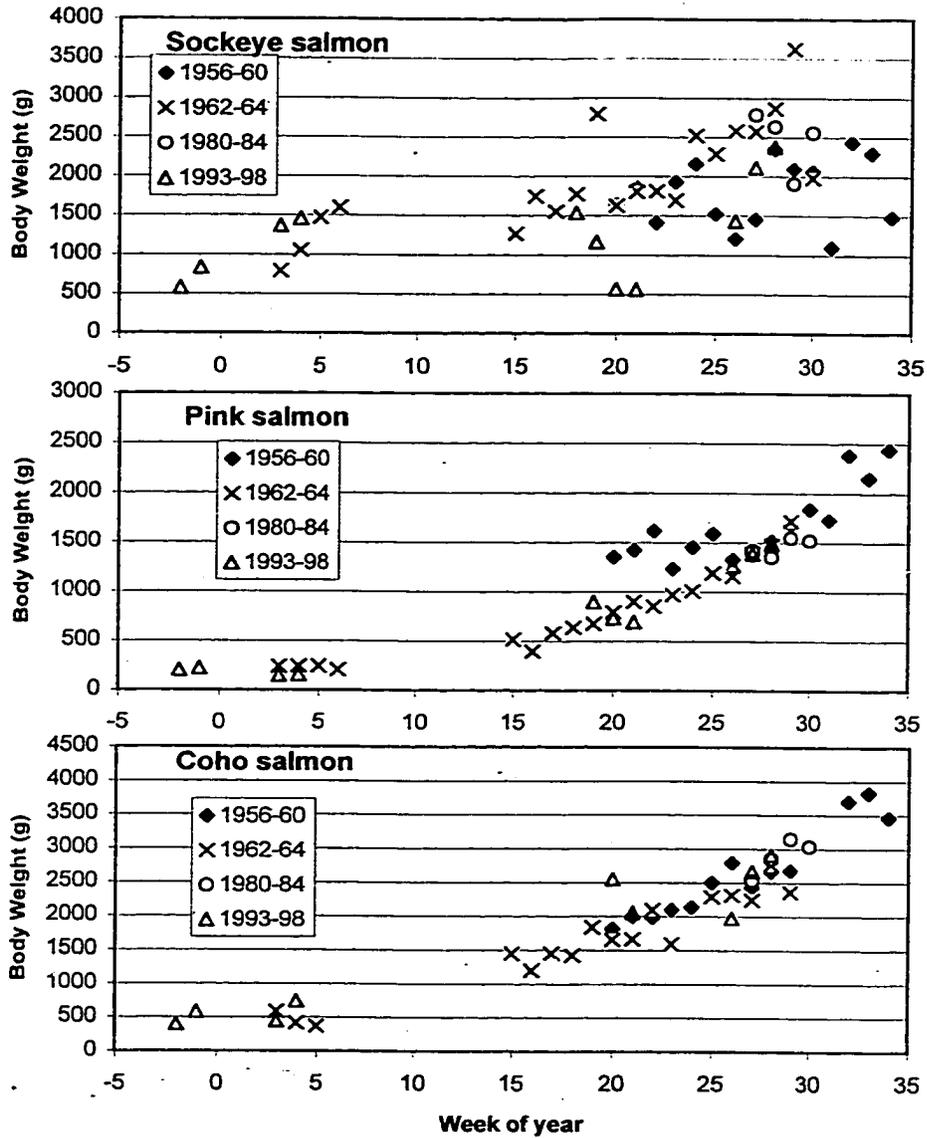


Figure 3.6. Seasonal trend in average salmon body weights. Average salmon body weights at all sampling locations by week and sampling period. Variation between sampling periods may be either due to interannual variability or differences in latitude and longitude of sampling. Negative weeks=December.

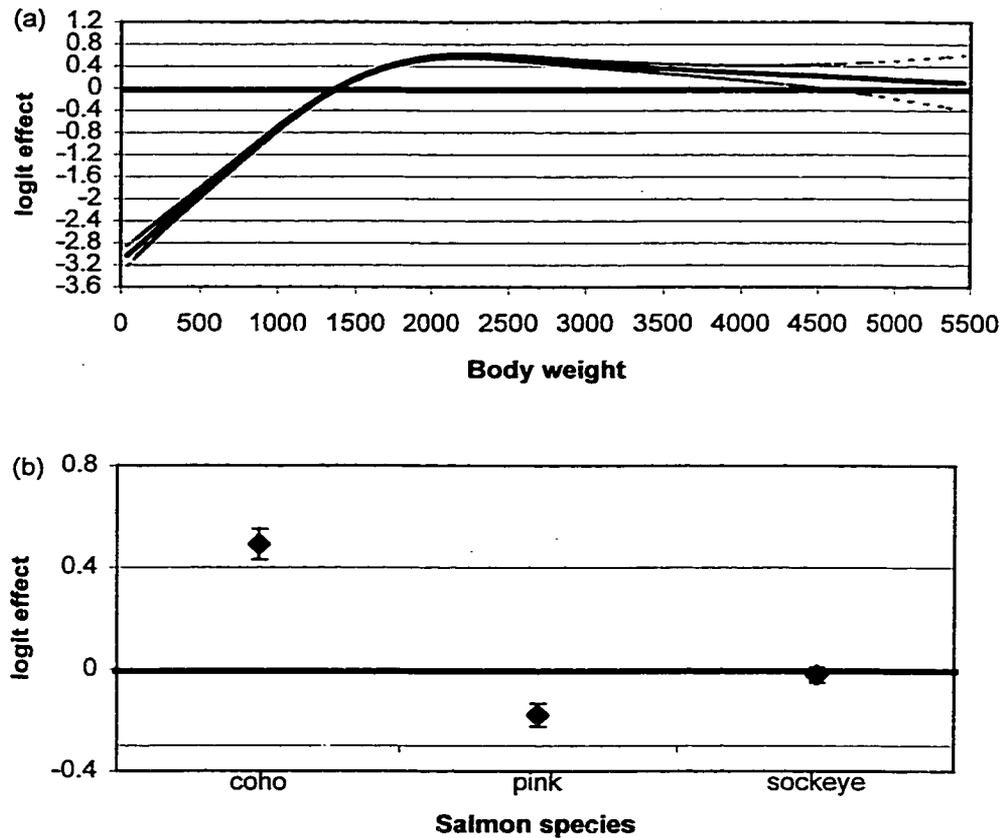


Figure 3.7. Fitted terms for fixed effects in the full model of Squid binary response, $\text{logit}(\text{squid}) = \text{constant} + s(\text{BW}) + \text{Species} + s(\text{Latitude}) + s(\text{Longitude}) + \text{Year} + s(\text{Week}) + \text{SST}$. All data are given in logit transformed probabilities. Each function is centered so that the average over all points=0. Dotted lines show standard error of partial residuals, calculated as outlined in Hastie (1993). Figure is continued on following two pages.

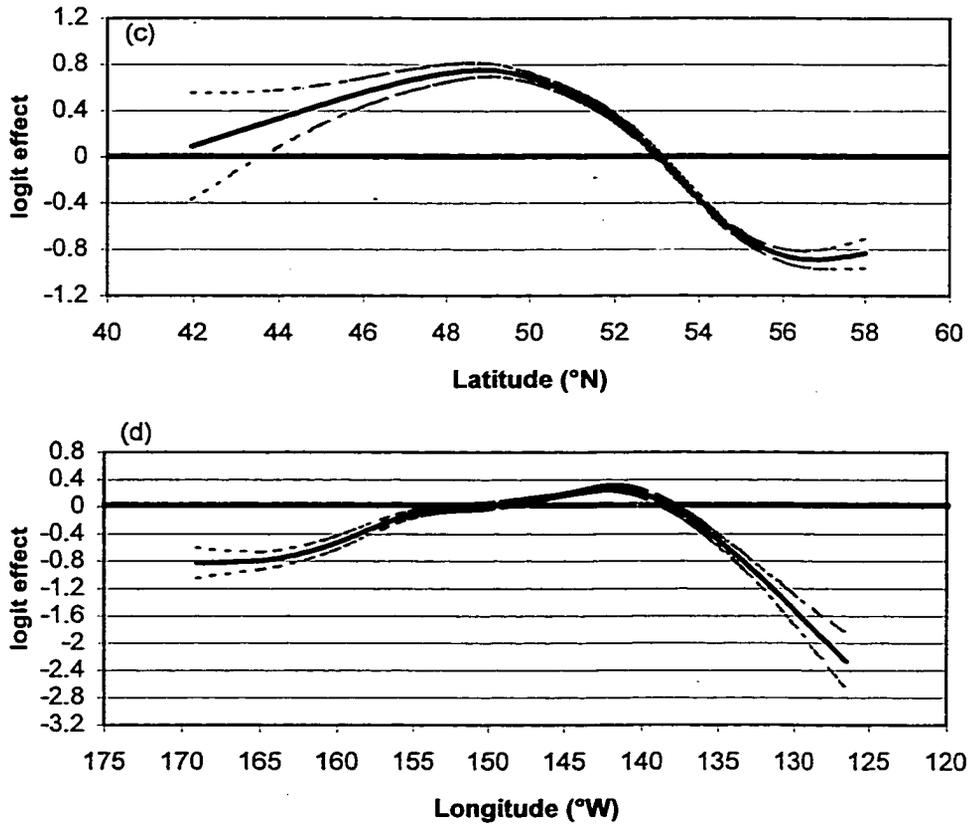


Figure 3.7(cont.) Fixed effects of full model.

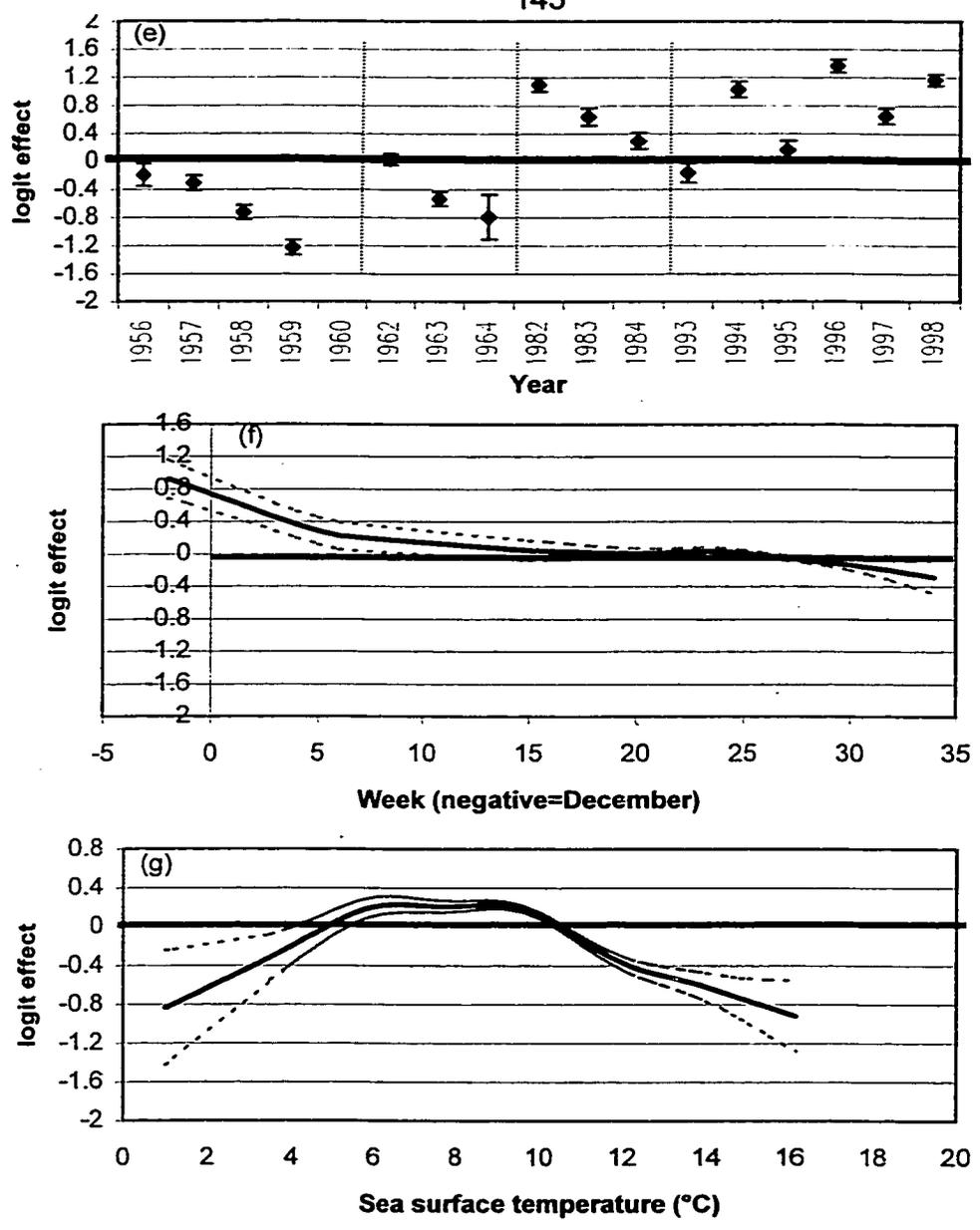


Figure 3.7(cont.) Fixed effects of full model. Vertical dotted lines in (e) show breaks between sampling periods. (*) in 1960 indicates low value (mean=-3.6).

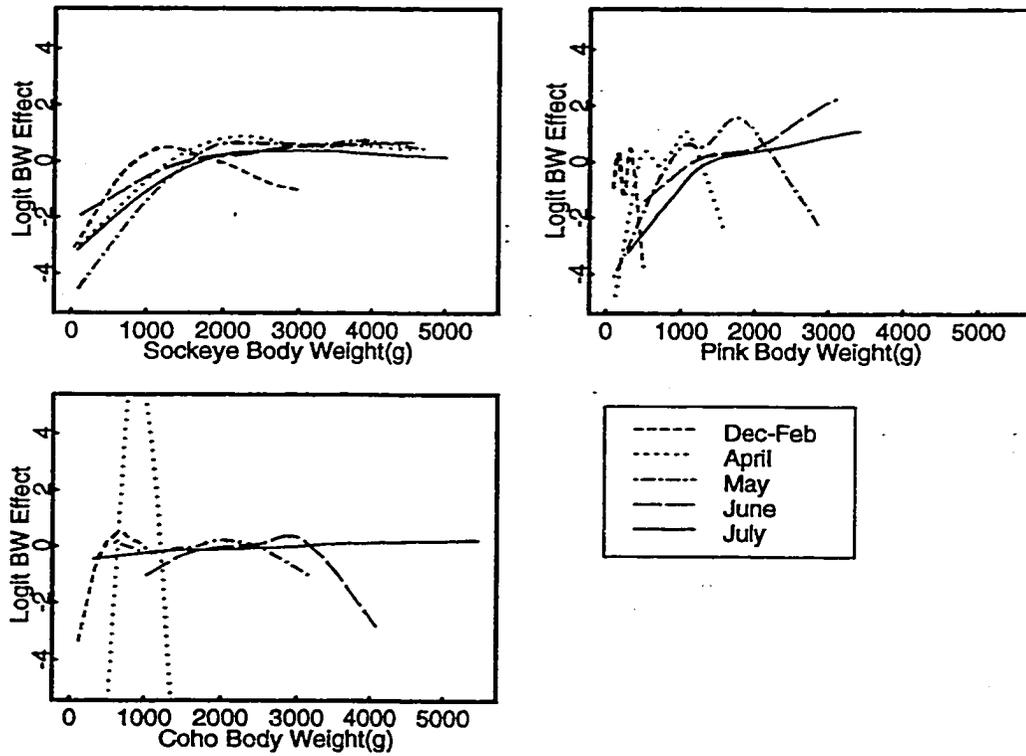


Figure 3.8. Body weight effect for each species, month. Body weight effect for each month and species, fitted to model $\text{logit}(\text{Squid}) = s(\text{Body weight}) + s(\text{Latitude}) + s(\text{Longitude}) + s(\text{SST})$, given month and species). Not all terms are significant: see Table 3.7 for significance values and offsets.

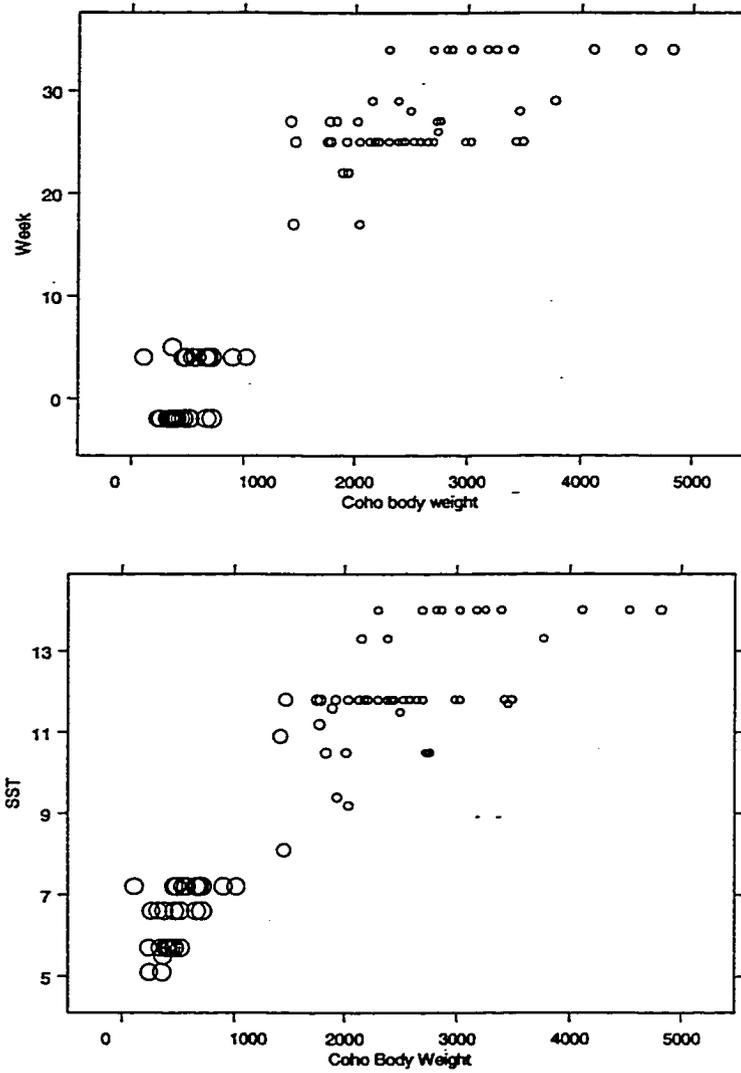


Figure 3.9. Coho response fitted to combined responses. Area of circles represents the logit response of coho salmon to squid, fitted to a function $s(\text{BW}, \text{week})$ in (a) and $s(\text{BW}, \text{SST})$ in (b).

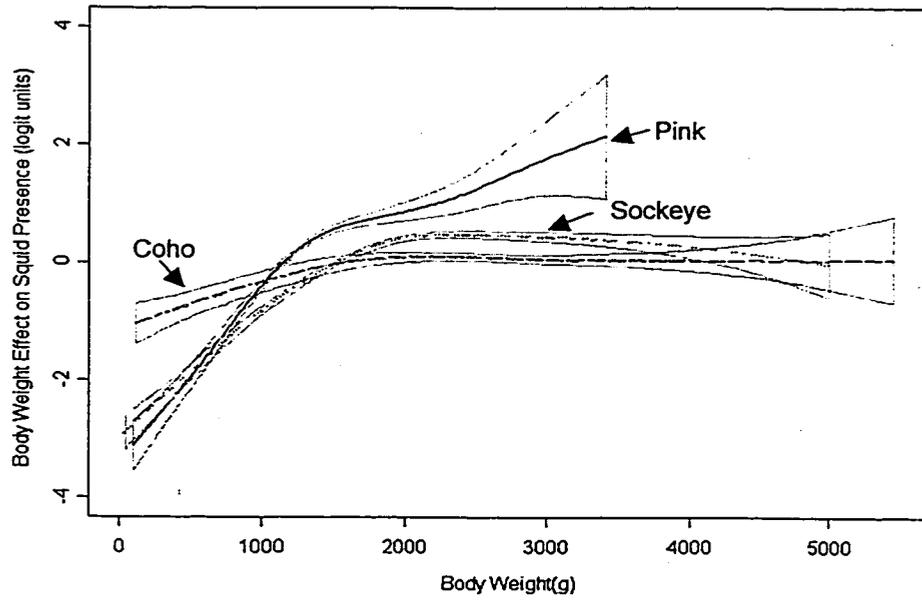


Figure 3.10. Body weight response curves for all three species. Shaded boxes indicate standard error of fit.

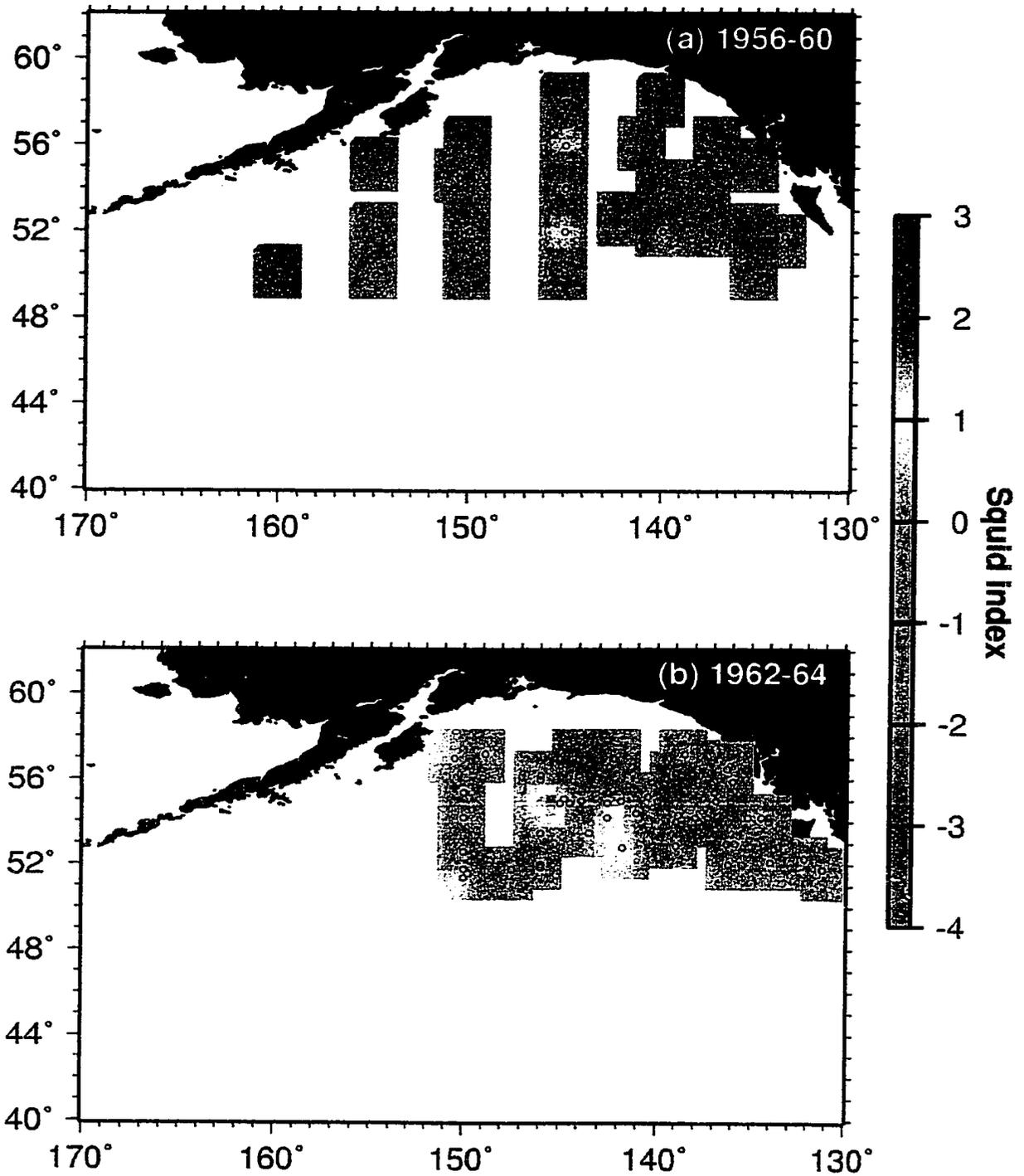


Figure 3.11. Squid index values by sampling period, pink, coho and sockeye salmon. Colors shown indicate the squid index values extrapolated over a (latitude)x(longitude) surface from the study locations shown by circles. Blank areas indicate no sampling within 1° of latitude or longitude. Figure is continued on following two pages.

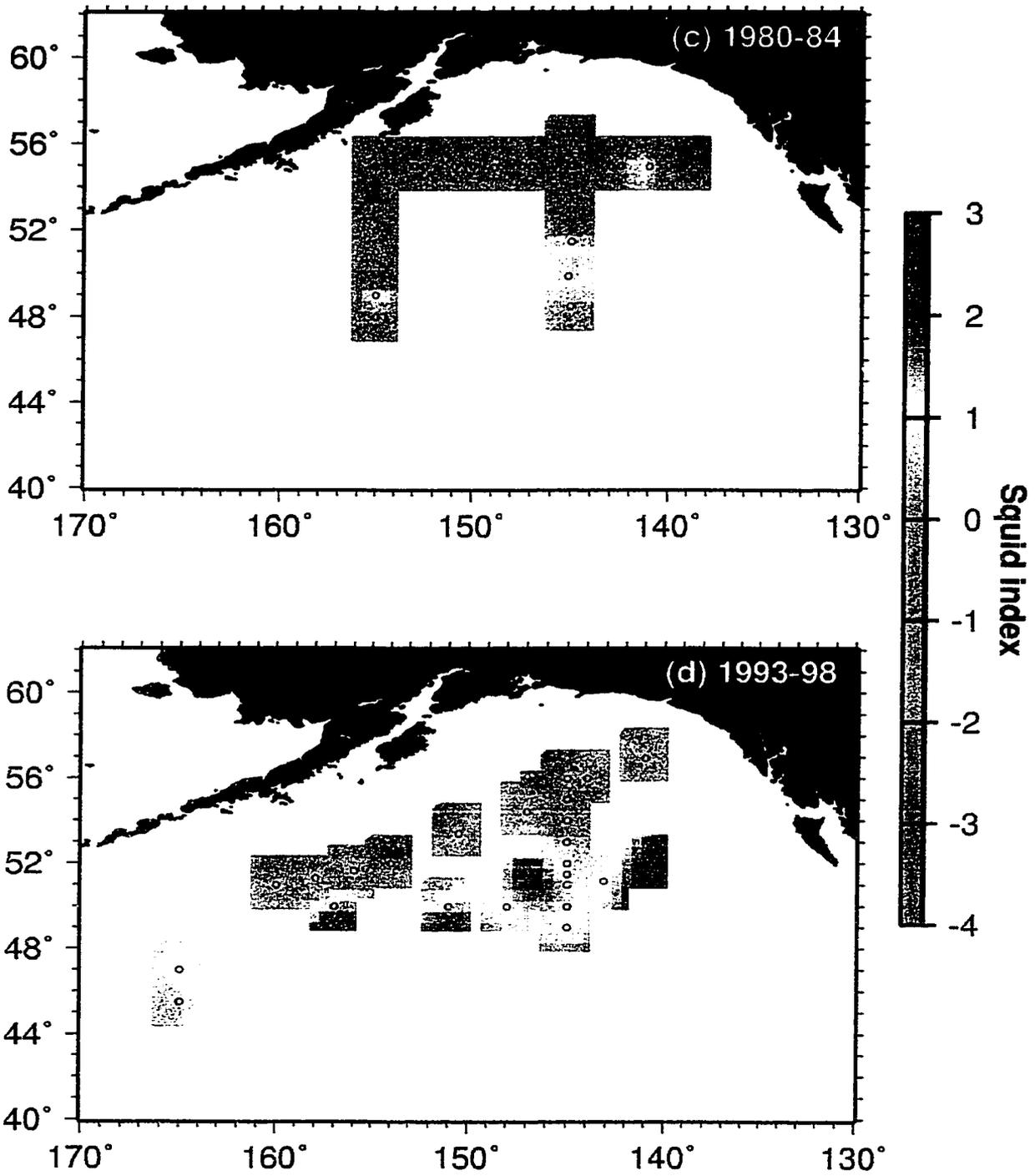


Figure 3.11(cont.) Squid index values by sampling period.

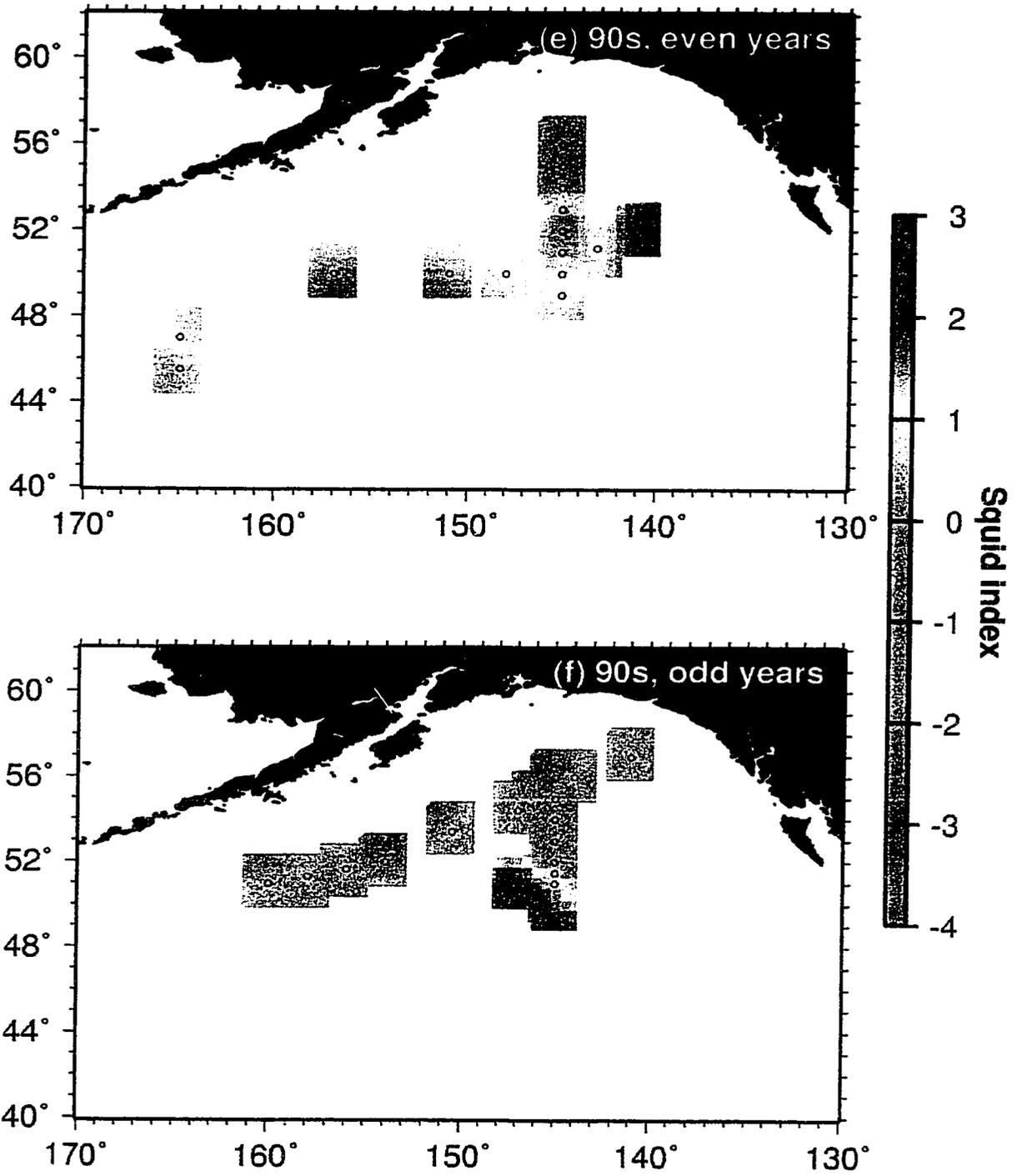


Figure 3.11(cont.) Squid index values by sampling period.

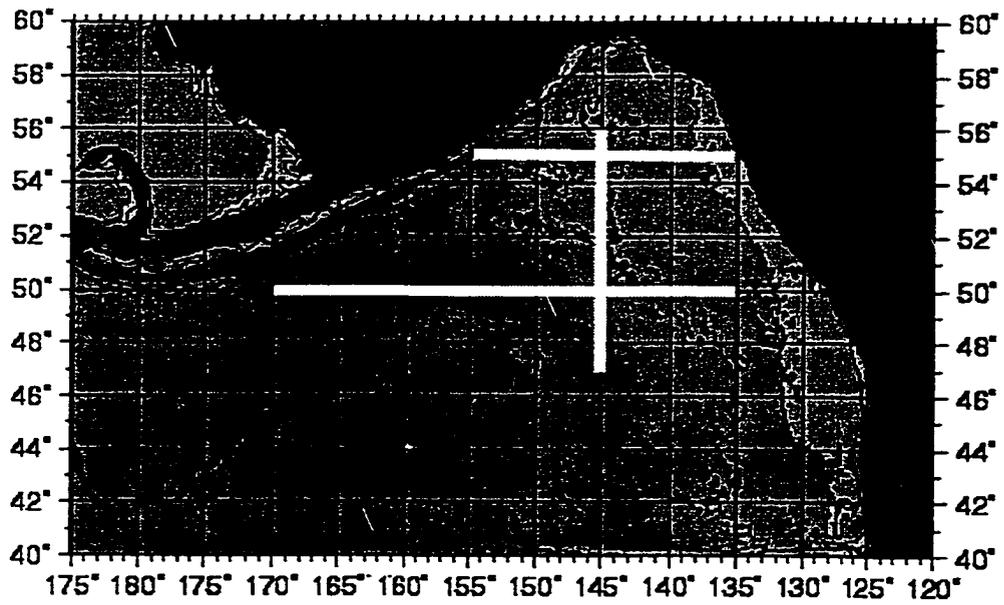


Figure 3.12. Three most-heavily sampled July transect lines. While lines indicate center of data pooled along each transect.

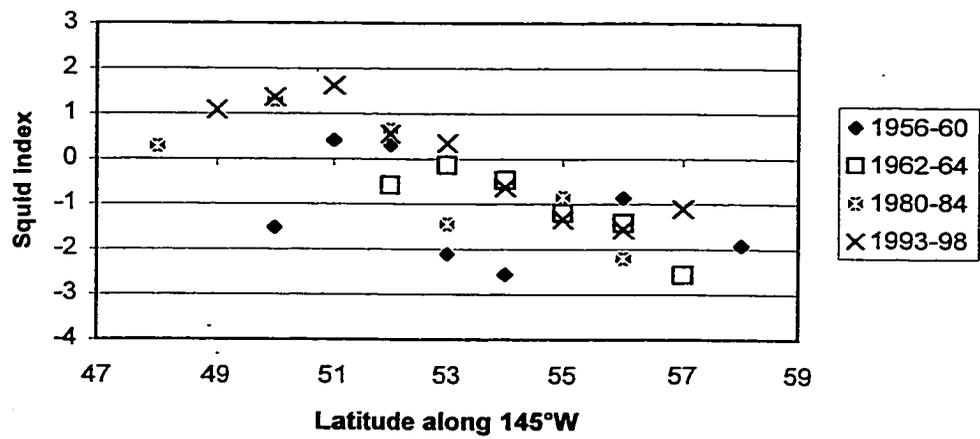


Figure 3.13. Squid index values for salmon along 145° W. Each point represents data from fish within a single years, and pools fish within 1° of the plotted latitude and within 5° longitude on either side of 145°W.

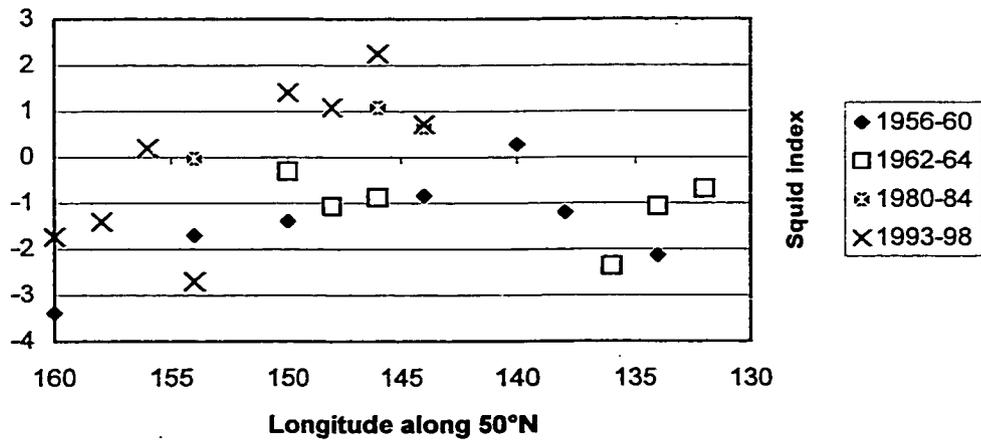


Figure 3.14. Squid index values for salmon along 50° N. Each point represents data from fish within a single years, and pools fish within 2° of the plotted longitude and within 2° latitude on either side of 50° N.

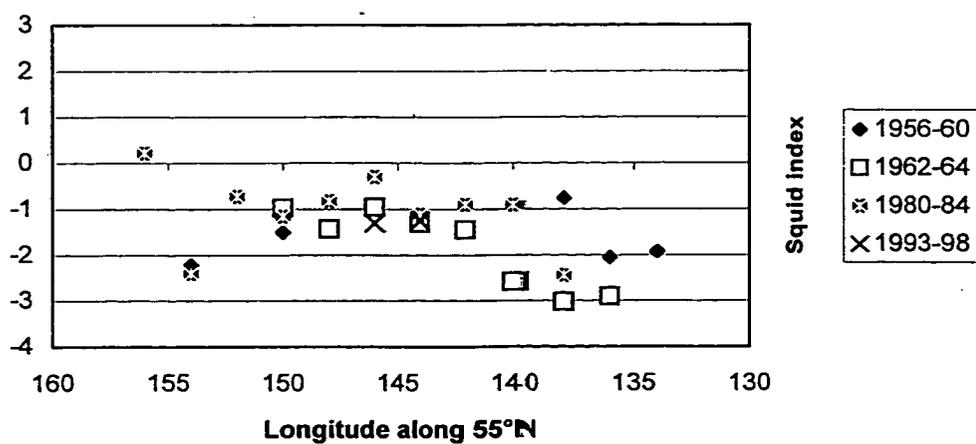


Figure 3.15. Squid index values for salmon along 55° N. Each point represents data from fish within a single years, and pools fish within 2° of the plotted longitude and within 2° latitude on either side of 55° N.

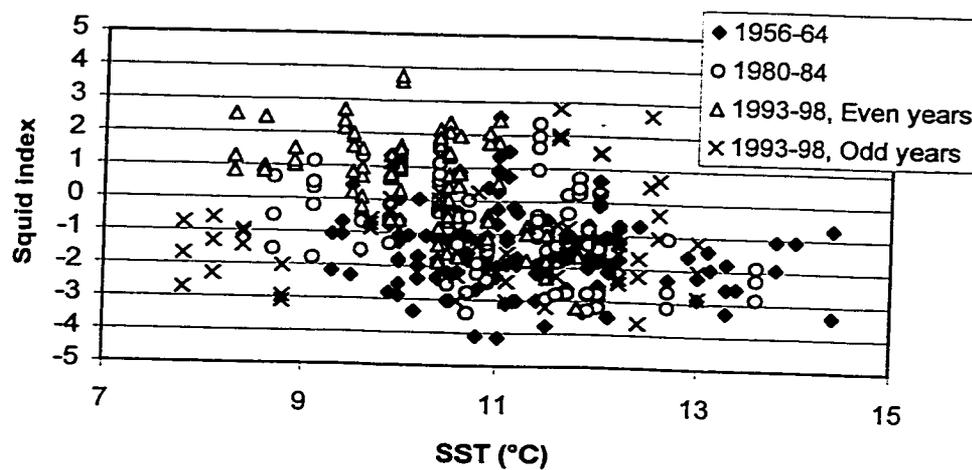


Figure 3.16. Squid index vs. sea surface temperature. Squid index values for all July stations plotted as a function of sea surface temperature.

4 Trophic and oceanographic aspects of the summer distribution of salmon prey in the Gulf of Alaska and consequences for salmon growth rates

4.1 Introduction

The models describing the relationship between adult Pacific salmon body weights and environmental factors in the North Pacific Ocean have, to date, focused on large-scale correlations rather than on mechanisms. For example, several studies have reported a negative relationship between annual ocean temperature anomalies over large areas and the adult body weights measured in many North American stocks of Pacific salmon (Hinch et al. 1995; Cox and Hinch 1997; Pyper and Peterman 1999).

Large-scale correlations are useful for prediction, provided that the mechanisms behind them are constant over time. If correlations are extrapolated over long time periods, it is important to determine if they have the potential to "break down" in the face of large scale climatic change. Investigating the mechanisms behind annual-scale correlations requires measuring processes on smaller scales. Due to the difficulty of sampling on a fine scale across the North Pacific, relationships between ocean conditions and salmon growth remain open to speculation (e.g., Welch et al. 1998).

Figure 4.1 shows a chain of causal relationships that may lead to variation in the summer growth rate of salmon (relationships highlighted in bold). Salmon put on 50-90% of their final body weight during the summer immediately prior to maturation (Ishida et al. 1998). Correlations between measurable environmental conditions and salmon body size may be the result of two mechanisms, shown by the bold arrows in Figure 4.1. The first mechanism is the result of temperature or other water conditions directly

affecting the physiology of salmon growth (line A). The second mechanism is the result of prey abundance affecting salmon growth (line B).

If the mechanism A is the predominant source of year-to-year variation in salmon growth, the correlation between the abiotic environmental factors and salmon body size is a direct mechanistic link. In this case, oceanographic models may legitimately link long-term climate change to salmon growth by modeling the effect of long-term climate change on the annual abiotic factors in question. This approach was taken by Welch et al. (1998), in which a model relating future sea surface temperature to global greenhouse warming was used to predict a decreased area of high seas salmon distribution with increased CO₂ concentration. They described a correlation between salmon distribution limits and sea surface temperature (line A) and extrapolated, by the climate model, a link between long-term climate change and salmon distribution.

However, if mechanism B is responsible for the correlation between abiotic factors and salmon growth, such long-range predictions may be inaccurate. The correlation between abiotic conditions with prey as an intermediary may show a similar correlation on the short term, but may break down on the long term if climate change affects the distribution of prey (line C).

In this chapter, I explore oceanographic variables, including sea surface temperature, salinity, and upper-layer mixing processes, in relation to prey distribution and modeled salmon growth rates. In Section 4.2, I present the results of food habits studies from five years of high seas salmon research cruises along a July transect in the northeastern Pacific (50°-56°N, 145°W, 1994-98). The results suggest that there are two distinct latitudinal summer feeding zones for salmon associated with the July latitudinal sea surface temperature minimum. The southern zone (south of 51°-54° N) is high in micronektonic squid between 6-12 cm mantle length, primarily the species *Beryteuthis anonychus*. The northern zone is higher in mesozooplankton in

both net samples and salmon stomachs. Moreover, temporal variation occurs in the biogeography of this food web, with the geographic overlap between salmon and squid varying from year to year. The difference in the diet and feeding rates of pink, coho, and sockeye salmon is substantial between the two regions.

In section 4.3, I describe the results of a set of bioenergetics models constructed using data from the experiments performed in Section 4.2. The results compare, within the range of variation present during the sampling period, the quantitative importance of mechanism A and mechanism B in determining the variation in measured salmon growth, especially with respect to the north/south zones.

If this zonal boundary extends across the northeast Pacific, the year-to-year variation in the size of the southern zone may be up to 2 million km². This variation in the biogeography of salmon prey may explain part of the previously noted relationship between ocean sea surface temperature and the adult body weight of salmon. In Section 4.4, I use sea surface temperature data from 1950-1998 as an index to the overlap area of salmon and squid to investigate the annual and decadal variation in the size of the overlap region. A more complete model of salmon growth must contain data on seasonal variation and salmon diet change with body size, and is presented in Chapter 5.

4.2 Variation in summer distribution of the prey of Pacific salmon in the offshore Gulf of Alaska in relation to oceanographic conditions, 1994-98

4.2.1 Introduction

This section reports the results of five years of summer salmonid food habits studies, conducted between 1994-98. Specifically, I examine the link

between physical ocean conditions and salmon prey variation during the sampling period. I examine prey distribution with respect to the temperature and salinity of the water column, and with respect to the annual variability of the position of oceanographic features such as fronts, water masses, and eddies. In doing so I pay particular attention to the changing proportions of micronektonic squid and zooplankton in salmon diets.

In studying trends in the ocean, an important question to ask is "what is a fixed point?" If data are taken at a fixed latitude and longitude over a number of years, a biological trend at that location may result from changes occurring within a single water mass, or from the shifting spatial positioning of an adjacent water mass. Many physical properties of the water column may be correlated during a single sampling period. For example, sea surface temperature may show a strong correlation with mixed-layer depth. If a biological variable is related to either variable, it would not be clear which of the physical variables has a direct mechanistic link to the biological process. This is important to consider if scenarios of climate change predict changes in the relationships between physical variables.

Within the Gulf of Alaska, several distinct water masses distinguish the upwelling center of the Alaskan Gyre (Ridge Domain) from the Subarctic Current on the south, the Alaskan Stream to the north, and the Alaskan Current to the northeast (Figure 4.2 and Chapter 2). The Gyre itself may shift from east to west on an interannual basis (Royer and Emery 1987), while the Subarctic Current may shift its waters to the north and south (Hollowed and Wooster 1992).

A study of salmon food habits by Percy et al. (1988) found that the Ridge Domain was high in zooplankton prey, while the Subarctic Current region was high in the micronektonic squid *Beryteuthis anonychus*. However, at the time not enough data existed to examine this hypothesis against a background

of shifting oceanographic boundaries. A primary purpose of this section is to examine salmon prey in relation to these shifting water masses.

4.2.2 Materials and methods

4.2.2.1 Study area

The data for this study were collected by the Japanese research vessel *Oshoro maru* along a transect line running from 50°N to 56° N along 145°W in 1994-98 (Figure 4.2). Stations were sampled between 1 July and 11 July in each year. Gillnet sampling was conducted at every degree of latitude, while oceanographic and plankton sampling were conducted at every half degree. In 1994, oceanographic and plankton data collection alternated between 145°W and 146°W; this relatively slight longitudinal variation was ignored in the analysis. Due to weather conditions and time limitations in 1995, fishing stations at 50°, 51° and 52° N were cancelled and replaced with a single fishing station at 51.5° N. The sampling methods and resulting oceanographic data from each cruise are published annually by Hokkaido University (e.g., Faculty of Fisheries 1998).

4.2.2.2 Oceanographic and zooplankton sampling

Vertical casts to 1500 or 3000 meters depth were made with a Neil Brown Mark IIIB CTD at each half degree of latitude. Temperature (°C) and salinity (psu, practical salinity units) were recorded continuously. Values of σ_t , the water density anomaly from 1000g/m³, were calculated by shipboard computer.

Zooplankton samples were collected by a 150m depth-to-surface tow of a twin plankton NORPAC net (0.45m ring diameter; 0.35mm mesh size (#200 filtering cloth; 1.8m length) while the ship drifted (speed 0 knots). Samples

were bottled with formalin and wet weight of each sample was determined. For most samples, gelatinous zooplankton was removed before bottling.

4.2.2.3 Salmon sampling

During July in the offshore Gulf of Alaska, maturing stocks of sockeye salmon and pink salmon east of 155° W longitude are primarily fish from Central Alaska, Southeastern Alaska, British Columbia, and Washington. In addition, immature sockeye are found from other North American stocks including Bristol Bay, although their numbers increase to the west of 155° W, south of the Aleutian Islands. Coho salmon may be from any North American stock. Immature chum salmon in the region are a mix of North American and Asian fish (Myers et al. 1996, Urawa et al. In press). Variation in prey availability in the study region may affect any or all of these stocks. Other salmonid species were not caught in large enough numbers to be analyzed in this study.

Salmon surface gillnet gear (0-6m fishing depth) was set prior to sunset and retrieved at sunrise at each station. The gillnet consisted of 47 to 49 panels of 50m-long tans (total length 2.45 km). The net was divided into panels of commercial gear and research gear, with 25-30 tans of research gear (multiple mesh sizes for non-size selective sampling) used at each station.

Biological data—scale samples, species, fork length (mm), body weight (g), sex, and gonad weight (g)—were taken from the first 60 fish of each species from each mesh size, which included almost all fish from the research mesh. Stomach contents were examined from up to 30 fish of each species in each gillnet set. Stomachs were sub-sampled from both commercial and research meshes as fish were being processed, with an attempt to apportion the collection among all size classes present. The methods used for stomach examination were similar to those of Pearcy et al. (1988), and are described in Kaeriyama et al. (in press). Total prey weights were determined, and percent volume of each identifiable prey type was estimated visually.

4.2.3 Data analysis

4.2.3.1 Oceanographic analysis

Summary CTD data at standard depths were used to determine latitude/depth isopleths using the Generic Mapping Tools software package (Smith and Wessel 1990; Wessel and Smith 1995). The depths of the top and bottom of both the seasonal and permanent pycnoclines at each station were estimated by locating the standard depths closest to the inflection points of curves fitted to the σ_t plot. The strength of the density gradient across the pycnocline was calculated as the buoyancy frequency N (Mann and Lazier 1996, pg. 62) across each pycnocline. Buoyancy frequency is proportional to the gradient of density across a pycnocline. Due to the smoothing procedure used across standard depths, the pycnocline depth was not resolvable to an accuracy greater than +/-5m. Daily mixing and precipitation was evident in the upper 10m of the water column, so stratification in the upper 10m could not be determined reliably.

Principle Components Analysis (PCA) was used to determine the common modes of variability for eight oceanographic variables: sea surface temperature (SST) and salinity, 100m temperature and salinity, seasonal pycnocline depth and maximum buoyancy frequency, and permanent pycnocline depth and maximum buoyancy frequency (Mathsoft 1995). These principle components were used to determine relationships between physical and biological properties.

4.2.3.2 Oceanographic domain determination

Two data sources were used to determine regional oceanographic boundaries. The first set of data was the CTD temperature, density, and salinity data collected along the transect. The second set was the July monthly averaged 1° x 1° resolution SSTs for the years 1981-present, calculated as

described in Reynolds and Smith (1994) and published electronically in the Integrated Global Ocean Services System Products Bulletin (IGOSS 2000). All boundaries were considered to occur halfway between two sampling stations, so every station was placed on one side of an oceanographic boundary.

From south to north, the distinct oceanographic domains along the transect line were the Subarctic Current, the Ridge Domain, and the Alaska Stream/Current (Figure 4.2). The boundary between the Subarctic Current and the Ridge Domain was placed each year between the two CTD stations showing the largest change in depth of the 4°C temperature isotherm, which rises from below 300m in the Subarctic Current to near 100m in the Ridge Domain. Pearcy et al. (1988) use a slightly different definition of the Ridge Domain, describing it as the latitude at which the 4° C isotherm reaches 100m depth. However, the isotherm did not reach that depth at any time during this study. The boundary between the Ridge Domain and the Alaska Current was placed at the latitude of northern descent of the 4°C isotherm from 100m to below 300m (Pearcy et al. 1988).

A plot of a single year of IGOS data along the transect shows that the SSTs along 145° W between 40°N and 58°N in a given year may be fit with little error to a quadratic curve with three parameters: the latitude of minimum temperature (MinLat), the minimum temperature (TMin), and the "curvature distance" (D) or rate of change of the north/south warming trend (Figure 4.3). These three parameters were fitted to the curve for each year by minimizing the sum of squares error between the curve and the data using an exhaustive fitting routine at the resolution of 0.05° latitude or 0.05°C. The calculated latitude of minimum temperature (hereafter SST minimum) was used as a boundary distinct from the Subarctic Current/Ridge Domain boundary.

The Alaska Current may create eddies, which move into the Ridge Domain, obscuring the Ridge Domain's presence while transporting coastal

water, or water from the southern portions of the Subarctic Current, into the Ridge Domain (Thomson and Gower 1998). Locations where mesoscale features appeared in the CTD data were noted in the analysis and examined for possible correlations with biological variables.

4.2.3.3 Zooplankton analysis

Zooplankton density measurements (mg/m^3) were log-transformed, and all stations at which $\ln[\text{density}]$ (representing the combined weights of gelatinous and non-gelatinous zooplankton) was greater than 7 were excluded from the analysis. The cutoff was determined after examining the statistical distribution of the raw data. Therefore, the samples should not be considered to represent concentrations of gelatinous zooplankton.

Due to this exclusion, and equipment difficulties, raw zooplankton measurements were not available at all stations. For each station, I averaged all undiscarded log-transformed zooplankton measurements taken within a 100km radius during the same year. The distance of 100km was chosen because (1) it would include multiple measurements at most gillnet stations, (2) it would leave mesoscale features, generally 200+km in size, resolvable, (3) it would provide smoothing over the area in which a salmon travelling 30-50km a day may have been feeding, and (4) a spatial study by Rand and Hinch (1998) showed that zooplankton concentrations in the Gulf were strongly autocorrelated to a range of 100km, with correlation in some years falling off sharply outside that distance.

The difference in total zooplankton wet weight between day and night sampling in 0-150m NORPAC samples was found to be non-significant in high latitude areas in the summer (Sugimoto and Tadokoro 1997), and day and night differences are not taken into account in this analysis. Phytoplankton data were also considered, as proxied by secchi depth (Sugimoto and Tadokoro 1997).

However, due to the amount of error inherent in this method, limited analysis was performed on these data.

4.2.3.4 Salmon CPUE and body weight

Catch-per-unit-effort (CPUE) of each gillnet operation was calculated from the total number of each species of salmon caught in the research (non-selective) gillnet. The research gear from an overnight net set, or approximately 30 tans of mixed-mesh gear, was considered to be a single unit of effort.

The freshwater and ocean age class of each fish was determined by counting the number of freshwater and ocean annuli on acetate impressions of scales. Maturity of salmonids in the samples was determined from gonad weights. The criteria used for determining maturity is reported by Takagi (1961). To determine the CPUE of individual age and maturity classes, the total number of each species caught in a single set was multiplied by the proportion of each age or maturity class in the catch.

For the analysis, log-transformed CPUE values were derived from the formula $\ln[CPUE+1]$. Salmon catch has been found to conform to a negative binomial distribution rather than to a lognormal distribution (Welch and Ishida 1994), so the parametric statistical tests used to analyze CPUE in this section may not provide an accurate accounting of error probabilities.

Salmon body weights were stratified by species, age, and maturity, and log-transformed prior to analysis.

4.2.3.5 Salmon stomach contents and squid density estimation

The patchy nature of prey distribution requires the use of detailed bioenergetics simulation modeling and Monte Carlo techniques to determine the effect of each prey type on salmon growth. Details of the abundance and importance individual prey types in the salmon diet are presented in Kaeriyama

et al. (in press), while differences in growth resulting from prey variation are discussed in Section 4.3.

For each gillnet station, I calculated the index of micronektonic squid density derived in Chapter 3, using food habits data from pink, sockeye, and coho salmon. Chum salmon do not feed on squid often enough to be used for this index. The formula used was:

$$SquidIndex = \ln \left[\frac{N_{squid,species} + \frac{1}{2}}{N_{total,species} - N_{squid,species} + \frac{1}{2}} \right] - \alpha_{species}$$

$BW \geq BW_{cutoff}_{species}$
 $species = \{pink, coho, sockeye\}$

This formula gives three comparable estimates of the squid index at each station, provided all three species (pink, coho, and sockeye salmon) are sampled at the station. $N_{total,species}$ is the number of fish stomachs sampled in a given species, where only fish with body weights above BW_{cutoff} are used. $N_{squid,species}$ is the number of those fish with stomachs containing non-larval squid. The correction α is used to calibrate the estimates with respect to each other. The body weight cutoff and correction α for each species are given in Table 4.1.

The squid index is an empirical logistic variable (Cox and Snell 1989). If prey capture is considered to be a Poisson process, the squid index is approximately proportional to $\ln[\text{density}]$ in the range $-3 < \text{Index} < 3$, where $[\text{density}]$ is the numerical density of squid in the foraging area (Chapter 3). Thus, this corrected squid index may be treated as a log-CPUE index, which uses the salmon as the sampling gear, and the differing α for each of pink, sockeye and coho constituting empirical "gear corrections" for species-specific behavior. In this study, the three estimates of squid density were pooled into a single estimate for each gillnet station.

4.2.3.6 Determining relationships between variables

Each of the biological variables described above—zooplankton density, squid index values, CPUE and body weight of salmon (by species and age) and the prey weight—was analyzed with respect to physical variables. The physical variables considered were year, latitude, ocean domain/boundaries, and the principle components of the eight water column variables. The relationship between biological and physical variables were examined by constructing Generalized Linear Models (GLMs) for the potential biological/physical relationships (McCullagh and Nelder 1989).

The process used to select the best statistical models for each variable was a manual stepwise model selection procedure, where linear first-order interactions of each of the physical variables were examined in turn, and second- and higher-order interactions were examined where appropriate.

4.2.4 Results

CTD sampling occurred at 83 stations while NORPAC sampling included 131 zooplankton samples over these stations, 5 of which were discarded due to the presence of gelatinous material. A total of 876 pink, 1,124 sockeye, 412 coho and 1,320 chum salmon was measured at 33 gillnet stations. From these, a total of 2,471 stomach samples was taken. For sockeye and chum, ocean ages .1-.3 made up over 99% of the samples. For calculating the squid index, 1,738 pink, coho and sockeye stomachs came from fish with body weights above the species-specific cutoffs, with at least 22 and an average of 51 being sampled for squid at each station.

4.2.4.1 Oceanographic variables along 145°W, 1994-98

In 1995, precipitation caused measurements of sea surface salinity to be anomalously low at a few stations (<29 psu). These salinity values were

replaced with salinity values at 1m depth, which were all greater than 32 psu. No other corrections were made in the oceanographic data prior to analysis.

In all years, a seasonal thermocline was visible between 20-50m depth (Figure 4.4). At most stations, the seasonal thermocline was the point of highest buoyancy frequency in the water column, although in 1995 and 1998 some strong surface stratification was visible in the top 5m (Figure 4.5). In all years, mixed-layer water temperatures were high in the south, decreased to a minimum between 51-53°N, and increased again in the north. The mixed layer was generally shallower and stronger in the north and weaker and deeper in the south. Temperatures were warmest in 1997 and cooler in 1996 and 1998. In 1997, the mixed layer was shallow with strong stratification along the entire transect.

Salinity at the sea surface south of 56°N was similar in all years, although surface precipitation in 1995 made it highly variable (Figure 4.6a). North of 56°N, the low saline surface water in 1994 and 1995 is evidence of the Alaska Stream. At 100m depth, there is an interannual difference in salinity values between 51°-53°N: in 1995 and 1998, this region is more saline than 33 psu, while in the other years it is less saline than 33 psu (Figure 4.6b). Water fresher than 33 psu at 100m depth is one indicator of the Dilute Domain (Chapter 2), so the Dilute Domain may be in evidence in 1994, 1996, and 1997 between 51-53°N.

The maximum gradient in the permanent pycnocline occurs between 80-120m at most stations (Figure 4.5). The exceptions are between 51-53°N in 1997, when the pycnocline was deeper, and between 55-57°N in 1995, when the pycnocline was not visible. This latter anomaly is due to the presence of a strong downwelling (clockwise) eddy between 55-57°N, which is also shown by the intrusion of 6°C water to depths of 200m. Dynamic topography maps confirm the presence of this eddy in 1995 (Onishi et al. 2000). Downwelling

eddies also occurred between 52-54°N in 1998, and near 52°N in 1994. Weaker downwelling eddies were reported in all years (Onishi et al. 2000).

4.2.4.2 Principle components analysis

SST was positively correlated with seasonal mixed-layer strength, and negatively correlated with seasonal mixed-layer depth (Table 4.2). Seasonal pycnocline depth and strength showed a significant negative correlation. This result is expected, because surface warming is the primary factor affecting the seasonal mixed-layer strength and depth (Tully 1965). Because the permanent pycnocline represents a sharp halocline, there is a significant negative correlation between permanent pycnocline depth and salinity at 100m. More dilute southern waters in 1994, 1996 and 1997 may be characteristic of the dilute domain, but it is not possible to determine this with the available data.

The first two principle components (PCs) derived from this correlation matrix account for 58% of the variation in the data set, while the first five PCs account for 91% of the variation (Table 4.3). By convention, only variables accounting for the first 90% of the variation are retained for further analysis (Mathsoft 1995). An examination of PC5 revealed that it was the result of a single anomalous data point in 1995 at 55.5°N, where the permanent pycnocline was not evident. Therefore, PCs 5-8 were not analyzed further.

PC1 is primarily a measure of the properties of the seasonal thermocline. It represents the combined surface water characteristics of sea surface temperature, mixed-layer depth, and mixed-layer strength. Stations with maximum values of PC1 show very warm surface-layer temperatures with SSTs between 12-14°C, while stations with minimum values have surface-layer temperatures below 10°C. PC1 values show interannual variability, with 1997 having a warmer, shallower mixed layer, and 1996 and 1998 being cooler and more well-mixed on the surface. PC1 values tend to increase from south to north (Figure 4.7).

The remaining three principle components reflect processes in the permanent pycnocline that are associated with the oceanic domains. High values of PC2 indicate dilute surface waters and a deeper, less stratified permanent pycnocline, typical of the Alaskan Stream. PC3 and PC4, both possess temperature at 100m as an important contributor. The colder temperatures at 100m are indicative of the doming of the Ridge Domain, and high values of PC3 and PC4 occur within the Ridge Domain. Because PC2-PC4 are indicators of oceanographic domain characteristics, they are redundant with the domain definitions (Subarctic Current, Ridge Domain, Alaska Current) determined by examination of the TS plots.

4.2.4.3 Oceanographic boundaries

In all years, the Ridge Domain of $\sim 4^{\circ}\text{C}$ water was evident along the transect, rising from below 300m to depths of 100-200m (Figure 4.8). In 1994, the rise was between 50° and 51°N , and in 1995-97 the rise was between 51° and 53°N . In 1998, a weak rise occurred at 51°N and a sharper rise occurred between 53° and 54°N , with an intrusion of warmer water to 150m between the two rises. The sharper northern rise was chosen for the Ridge Domain boundary. In all years, north of 55° - 56°N the Ridge Domain was not evident, either due to eddy activity in the north or the presence of the Alaska Stream. The latitudes of the Ridge/Subarctic Current and Gyre/Alaska Stream boundaries are shown in Figures 4.8-9.

The SST minimum ranged between 50.5°N and 53.5°N . The minimum was furthest to the south in 1997 and furthest to the north in 1996 (Figures 4.8-9). The minima generally corresponded with locations of SST minima seen in the *Oshoro maru* data, except in 1995 when turbulent conditions may have affected shipboard measurements.

All three of the first-order models for PC1 (pooled by domain, pooled north or south of the SST minimum, and fit linearly to latitude) were significantly

better than the null model at explaining the latitudinal variation in PC1. However, the SST minimum explained a greater proportion of the variance (31% of the total variance) compared with 20% and 17% for latitude and domain, respectively (Table 4.4). Using latitude as an additive term in the two-pool SST minimum model did not increase the amount of variance explained. The exploration of 2nd- and 3rd-order nonlinear functions of latitude did not result in a significant decrease in the best model's residual variance. This result indicates that in any given year, variation in the common mode of sea surface temperature and seasonal mixed-layer variation is best explained by distinguishing two zones, with a discontinuity located at the yearly SST minimum. Water is warmer and more stratified north of this border, and cooler and less stratified south of this border.

4.2.4.4 Zooplankton

Zooplankton densities, averaged at 100km resolution, are shown by year and latitude in Figure 4.10. Stepwise linear model selection of the explanatory variables showed that log-transformed zooplankton measurements were significantly different between domains (1-way ANOVA, $P < 0.04$). The average zooplankton densities over all years were lowest in the Subarctic Current (average: 180 g/1000m³) and highest in the Ridge Domain (average: 253 g/1000m³). Values in the Alaska Current averaged 221 g/1000m³.

The north to south change from high to low zooplankton density along the transect was correlated with domain boundaries, and the change is steep and evident in the zooplankton data, especially between 1996-1998. Patches of high or low zooplankton densities co-occurred with anticyclonic eddies in 1994, 1995 and 1998 (eddies shown by arrows in Figure 4.10).

When the stations in the Alaska Stream were removed, the southern boundary between areas of high and low zooplankton densities was more strongly associated with the SST minimum than with the Ridge/Subarctic

Boundary. A 1-way ANOVA between the two models showed a significant difference in the amount of variance explained ($P < 0.05$), with the SST minimum break explaining 21% of the zooplankton variance south of the Alaska Current, while the Ridge/Subarctic Current partitioning explained only 11% (Table 4.5).

Zooplankton showed a weak positive correlation with phytoplankton as proxied by secchi depth ($R = 0.11$). This is probably due to the effect of mesoscale vertical concentration and dilution features, such as the 1998 eddy, acting on both phytoplankton and zooplankton (Figure 4.11). Relationships between zooplankton and either of PC1 or latitude were not significant.

4.2.4.5 Squid indices

In most years, salmon were not collected far enough to the north to examine squid or salmon in the Alaska Current. Therefore, all Alaska Current stations were removed from the analysis of squid density and salmon biological characteristics. Examination of squid specimens from stomachs indicated that over 90% of the squid found in salmon stomachs were *Berryteuthis anonychus*, with the remainder being *Gonatus onyx* or unidentified species.

Examined station-by-station, the squid index values calculated separately for pink, sockeye, and coho salmon were highly correlated ($R = 0.75$ to 0.85 , $P < 0.001$), confirming that most of the variation in index values was due to factors common to all three species varying between stations, such as the environmental density of squid. Values of the pooled index ranged from -2.5 and 2.5 across all stations. This corresponds to a range of from 5% to 95% of salmon with squid in stomachs.

The pooled squid index showed significant first-order interactions with latitude, PC1, and the SST minimum. In addition, several of the additive interactions between the three variables were significant (Table 4.6). However, it was not immediately possible to choose a "best" model from among the

multiple interactions of the three variables on squid densities, as the three explanatory variables were not independent.

To clarify the situation, squid index values were plotted versus both latitude and PC1 (Figure 4.12). While PC1 and latitude are not truly orthogonal, this graph shows the relationship of squid abundance to the three variables. Squid index values were higher in the south, and at colder surface temperatures with deeper seasonal mixed layers. More importantly, there is a sharp linear boundary between high and low squid index values (dotted line in Figure 4.12). In any given year, all positive squid index values were on the southern end of the transect, and all negative values were on the northern end of the transect.

The latitude of the cutoff varied from year to year (Figures 4.13-14). The latitude at which squid abundance drops and the SST minimum for each year are significantly correlated (Table 4.7). The correlation between the Ridge/Subarctic Boundary and the squid boundary is not significant. A clear distinction between northern and southern values for the squid index may also be observed by plotting estimates of the standard error of the index (Figure 4.15).

4.2.4.6 Interannual variation of salmon prey within each domain

Figure 4.16 shows the average value, by year, for each of PC1, zooplankton, and squid, for the sampling area north and south of the SST minimum. All variables showed significant differences between the two zones, both overall and within a single year. Within each zone, not all variables differed between zones. PC1 varied significantly in each zone across the five years, with high values in 1994 and 1997 (1-way ANOVA, $P < 0.005$). Zooplankton showed a significant increase in the northern zone between 1994 and 1998 (1-way ANOVA, $P < 0.005$), but did not vary significantly in the south. Squid index values were not significantly different between any of the years.

When the variables were examined on a station-by-station level within each year and region, there were no significant correlations.

4.2.4.7 Salmon CPUE

Log-transformed CPUEs for salmon showed few significant differences between ocean domains or across the SST minimum (Table 4.8). The exception was for ocean age .1 and .2 sockeye, which had higher CPUEs in the Ridge Domain than in the other two domains. All of the remaining species and ocean age classes, except for ocean age .3 chum salmon, showed a significant relationship between CPUE and latitude, with catches increasing from the south to the north. CPUEs of ocean age .1 sockeye salmon also showed a significant negative correlation with PC1. No other groups showed any response to this variable (Table 4.8). Pink salmon, ocean age .2 and .3 chum salmon, and ocean age .3 sockeye salmon showed significant differences in CPUE by year.

4.2.4.8 Salmon body weights

Of the 14 age and maturity classes caught in large enough numbers for analysis, seven groups showed significant size differences between the north and the south. All significant chum salmon differences showed larger body weights north of the SST minimum, while coho, pink, and maturing .2-.3 sockeye salmon showed significantly larger body weights to the south (Table 4.9).

Within the southern and the northern zones, several of the species/age-class combinations showed significant interannual variation in body weight. Specifically, the fish with the largest average body weights—coho, ocean-age .3 chum and maturing ocean-age .2 sockeye salmon—were largest in 1996 and 1998 and smallest in 1995 and 1997 (Figure 4.17a). Conversely, two of the smallest size groups—ocean age .1 sockeye salmon in the south and the north—were significantly larger in 1997 than in any other year (Figure 4.17c).

Groups in the middle size range showed no clear year-to-year trend (Figure 4.17b).

4.2.5 Discussion

The analysis of zooplankton and micronektonic squid along the transect line supports the existence of a biological boundary affecting salmon feeding ontogeny between 50-54°N, associated with the July sea surface temperature minimum (Tables 4.5-6 and Figures 4.10-12). This boundary was noted by LeBrasseur (1966), who described the predominance of squid in salmon diets in the Subarctic Current. Percy et al. (1988) similarly noted a biological boundary along 155°W in 1984 and 1985, but again associated the boundary with the border between the Subarctic Current and the Ridge Domain. However, our analysis shows that the SST minimum is more strongly correlated with the biological boundary than the Ridge/Subarctic border.

An examination of data in Percy et al. (1998), in comparison with the SST minimum for those two years, indicates that the SST minimum is a good fit to the boundary for those years as well. Part of the issue may lie in the definition of the Subarctic/Ridge boundary—it may be that the SST minimum was simply a better indicator of this boundary along 145°W during the sampling period.

South of this boundary, sea surface temperatures are cooler, and the seasonal mixed-layer is deeper with weaker stratification than is found north of the boundary. Zooplankton density is lower to the south and higher to the north, while the density of the micronektonic squid *Beryteuthis anonychus*, as indexed from salmon stomach sampling, is higher in the south than in the north. The latitude of this boundary varies from year to year between 51°N in 1997 and 54°N in 1998, a distance of over 300 km.

Within each of the two regions, the sea surface temperature/seasonal mixed-layer principle component varies from year to year. In the north, zooplankton density increased from 1994 to 1998 but it did not differ significantly in the south. Within each region, squid density did not vary significantly from year to year. Therefore, variation in the processes determining the latitude of the SST minimum may be more important to salmon prey distribution than the variation in the amount of food within each region. Zooplankton showed additional mesoscale structure associated with eddies in 1995 and 1998.

The importance of the SST minimum boundary in determining salmon growth is suggested by the body weights of the largest salmon, which would be expected to have the highest predation rates on squid. All of these species are larger in 1996 and 1998, when the boundary was farther to the north, and smaller in 1997 when the boundary was farther to the south (Figure 4.17). It is possible that sea surface temperature, which is warm in 1997 and cold in 1996 and 1998, is a contributing factor.

Ocean age .1 sockeye salmon, however, are larger in 1997 than in the colder years. If sea surface temperature alone was determining the growth rates of salmon, these smaller age classes would follow the same body weight pattern as the larger fish. However, these smaller fish, feeding mainly on zooplankton, grow larger in years in which their overlap with squid is minimized. This supports the idea that the difference in prey distribution on either side of the boundary is a determining factor in growth. In addition, it suggests that the squid are a competitor with the smaller sockeye for food, although there is no evidence of a negative correlation between squid and zooplankton on a station by station basis within each region.

The salmon CPUEs increasing from south to north show that migration patterns are probably more important for determining salmon distribution than

prey in late July. Pink salmon catches have been shown to be related to run sizes of central Alaskan pink salmon although it is not known if the other species show a similar relationship (K. Myers, School of Aquatic and Fishery Sciences, University of Washington, Seattle, unpublished data). The fact that ocean-age .2 sockeye do not show a latitudinal trend may indicate that they are primarily eastward-migrating British Columbian fish (S. McKinnell, Institute of Ocean Sciences, Fisheries and Oceans Canada, Sidney, British Columbia, pers. comm).

The mechanistic link between the SST minimum and the northern boundary of squid distribution is not clear. The SST minimum may represent a density or temperature gradient unsuitable for squid. Aydin et al. (1998) suggest that the SST minimum may be a proxy for a frontal structure between internal Alaskan Gyre waters and waters from the west, possibly indicating the presence of Oyashio waters within the Ridge Domain. Surveys conducted in the 1950s-1970s show that Oyashio waters are associated with a cold front within the Ridge Domain which varies substantially in its eastern extent from year to year (Favorite and Hebard 1961; USBCFBL 1969). This component of westward transport, associated with the SST minimum, may be linked to squid distribution.

Fronts may propagate across the North Pacific and vary substantially from year to year (Yuan and Talley 1996). Pearcy et al. (1998) found a similar biological border further to the south that was important for larger species such as Pacific pomfret (*Brama japonica*) and Neon Flying Squid (*Ommastrephes bartrami*). The role of fronts in salmonid feeding has been cause for speculation (e.g., Brandt 1993), and the behavior of these fronts under climate-change scenarios may be critical to determining changes in salmon biogeography.

Because the squid are sampled from salmon themselves, it is possible that the change is not representative of squid abundance but of the changing

ability of salmon to capture squid on one side of the border, or that at warmer temperatures, catching squid ceases to be profitable causing salmon to switch to zooplankton. However, the fact that the switch occurs in pink, sockeye, and coho salmon simultaneously, three species with differing energy budgets, suggests that the change is due to the presence or absence of squid.

4.2.6 Conclusions

The determination of the SST minimum as a proxy for the border between two distinct feeding modes of salmon has implications for both current salmon growth and future salmonid populations. If the boundary extends across the Alaskan Gyre, the interannual variation in the area of squid/salmon overlap may be over 2 million square kilometers (See Section 4.4). This large variation in a species range may have a profound impact on its predators, the salmon.

Because SST records exist, it would be worthwhile to examine the variation in this border back through time and relate it to large-scale salmonid growth trends, to determine the importance of this mechanism in salmon growth overall. Such retrospective studies, in combination with continuing modeling on salmon growth, would improve our ability to understand the consequences of global climate change.

4.3 *Bioenergetics models*

4.3.1 Introduction

Projections relating long-term changes in sea water temperature to salmon growth rates must take into account the nonlinear relationship between temperature, prey consumption, and salmon growth (Murphy 1995; Hinch et al 1995). The study of the metabolism of an animal's feeding with respect to their environment is known as bioenergetics. Bioenergetics models combine

laboratory-measured physiological parameters with field-measured environmental data to determine an instantaneous daily rate of somatic growth for a given fish, fed a given ration in a given environment. Parameter sets for many fish have been published (c.f. Hewett and Johnson 1992).

Bioenergetics models calculate a daily energy balance which assumes that all energy entering and leaving a fish must be accounted for. The general model formula is:

$$C = G + R + F + U$$

Where **C** is a fish's daily consumption (in food calories), **G** is the expected growth, and **R** (respiration) and **F+U** (egestion and excretion) are heat and material losses respectively, arising from the process of metabolism. The benefit of bioenergetics modeling is that **R** and **F+U** can be parameterized from laboratory experiments as functions of **C**, **G**, water temperature, and fish body size. The formulae, parameters and references for the models used for pink, sockeye, coho, and chum salmon are given in Appendix B.

Given the following four input variables for a salmon:

- Ambient water temperature
- Daily ration (**C** in the equation above)
- Prey quality (caloric density and the proportion that is indigestible)
- Body weight of the salmon

the model will predict the amount of somatic growth (**G**) experienced by the fish, and estimate the conversion efficiency of growth (material assimilated/material consumed). This version of the model is parameterized for a daily time increment. I designed the bioenergetics experiments in this section to: (1) determine the direct effects of each of the four sampled variables on growth rate, using the *natural range of variation* measured during the study described in Section 4.2, and (2) predict the effect of a systematic change (up or down) of each of the variables on the growth rates of salmon in the sampling region.

4.3.2 Methods

The input variables for the bioenergetics model are water temperature, salmon body weight, daily food ration (% predator body weight per day), and prey quality (prey caloric value). I calculated these quantities for sockeye, chum, pink and coho salmon from the study conducted in July along 145°W, between 1994-98, as described in Section 4.2. I used these quantities to predict the body weight-specific growth rates and conversion efficiencies of each salmon species, using the model parameters in Appendix B.

In performing the analysis, I pooled data into north and south groups, using the SST minimum shown in Figure 4.14 as the dividing line between the two groups. Unfortunately, sample sizes were not large enough to analyze body-weight specific variation between years within each region. Therefore, this analysis focuses on the difference in feeding conditions between the two regions. This is partially supported by Figure 4.16, which showed a greater difference in zooplankton and squid densities between regions than between years within each region.

4.3.2.1 Temperature and body weight measurements

Water temperatures were taken from CTD data at each ½ degree of latitude—10m increments were used from the sea surface to 40m depth. Body weight measurements came from the research-mesh gillnet as described in Section 4.2. For the re-sampling process described below, water temperatures were assumed to be normally distributed, while body weights were assumed to have a lognormal distribution. For determining diets and growth rates, salmon were subdivided by species and by 500g body weight categories.

4.3.2.2 Estimating daily consumption rates

The daily ration of a salmon as a percentage of its body weight was calculated from the weight of prey in its stomach, corrected for temperature-

specific digestion rate. For this correction, I used the sea surface temperature at the location of fish capture. This may result in an overestimate of prey consumption if the fish was actually digesting its food at a lower temperature, although the nighttime surface sampling ensured that the salmon captured had spent some time in surface waters.

As food eaten is being constantly digested, calculating the daily food consumption of a fish from "instantaneous" measurements of stomach contents weights requires making assumptions about both the feeding patterns and digestion rates of the fish. I used two methods of estimating daily ration, one using the assumption of a 12-hour feeding period, and one using a 24-hour (continuous) feeding period.

The 12-hour method assumes that salmon feed primarily during the night, and that salmon measured in the morning had empty stomachs prior to starting feeding on the previous evening. Under this assumption, food weight represents feeding during a single evening only. For simplicity, the evening period was taken as being 12 hours prior to the point of capture. This assumption roughly fits the "dusk and dawn" feeding pattern which has been noted in some salmonid species.

Under the assumption of a 12-hour daily feeding pattern, and assuming that the digestion rate is proportional to stomach contents weight, the total daily consumption can be determined by:

$$\text{Consumption / day} = \frac{12 \cdot D}{(1 - e^{-12 \cdot D})} \cdot S$$

Where D is the digestion rate in units of (hour^{-1}), and S is the measured stomach weight, in units of grams or percent of salmon body weight.

The 24-hour feeding pattern assumes that salmon feed at a constant rate 24 hours a day, and that the average measured stomach contents represent an "equilibrium" fullness level. In this case, the appropriate correction factor is:

$$\text{Consumption / day} = 24 \cdot D \cdot S$$

Digestion rate D is temperature dependent, and in this study is calculated for each fish by:

$$D = a \cdot e^{b \cdot T}$$

T is the ambient water temperature, which in this study approximated by sea surface temperature at the capture location. If digestion occurs in deeper, cooler waters, the sea surface temperature estimate for D may be 20-40% too high. However, the fish were caught near the surface and hauled in the morning, and during nighttime hours salmon are more surface-oriented (Walker et al. in press). The constants used for all pink, sockeye, and coho were $a = 0.053$, $b = 0.114$, while the a value used for chum was 0.106, or double that for the other species. For a review of estimates of digestion rate as a function of sea surface temperature, see Davis et al. (1998a) and references therein.

It is important to include the digestion rate correction in calculating feeding rates of fish. Welch et al. (1998) use the instantaneous prey weight S directly in bioenergetics models, without correcting for digestion. This results in an estimate of daily consumption which is approximately $\frac{1}{2}$ of the 12-hour estimate. Underestimating the daily consumption may overemphasize the direct effect of temperature on salmon growth rates, as at lower consumption rates, salmon growth is more sensitive to rising water temperatures within the range seen in the Gulf of Alaska surface waters in the summer.

4.3.2.3 Prey quality

Prey quality in bioenergetics models has two parts: caloric content (calories per gram wet weight) and percent indigestible. Based on Davis et al. (1998b), the %indigestible of all prey was set to 10%. The percent by volume of each of five prey guilds shown in Table 4.10 was used to determine the overall prey caloric content for each fish with food in its stomach.

Caloric values for each type of food came from previous laboratory studies, such as those listed in Table 3.1. Values were averaged for different prey types within a single group, and rounded to the nearest 100cal/g wet weight to give the prey caloric densities. Because a large proportion of the contents of chum salmon stomachs were unidentifiable, it was necessary to include unidentifiable material in chum salmon prey weight measurements, or measured prey weights would have been too low to sustain growth. Unidentified material in chum stomachs was given a caloric density halfway between gelatinous zooplankton and small hard-shelled zooplankton.

While laboratory experiments of hard-shelled zooplankton resulted in a small range of caloric densities between 600-800cal/g wet weight, squid showed a larger range of values between 1000-1500cal/g wet weight, possibly as a function of squid size. Because squid caloric densities are central to the results, the bioenergetics models were run twice, one with squid caloric density set at 1000 cal/g wet weight, one with squid caloric density set at 1500 cal/g wet weight.

4.3.2.4 Average diet composition and trophic level

The total digestion-corrected wet weight (g) of each prey type was summed over all fish within a single species, body weight category, and region, and this total was divided by the total wet weight of all prey items to determine the percent-by-weight of each type of prey in the salmon diets. Trophic level was determined by weighting the trophic level of each type of prey, given in Table 4.10, by its percentage in the diet. The trophic levels shown in Table 4.10 are approximate, and based on a small zooplankton's diet consisting of 50% phytoplankton (trophic level 1) and 50% microzooplankton (trophic level 2).

The overall diet proportions for salmon of a given species and body weight category over all regions was calculated by weighting the total wet weights for each region by the catch of salmon in the research gillnet in each

region. As 13 gillnet stations were conducted in both the north and south regions, no corrections were made for sampling effort. Therefore, the formula for the diet over the pooled regions was:

$$WW_{pooled} = \frac{WW_{south} \cdot N_{south} + WW_{north} \cdot N_{north}}{N_{south} + N_{north}}$$

where ***WW_{pooled}*** is the wet weight of a given prey item pooled over north and south areas, ***WW(north, south)*** is the average wet weight of that prey in stomachs sampled in a given region, for a given species and body weight category. ***N(north, south)*** is the number of fish of the given species and body weight caught in research-mesh gillnet in north or south regions. Once a pooled wet weight was calculated for all prey types, these were used to calculate the pooled diet proportions and trophic levels.

4.3.2.5 Monte Carlo simulations to estimate daily growth rate

The patchy nature of prey distribution in the ocean assures that, given a salmon sampled in the wild, some may have filled their gut, while some may not have foraged for many hours before the time of capture. Prey weights for individual fish generally have a Poisson or negative binomial distribution. Calculating “instantaneous” growth rates using prey weights drawn from such distribution would give poor results, as it would indicate that most of the fish were growing with a negative growth rate (no food in the stomachs), while a small number of fish would be growing at a physiologically impossible rate, with estimates of daily consumption more than 3-5 times the physiological maximum.

However, the range of natural variation is an important component of this analysis. Rather than calculate the average growth in a given time, I emphasize the range of natural variation in growth experienced during the study. I do this by creating replicate “samples” of fish using the Monte Carlo techniques. In averaging daily ration and prey caloric values, I decided to use a sample size of 30 fish as a unit of measure. While this number is somewhat

arbitrary, it normalizes the data without removing a substantial amount of the variation. Moreover, a sample of 30 fish may be considered to represent a single fish over the period of a single month—thus, the variation in daily ration reported below represents an approximation the variation experienced by a single fish during a single month of summer (June or July).

In reality, “daily” feeding rates in an individual fish are averages of many days of foraging in patchy environments, as a fish may capture more than it may digest in a single day, or may be caught in nets before it begins another foraging period. Therefore, the mean and standard deviation of prey weights as a percentage of body weight for each species and age class were computed by taking the average prey weights in the stomachs of 30 fish selected from the sampled fish at random with replacement.

The “30-fish” resampling was repeated to create a normally-distributed sample of prey weights for each species and body weight class. The standard deviation therefore represents the standard deviation of the mean of a sample of 30 fish, or 1 fish over 30 days, rather than of a single fish in a single day. There were not enough stomachs sampled to partition sockeye or chum diets by age or maturity status.

For each estimate daily of growth rate:

1. The fish from the food habits data set were divided into north and south groups based on the SST minimum. Fish were further grouped by species and by body weight into 500g categories.
2. A single water temperature was drawn from a normal distribution with the mean and variance calculated from the field data within the region.
3. A single salmon body weight was drawn from a lognormal distribution measured from research gillnet catches, truncated to reflect the boundaries of the body weight bin.

4. Thirty stomach samples of the given body weight x species category were drawn from all the fish that were sampled in that category in that region, with replacement. The gut contents of each fish were converted to a specific daily consumption rate (g/g/day), using the 12-hour or 24-hour feeding assumption, as above. Fish with empty stomachs were included with daily consumption defined as 0. The average daily consumption values from the 30 fish were averaged into a single value.
5. Thirty fish of the given body weight x species category were drawn with replacement from all the fish in that category and region with at least trace amounts of food in their stomachs. The caloric content of each stomach was determined, and averaged together.
6. From these four values (water temperature, body weight, daily consumption and caloric content), a single estimate of daily growth was made. This procedure was repeated, and averaged with previous estimates, until the standard error of the estimated growth rate was less than 0.1% of the mean. This required 2,000-10,000 repetitions depending on the species and region. Standard error was calculated by dividing the estimated standard deviation of the estimated value by the square root of the number of repetitions.

Estimates were made using all eight combinations of:

1. sea surface temperatures vs. 0-40m water temperatures;
2. the 12-hour vs. 24-hour feeding period; and
3. 1000 vs. 1500 calories/g wet weight for squid caloric values.

4.3.2.6 Determining the importance of natural variation and systematic change

To isolate the effect the natural range of variation of the four input variables had on the calculated growth rates, the above procedure was

repeated four additional times. In each of these additional experiments, three of the variables were fixed at their average value, while one was drawn at random as described above. The resulting coefficient of variation (C.V.) of growth rate estimates was recorded for each experiment.

Further, to investigate the effect of a systematic change of each of the input variables, the chosen variable was set at +/- 10% from its mean value, and the rest of the variables were chosen at random as above.

4.3.3 Results: Measured range of growth conditions, 1994-98

4.3.3.1 Water temperature

Table 4.11 shows mean, minimum, maximum, and standard deviation of water temperatures of the upper 40 meters of the water column at all oceanographic stations, reported at 10 meter depth increments. Overall, the 0-40m average temperature was similar in the north and south (9.6°C and 9.5°C, respectively). However, the structure of the water column differed: sea surface temperatures were warmer in the north than in the south, while temperature at 40m was cooler in the north than in the south. Therefore, the stratification of the thermocline was stronger in the northern region, and the standard deviation of water temperatures at all depths was greater in the north.

4.3.3.2 Salmon body weights

The differences in salmon weight-at-age between the north and south regions were discussed in Section 4.2 and are shown in Table 4.9: Chum salmon were generally larger in the north, while coho, pink, and age 2+ sockeye salmon were larger in the south. Table 4.12 shows the total catch of salmon stratified by body weight categories in the north and south. The bold numbers in Table 4.12 show the body weight categories from which stomach samples

were taken in all years in both regions: only these categories were used for bioenergetics simulations.

4.3.3.3 Prey composition and trophic level

The percent consumption by weight of each prey type, and the overall trophic level by body weight category, is shown in Figures 4.18-4.21. The "combined" north and south prey composition (Graph (c) in each of Figures 4.18-4.21) weighted the total prey weight in each region by the relative catch of that body weight category in that region.

Sockeye salmon in the north fed primarily on small zooplankton, even up to body weights of 3 kg (Figure 4.18a). However, in the south, only the smallest sockeye fed on zooplankton, while the diets of fish above 1 kg body weight consisted entirely of squid (Figure 4.18b). Taking into account the greater preponderance of larger fish in the south, the overall pattern is one of increasing trophic level as body weight increases (Figure 4.18c).

Chum salmon do not show a great difference in diet between north and south regions (Figure 4.19a-c), nor do they show a significant difference in diet composition with body weight. However, the large amount of unidentified material in the stomachs of chum salmon prevents the full assessment of possible diet changes.

Pink salmon show a pattern similar to sockeye salmon, with all size categories present in the north feeding primarily on small zooplankton, while all size categories in the south feed primarily on squid (Figure 4.20a,b). Again, due to the greater number of larger fish in the south, the combined regions give the appearance of the pink salmon increasing in trophic level as they grow larger, by switching from zooplankton to squid (Figure 4.20c).

Finally, coho salmon above 1.5 kg body weight fed primarily on squid in both regions (Figure 4.21a-c). Coho smaller than 1.5 kg were only caught in the north, and primarily fed on small zooplankton.

4.3.3.4 Salmon prey quantity

The daily ration of the salmon in the study, calculated using the 24-hour (continuous) feeding assumption, are shown in Table 4.13. In the south, the daily rations were extremely high for coho salmon, pink salmon, and sockeye salmon above 1.5 kg body weight. Estimates of southern rations for these groups ranged between 3.1-9.5% body weight per day, in contrast with a range between 1.4-3.0% body weight per day in the north. Chum salmon, on the other hand, had a higher daily ration in the north (2.7-3.4%bw/day) than in the south (1.8-2.6%bw/day). This difference between north and south was significant for most body weight categories (Table 4.13).

The daily ration may be presented as a "P-Value", or proportion of maximum consumption rate per day. A P-Value of 1.0 indicates a ration corresponding to the maximum body-weight specific physiological consumption rate. This physiological maximum is a long-term average, so measurements made from instantaneous measurements of stomach contents may have P-Values exceeding 1.0 (J. Kitchell, Center for Limnology, University of Wisconsin, Madison, pers. comm.).

The 24-hour feeding assumption produced estimates which were at or above the maximum daily ration in many cases, especially in the south (Table 4.14). On the other hand, the 12-hour (night feeding only) feeding assumption resulted in significantly lower P-Values which were near the maintenance ration, or the ration required to meet metabolic demands while providing no excess energy for growth.

Previous studies have estimated that the consumption rates of salmon during this period of their life must be near their maximum values to account for their observed growth (Davis et al. 1998b; Nishiyama et al. 1977). The results in Table 4.14 indicate that the salmon population as a whole must be assumed to feed for more than 12 hours a day to maintain growth rates measured in previous studies, although an individual salmon might feed for only a portion of the day. For the rest of the reported results, I used only the 24-hour assumption, although the "true" feeding pattern may lie between the two assumptions.

4.3.3.5 Salmon prey quality

Prey caloric values for individual fish showed a binomial distribution for all salmon species. In general, most individual fish were found to contain a single prey type when considering the broad categories listed in Table 4.10, although the zooplankton category itself might contain many taxa which may have differing caloric values. Table 4.15 shows the average caloric values for two assumptions: Table 4.15a shows the caloric contents assuming squid to have a caloric content of 1000cal/g wet weight, while Table 4.15b shows results assuming 1500 cal/g wet weight for the squid.

In either assumption, the caloric content of coho, pink, and larger sockeye salmon was higher in the south than in the north, due to the presence of the squid in the stomachs of fish caught in the region. Chum salmon showed slightly higher values in the north.

4.3.3.6 Predicted rate and efficiency of growth

Using the minimal assumption of squid containing 1000cal/g wet weight produced growth rates shown in Table 4.16 and Figure 4.22. The highest daily rates of growth were measured in the south, for pink, coho and sockeye salmon. Growth rates were above 1%bw/day for 1.5-2.5 kg fish of these three

species in the south, although this maximum rate decreased for larger fish (Figure 4.22, Table 4.16). For the smallest category of sockeye salmon, between 0.3-0.5 kg, the model predicted a negative growth rate (weight loss) in the south, although this is based on a sample size of only three fish. However, it is worth noting that only 8 fish in this category were caught in the south during the five years of the study, possibly indicating a region of poor growth for this category, which consisted entirely of ocean age .1 sockeye.

In the north, the model predicted lower growth rates for pink, sockeye, and coho salmon, ranging between 0.3%-0.5% bw/day for all body weight categories. Predicted growth rates for chum salmon were lower in the south (0.25-0.27%bw/day) than in the north (0.4-0.67%bw/day), although the differences between the two regions were less pronounced for this species.

If squid were assumed to have a caloric content of 1500cal/g, the growth rates in the south for pink, coho, and sockeye would be significantly higher, between 1.5-2.0%bw/day, while growth rates for all fish in the north would be similar to the 1000cal/g model (Figure 4.23).

While growth rate varied significantly between northern and southern regions, the efficiency of energy and matter transfer between predator and prey did not vary. Table 4.17 shows the efficiency of caloric assimilation, or total calories of predator growth divided by the total prey calories eaten, with the rest being lost as metabolic heat. Caloric conversion efficiencies varied between 26-53%, while most ranged between 40-50%. Ocean-age .1 sockeye lost caloric value in spite of their intake.

Biomass assimilation, or wet weight of predator growth divided by wet weight of prey eaten, was lower than caloric conversion, as energy is packed more densely in salmon than in their prey. Biomass conversion efficiency ranged between 10-26%, and did not vary significantly between regions for most categories (Table 4.18).

4.3.3.7 The source of natural variation in growth rates

The importance of natural variation of each input variable in determining the predicted growth rate is shown in Figure 4.24. Results are averaged for all body weight categories of each fish species. Figure 4.24 shows, for each input variable, the coefficient of variation of growth rate obtained by allowing that input variable to vary within its sampled range, while all other input variables are fixed at their average measured value. In both the north and the south, variation in body weight (within each body weight category), temperature, and prey caloric density, contributed little to the C.V. (standard deviation/mean) of growth rate estimates, with C.V.s of less than 10% for all variables. However, when daily ration was allowed to vary within its measured distribution, the C.V. of estimated growth rates was higher for all species. The C.V. was between 30-40% in the north for all species (Figure 4.24a). In the south, pink, sockeye and coho salmon had a lower C.V. from variation in daily ration, between 10-20%, while the C.V. in growth rates for chum was above 40% (Figure 4.24b). In the south, daily ration for pink, sockeye, and coho salmon showed much less variance, as all species showed daily rations with consistently high quantities of squid.

The C.V. of daily growth rate estimates when all input variables were allowed to vary within their measured distribution was slightly lower than that for daily ration alone, as allowing all quantities to vary stabilized the variance somewhat (rightmost column in Figures 4.24a-b).

4.3.3.8 The effect of systematic changes in input variables

The effects of a systematic +/-10% change in the measured mean value of each input variable is shown in Tables 4.19-4.22.

An 10% increase in body weight led to slight changes in growth rates, with the direction depending on species and size range (Table 4.19), although it is generally negative. This results from a predicted physiological slowing of

growth processes as the salmon increases in size. The effect of body weight is relatively minor compared to the effect of increasing ration or caloric value of the food by 10% (Tables 4.20 and 4.21). The increase of daily ration of 10% increases growth rates for all species in the north, and for chum in the south between 9-15%.

However, the increase is less for coho, pink and sockeye salmon in the south, with a 10% increase in daily ration only leading to a 1-6% increase in growth rate. This indicates that their ration is already near its maximum in the south. Ocean age .1 sockeye growth rate goes down in the south as its ration goes up, indicating that, within its measured range, the energy required to process 10% more food is greater than the additional growth obtained from it, assuming the caloric density of prey was correctly estimated.

A 10% increase in caloric content of the food generally leads to a 10-15% increase in growth for all species and size categories, except for the smallest sockeye salmon in the south. As growth rate is measured in biomass, this result is due to the higher biomass conversion efficiency resulting from higher energy food sources.

Finally, a 10% increase in the 0-40m water temperature predicts changes in growth rate which differ between species, body weight category, and region (Table 4.22 and Figure 4.25). The fish primarily feeding on small zooplankton and gelatinous material show a decrease in growth rates with increasing water temperature. These groups include all pink and sockeye in the north, smaller pink and sockeye in the south, and chum salmon in both regions.

In contrast, the groups in the south with high growth rates, resulting from feeding on squid—coho, larger pink, and larger sockeye—show an increase in growth rates with increasing water temperature (Figure 4.25). Finally, coho in the north show very little change with changing sea surface temperatures.

Figure 4.26 shows results similar to those in 4.25, but assuming that salmon are permanently maintained at sea surface temperature, and that sea surface temperature increases by 10%. In this case, all species and body weight categories decrease in the north, while results in the south are unchanged, although the increase in coho growth in the south is less than shown in Figure 4.25. This difference is magnified in the north as the difference between sea surface temperatures and 0-40 meter temperatures is greater in the north than in the south (Table 4.11).

4.3.4 Discussion

During the period July 1994-98, the greatest difference in predicted growth rates between fish in a single category arises from the difference in the daily ration and food quality between the north and south zones, as shown in Figure 4.22. This result is most pronounced for salmon which depend on squid in the southern zone, primarily pink, larger sockeye and coho salmon.

Within each region, the natural variability in daily ration gave rise to a greater variation in growth rates than did the natural variation in body weight, water temperature, or prey caloric values (Figure 4.24). This was true whether or not salmon were assumed to maintain body temperatures at sea surface or 0-40m water temperatures. The variation in prey caloric values was probably higher than noted, as prey may vary in caloric content, based on size for squid or on species for zooplankton. More detailed examination of year-to-year variation in prey caloric contents would provide an interesting comparison.

It is worth noting that the high level of squid in the south tended to decrease the variance caused by differences in daily ration for pink, coho, and sockeye salmon in the south (Figure 4.24b). In conjunction with the decreasing growth rates shown for these species in the south as they grew larger, this indicates that the fish in the south were feeding at their maximal rates during all years of the study.

As shown by Figures 4.18-4.21, the trophic level of pink and sockeye salmon tended to increase with body weight, mainly through increased consumption of squid. However, this effect is confounded by the differential distribution of large and small salmon, with larger pink and sockeye salmon being caught in greater numbers in the south. This presents a "chicken-or-egg" type of problem: it is not clear if salmon stay in the southern regions to feed on squid because they are larger, or are larger because they feed on squid. This is further confounded by the fact that salmon in the two regions may represent different stocks of fish.

The predicted effects of a systematic 10% increase in sea surface or 0-40 water temperatures, shown in Figures 4.25 and 4.26, are especially interesting. The results predict that in the southern regions, an increase in sea surface temperature would actually *favor* squid-feeders, as they currently find enough food to benefit from increased metabolic activity associated with warmer water. This is true even in the overall warm climate that typified the 1990s.

Most previously-reported comparisons of sea surface temperature and the stock-specific adult body weights of salmon show a negative correlation (Pyper and Peterman 1999; Rogers and Ruggione 1993). Hinch et al. (1995) and Welch et al. (1998) suggest that this may result from the direct physiological effects of increased water temperature. However, the results here suggest that the direct physiological link might act in the opposite direction in the open ocean, or at least in the squid-feeding areas by squid-eating salmon.

There are a few likely scenarios which would reconcile this pattern. First of all, changing sea surface temperatures may affect prey quantities within each region, in a manner not detected in this study. A change in the highly variable daily ration resulting from a changing prey distribution may give rise to the noted correlations.

Secondly, sea surface temperatures at a single point may be correlated with the latitude of the north/south division, and may indicate the total extent or size of the ocean region in which salmon and squid overlap. Rather than representing a direct physiological effect, the sea surface temperature/adult body size link may be a manifestation of the year-to-year shift in biogeography of prey. This is explored more fully in Section 4.4.

A final scenario may result from the geographic pattern of variation seen in ocean temperatures. A salmon feeding in the southern "high squid" zone must pass through the food-poor northern zone to return to Alaska, and pass through coastal waters to return to British Columbia. During this period of rapid migration, feeding rates may be lower due to lack of prey or the requirements of migration. When feeding rates are lower, increases in water temperature depress growth as shown in Figure 4.26a.

Moreover, coastal stratification and warming would lead to higher temperatures in coastal waters than those seen in the open ocean: the anomalous warm waters in 1997 were highest in coastal waters. While feeding in the southern waters may remain rich in squid, the coastal temperature gauntlet through which the salmon must pass may be the ultimate arbiter of final body size. This gauntlet may vary in width, and may also vary in the severity of warmer temperatures encountered.

It is interesting to compare this model with the global warming scenario presented by Welch et al. (1998). Based on increasing global sea surface temperatures, they predict that salmon will move further north and not survive in southern waters. However, if temperature increases have the largest impact on growth in coastal waters, the pattern may be different. In this case, the "southern" waters between 48-52°N may provide the only remaining cooler water refuge in which feeding is sufficient for the larger salmon. "Fleeing north"

may be the worst option which the salmon might pursue, as they would lose access to the richer squid feeding grounds in the summer.

As McKinnell (1994) shows, the center of distribution of Fraser River sockeye salmon overlaps to the greatest extent with the squid-feeding zone in July. The stocks which must travel further through coastal water, such as Bristol Bay and Central Alaskan stocks, may suffer a greater impact than those in British Columbia or Southeast Alaska.

These relatively simple bioenergetics models cannot take into account some aspects of salmon growth which may affect these results. Differential allocation of growth between gonadal and somatic development may impact growth rates, as may differences in hormonal levels determined earlier in the season. Also, while these models have been used repeatedly for adult fish, the initial calibrations were performed on juvenile fish: clearly, a greater emphasis on laboratory measurements of adult salmon bioenergetics would improve these models. This is especially true for chum salmon, whose bioenergetics are relatively poorly understood.

Our understanding of foraging processes on the open ocean is limited—while it is possible to predict differences in growth rates based on the caloric contents of prey, the energetic demands between the two foraging modes of catching zooplankton vs. catching squid are not understood. Direct observation of salmon foraging behavior, perhaps using an ROV under differing light conditions and time of day, would greatly improve our understanding of the feeding processes. Additionally, Individual Based Models (IBMs) could be used to incorporate this information into the migration patterns of specific salmon stocks. An IBM of Fraser River sockeye salmon presented by Rand et al. (1997) is a good first step, but future generations of such models must take into account the year-to-year variation in prey type and distribution reported here.

Such models would help to determine the patterns in growth which would be expected in the face of future environmental change.

4.3.5 Conclusions

In the offshore Gulf of Alaska, the natural range of variation of the daily ration of salmon caused a greater variation in predicted growth rates than did water temperature, body weight, or prey caloric value, within the summer study period. This variation was especially pronounced between the north and south regions divided by the latitudinal sea surface temperature minimum. The most notable characteristic of the southern region was the high growth rate in coho and larger pink and sockeye salmon resulting from the presence of micronektonic squid. The variation in the northern extent of squid may be the largest determinant of adult salmon biogeography in this region.

Water temperature itself has a lesser direct effect on salmon growth in this region, and increasing temperatures might actually improve growth rates by increasing the area of overlap in squid and salmon distribution. In light of this fact, if increasing water temperature is related negatively to final adult body size, it must be either through changes in prey distribution and caloric density, or through the influence of the warmer coastal regions around the Gulf.

In addition to increased physiological sampling in the Gulf, the construction of multiple Individual Based Models for different salmon stocks would greatly improve projections of growth in the face of future climate change.

4.3 Trends in potential squid/salmon overlap area, 1950-99, and relation to salmon body weights

4.3.1 Introduction

The results of Section 4.2 demonstrate the existence of a latitudinal biological boundary in the northeast subarctic Pacific between 140-165°W. South of this boundary, pink, coho and sockeye salmon above 1000g body weight primarily consume the micronektonic squid *Beryteuthis anonychus* during the summer. North of this boundary, the fish consume zooplankton, or nothing, until they reach the continental shelf. The results of Section 4.3 suggest that the differences in salmon growth rates between the two regions can be large for the squid-consuming salmon (Figs. 4.22-23).

The boundary between squid and zooplankton was correlated with the July latitudinal sea-surface temperature minimum (Tmin) during feeding surveys conducted in the 1990s. During the 5 years of the study, this boundary varied between 50-53°N, a distance of over 300 km (Figs. 4.13-14). If this boundary is extended east/west, this amounts to a difference of approximately 58,000 km² of ocean surface area for every degree of longitude over which the boundary extends.

As shown in Figure 3.2, *B. anonychus* distribution extends considerably into the subtropical domain, and it is a chief component of the diet of transitional fish species such as Pacific pomfret (*Brama Japonica*). Salmon distribution does not extend as far south; however, repeated surveys (e.g., Faculty of Fisheries 1998) have shown that most salmon species are rare on the high seas south of the subarctic boundary. It is not known exactly what factors influence the southern limit of salmon distribution. One suggestion is that SST is a limiting factor (Welch et al. 1998), but it is possible that SST is a proxy for

the position of oceanographic fronts that make up the transition region (Table 2.1).

Therefore, both the southern and northern borders of the *B. anonychus* / salmon range of overlap may vary from year to year, as may the total ocean surface area between the borders (hereafter known as overlap area). It is possible that this biogeographic variation may be a source of interannual variation in salmon growth. The remaining question is: does variation in the overlap area scale up to year-to-year differences in adult salmon body size? If so, how does this source of variation compare to either the physiological effects of water temperature on salmon, or to density-dependence arising from high salmon numbers?

In order to evaluate the role of each of these sources of variation, historical trends in the overlap area must be compared to historical changes in salmon body weights in the region. Fortunately, both the northern and the southern boundaries of this area are indexed to SST. July SST records of useable resolution exist back to 1950 for the Gulf of Alaska. This section uses these data to revisit previously-reported relationships between salmon body size, salmon numbers, and oceanographic conditions.

The results presented here rely on correlations between ocean conditions and adult salmon body size, measured on an annual scale. As discussed in Chapters 1 and 2, these correlations do not directly confirm any mechanistic hypotheses. However, if patterns of correlations are observed across many salmon stocks covering a wide geographic range, the relationships, in conjunction with the detailed food habits studies of Sections 4.2 and 4.3, may allow the formation of mechanistic hypotheses that clarify the relationships shown in Figure 4.1.

It is important, before proceeding on correlative studies, to define precisely what is meant by salmon individual "size." Some of the previous

studies have used adult salmon length (nose-fork or eye-fork) as an index of "size," while other studies have used adult salmon body weights. In addition, some studies have used measurements of salmon scales—either the number or width of rings on a scale—as an index of salmon growth.

The three types of growth are intimately related. In many cases, one may serve as a proxy for the other. However, it is worth noting that differential growth in length, weight, and scale patterns may result in each type of measurement recording a slightly different process.

A second difficulty in examining size trends arises in species with multiple ages of maturation, in this study, sockeye, chum, and chinook salmon. Multiple ages of maturation in a population of salmon may lead to counterintuitive results, even if age-specific size measurements are used. In years of poor growth, only the larger salmon may mature, leading to larger average size-at-age in poor growth years.

A final difficulty is that of stock aggregation: unless measurements are taken on specific spawning grounds, the year-to-year variance in the relative population sizes of genetically distinct stocks within a sample may skew results, as a process which correlates with "larger" fish overall may simply favor a stock which happens to have a genetic predisposition to larger body sizes. This kind of stock aggregation issue is especially prevalent if records from commercial fisheries catch are used to obtain the average age of fish.

Unfortunately, the lack of historical records of body sizes of many stocks prevents these difficulties from being satisfactorily addressed in broad-scale studies. The approach taken here is to use multiple types of records of body size where available, including age-specific and non age-specific data, length and weight data, commercial catch and non-commercial catch data, and data from multiple species and regions throughout North America. These records are not pooled before analysis, but individually examined for correlative

relationships. While this increases the chance of spurious significant correlation (Type I Error), this can be mitigated by only accepting the significance of correlations if they are seen in multiple data sources.

Previous studies correlating annual salmon growth or body weights with summer SSTs have used data from geographically fixed points or regions. For example, McKinnell et al. (1999) found a highly significant relationship between the temperature at 53°N, 145°W and the proportion of Fraser River sockeye salmon migrating north vs. south around Vancouver Island.

Along 145°W, 53°N latitude is near T_{min}, which brings up an interesting question. If the temperature rises at 53°N, is this a result of the “bowl” shown in Figure 4.3 moving up and down (increasing uniformly in temperature) or moving north to south, sliding the temperature at 53°N up the surface of the bowl? The distinction between these two types of SST variation at a fixed geographical point near T_{min} may have profound biological significance, which might be ignored by the geographical correlation. To that end, the correlations between salmon trends and physical variables are taken with respect to the “oceanographically-fixed” feature of the July SST bowl, rather than with respect to any specific latitude and longitude.

4.3.2 Methods

4.3.2.1 Setting

The latitudinal sea surface temperature minimum exists in the summer in the Gulf of Alaska between 140-165°W (Figure 4.27). The features of the July minimum vary across the gyre (Figure 4.28). The SST minimum does not exist in the warmest coastal waters along 135°W, but the “bowl” of cold temperatures is quite evident between 140-160°W. The northern “lip” of the bowl moves southward for progressively further western transects, generally following the Aleutian shelf. West of 165°, the minimum no longer exists, and temperatures

are uniformly cooling from 40°N, through the Aleutian Islands and into the Bering Sea (Figure 4.28).

The latitudinal SST minimum in the center of the gyre does not exist year-round. The long-term climate record along 145°W shows that in March, SST is coolest along the transect, and a possible SST minimum exists farther to the north near 55-56°N (Figure 4.29a). As the water warms in Spring, shelf waters warm more swiftly than central gyre waters until by June, the SST minimum is near 52-53°N, where it remains until August. Between August and September, the northernmost shelf waters cool more quickly than the waters near 52-53°N and the minimum moves again to the north, where it remains as the water cools uniformly throughout the fall (Figure 4.29b). It is not clear how this seasonal process affects the movement of squid or salmon.

The correlation between the SST minimum and *B. anonychus* distribution has only been examined directly for the month of July in Section 4.2 and 4.3. Therefore, it is not clear if squid move with this seasonal boundary, or if the oceanographic process responsible for this boundary and the biological process responsible for squid distribution correspond throughout the year.

4.3.2.2 Oceanographic and salmon run size data

Average July sea surface temperature measurements were obtained for the Gulf of Alaska on a 1°lat. x 1°lon. resolution for the period 1982-1999 (IGOSS 2000), and a 2°x2° resolution for the period 1950-1992 (COADS 1994); reported at odd latitudes and longitudes only). The SST data set is derived from a combination of satellite, shipboard and buoy data (Reynolds and Smith 1994).

Figure 4.27 shows the long term average (1950-1999) July SSTs in the Gulf of Alaska, showing the ocean surface area used in this analysis (colored box). The southern border of this box was chosen as 43° latitude which

encompassed the 13°C isotherm in almost all years. The northern border was staggered to stop short of the continental shelf, from 51°N at 165°W to 59°N at 141°W.

The eastern and western boundaries of the region were chosen by examining long term means of July SST transects along longitude lines (Figure 4.28). Water is warmest on the eastern side of the gyre, and water along 135°W does not show a temperature minimum, possibly due to the influence of warm waters off the British Columbian shelf. The SST minimum is clear and apparent on transects between 140°-160°W longitude, but becomes weaker at 165° and vanishes at 170°W, where water cools continuously between the Subtropical Region and the Bering Sea.

The “bowl” along a single line of latitude was described by a quadratic curve parameterized ***MinLat*** (the latitude (°N) at which SST is at a minimum), ***Tmin*** (the SST (°C) at that minimum) and ***Dist 1°C*** (the distance traveled north or south, in degrees latitude or kilometers, between the minimum latitude and where the temperature is 1°C warmer than at the minimum latitude; Figure 4.3). The temperature increase of 1°C is arbitrary: ***Dist 1°C*** is simply a rescaling of the curvature into a meaningful physical quantity. The units of this last parameter are (lat^{1/2}/°C): a high value of ***Dist 1°C*** indicates a “shallow” bowl with less of a temperature difference along a transect

Parameters ***MinLat***, ***MinTemp***, and ***D 1°C*** were fitted by minimizing sum of squares error through an exhaustive search of the parameter space at a resolution of 1% of the estimated parameter value. The quadratic curve was fitted in every year 1950-99 along each odd degree of longitude between 141°-165° W, giving three parameters for each transect and year. The latitude of the 13°C isotherm along each transect was calculated from the fitted parameters. Finally, the total overlap area was calculated by converting the distance

between MinLat and the 13° isotherm into “wedges” of 2° longitude width centered on each transect.

As the SST data used was averaged and smoothed over a monthly time period, the patterns would be expected to reflect smoothed seasonal processes, rather than daily heating and mixing processes characteristic of individual measurements of pelagic water temperatures. Therefore, the “minimum” reflected in the monthly data may not represent a SST minimum experienced by a fish on a given day, but rather be a more conservative measure of overall oceanographic processes.

For comparison with other oceanographic processes, these data were compared with the annual PDO and ENSO 3.4 indices as provided by Steve Hare and documented in Mantua et al. 1997 (see Chapter 2 for a description of PDO and ENSO indices).

4.3.2.3 Pacific salmon data

Salmon size data was taken from several published sources for the years 1954-97 (Table 4.23). Regional average body weights of Alaskan commercial harvests of sockeye, pink, chum, coho, and chinook data were provided by Brian Bigler from the data published in Bigler et al. (1996). These data covered the years 1969-96 and were divided into Ketchikan, Cook Inlet, Kodiak, Bristol Bay, Kuskowim, and Yukon fishing areas. Not all species were caught in all areas.

For sockeye salmon, two additional sources of data were obtained. Normalized age-specific regional aggregated lengths (either eye to fork or nose to fork) were reported by Pyper et al. 1999 for 5 regions: Bristol Bay, Cook Inlet, Fraser River, Copper River, and Skeena River. These data values were visually taken from Figure 3 of Pyper et al. 1999: years of data coverage varies by region. In addition, the average body weight of sockeye from three

Canadian commercial catch areas (Areas 12, 13, and 20) was provided from Canadian Department of Fisheries and Oceans (DFO circular) statistical information for the years 1982-97. The sockeye caught in these regions are almost entirely Fraser River fish, dominated by age 1.2 fish (S. McKinnell, Institute of Ocean Sciences, Fisheries and Oceans Canada, Sidney, British Columbia, pers. comm.).

The total yearly run sizes of all combined North American pink and sockeye stocks (numbers of salmon) were obtained for the years 1950-98 from Rogers (1999) and used as an index of total salmon abundance in the Gulf of Alaska. Coho and chinook salmon were less than 10% of total salmon in the region and not included. Chum salmon, while making up a higher percentage of total salmon, were not included: the majority of chum in the world are of Japanese origin, and it is unclear what proportion of these fish enter the Gulf of Alaska, although their contribution to competition may be considerable.

4.3.2.4 Comparative studies

Correlative studies between variables were performed by measuring the simple correlation coefficient R between each pair of variables. The significance of correlations was measured using an F-test and the formula $F=(1+|R|)/(1-|R|)$ (Zar 1984). Further investigative studies included multiple regression and principle components analyses. These latter analyses did not substantially change interpretations of the results, and are not presented.

One problem with simple correlation studies lies in the amount of temporal autocorrelation that may be present in the data set. Specifically, when faced with a "regime" such as that in 1976-77, many variables may shift at once with a single, underlying cause. Correlations will be more likely to be significant as a result, even if one of the variables did not "cause" a change in the other.

To address this, the correlation coefficients were calculated on time series across all years, and were also calculated on data broken into two time periods; 1950-1977 and 1978-98. 1977 was included in the "pre" period based on a possible lag between physical and biological response. This method does not remove all temporal autocorrelation and requires the presupposition of the regime shift. In particular, a second regime shift in 1989 may have increased correlation coefficients: this possibility is addressed in the results and discussion.

Finally, when viewing many correlation coefficients, the risk of a spurious (Type I) error is heightened. Two steps are taken to filter out Type I errors. First, the significance level required to report a correlation was $P(F) < 0.01$ rather than $P(F) < 0.05$. Secondly, patterns in correlations between salmon body size and physical variables were only considered as relevant if they occurred in multiple stocks.

4.3.3 Results

4.3.3.1 Fitting of oceanographic parameters

The quadratic fitting of D , T_{min} and $MinLat$ to $2^\circ \times 2^\circ$ sea surface temperatures gave three time series \times 13 lines of longitude between 141° and 165° W inclusive (odd longitudes only), a total of 39 time series running from 1950-1999. Examination of the residual error of fits showed standard errors from nonlinear fitting of less than 5% for all parameters on almost all longitude transects and years, except for years prior to 1954, for which available data was sparse. Trends prior to 1954 were therefore discarded.

No significant differences in fits occurred when higher resolution $1^\circ \times 1^\circ$ IGOSS data was substituted for $2^\circ \times 2^\circ$ COADS data in years for which both data sets existed (correlation $R > 0.90$ for all individual parameters 1982-92). Varying

the southern starting point of transects between 39-45° had little effect on the estimated parameter values.

An additional sensitivity test was conducted by varying the southern cutoff temperature for salmon distribution between 13-15°C. The former test had no noticeable effect on the results. While increasing the temperature of the southern isotherm increased the overlap area 10-20% in all years, it did not affect the relative change in the area over time, as the change between 13-15°C along the southern edge of the study area occurred over a short latitudinal distance (Figure 4.27).

4.3.3.2 Patterns in oceanographic trends

Examining longitudinal autocorrelation for each parameter showed high correlations within each variable between adjacent transect lines. The autocorrelation patterns of each time series suggested that the 13 lines of longitude could be reduced into four east/west areas, with strong temporal correlation within each area and weaker correlation between areas. Three of the areas cover 4 longitude lines each: 141°-147°W, 149°-155°W, and 157°-163°W. These regions are hereafter known as East, Mid, and West gyre regions respectively (dashed lines in Figure 4.27).

The 165°W transect, furthest to the west, showed low parameter correlations with all other transects, including transects immediately to the east. Since this transect may be outside the central gyre and does not possess a temperature minimum in many years (Figure 4.28), it was discarded from subsequent analysis.

Longitudinal parameters within the East, Mid, and West regions were averaged by year to give three time series, East, Mid, and West, for each of the three parameters D, MinLat, and MinTemp. In addition, overlap area (surface area between the 13°C isotherm and MinLat) was calculated for each of the

three regions and summed to calculate the total overlap area. Thus, a total of 17 physical variables were available for comparison with trends in salmon production (Table 4.24)

Figure 4.30 shows the SST, MinLat and 13° isotherm for 1993-98. The total overlap area is the area between the two lines and is bounded by 140°W and 164°W. Circles in Figure 4.30 show the stations at which salmon were sampled for squid, and the squid index values for those stations are shown (see Section 4.2.3.5 for calculation method). The sampling locations include the 145° W line transect discussed in Section 4.2 as well as additional (non-transect) stations sampled during the same research cruises.

The total overlap area varied from a high of 4.3 million km² in 1971 to a low of 1.9 million km² in 1997, and averaged 3.3 million km² over the period 1954-99 (Figure 4.31). Prolonged periods with a higher than average overlap area occurred between 1965-66, 1971-75 and 1985-88. A low period existed between 1976-84 and 1989-98, with the area increasing again in 1999.

This variation was not uniform across the gyre's east/west extent (Figure 4.32). While the peak in the 1960s and 1970s was seen across the gyre, the decrease in the overlap area after 1988 was almost entirely due to changes in the eastern portion of the gyre (Figure 4.32c).

The three component variables of the overlap area were not wholly independent. D was positively correlated with both MinLat and Tmin, indicating that D increased both as the "bowl" moved north/south or as the temperature of the bowl moved up/down. MinLat was negatively correlated with Tmin: as the latitude of the minimum moved north, the temperature of the minimum became cooler. The total area shows a strong correlation with MinLat and Tmin but a weak correlation with D (Table 4.25).

MinLat patterns varied across the gyre. Two points in which the minimum was farthest to the south in the east were during the 1983 and 1997

“El Nino North” periods (Figure 4.33c). MinLat shows a negative correlation with the PDO across all years, but not in the pre- or post- regime time periods separately. This negative correlation is probably due to the few years of northerly minimum latitudes in the 1970s.

A rise in T_{min} in the east is the main source of the decrease in overlap area between 1988-89 (Figure 4.34c). A positive correlation with the PDO occurs in T_{min} values across all years but not within the pre- or post- regime time periods, possibly due to the warm temperatures in the 1990s. T_{min} east was highly correlated with the temperature at 53°N, 145°W due to that point's closeness to minLat ($R > 0.80$). Previous analyses which used the temperature at 53°N, 145°W as a variable (c.f. McKinnell et al. 1999) would not differ in conclusions if T_{min}East had been used.

Finally, a positive correlation occurs between D (the curvature in the SST “bowl”) in the eastern portion of the gyre and the PDO index (Table 4.26). Much of this correlation is due to the extreme jump in D east between 1977 and 1978 (Figure 4.35). This corresponds with the PDO pattern of warming northern waters and cooling southern waters which would lessen the curvature from north to south across the gyre. If D contains some component of the PDO, it is interesting to note that its return to low levels has been gradual throughout the 1990s rather than abrupt as may be expected if a “reverse” regime shift had occurred in the late 1990s.

4.3.3.3 Interrelations with salmon numbers and body sizes

Total North American pink and sockeye salmon run sizes increased suddenly after the 1976 regime shift. Pink salmon numbers increased from an average of 109 million between 1954-77 to an average of 267 million between 1978-97. This latter period showed two periods of increase, one between 1978-85, with a slight decrease between 1986-88 followed by a large increase in 1989 (Figure 4.36).

Prior to 1977, sockeye salmon numbers were dominated by a 4-5 year cycle of western Alaskan (Bristol Bay) fish and averaged 33 million annually between 1954-77. This number increased to 80 million between 1978-80. Sockeye remained near 80 million until 1985. Between 1986-88, sockeye salmon numbers decreased to nearer 60 million, jumping again in 1989 to near 90 million (Figure 4.36). Most of this increase came from western Alaskan stocks, primarily Bristol Bay, although other Alaskan and British Columbian stocks increased during the 1980s as well.

Numbers of pink and sockeye salmon show a strong positive correlation in both pre- and post- regime periods (Table 4.27). Numbers show a strong positive correlation with the PDO index over the time period as a whole; however, when divided into pre- and post- regimes, this correlation is no longer significant. Salmon numbers also show a pattern of negative correlation with MinLat and a positive correlation with D, although this also disappears in the individual time periods. The correlation between Tmin and numbers exists in the post-regime and over the entire time period, but does not exist in the pre-regime era.

All time series of sockeye, pink, and chum catch weights and sockeye age-specific lengths showed a decline between 1976-97. All of the chinook catch weights except for Ketchikan also showed a decrease, while Ketchikan chinook catch weights showed an increase. Coho salmon body weights did not show a decrease: the patterns of these trends are shown in detail in Pyper et al. 1998 and Bigler et al. 1996. When correlated with physical variables for all of the available years, many of the pink, sockeye, chum and chinook stocks showed a significant negative correlation with salmon numbers (Table 4.28). A smaller number of time series, specifically those of British Columbian area sockeye catch weights, showed a significant negative correlation with Tmin and a significant positive correlation with overlap area.

When divided into pre- and post- regime groups, the pattern changes. No physical or run size variables show significant correlations with more than a few salmon size variables in the 1954-77 time period (Table 4.29). However, in the post-regime period, both salmon numbers and overlap areas are significantly correlated with several of the size time series (Table 4.30).

4.3.3.4 A close examination of Fraser River stocks

This interaction between salmon numbers, overlap area, and salmon size was explored further for Fraser River sockeye. For Fraser River stocks, both age-specific length data (FR 1.1, 1.2, and 1.3) and catch body weight (BC areas 12,13, and 20) were available. Most of the Fraser River catch consists of age 1.2 fish: therefore, trends in BC area catch weights are most comparable to FR1.2 fish (S. McKinnell, Institute of Ocean Sciences, Fisheries and Oceans Canada, Sidney, British Columbia, pers. comm.).

As seen in Tables 4.28 and 4.30, there are significant relationships between Fraser River time series, salmon numbers, and the physical characteristics of the eastern gyre in the post-1977 period. Figure 4.37 shows annual anomalies for (a) BC areas 12, 13, and 20 average sockeye body weight; (b) FR1.2 lengths; (c) overlap area east; (d) inverted TminEast (shown inverted); (e) salmon numbers (shown inverted); (f) ENSO (shown inverted) and (g) PDO (shown inverted). Between 1954-77 no correlations are significant between FR1.2 lengths and the other time series. (Table 4.31; BC area body weight data is not available during this time period). However, the 1978-97 period shows significant correlations between body length and weight, sockeye numbers, SST, and overlap area (Figures 4.37 and 4.38; Table 4.31). Each time series shows a distinct low-high-low pattern between the periods 1978-85, 1986-89, and 1990-97. One interesting note is that while FR1.2 body length has a much stronger correlation with sockeye run size than with overlap area,

the body weight time series shows a stronger correlation with the overlap area than with the run size data (Figure 4.38; Table 4.31).

4.3.3.5 Interactions between salmon run sizes and overlap area

Rather than perform a multiple regression on Tmin and salmon numbers, the colinearity of the two data series combined with the possible interaction of the two variables suggests a different approach. As mentioned above, TminEast and overlap area (east) show a strong correlation (Figure 4.39a). This suggests that any given year can be described as a “cold large-overlap” or a “warm small-overlap” year. These roughly correspond to the positive anomalies (“cold-large”) and negative anomalies (“warm-small”) in Figure 4.37(b) and (c). Note from Figure 4.37 that prior to 1989 there were more cold-large than warm-small years, and all years between 1989-97 were warm-small.

Similarly, the time series of salmon run sizes can be divided into years of “many fish” and “few” fish: years of “few” fish are positive anomalies in Figure 4.37e (Figure 4.39b). Pink salmon and sockeye salmon showed the same positive and negative anomalies, therefore it does not matter which of these two time series is used to make the division. Note that all of the years with “few” fish are prior to 1978. The “cold-large/ small-warm” and “few/many” states are not independent (χ^2 -test, $P < 0.05$) although a small number of cold-large/few small-warm/many years do exist (Table 4.32).

With these divisions, the question can be asked: did the overlap area (or Tmin) - body size relationship change between years of few fish and years of many fish? Conversely, did the relationship between sockeye run sizes and body size change in “cold-large” vs. “warm-small” years? As the change in the causative relationship is an issue, regression, rather than correlation, is used to answer these questions.

Regressions were performed on the subset of 12 salmon size indices that showed significant correlations with both salmon numbers and either overlap area or Tmin in at least one of the time periods in Tables 4.28-4.30. The results of the regressions are shown in Table 4.33-4.34. Table 4.33 shows regressions of size vs. overlap area and size vs. Tmin, given that salmon numbers are "few" or "many" respectively. In years with few pink and sockeye salmon in the gyre overall, only two time series—FR 1.3 and CK1.2—show a significant relationship with Area or Tmin (Table 4.33). The relationship that exists in years of few fish for FR1.3 and CK1.2 stocks is opposite that seen for most stocks in Tables 4.28-4.30: fish length is positively correlated with Tmin and negatively correlated with ocean area.

However, in years with "many" fish, 8 of the 12 time series examined show a regression with a significant positive relationship with the overlap area east, although only 2 of the 12 stocks show a negative relationship with Tmin (Table 4.33). Note that with $P < 0.05$ as a significance level, between 1-2 spurious correlations are to be expected with these 24 comparisons. Figure 4.40 shows the regressions for FR1.2 fish. When there are "many" fish in the environment, a significant positive correlation exists between overlap area and body length, and a significant negative correlation exists between Tmin and body length (Figure 4.40(a) and (b)). There is no significant relationship when there are "few" fish in the environment.

When years are divided into "small-warm" and "large-cold" and regressed against salmon run sizes, a negative relationship between body size and run sizes is apparent for the stocks regardless of the "small-warm" or "large-cold" status (Table 4.34). For FR1.2 fish, the slope of the relationship does not seem to change with temperature or overlap area (Figure 4.40c). However, when all of the regressions are examined side by side (Figure 4.41), it is apparent that, for almost all stocks tested, the density-dependent slope is steeper (or the average body size is lower) in warm-small years than in cold-large years.

4.3.4 Discussion

Fraser River fish were chosen for the detailed analysis because, in addition to having both length and weight data, they are the salmon whose distribution may make them the most affected by both changes in the squid/salmon overlap area. McKinnell (1994) showed that the center of Fraser River salmon distribution was near the center of the salmon/squid overlap area. Table 4.31 shows that Fraser River fish were sensitive to both the size of the overlap area and the total run sizes of salmon in the 1977-98 time period.

One interesting result of the analysis of Fraser River fish is the fact that length is more closely related with salmon numbers, while body weight is more closely related to overlap area, at least after 1977 (Figure 4.40). An examination of the condition factor ($\text{body weight}/\text{length}^3$), pooled by month over 6,000 sockeye and pink collected in the Alaska Gyre (data in Chapter 3), shows that between January and April, the salmon condition factor remains constant for pink and sockeye salmon, indicating that their length and weight are increasing proportionately without a change in relative girth (Figure 4.42). However, the increase in the condition factor between April and August indicates that during this latter period, weight is increasing more quickly than length.

These two facts, taken together, suggest that the density-dependent relationship is most important to salmon growth when length and weight are growing similarly, in the winter or early spring. On the other hand, the relationship between body weight and overlap area is important in the summer, when body weight increases faster than length^3 indicating an increase in the girth of the fish.

Western Alaskan sockeye salmon leave the Alaska Gyre by the middle of spring (Myers et al. 1996). If density-dependent salmon growth is occurring on the scale of the entire gyre, it may be most prevalent in the winter and early

spring, when there are more fish in the gyre than in the summer. On the other hand, if the area of overlap with squid is a limiting factor in growth, this limitation probably occurs in the summer, as temperatures become warmer, and growing sockeye and pink become large enough to eat squid (Chapter 3).

As the proposed squid/salmon overlap area is negatively correlated with SST near the minimum, it is not possible to conclude with certainty whether the direct causal mechanism between water temperature and salmon body weights is physiological or a result of the changing distribution of squid and salmon, as both warmer temperatures and a smaller overlap area would affect salmon body size negatively. However, the correlative evidence of Table 4.33 suggests that the overlap area may offer a slightly better explanation than T_{min} for salmon growth variation.

The changing relationship between salmon run sizes, overlap area, and body size is difficult to untangle due to the colinearity of salmon run sizes and overlap area, and the temporal autocorrelation that occurs in all of the time series as the results of regime shifts (Figure 4.37). However, the patterns of changing regressions in Tables 4.33 and 4.34 suggest two possible hypotheses:

- 1. As salmon numbers have increased and foraging has become more competitive, salmon are more sensitive to the physiological effects of temperature and/or the distribution of prey in the Alaska Gyre, especially the micronektonic squid *B. anonychus*.** Peterman (1987) suggested that salmon density-dependent growth curves would change with the physiological demands of increased water temperature by decreasing the salmon body size independently of density-dependence (Figure 4.43). Figure 4.41 suggests another possibility, that changes in prey distribution or water temperature might steepen the negative

density-dependent slope in some cases. Mechanisms for this change in slope are presented in Sections 5.3 and 5.4.

- 2. The change in ocean conditions either changed the distribution of *B. anonychus*, or led to a significant increase in the importance of this species in salmon diets, and thus to the importance of this species' biogeography in determining salmon growth.** Chapter 3 suggests that *B. anonychus* abundance level may have substantially increased between the 1960s and the 1980s. It is possible that the relationship between overlap area, T_{min} and salmon body weight, did not exist prior to the 1977 regime shift because squid was a less important player in the ecosystem at that time. However, it is worth noting that these squid have been reported as important diet components for salmon throughout the 1950s and 60s (LeBrasseur 1966).

It is interesting to note that if squid have increased in abundance since 1977, it might be expected that increased temperature would be physiologically beneficial to salmon: Figure 4.25 shows that in areas of high squid consumption, larger salmon would benefit from the increase in metabolism that might allow them to digest more squid. The fact that the relationship between T_{min} and salmon is negative suggests that direct physiological concerns are less responsible than the changing overlap area for determining salmon growth on the high seas.

This does not mean that future increases in temperature will be beneficial to salmon: much of the variation in the overlap area comes from the variation in the southern location of the 13° C isotherm. The future of salmon with respect to temperature may depend on what actual mechanism underlies the relationship of the fish with their southern limit of distribution.

A second regime shift in 1989 is visible in the time series in Figure 4.39. The time series of gyre shape in Figure 4.32-35 show that the change in

conditions after 1989 differed from the changes in 1977: the effect of the 1989 regime shift has been reported in multiple sources (Hare and Mantua 1999).

Using sea surface temperatures as a proxy for the squid/salmon overlap area may not capture their full range of biogeographical variation. The 13° isotherm as a southern limit for salmon distribution is specific to sockeye, and it is possible that the concentration of predators and prey at frontal structures may override overreaching temperature patterns in determining fish distribution (Brandt 1993; Murphy 1995). However, the SST proxy may serve as a useful comparison if it explains a portion of the previously noted correlations between sea surface temperature and salmon body weights.

As a final note, it should be realized that even if the changing overlap area of squid/salmon explains a proportion of salmon growth variation, this does not imply that the mechanism is a simple limitation of squid as a prey supply. The migratory behavior of the salmon means that the explanation may lie in a combination of feeding and movement behavior, of which feeding on squid is a small part. As mention in section 4.3, the use of detailed individual-based models of salmon movement and foraging would be a useful next step in examining this.

If the correlations presented in this section show little else, they show that salmon response to climate change may arise from complex combinations of abiotic conditions and prey distribution. In light of the possibility of global warming, it is important to realize that simple extrapolations and predictions based on current trends must take into account the complexity of the physical and biological environment in which the salmon live and grow.

Table 4.1. Estimated empirical corrections for calculating a squid density index from sockeye, pink, and coho salmon, from Table 3.8. Corrections were calculated from over 11,000 fish sampled between 1956-98.

Species	Body weight cutoff (g)	Alpha offset (intercept)
Sockeye	1000	-0.03
Pink	1000	-0.41
Coho	500	+0.60

Table 4.2. Correlations between selected oceanographic variables. Variables in the left-hand column are temperature (°C) and salinity (psu) at the surface (T0 and S0), temperature and salinity at 100m (T100 and S100) seasonal pycnocline depth (meters) and strength (buoyancy frequency) (Sdepth and Sstrn) and permanent pycnocline depth and strength (Pdepth and Pstrn).

	<i>T0</i>	<i>S0</i>	<i>T100</i>	<i>S100</i>	<i>Sdepth</i>	<i>Sval</i>	<i>Pdepth</i>	<i>Pval</i>
<i>T0</i>	1							
<i>S0</i>	0.02	1						
<i>T100</i>	-0.06	-0.23	1					
<i>S100</i>	-0.05	0.27	-0.16	1				
<i>Sdepth</i>	-0.57(*)	0.11	-0.01	0.00	1			
<i>Sstrn</i>	0.79(*)	0.21	-0.21	0.11	-0.53(*)	1		
<i>Pdepth</i>	0.00	-0.27	0.17	-0.83(*)	0.01	-0.16	1	
<i>Pstrn</i>	-0.24	0.35	-0.21	0.07	0.25	-0.10	-0.30	1

(*) Significant at the $P < 10^{-5}$ level (two-tailed F-test, 82 d.f.).

Table 4.3. Principle components of oceanographic data. The eigenvectors (loading coefficients) are shown for all eight principle components. Variables in the left-hand column are the same as in Table 2. The individual and cumulative percent of variance explained by each component are also shown. For the first four PCs, coefficients with absolute values >0.35 are shown in bold (cutoff is arbitrary).

Variable	Principle Component							
	PC1	PC2	PC3	PC4	PC5	PC6	PC7	PC8
T0	0.55	0.22		-0.11		-0.40	-0.68	
S0	0.14	-0.39	0.40	-0.45	-0.57	0.34	-0.11	
T100	-0.17	0.25	-0.46	-0.82				
S100	0.20	-0.49	-0.49	0.10	-0.13			0.67
Sdepth	-0.46	-0.24	0.12		-0.35	-0.77		
Sstrm	0.59		0.17			-0.31	0.72	
Pdepth	-0.21	0.53	0.38		-0.20	0.13		0.67
Pstrm	-0.11	-0.40	0.44	-0.29	0.70			0.25
Percent of variance explained								
Individual	30	28	15	10	8	6	2	1
Cumulative	30	58	73	83	91	97	99	100

Table 4.4. Results of 1-way ANOVA comparing Ridge Domain/Subarctic Current break with SST minimum break as an explanation for the first oceanographic principle component (PC1). All listed models were significantly better than the null model (F-test, $P < 0.001$).

Model	Residual DF	Residual Deviance
Null Model	59	101
PC1 ~ Latitude	58	80
PC1 ~ North or South of SST minimum	58	(*)69
PC1 ~ Domain	57	83
PC1 ~ North or South of SST minimum + Latitude	57	69

(*) best model.

Table 4.5. Results of 1-way ANOVA comparing Ridge Domain/Subarctic Current break with SST minimum break as an explanation for zooplankton densities.

Model	Residual DF	Residual Deviance	F-value (comparison with null model)	P (F)
Null Model	58	11.9		
Ln (Zoop) ~ North or South of SST minimum	57	9.4	14.96	<0.0003
Ln (Zoop) ~ Ridge or Subarctic Current Domains	57	10.6	6.64	<0.0125

Table 4.6. Residual degrees of freedom and deviance from all first order interactions using the squid index as the dependent variable and N/S boundary, Latitude, and PC1 as the three explanatory variables.

Model	Residual DF	Residual Deviance
Null Model	27	49
Single term models		
Squid ~ North or South of SST minimum	26	29
Squid ~ Latitude	26	33
Squid ~ PC1	26	29
Two term models		
Squid ~ N/S + Lat.	25	28
Squid ~ N/S + PC1	25	24
Squid ~ Lat. + PC1	25	22
Three term model		
Squid ~ N/S + Lat. + PC1	24	22

Table 4.7. Correlation between the latitude of the yearly boundary between high and low squid index values and the yearly boundary between the IGOSS SST minimum and the Ridge/Subarctic Boundary. Two methods of determining the squid cutoff latitude: one uses the switch between positive and negative values, and one uses the dotted line in Figure 4.13.

	<i>Ridge/Subarctic Border</i>	<i>IGOSS SST minimum</i>	<i>Squid positive/negative cutoff</i>
IGOSS SST minimum	0.12		
Squid positive/negative cutoff	0.42	0.86(*)	
Squid latitude/PC1 cutoff	0.37	0.97(**)	0.90(*)

(*) P<0.05 (**) P<0.01

Table 4.8. The best statistical model for CPUE of each species or age class. All latitude trends are positive correlations, while the trend with PC1 is a negative correlation. Yearly trends show significant differences between years and do not indicate direction of the differences. Best models were chosen by stepwise model selection.

Species	Best model
Sockeye	Latitude
Chum	Latitude
Pink	Latitude + Year
Coho	Latitude
All four species	Latitude
Age .1 Sockeye	Domain – PC1
Age .2 Sockeye	Domain
Age .3 Sockeye	Latitude
Age .1 Chum	Latitude
Age .2 Chum	Latitude + Year
Age .3 Chum	Year

Table 4.9. Average body weights by species, ocean age, and maturity status, of salmon caught south and north of the SST minimum. North/South split P shows significance of difference between north and south for all years pooled (2-tailed t-test). Significant values are listed as higher in the north or in the south. North-by-year and South-by-year show P-values for 1-Way ANOVA of between-year variation for each fish group and region.

Species	Ocean		N	Body	Body	North/South Split P	Higher in:	North by	South
	Age	Maturity		Weight	Weight			Year P	By Year P
				(kg)	(kg)				
Chum	.1	IM	332	0.75	0.67	3.04E-05	North	0.92	0.01
		MT	28	0.77	0.84	0.55		9.93E-05	
	.2	IM	763	1.29	1.18	4.82E-07	North	2.73E-22	0.15
		MT	100	1.52	1.41	0.21		3.70E-06	0.65
	.3	IM	54	1.68	1.59	0.62		0.47	0.48
		MT	43	2.60	1.93	0.01	North	5.74E-09	0.05
Coho	.1	MT	412	2.82	3.06	0.01	South	1.94E-03	0.20
Pink	.1	MT	876	1.30	1.53	2.17E-16	South	2.47E-04	0.00
Sockeye	.1	IM	68	0.50	0.54	0.10		1.57E-03	0.15
		MT	39	0.79	0.95	0.57		1.37E-03	0.70
	.2	IM	82	1.75	2.01	0.07		2.80E-05	0.00
		MT	641	2.27	2.65	5.36E-16	South	0.03	0.01
	.3	IM	2	2.78	-				
		MT	292	2.96	3.15	0.03	South	0.02	0.01

Table 4.10. Prey categories, prey caloric density (calories/gram) and trophic level of prey assumed for the analyses in Section 4.3. See Table 3.x for a more detailed list of prey types. Trophic levels are approximate and based on Pauly and Christensen 1996. Caloric density is to the nearest 100cal/g.

	Included genera	Trophic Level	Calories/gram wet weight.
Small Zooplankton	Copepods, pteropods, euphausiids, amphipods	2.5	700
Large Zooplankton	Large decapods, chaetognaths, polychaetes	3.0	900
Fish	Myctophids	3.5	1300
Squid	Gonatid spp.	3.5	1000 or 1500 (see text)
Gelatinous material	Salps	3.0	100
Unidentified material	Assumed gelatinous or small zooplankton	-	300

Table 4.11. Water temperatures along transect line, 1994-98, north and south of the SST minimum. Temperatures (°C) are from CTD sampling and reported at 10 meter depth increments.

A. SOUTH		Temperature (°C)			Standard deviation
Depth	N	Mean	Minimum	Maximum	
Sea surface	30	10.2	9.2	12.2	0.78
10 m	30	10.1	9.2	11.5	0.66
20 m	30	9.9	8.9	11.4	0.73
30 m	30	9.0	7.3	10.6	0.71
40 m	30	8.0	7.1	9.7	0.63
0-40 m	150	9.5	7.1	12.2	1.09

B. NORTH		Temperature (°C)			Standard deviation
Depth	N	Mean	Minimum	Maximum	
Sea surface	34	11.1	9.5	12.8	0.93
10 m	34	11.0	9.5	12.8	0.98
20 m	34	10.4	8.2	12.7	1.19
30 m	34	8.5	6.7	11.9	1.11
40 m	34	6.9	5.6	8.6	0.76
0-40 m	170	9.6	5.6	12.8	1.93

Table 4.12. Catch of salmon in research (non-size selective) gillnet, 1994-98. Sampling effort was the same in north and south regions. Significance of north/south body weight differences are listed by age class in Table 4.9. Bold numbers indicate categories for which catch was distributed evenly enough over all years to be included in growth simulations.

Body weight Category (g)	Chum		Coho		Pink		Sockeye	
	North	South	North	South	North	South	North	South
300-499	7	14					35	8
500-999	257	191			116	21	45	19
1000-1499	496	203	11	2	366	94	51	6
1500-1999	182	38	20	7	124	97	146	28
2000-2499	22	4	63	19	26	32	256	73
2500-2999	7		83	24	3	2	222	92
3000-3499	9	2	62	39			89	69
3500-3999	3		50	14			44	19
4000-4499	1	1	3	7			11	5
4500-4999	2		1	3			2	1
5000-5499			1	1				1
5500-5999	1			1				
Grand Total	987	453	294	117	635	246	901	321

Table 4.13. Daily ration: re-sampled mean, minimum, maximum, and standard deviations of as a percentage of salmon body weight for each salmon species and weight class, corrected for digestion rate. Re-sampling was performed by drawing 10,000 replicate samples of 30 fish each from the data set with replacement. N is the number of fish in the original data set. Digestion assumed a 24-hour feeding period. P indicates result of a two-tailed T-test between north and south samples, assuming sample sizes of 30. * indicates significance <0.01; ** indicates significance <0.00001.

	Body weight Category (g)	North			South			P
		N	mean	sd	N	Mean	sd	
Chum	500-999	116	3.4%	0.7%	95	1.8%	0.5%	1.8E-26 **
	1000-1499	135	2.7%	0.8%	102	2.5%	0.9%	0.20
	1500-1999	88	3.0%	1.0%	50	2.6%	0.7%	9.5E-03 *
Coho	1500-1999	34	2.1%	0.6%	15	4.5%	0.9%	8.0E-13 **
	2000-2499	73	1.4%	0.5%	29	9.5%	1.6%	2.2E-34 **
	2500-2999	97	2.8%	0.9%	46	4.9%	0.9%	3.0E-18 **
	3000-3499	75	2.2%	0.7%	38	5.1%	0.9%	2.3E-23 **
	3500-3999	55	1.8%	0.6%	20	3.1%	0.6%	6.6E-11 **
Pink	500-999	28	1.8%	0.4%	8	1.6%	0.5%	0.31
	1000-1499	211	2.5%	0.6%	100	4.8%	1.0%	3.8E-29 **
	1500-1999	103	2.0%	0.5%	110	4.8%	1.0%	1.6E-34 **
	2000-2499	18	1.9%	0.4%	21	4.5%	0.9%	1.4E-16 **
Sockeye	300-500	18	2.5%	0.7%	3	0.3%	0.1%	4.2E-19 **
	500-999	20	2.9%	0.6%	10	2.6%	1.0%	0.44
	1500-1999	60	1.9%	0.5%	33	6.4%	1.2%	9.7E-29 **
	2000-2499	118	2.3%	0.7%	100	5.8%	1.1%	3.8E-34 **
	2500-2999	99	1.7%	0.4%	86	5.4%	1.2%	1.6E-35 **
	3000-3499	47	3.0%	0.9%	45	5.6%	0.9%	8.0E-20 **

Table 4.14. P-values, or proportion of maximum physiological feeding rate, as calculated by bioenergetics models. P-values greater than 1 may result from stomach sampling after intense feeding bouts. Sample sizes and significance values are as in Table 4.13.

	Body weight Category (g)	North		South		P
		Mean	sd	Mean	sd	
Chum	500-999	0.64	0.15	0.34	0.09	1.8E-25 **
	1000-1499	0.57	0.17	0.54	0.19	.19
	1500-1999	0.71	0.24	0.61	0.18	8.5E-03 *
Coho	1500-1999	0.73	0.28	1.47	0.31	7.7E-11 **
	2000-2499	0.51	0.24	2.00	0.03	2.9E-50 **
	2500-2999	1.07	0.40	1.73	0.28	1.1E-16 **
	3000-3499	0.89	0.36	1.82	0.24	2.5E-23 **
	3500-3999	0.78	0.32	1.26	0.28	2.7E-08 **
Pink	500-999	0.44	0.11	0.40	0.11	.3
	1000-1499	0.70	0.18	1.33	0.28	1.5E-28 **
	1500-1999	0.62	0.16	1.47	0.29	2.1E-34 **
	2000-2499	0.63	0.15	1.47	0.29	1.5E-16 **
Sockeye	300-500	0.44	0.13	0.05	0.01	5.0E-18 **
	500-999	0.71	0.16	0.64	0.23	.43
	1500-1999	0.59	0.15	1.83	0.23	1.2E-35 **
	2000-2499	0.76	0.24	1.80	0.25	1.5E-37 **
	2500-2999	0.59	0.16	1.78	0.28	7.9E-41 **
	3000-3499	1.10	0.32	1.88	0.19	2.3E-20 **

Table 4.15. Prey caloric densities in salmon stomachs: re-sampled mean, minimum, maximum, and standard deviations of prey caloric density (calories per gram wet weight) for each salmon species and age class are shown, corrected for digestion rate (see text). N and significance values are as in Table 4.13. (A) shows results assuming squid density=1000 cal/g; (B) shows results assuming squid density=1500cal/g.

A	Body weight Category (g)	North		South		P
		Mean	sd	Mean	sd	
Chum	500-999	536	40	504	40	3.3E-07 **
	1000-1499	456	43	374	37	8.6E-23 **
	1500-1999	472	48	431	39	9.2E-07 **
Coho	1500-1999	976	23	1014	8	7.3E-12 **
	2000-2499	966	27	998	2	4.4E-14 **
	2500-2999	958	27	1000	27	5.0E-12 **
	3000-3499	962	24	995	11	8.0E-15 **
	3500-3999	972	21	1008	6	6.8E-17 **
Pink	500-999	689	30	877	26	1.5E-24 **
	1000-1499	713	29	947	27	2.4E-57 **
	1500-1999	763	32	949	24	4.3E-48 **
	2000-2499	820	33	891	30	2.9E-09 **
Sockeye	300-500	722	34	700	34	0.32
	500-999	710	41	833	30	3.0E-13 **
	1500-1999	764	20	989	18	8.9E-52 **
	2000-2499	777	26	978	18	6.0E-57 **
	2500-2999	797	37	993	7	2.2E-50 **
	3000-3499	836	48	970	28	1.8E-23 **
B	Body weight Category (g)	North		South		P
		Mean	sd	Mean	sd	
Chum	500-999	536	40	504	40	3.3E-07 **
	1000-1499	456	43	387	46	4.4E-17 **
	1500-1999	472	48	445	46	1.9E-03 *
Coho	1500-1999	1371	46	1491	5	1.0E-21 **
	2000-2499	1292	56	1496	4	9.3E-38 **
	2500-2999	1310	55	1501	55	5.3E-27 **
	3000-3499	1344	51	1472	25	4.2E-25 **
	3500-3999	1370	47	1491	4	1.6E-26 **
Pink	500-999	713	39	1172	70	5.0E-25 **
	1000-1499	764	46	1339	54	1.4E-64 **
	1500-1999	872	61	1351	53	2.5E-54 **
	2000-2499	921	53	1251	61	1.7E-25 **
Sockeye	300-500	722	34	700	34	.32
	500-999	729	44	1014	70	5.1E-17 **
	1500-1999	875	52	1410	41	9.8E-52 **
	2000-2499	920	61	1453	36	5.6E-61 **
	2500-2999	920	63	1481	19	2.2E-62 **
	3000-3499	1051	78	1445	46	9.0E-37 **

Table 4.16. Predicted growth rates (%body weight per day) of salmon by body weight category and north/south region, assuming squid caloric density=1000cal/g wet weight. Sample size and significance values are as in Table 4.13.

	Body weight Category (g)	North		South		P
		mean	Sd	mean	Sd	
Chum	500-999	0.67%	0.19%	0.25%	0.12%	7.4E-27 **
	1000-1499	0.40%	0.17%	0.28%	0.15%	1.8E-07 **
	1500-1999	0.50%	0.21%	0.37%	0.15%	1.8E-04 *
Coho	1500-1999	0.45%	0.17%	0.99%	0.16%	4.1E-15 **
	2000-2499	0.24%	0.14%	0.97%	0.12%	6.5E-34 **
	2500-2999	0.48%	0.17%	0.78%	0.11%	1.3E-18 **
	3000-3499	0.35%	0.14%	0.69%	0.09%	3.9E-23 **
	3500-3999	0.27%	0.11%	0.50%	0.09%	6.9E-13 **
Pink	500-999	0.32%	0.11%	0.39%	0.15%	.22
	1000-1499	0.48%	0.14%	1.23%	0.20%	6.3E-40 **
	1500-1999	0.39%	0.12%	1.13%	0.16%	2.3E-43 **
	2000-2499	0.38%	0.10%	0.92%	0.13%	1.1E-20 **
Sockeye	300-500	0.52%	0.20%	-0.12%	0.03%	1.7E-18 **
	500-999	0.60%	0.16%	0.65%	0.27%	.55
	1500-1999	0.36%	0.11%	1.32%	0.11%	3.7E-44 **
	2000-2499	0.43%	0.15%	1.13%	0.10%	2.8E-44 **
	2500-2999	0.30%	0.10%	1.02%	0.10%	4.2E-49 **
	3000-3499	0.54%	0.15%	0.93%	0.07%	8.8E-23 **

Table 4.17. Predicted percent caloric conversion efficiency (calories of salmon growth/calories prey eaten) of salmon by body weight category and north/south region, assuming squid caloric density=1000cal/g wet weight. Sample size and significance values are as in Table 4.13.

	Body weight Category (g)	North mean	sd	South mean	Sd P	
Chum	500-999	50%	4%	35%	14%	3.1E-14 **
	1000-1499	44%	12%	35%	41%	.052
	1500-1999	45%	33%	43%	12%	.61
Coho	1500-1999	46%	14%	48%	4%	.49
	2000-2499	34%	63%	26%	6%	.26
	2500-2999	46%	72%	43%	6%	.72
	3000-3499	46%	19%	41%	7%	.042
	3500-3999	45%	18%	50%	3%	.066
Pink	500-999	44%	8%	47%	11%	.53
	1000-1499	50%	4%	53%	3%	5.0E-06 **
	1500-1999	50%	5%	51%	4%	.19
	2000-2499	51%	4%	50%	4%	.51
Sockeye	300-500	46%	9%	-113%	82%	1.5E-03 *
	500-999	51%	4%	48%	159%	.95
	1500-1999	49%	6%	43%	6%	3.3E-05 *
	2000-2499	50%	31%	44%	6%	.048
	2500-2999	49%	6%	44%	7%	1.2E-06 **
	3000-3499	52%	4%	42%	6%	5.5E-13 **

Table 4.18. Predicted percent biomass conversion efficiency (wet weight of salmon growth/wet weight of prey eaten) of salmon by body weight category and north/south region, assuming squid caloric density=1000cal/g wet weight. Sample size and significance values are as in Table 4.13.

	Body weight Category (g)	North mean	sd	South mean	sd	P
Chum	500-999	19%	2%	13%	5%	8.4E-16 **
	1000-1499	15%	4%	10%	10%	2.3E-05 *
	1500-1999	16%	11%	14%	4%	.14
Coho	1500-1999	20%	6%	22%	2%	.20
	2000-2499	14%	26%	11%	2%	.32
	2500-2999	17%	28%	16%	2%	.93
	3000-3499	15%	6%	14%	2%	.14
	3500-3999	14%	6%	16%	1%	.013
Pink	500-999	17%	3%	23%	6%	6.5E-03 *
	1000-1499	19%	2%	26%	2%	1.1E-38 **
	1500-1999	19%	2%	24%	2%	1.4E-24 **
	2000-2499	19%	2%	21%	2%	.025
Sockeye	300-500	20%	4%	-48%	35%	1.4E-03 *
	500-999	20%	2%	23%	77%	.93
	1500-1999	19%	2%	21%	3%	9.6E-05 *
	2000-2499	18%	12%	20%	3%	.08
	2500-2999	17%	2%	19%	3%	2.2E-06 *
	3000-3499	18%	2%	17%	3%	.014

Table 4.19. Growth rate change, as a proportion of the mean growth rate shown in Table 4.16, resulting from increasing or decreasing the body weights in each category by 10% of measured values.

Species	Body Weight	North		South	
		-0.10	+0.10	-0.10	+0.10
Chum	500-999	0.00	0.00	-0.02	0.01
	1000-1499	-0.01	0.01	-0.01	0.01
	1500-1999	0.00	0.00	-0.01	0.01
Coho	1500-1999	0.04	-0.03	0.05	-0.05
	2000-2499	0.04	-0.03	0.08	-0.07
	2500-2999	0.06	-0.05	0.07	-0.06
	3000-3499	0.06	-0.05	0.08	-0.07
	3500-3999	0.06	-0.05	0.07	-0.06
Pink	500-999	0.00	0.00	0.00	0.00
	1000-1499	0.01	-0.01	0.03	-0.03
	1500-1999	0.02	-0.02	0.04	-0.03
	2000-2499	0.02	-0.02	0.04	-0.04
Sockeye	300-500	0.00	0.00	0.04	-0.04
	500-999	0.01	-0.01	0.01	-0.01
	1500-1999	0.02	-0.02	0.05	-0.04
	2000-2499	0.03	-0.03	0.05	-0.05
	2500-2999	0.03	-0.03	0.05	-0.05
	3000-3499	0.04	-0.04	0.06	-0.05

Table 4.20. Growth rate change, as a proportion of the mean growth rate shown in Table 4.16, resulting from increasing or decreasing the daily ration shown in Table 4.13 by 10% of measured values.

Species	Body Weight	North		South	
		-0.10	+0.10	-0.10	+0.10
Chum	500-999	-0.12	0.12	-0.17	0.17
	1000-1499	-0.14	0.13	-0.15	0.15
	1500-1999	-0.12	0.12	-0.13	0.13
Coho	1500-1999	-0.12	0.12	-0.07	0.06
	2000-2499	-0.14	0.14	0.00	0.00
	2500-2999	-0.10	0.09	-0.05	0.03
	3000-3499	-0.11	0.11	-0.04	0.02
	3500-3999	-0.12	0.11	-0.09	0.08
Pink	500-999	-0.14	0.14	-0.13	0.13
	1000-1499	-0.12	0.11	-0.08	0.07
	1500-1999	-0.12	0.12	-0.07	0.06
	2000-2499	-0.12	0.12	-0.07	0.06
Sockeye	300-500	-0.14	0.13	0.07	-0.07
	500-999	-0.12	0.11	-0.11	0.11
	1500-1999	-0.12	0.12	-0.03	0.02
	2000-2499	-0.11	0.11	-0.04	0.02
	2500-2999	-0.12	0.12	-0.04	0.03
	3000-3499	-0.09	0.09	-0.03	0.01

Table 4.21. Growth rate change, as a proportion of the mean growth rate shown in Table 4.16, resulting from increasing or decreasing the prey caloric density shown in Table 4.14(a) by 10% of measured values.

Species	Body Weight	North		South	
		-0.10	+0.10	-0.10	+0.10
Chum	500-999	-0.13	0.13	-0.18	0.18
	1000-1499	-0.14	0.14	-0.16	0.16
	1500-1999	-0.13	0.13	-0.14	0.14
Coho	1500-1999	-0.13	0.13	-0.11	0.11
	2000-2499	-0.15	0.15	-0.11	0.11
	2500-2999	-0.12	0.12	-0.11	0.11
	3000-3499	-0.13	0.13	-0.11	0.11
	3500-3999	-0.13	0.13	-0.12	0.12
Pink	500-999	-0.15	0.15	-0.14	0.14
	1000-1499	-0.13	0.13	-0.11	0.11
	1500-1999	-0.13	0.13	-0.11	0.11
	2000-2499	-0.13	0.13	-0.11	0.11
Sockeye	300-500	-0.14	0.14	0.07	-0.07
	500-999	-0.13	0.13	-0.12	0.12
	1500-1999	-0.13	0.13	-0.11	0.11
	2000-2499	-0.12	0.12	-0.11	0.11
	2500-2999	-0.13	0.13	-0.11	0.11
	3000-3499	-0.11	0.11	-0.11	0.11

Table 4.22. Growth rate change, as a proportion of the mean growth rate shown in Table 4.16, resulting from increasing or decreasing the 0-40m water temperatures shown in Table 4.11 by 10% of measured values.

Species	Body Weight	North		South	
		-0.10	+0.10	-0.10	+0.10
Chum	500-999	0.02	-0.02	0.06	-0.07
	1000-1499	0.03	-0.04	0.05	-0.05
	1500-1999	0.02	-0.03	0.03	-0.04
Coho	1500-1999	-0.01	-0.01	-0.07	0.04
	2000-2499	0.02	-0.03	-0.11	0.09
	2500-2999	-0.04	0.02	-0.09	0.06
	3000-3499	-0.02	0.00	-0.10	0.07
	3500-3999	-0.01	0.00	-0.04	0.02
Pink	500-999	0.04	-0.04	0.03	-0.04
	1000-1499	0.02	-0.02	-0.01	0.01
	1500-1999	0.02	-0.02	-0.02	0.01
	2000-2499	0.02	-0.02	-0.02	0.01
Sockeye	300-500	0.03	-0.04	-0.14	0.15
	500-999	0.02	-0.02	0.01	-0.02
	1500-1999	0.02	-0.03	-0.04	0.03
	2000-2499	0.01	-0.02	-0.04	0.03
	2500-2999	0.02	-0.03	-0.03	0.03
	3000-3499	-0.01	0.00	-0.04	0.03

Table 4.23. Data sources for individual salmon size time series (individual length or weight of returning adults).

Code	Detailed description	Years	Data source
Sockeye body length (eye-fork or nose-fork, normalized)			
FR1.1	Fraser River age 1.1	1954-97	Pyper et al. 1999
FR1.2	Fraser River age 1.2	"	"
FR1.3	Fraser River age 1.3	"	"
SK1.2	Skeena River age 1.2	1964-97	"
SK1.3	Skeena River age 1.3	"	"
CP1.2	Copper River age 1.2	1968-97	"
CP1.3	Copper River age 1.3	"	"
CP2.3	Copper River age 2.3	"	"
CK1.2	Cook Inlet age 1.2	1967-97	"
CK1.3	Cook Inlet age 1.3	"	"
CK2.2	Cook Inlet age 2.2	"	"
CK2.3	Cook Inlet age 2.3	"	"
BB1.2	Bristol Bay age 1.2	1957-97	"
BB1.3	Bristol Bay age 1.3	"	"
BB2.2	Bristol Bay age 2.2	"	"
BB2.3	Bristol Bay age 2.3	"	"
Sockeye body weight, commercial catch records			
BC Area20	Johnstone Straits BC (Fraser River)	1982-97	DFO circular
BC Area12	Juan de Fuca BC (Fraser River)	"	"
BC Area13	Juan de Fuca BC (Fraser River)	"	"
Ketchikan		1969-96	Bigler et al. 1996
Cook Inlet		"	"
Kodiak		"	"
Bristol Bay		"	"
Pink body weight, commercial catch records			
Ketchikan		"	Bigler et al. 1996
Cook Inlet		"	"
Kodiak		"	"
Bristol Bay		"	"
Coho body weight, commercial catch records			
Cook Inlet		"	Bigler et al. 1996
Kodiak		"	"
Kuskowim		"	"
Chum body weight, commercial catch records			
Ketchikan		"	Bigler et al. 1996
Cook Inlet		"	"
Kodiak		"	"
Bristol Bay		"	"
Kuskowim		"	"
Chinook body weight, commercial catch records			
Ketchikan		"	Bigler et al. 1996
Cook Inlet		"	"
Kodiak		"	"
Bristol Bay		"	"
Kuskowim		"	"
Yukon		"	"

Table 4.24. Oceanographic, climatological, and salmon run size time series used for analysis of salmon individual body size (length and body weight). All physical and run size variables were collected for the period 1954-98.

Code	Description	Years	Data source
Climate indices			
PDO	Pacific Decadal Oscillation index, annual average		Mantua et al.
ENSO	El Niño/Southern Oscillation (3.4) index, annual average		(1997)
North American population sizes of maturing Pacific salmon (catch + escapement)			
N.Am.Pink	North American pink salmon		Rogers (1999)
N.Am.Sock	North American sockeye salmon		
Indices of Alaska Gyre July SST latitudinal transects			
Deast	Latitudinal curvature distance ($^{\circ}\text{lat}^{1/2}$)/ $^{\circ}\text{C}$ for eastern, mid, and western Alaska Gyre transects. See text for definition of regions.		
Dmid			
Dwest			
MinLatEast	Latitude ($^{\circ}\text{N}$) of July sea surface temperature (SST) minimum along latitudinal transects for eastern, middle, and western Alaska Gyre.		
MinLatMid			
MinLatWest			
TminEast	July SST ($^{\circ}\text{C}$) at latitude of minimum temperature in eastern, middle and western Alaska Gyre.		Calculated in this dissertation (methods in Section 4.4.2)
TminMid			
TminWest			
AreaEast	Total ocean surface area (million km^2) between MinLat (north) and the 13°C SST isotherm (south) for eastern, middle, and western Alaska Gyre.		
AreaMid			
AreaWest			
TotArea	Total ocean surface area (million km^2) between MinLat (north) and the 13° SST isotherm (sum of AreaEast, AreaMid, and AreaWest).		

Table 4.25. Significance level of Pearson's correlation coefficient R between the hypothesized total overlap area of salmon/squid and component variables Tmin, MinLat, and CurveDist in west, mid, and east gyre regions. '+' symbols indicate significant positive correlation while '-' symbols indicate significant negative correlation (F-test). The number of symbols indicates the negative logarithm of the maximum P-Value. For example, '++' or '--' indicates $0.01 > P \geq 0.001$; '+++'' or '---' indicates $0.001 > P \geq 0.0001$, etc. P-values ≥ 0.01 are considered insignificant.

	Overlap Area (TotArea)		
	1954- 1998	1954- 1977	1978- 1998
DEast		++	
DMid	+	++	
DWest	+	+	+
MlatEast	+++++	++++	++
MlatMid	+++++	++++	+
MlatWest	++++	++	+
TMinEast	---	-	---
TMinMid	---	---	---
TMinWest	---	---	---

Table 4.26. Significance level of Pearson's correlation coefficient R between calculated oceanographic variables in Table 4.24 and PDO, and ENSO indices, for three time periods. '+' symbols indicate significant positive correlation while '-' symbols indicate significant negative correlation (F-test). The number of symbols indicates the negative logarithm of the maximum P-Value. For example, '++' or '- -' indicates $0.01 > P \geq 0.001$; '+++ or '- - -' indicates $0.001 > P \geq 0.0001$, etc. P-values ≥ 0.01 are considered insignificant.

	Climate Indices					
	1954-1998		1954-1977		1978-1998	
	PDO	ENSO	PDO	ENSO	PDO	ENSO
DEast	++	+	-		+	+
DMid	+	++		+	+	+
DWest			-			
MlatEast	-				-	
MlatMid	-			+	-	
MlatWest	-		-		-	
TMinEast	+	+				+
TMinMid	+					
TMinWest	+					
AreaEast		-				
AreaMid						
AreaWest	-		-			
TotArea	-					

Table 4.27. Significance level of Pearson's correlation coefficient R between calculated oceanographic variables in Table 4.24 and run sizes (millions of fish) of North American pink and sockeye salmon for three time periods. '+' symbols indicate significant positive correlation while '-' symbols indicate significant negative correlation (F-test). The number of symbols indicates the negative logarithm of the maximum P-Value. For example, '++' or '--' indicates $0.01 > P \geq 0.001$; '+++' or '---' indicates $0.001 > P \geq 0.0001$, etc. P-values ≥ 0.01 are considered insignificant.

	Salmon run sizes (North America)					
	1954-1998		1954-1977		1978-1998	
	Pink	Sock.	Pink	Sock.	Pink	Sock.
PDO	+++	++++			-	
ENSO		+				
DEast	+	++			-	
DMid	+	+				
DWest						
MlatEast	-			+		
MlatMid	-	-				
MlatWest	-	-				
TMinEast	+++	++	+	-	+	++
TMinMid	+	+		-		
TMinWest	+					
AreaEast	-	-	-	+	-	-
AreaMid						
AreaWest						
TotArea	-					

Table 4.28. Significance level of Pearson's correlation coefficient R for relationships between salmon body size indices from Table 4.24 and oceanographic climate, and salmon run size indices from Table 4.23, for the time period 1954-97. '+' symbols indicate significant positive correlation while '-' symbols indicate significant negative correlation (F-test). The number of symbols indicates the negative logarithm of the maximum P-Value. For example, '++' or '- -' indicates $0.01 > P \geq 0.001$; '+++ ' or '- - -' indicates $0.001 > P \geq 0.0001$, etc. P-values ≥ 0.01 are considered insignificant.

	Climate Indices		Salmon Numbers		Curvature Distance			Latitude of Tmin			SST at Tmin			Overlap Area			Total Area
	PDO	ENSO	Pink	Sock.	E	M	W	E	M	W	E	M	W	E	M	W	
Sockeye length																	
FR1.1	-		---	---				++	++	++							
FR1.2	-		---	---										++			
FR1.3			-	---													
SK1.2			-	---													
SK1.3			-	---													
CP1.2			-	---													
CP1.3			-	---													
CP2.3			-	---													
CK1.2			-	---													
CK1.3			-	---													
CK2.2			-	---													
CK2.3			-	---													
BB1.2			-	---													
BB1.3			-	---													
BS2.2			-	---													
BB2.3			-	---													
Sockeye catch wt.																	
BC Area20			-	---										++	++		++
BC Area12			-	---										++	++		++
BC Area13			-	---										++	++		++
Ketchikan			-	---										++	++		++
Cook Inlet			-	---													
Kodiak			-	---										++			
Bristol Bay			-	---													
Pink catch wt.																	
Ketchikan			-	---													
Cook Inlet			-	---													
Kodiak			-	---										++			
Bristol Bay			-	---													
Coho catch wt.																	
Cook Inlet																	
Kodiak																	
Kuskowim														++			
Chum catch wt.																	
Ketchikan			-	---													
Cook Inlet			-	---													
Kodiak			-	---										++			
Bristol Bay			-	---													
Kuskowim			-	---													
Chinook catch wt.																	
Ketchikan			+++++	+++++													
Cook Inlet			+	+													
Kodiak			-	---										++			
Bristol Bay			-	---													
Kuskowim			-	---				++	++					++			
Yukon			-	---				++	++					++			

Table 4.29. Significance level of Pearson's correlation coefficient R for relationships between salmon body size indices from Table 4.24 and oceanographic climate, and salmon run size indices from Table 4.23, for the time period 1954-77. '+' symbols indicate significant positive correlation while '-' symbols indicate significant negative correlation (F-test). The number of symbols indicates the negative logarithm of the maximum P-Value. For example, '++' or '- -' indicates $0.01 > P \geq 0.001$; '+++' or '- - -' indicates $0.001 > P \geq 0.0001$, etc. P-values ≥ 0.01 are considered insignificant. Gray data series contained no data during this time period.

	Climate Indices		Salmon Numbers		Curvature Distance			Latitude of Tmin			SST at Tmin			Overlap Area			Total Area
	PDO	ENSO	Pink	Sock.	E	M	W	E	M	W	E	M	W	E	M	W	
Seckeye length																	
FR1.1								++	++	++							
FR1.2																	
FR1.3							++				++						
SK1.2																	
SK1.3																	
CP1.2																	
CP1.3																	
CP2.3																	
CK1.2											++	++					-
CK1.3																	
CK2.2													++				
CK2.3																	
BB1.2																	
BB1.3				-													
BB2.2				-													
BB2.3				-													
Seckeye catch wt.																	
Ketchikan	++																
Cook Inlet																	
Kodiak																	
Bristol Bay																	
Pink catch wt.																	
Ketchikan	++																
Cook Inlet																	
Kodiak																	
Bristol Bay																	
Coho catch wt.																	
Cook Inlet																	
Kodiak																	
Kuskowim																	
Chum catch wt.																	
Ketchikan																	
Cook Inlet																	
Kodiak																	
Bristol Bay																	
Kuskowim																	
Chinook catch wt.																	
Ketchikan																	
Cook Inlet																	
Kodiak	++																
Bristol Bay																	
Kuskowim																	
Yukon																	

Table 4.30. Significance level of Pearson's correlation coefficient R for relationships between salmon body size indices from Table 4.24 and oceanographic climate, and salmon run size indices from Table 4.23, for the time period 1978-97. '+' symbols indicate significant positive correlation while '-' symbols indicate significant negative correlation (F-test). The number of symbols indicates the negative logarithm of the maximum P-Value. For example, '++' or '- -' indicates $0.01 > P \geq 0.001$; '+++' or '- - -' indicates $0.001 > P \geq 0.0001$, etc. P-values ≥ 0.01 are considered insignificant.

	Climate Indices			Salmon Numbers			Curvature Distance			Latitude of Tmin			SST at Tmin			Overlap Area			Total Area		
	PDO	ENSO		Pink	Sock.		E	M	W	E	M	W	E	M	W	E	M	W			
Sockeye length																					
FR1.1																					
FR1.2				-	-																
FR1.3				-	-																
SK1.2																					
SK1.3				-	-																
CP1.2																					
CP1.3																					
CP2.3																					
CK1.2					-																
CK1.3				-	-																
CK2.2				-	-																
CK2.3					-																
BB1.2																					
BB1.3																					
BB2.2																					
BB2.3																					
Sockeye catch wt.																					
B/C Area20													-	-	-				++	++	++
B/C Area12													-	-	-				++	++	++
B/C Area13													-	-	-				++	++	++
Ketchikan																			++	++	++
Cook Inlet																			++	++	++
Kodiak																					
Bristol Bay																			++	++	++
Pink catch wt.																					
Ketchikan																					
Cook Inlet																					
Kodiak																					
Bristol Bay																					
Coho catch wt.																					
Cook Inlet																					
Kodiak																					
Kuskowim																					
Chum catch wt.																					
Ketchikan																					
Cook Inlet																					
Kodiak																					
Bristol Bay																					
Kuskowim																					
Chinook catch wt.																					
Ketchikan																					
Cook Inlet																					
Kodiak																					
Bristol Bay																					
Kuskowim																					
Yukon																					

Table 4.31. Pearson's correlation coefficient R of Fraser River age 1.2 fish length and body weights (commercial catch averages) with PDO, ENSO, N.Am.Sock, TMinEast and AreaEast time series, 1982-97.

<i>Pearson's R for 1982-97</i>	<i>PDO</i>	<i>ENSO</i>	<i>NAmSock</i>	<i>TminEast</i>	<i>AreaEast</i>
BC Area20 Body Weight	-0.06	-0.16	-0.62	-0.69	0.66
BC Area12 Body Weight	0.08	0.02	-0.59	-0.66	0.64
BC Area13 Body Weight	0.02	-0.11	-0.64	-0.70	0.65
FR1.2 Body length	0.03	-0.21	-0.75	-0.50	0.57

Table 4.32. Number of years classified as Large/Cold or Small/Warm (referring to salmon/squid overlap area and SST) or as Few/Many years (referring to total catch + escapement of North American pink and sockeye salmon, 1954-97.

	Few Fish	Many Fish	Total
Large/Cold	16	5	21
Small/Warm	9	14	23
Total	25	19	44

Table 4.33. Regression results of body size vs. AreaEast and body size vs. TminEast for years with run sizes categorized as "few" and "many" fish. Only selected stocks are shown.

OVERLAP AREA

	FEW					MANY				
	N	Slope	Int.	R2	P	N	Slope	Int.	R2	P
FR1.2	25					19	0.48	-0.55	0.27	*
FR1.3	25					19	0.37	-0.40	0.21	*
CK1.2	12	-0.44	0.92	0.33	*	19	0.41	-0.40	0.31	*
CK2.2	12					19	0.36	-0.42	0.27	*
PINK-KETCHIKAN	10					18				
PINK-COOK INLET	10					18	0.46	-0.43	0.27	*
PINK-KODIAK	10					18				
SOCKEYE-KODIAK	10					18	0.42	-0.41	0.25	*
CHUM-COOK INLET	10					18	0.66	-0.05	0.38	**
CHINOOK-BRISTOL BAY	10					18	0.55	-0.31	0.33	*
CHINOOK-KUSKOKWIM	10					18				
CHINOOK-YUKON	9					18				

Tmin

	FEW					MANY				
	N	Slope	Int.	R2	P	N	Slope	Int.	R2	P
FR1.2	25					19	-0.54	-0.41	0.23	*
FR1.3	25	0.47	0.55	0.21	*	19				
CK1.2	12	0.47	1.03	0.40	*	19				
CK2.2	12					19				
PINK-KETCHIKAN	10					18				
PINK-COOK INLET	10					18				
PINK-KODIAK	10					18				
SOCKEYE-KODIAK	10					18				
CHUM-COOK INLET	10					18	-0.74	0.17	0.36	**
CHINOOK-BRISTOL BAY	10					18				
CHINOOK-KUSKOKWIM	10					18				
CHINOOK-YUKON	9					18				

* P<.05

**P<.01

***P<.001

****P<.0001

Table 4.34. Regression results of body size vs. run size of pink and sockeye salmon, respectively, in years categorized as "Small Warm" and "Large Cold" oceanographic conditions. Only selected stocks are shown.

PINK	SMALL WARM					LARGE COLD				
	N	Slope	Int.	R2	P	N	Slope	Int.	R2	P
FR1.2	23	-0.71	0.03	0.39	**	21	-0.41	0.10	0.20	*
FR1.3	23	-0.60	0.07	0.31	**	21		0.12		
CK1.2	17	-0.66	0.21	0.32	*	14	-0.55	0.21	0.40	*
CK2.2	17	-0.83	0.32	0.57	***	14	-0.66	0.21	0.46	**
PINK-KETCHIKAN	14		0.02			14	-0.66	0.27	0.34	*
PINK-COOK INLET	14	-1.06	0.47	0.74	****	14	-0.40	0.43	0.31	*
PINK-KODIAK	14	-0.62	0.03	0.30	*	14	-0.61	0.40	0.54	**
SOCKEYE-KODIAK	14	-0.59	0.03	0.55	**	14	-0.69	0.36	0.34	*
CHUM-COOK INLET	14		-0.18			14		0.49		
CHINOOK-BRISTOL BAY	14		0.23			14		0.31		
CHINOOK-KUSKOKWIM	14	-0.58	0.14	0.42	*	14		0.30		
CHINOOK-YUKON	14	-0.81	0.45	0.38	*	13	-0.58	0.23	0.42	*

SOCKEYE	SMALL WARM					LARGE COLD				
	N	Slope	Int.	R2	P	N	Slope	Int.	R2	P
FR1.2	23	-0.73	-0.01	0.52	****	21	-0.50	0.10	0.22	*
FR1.3	23	-0.67	0.05	0.49	***	21		0.02		
CK1.2	17	-0.84	0.35	0.58	***	14	-0.81	0.15	0.50	**
CK2.2	17	-0.71	0.23	0.47	**	14	-0.96	0.14	0.57	**
PINK-KETCHIKAN	14		-0.22			14		0.26		
PINK-COOK INLET	14	-0.90	0.40	0.54	**	14		0.42		
PINK-KODIAK	14		-0.06			14	-0.90	0.34	0.70	***
SOCKEYE-KODIAK	14	-0.57	0.05	0.50	**	14	-1.00	0.29	0.43	**
CHUM-COOK INLET	14		-0.08			14		0.43		
CHINOOK-BRISTOL BAY	14	-0.77	0.38	0.37	*	14		0.28		
CHINOOK-KUSKOKWIM	14	-0.78	0.40	0.78	****	14		0.21		
CHINOOK-YUKON	14	-0.93	0.64	0.50	**	13	-0.75	0.19	0.43	*

* P<.05

**P<.01

***P<.001

****P<.0001

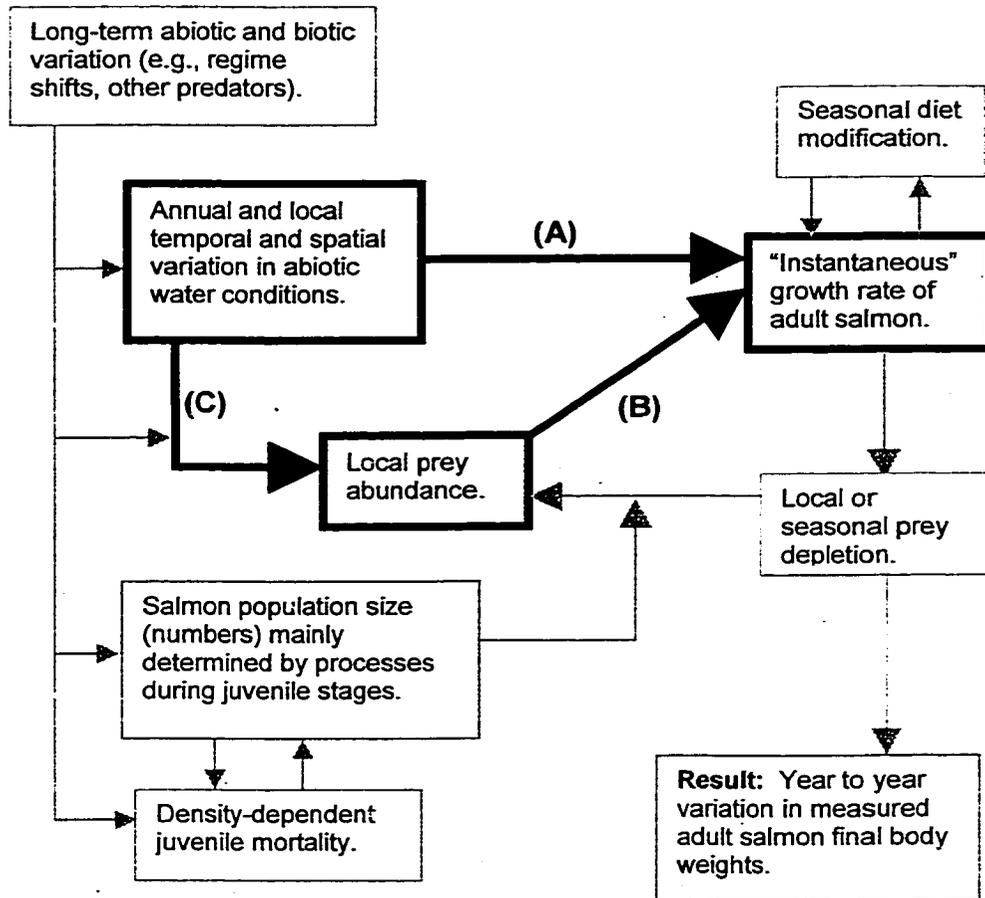


Figure 4.1. Conceptual model of factors influencing salmon growth rates, highlighting sections discussed in Chapter 4 (see text for details).

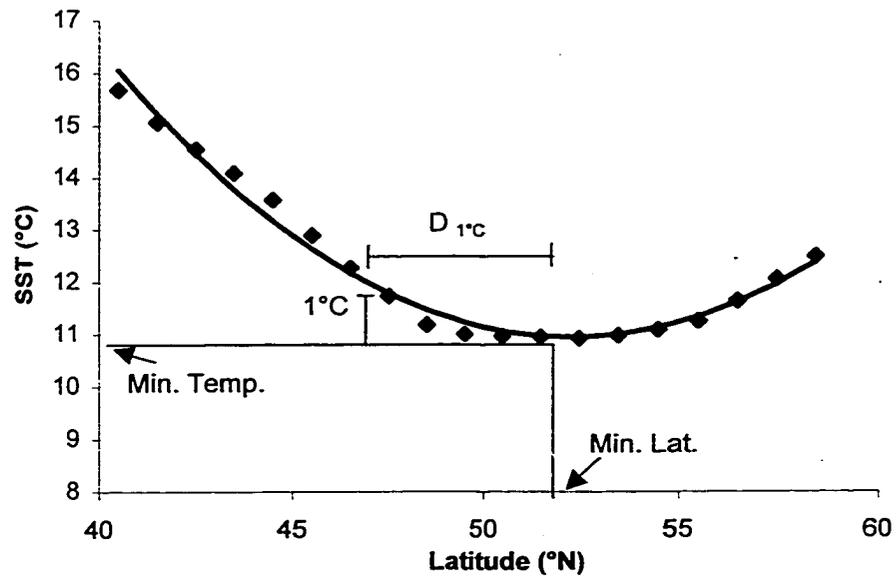


Figure 4.3. Points show actual $1 \times 1^\circ$ IGOSS sea surface temperatures for a single year. The solid line represents the smoothed 2nd degree curve fit using three parameters. The parameters may be manipulated to have specific physical meaning. In this case, the three parameters are minimum latitude (the latitude at which temperature is at a minimum), minimum temperature (the fit temperature at this minimum) and $D(1^\circ)$, or the distance in degrees latitude required for the temperature to rise 1°C from the minimum.

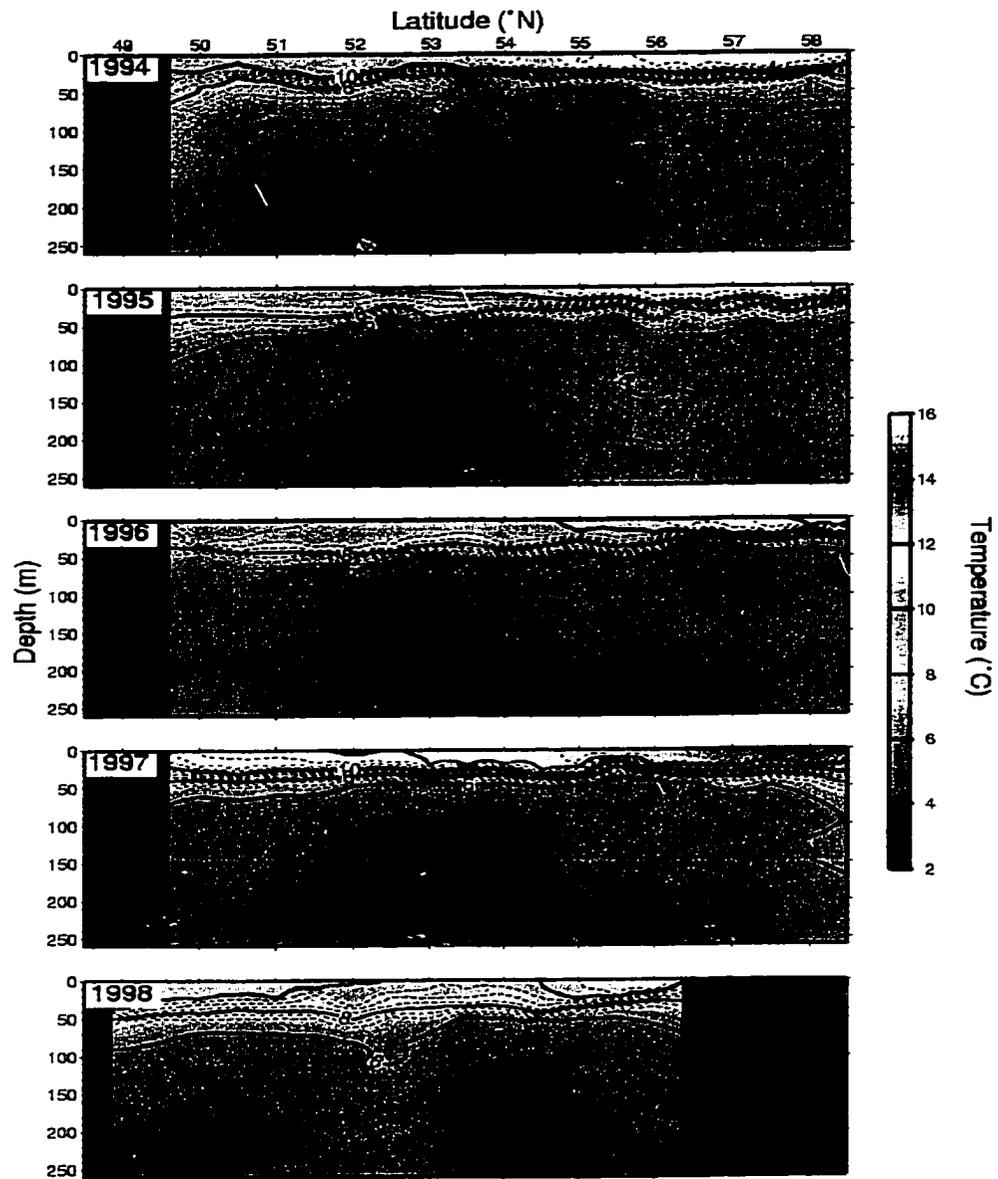


Figure 4.4. Surface to 250 meter water temperatures from CTD data, 145°W, July 1994-98.

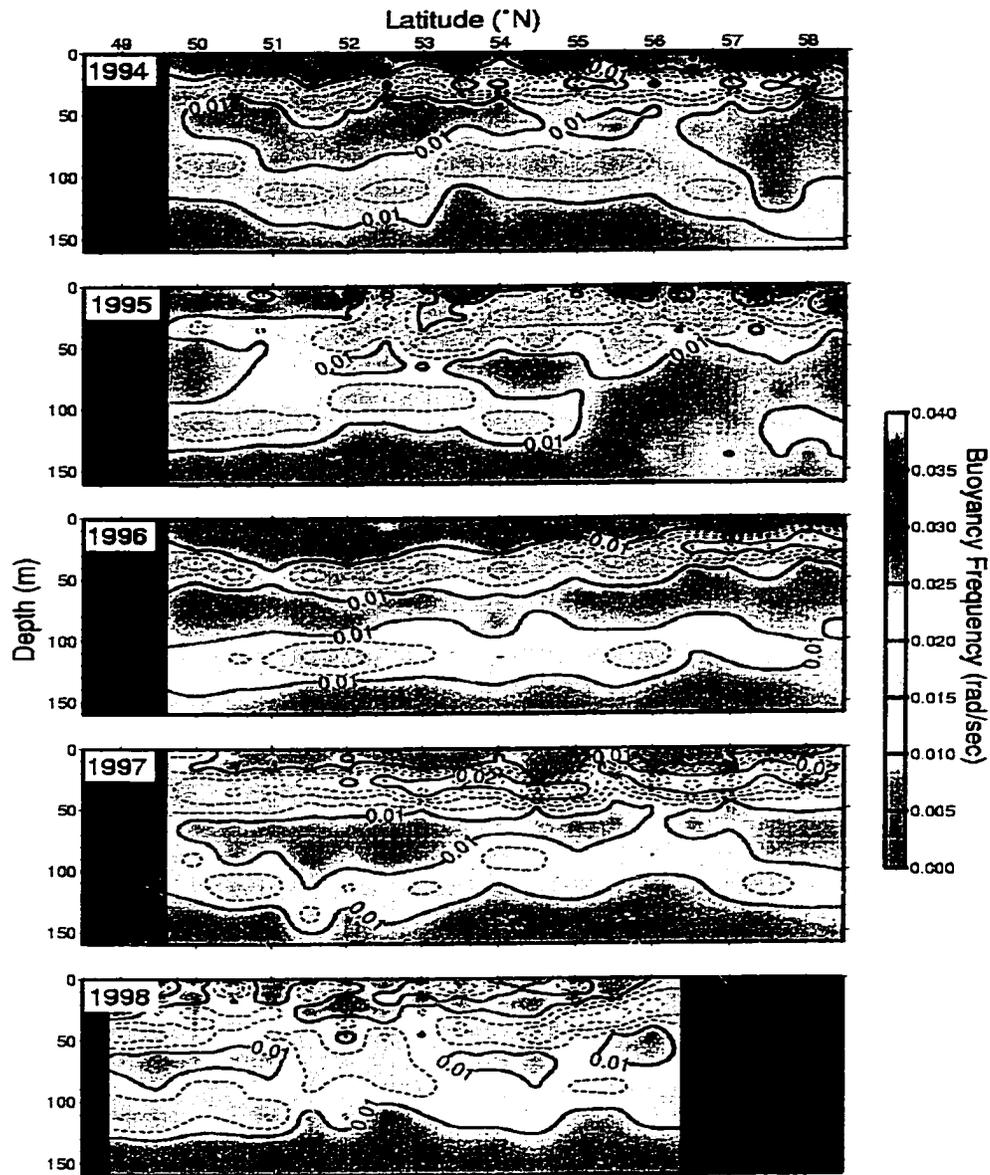


Figure 4.5. Surface to 150 meter buoyancy frequency from CTD data, 145°W, July 1994-98. Green/yellow bands show thermocline (shallow band) and halocline (deep band).

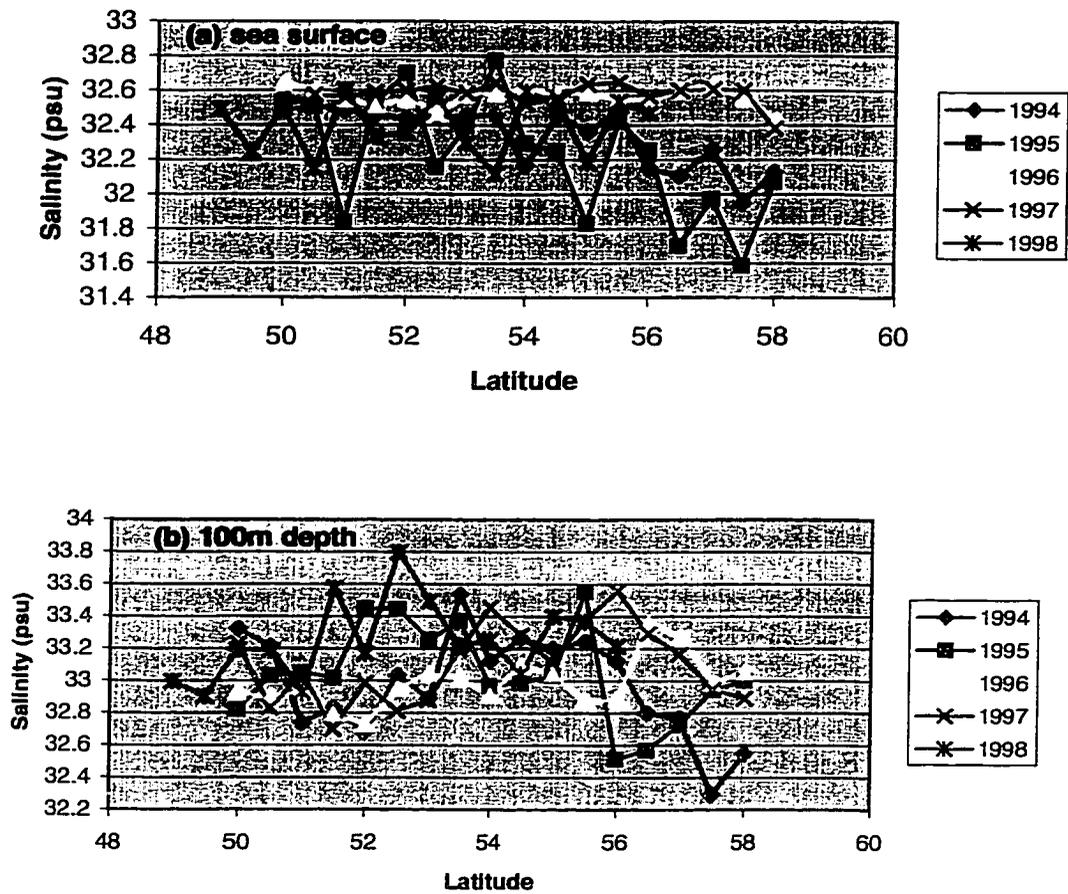


Figure 4.6. Salinity at (a) surface and (b) 100 meters from CTD data, 145°W, July 1994-98.

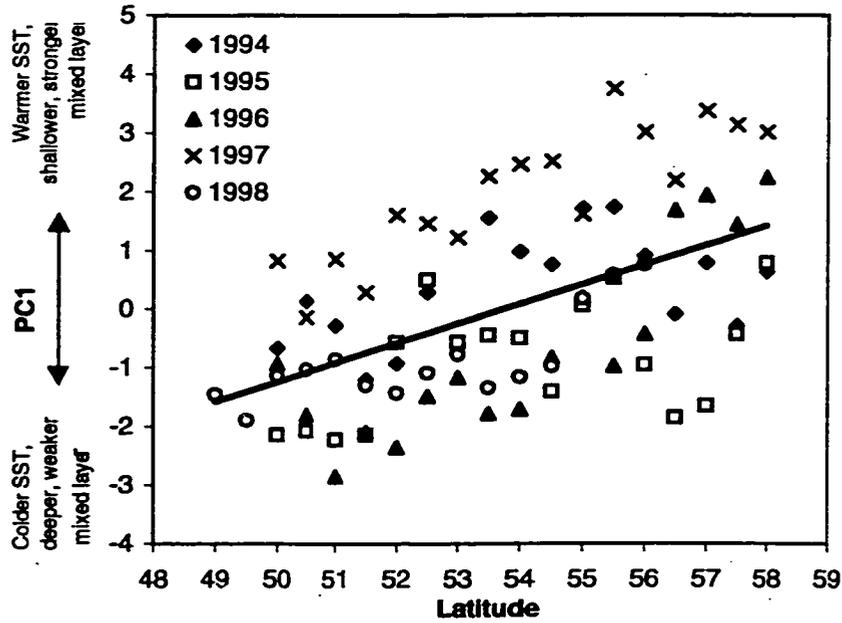


Figure 4.7. The first principle component of the eight oceanographic variables sea surface temperature and salinity, 100m temperature and salinity, mixed-layer depth and maximum buoyancy frequency, and permanent pycnocline depth and maximum buoyancy frequency, regressed vs. latitude. The first PC's primary components are SST, mixed-layer depth, and mixed layer buoyancy frequency.

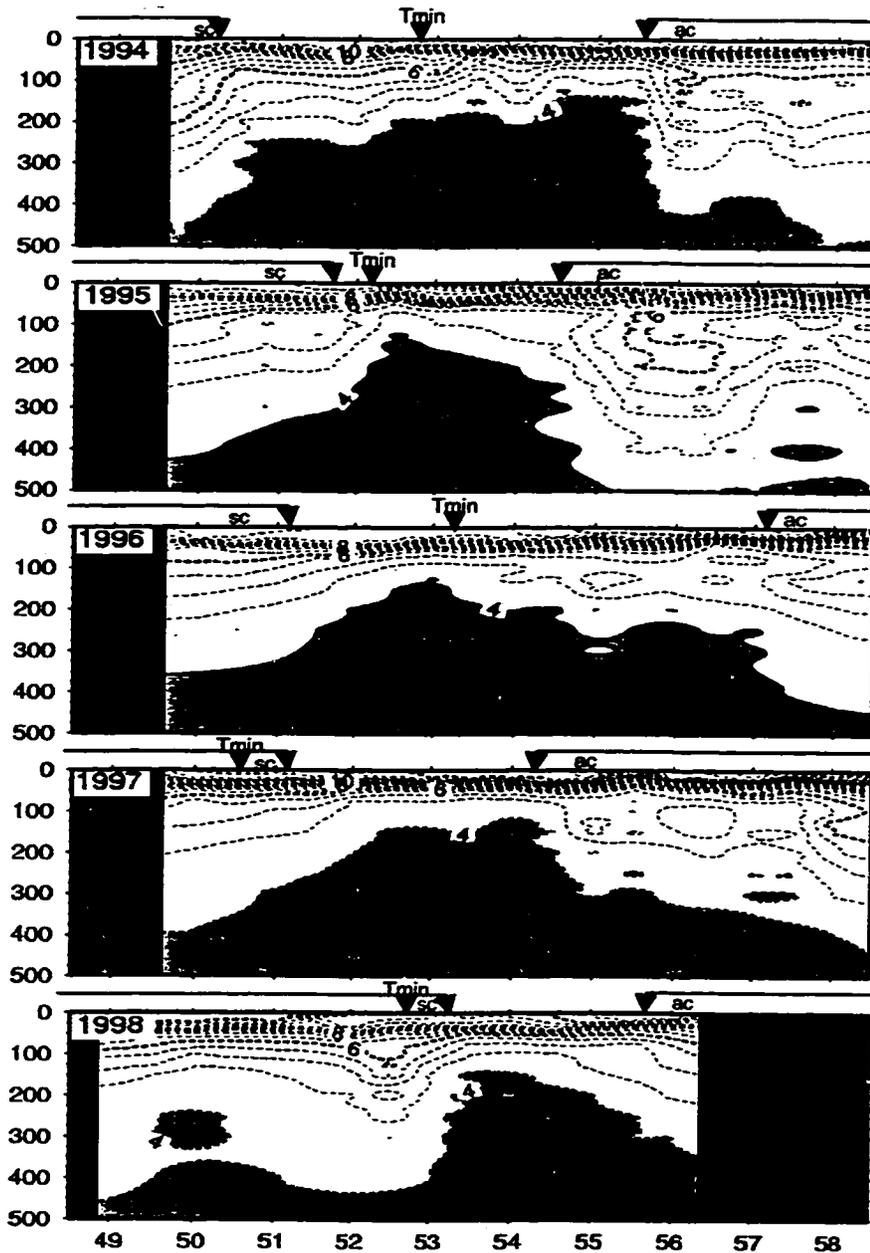


Figure 4.8. Sea surface to 500m water temperatures from CTD data, emphasizing 4°C isotherm (shaded areas are below 4°C). Oceanographic boundaries defined by the rising of the isotherm mark the edges of the Subarctic Current (sc) and the Alaska Current (ac). Tmin shows the location of the latitudinal sea surface temperature minimum from monthly mean temperature values.

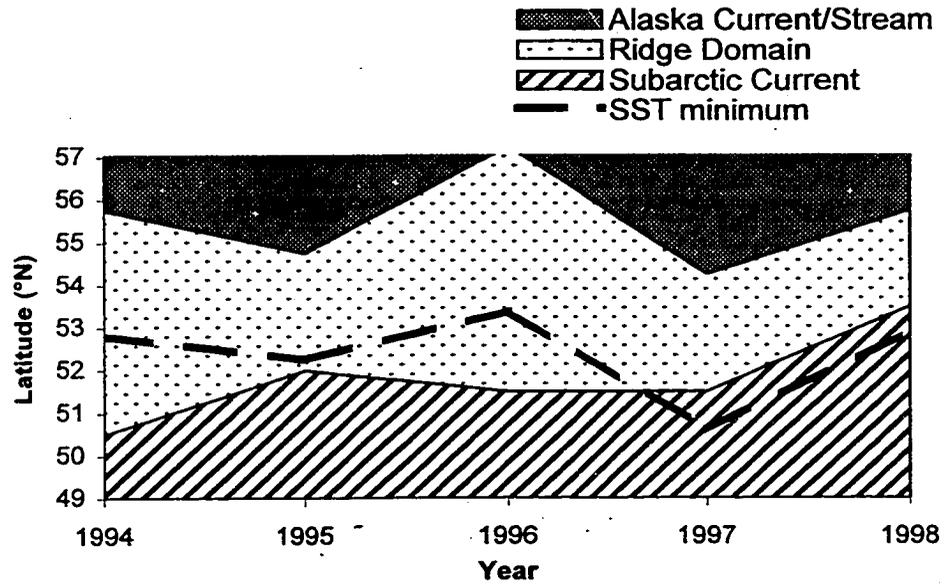


Figure 4.9. Oceanographic Boundaries as determined from temperature and salinity data for all years between the Subarctic Current and the Alaskan Stream. The SST minimum is calculated from quadratic fitting to July IGOSS data as shown in Figure 3.

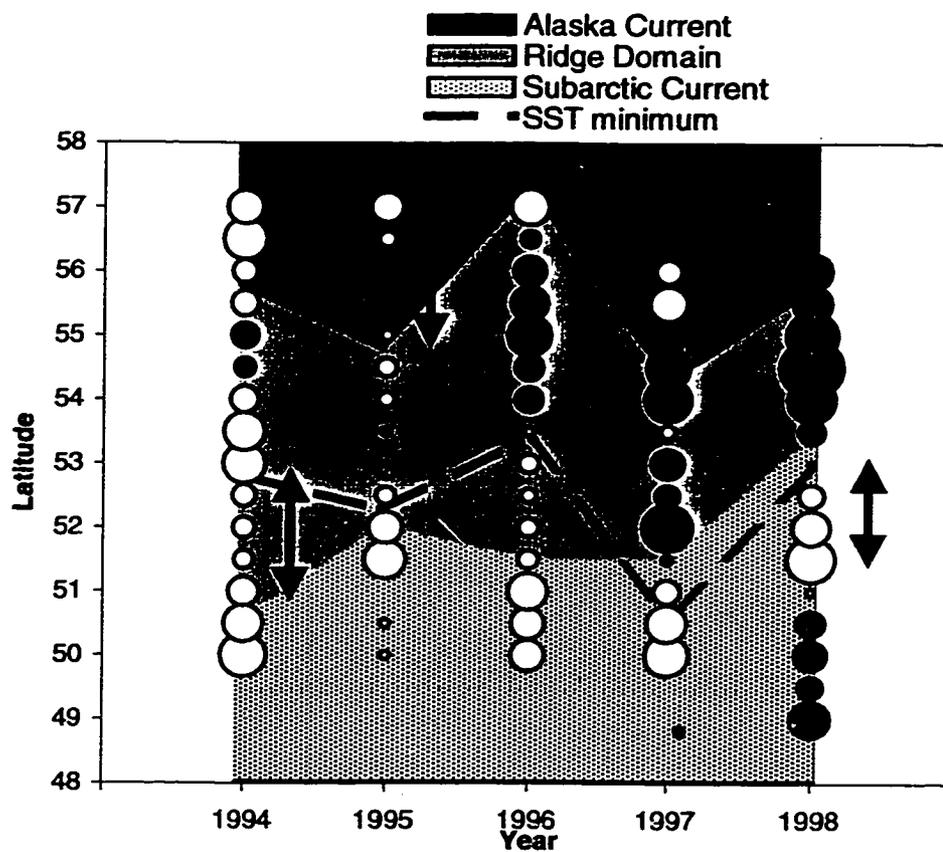


Figure 4.10. Zooplankton densities (mg/m^3 wet weight; black or white circles) at 0-150m by year and latitude, superimposed on oceanographic domains. The area of each circle is proportional to the deviation of the zooplankton density at that station from the mean density over all stations. Area of the circles represents distance of values from the mean; larger circles show larger standard deviations from the mean. Black circles show positive deviations, while white circles show negative deviations. The largest circles are approximately ± 3 s.d. from the mean. Arrows show the locations of the three anticyclonic eddies with the greatest volume transport during the study period, as reported by Onishi et al. (2000).

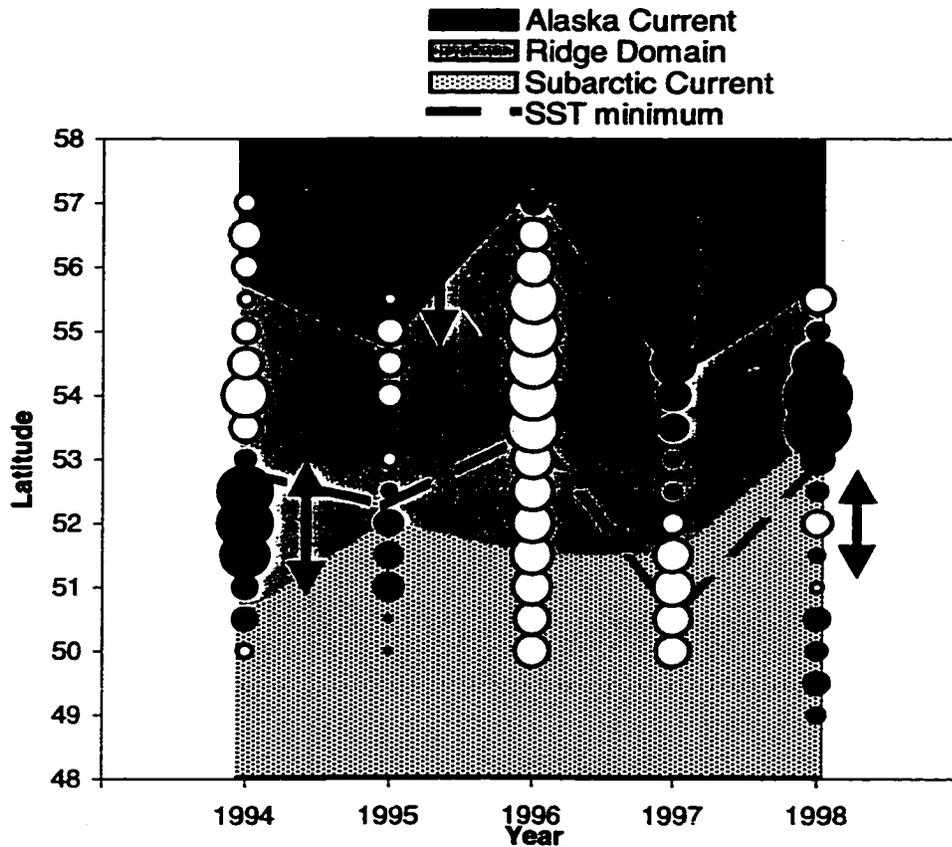


Figure 4.11. Phytoplankton densities estimated from ocean color measurements, by year and latitude, superimposed on oceanographic domains. The area of each circle is proportional to the deviation of the phytoplankton density at that station from the mean density over all stations. Area of the circles represents distance of values from the mean; larger circles show larger standard deviations from the mean. Black circles show positive deviations, while white circles show negative deviations. The largest circles are approximately ± 3 s.d. from the mean. Arrows show the locations of the three anticyclonic eddies with the greatest volume transport during the study period, as reported by Onishi et al. (2000).

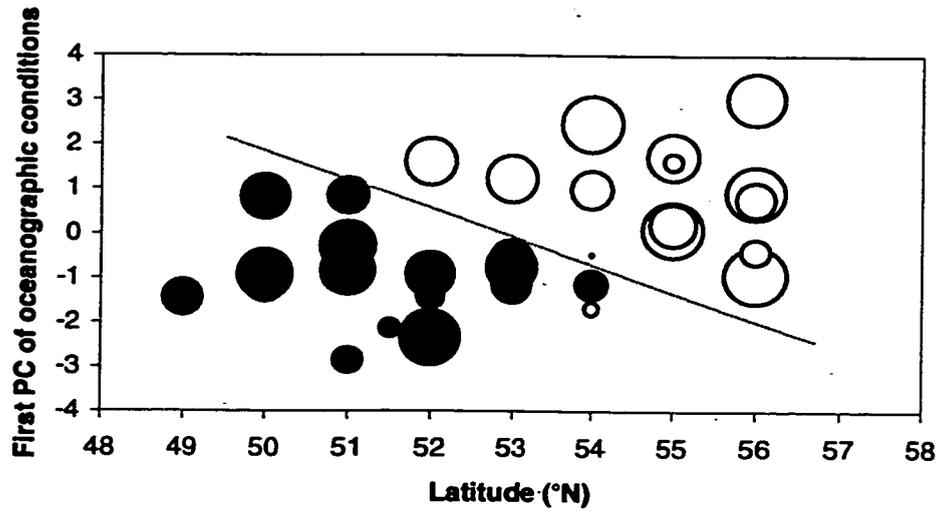


Figure 4.12. Squid index values plotted by latitude and the first principle component of oceanographic conditions for all stations, 1994-98. The area of each circle is proportional to the deviation of the squid index value at that station from the mean density over all stations. The largest circles are approximately ± 2.5 squid index units from the mean. The dotted line shows the division between high and low squid densities fitted by eye.

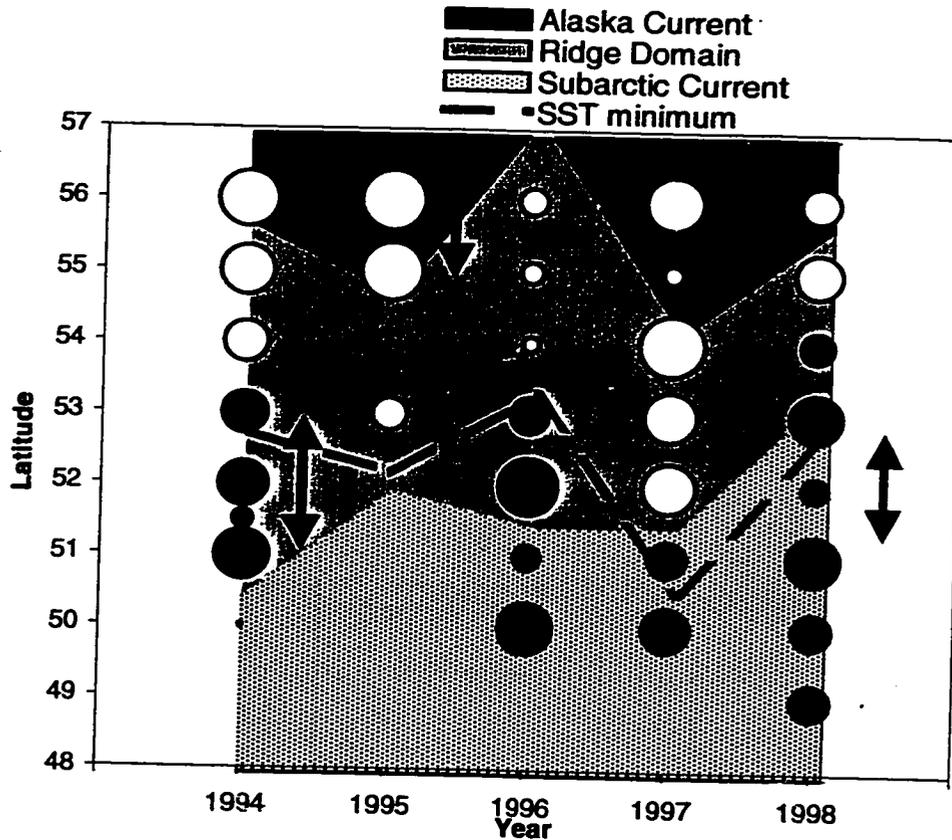


Figure 4.13. Squid index values by year and latitude, superimposed on oceanographic domains. The area of each circle is proportional to the deviation of the squid index value at that station from the mean density over all stations. Area of the circles represents distance of values from the mean; larger circles show larger standard deviations from the mean. Black circles show positive deviations, while white circles show negative deviations. The largest circles are approximately ± 3 s.d. from the mean. Arrows show the locations of the three anticyclonic eddies with the greatest volume transport during the study period, as reported by Onishi et al. (2000).

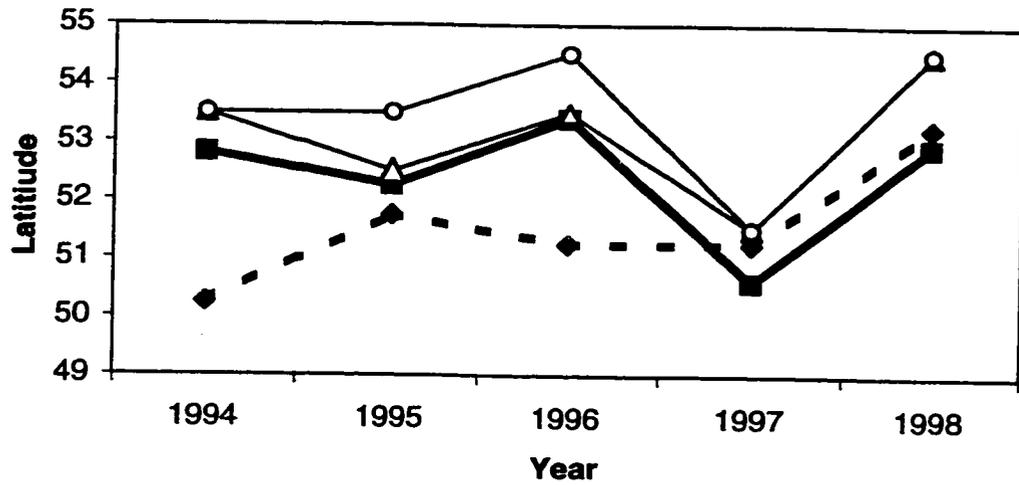


Figure 4.14. Latitude of north/south border using four criteria. The dotted line shows the latitude of the Ridge/Subarctic Boundary, while the solid bold line shows IGOS temperature minimum. The two lines with open circles/triangles show latitudes of abrupt changes in squid density values. Circles indicate the cutoff determined by the dotted line in Figure 4.12, while triangles indicate the latitude south of which all squid index values are positive, north of which all values are negative.

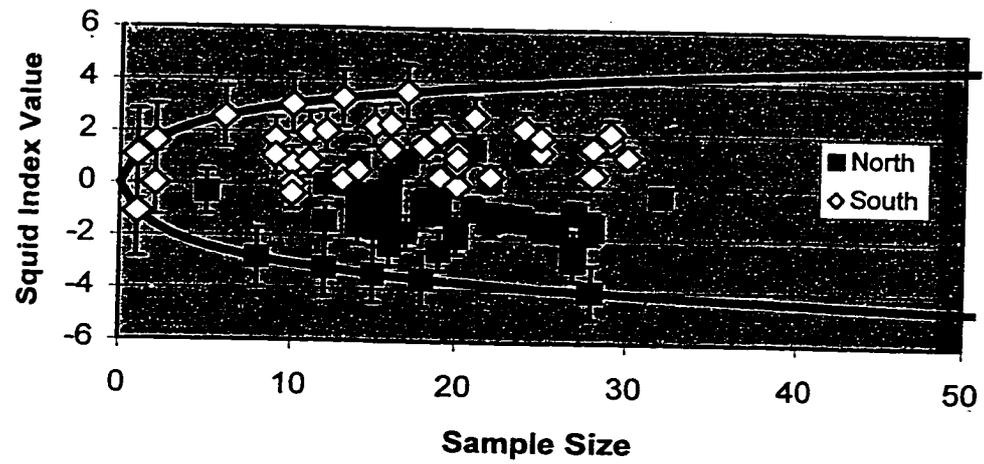


Figure 4.15. Squid index values for north and south of the SST minimum, as a function of sample size of salmon, shown with estimated standard deviations calculated as in Chapter 3 (error bars). The solid line shows the minimum and maximum possible values for the squid index given the sample size.

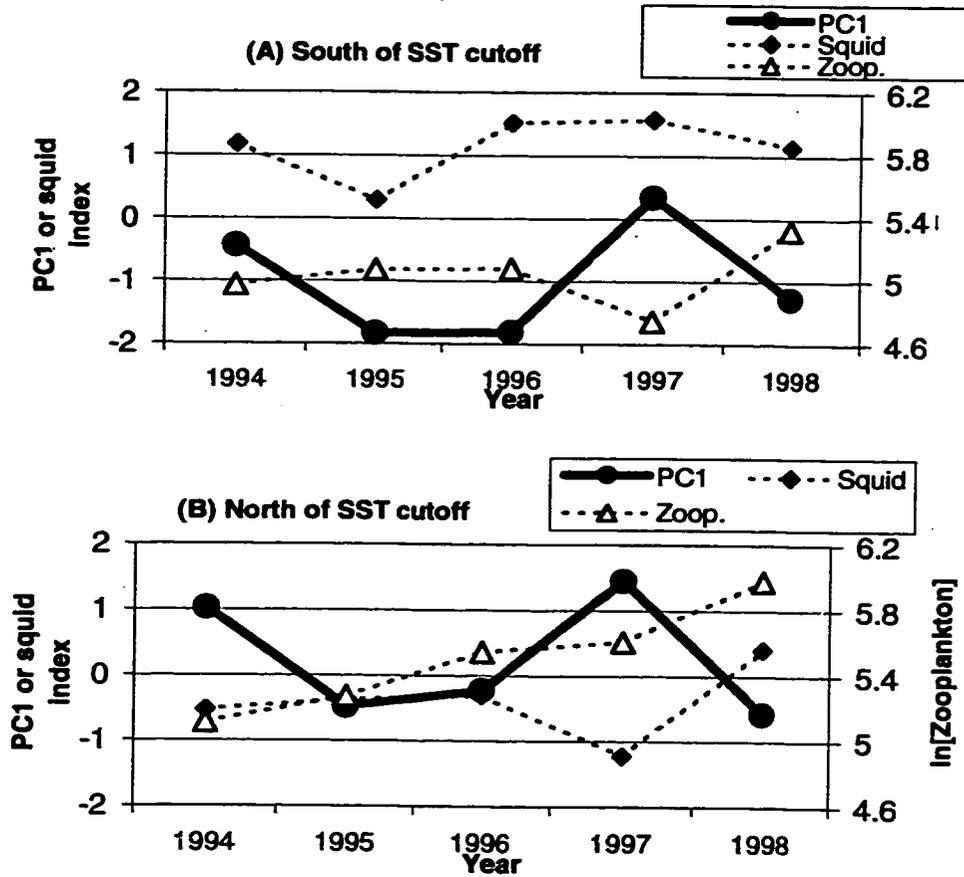


Figure 4.16. PC1, Zooplankton, and squid index values averaged (A) south and (B) north of the latitude of minimum SST, averaged by year. Bold lines showed a significant difference between years ($P < 0.005$), while dotted lines showed no significant difference between years ($P > 0.05$).

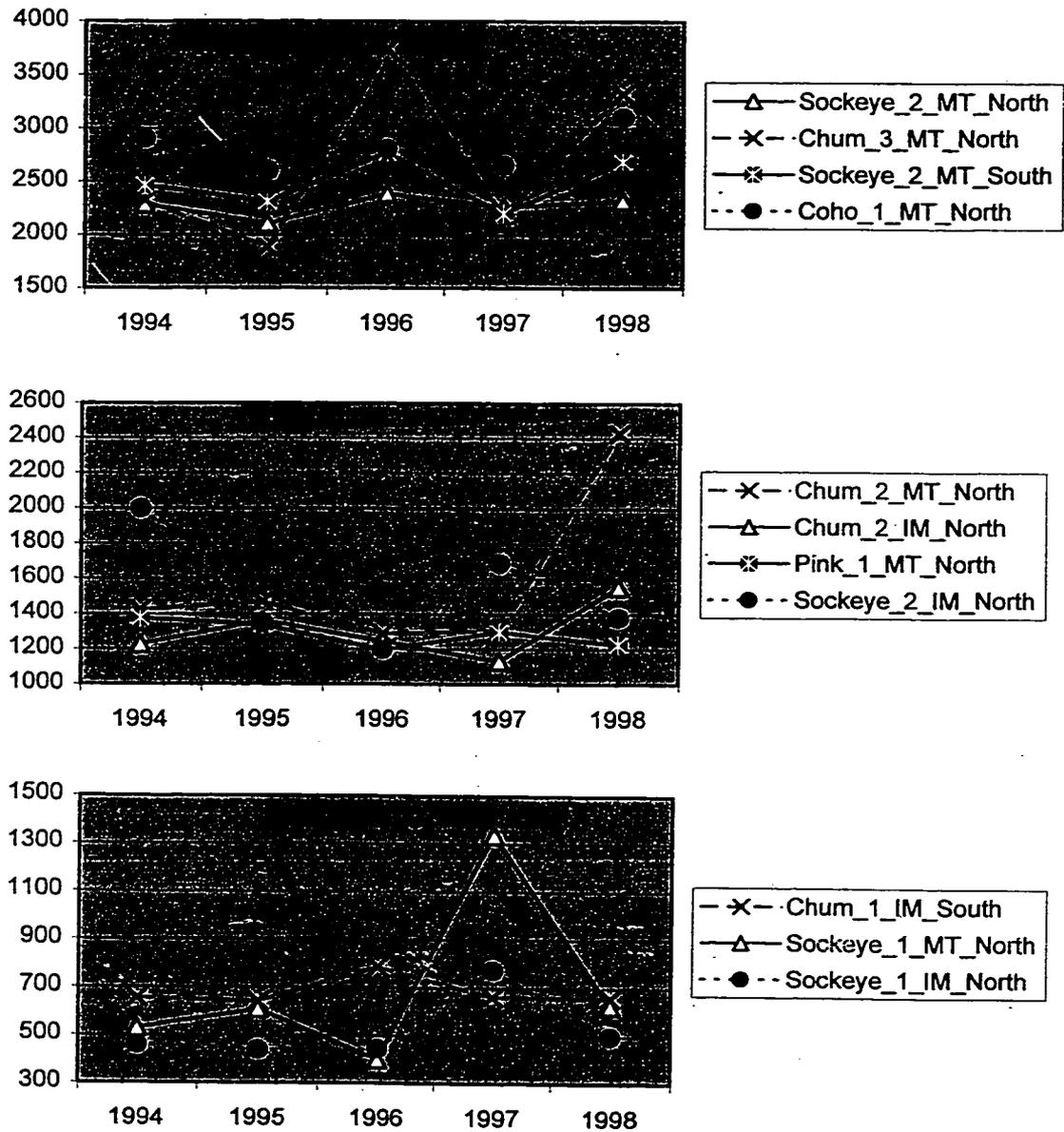


Figure 4.17. Year to year trend in body weights of salmon divided by species, age class, maturity status, and location south or north of the SST minimum. Only series with catches in all years which showed significant differences between years are shown. (A) shows the 4 series with the largest overall mean size (above 1.9 kg), (B) shows 4 series with middle mean sizes (1.2-1.8 kg) and (C) shows 3 series with smallest mean sizes (0.5-0.8 kg). Numbers indicate ocean ages while MT or IM indicate maturity status.

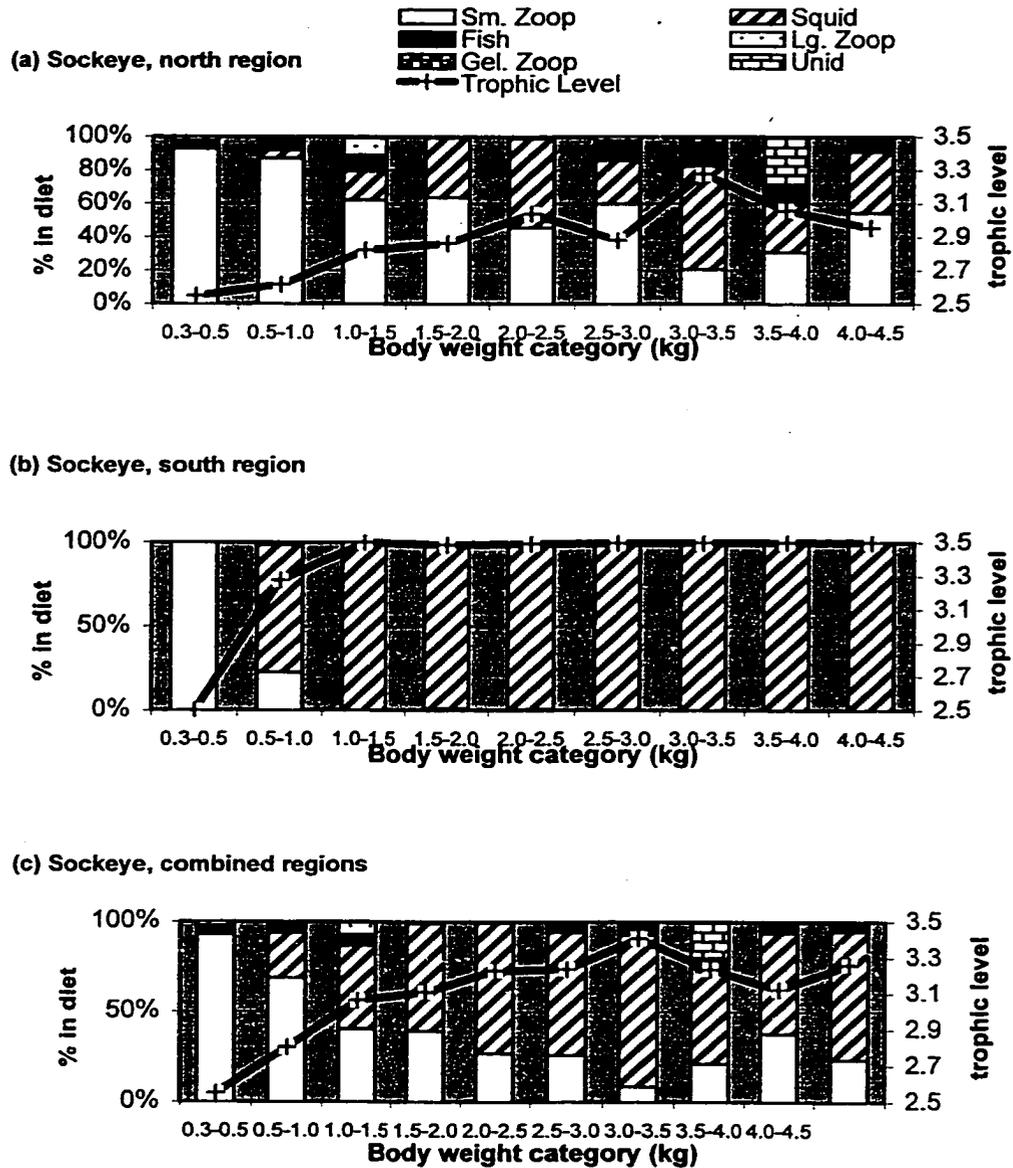


Figure 4.18. Diet composition of sockeye salmon by body weight, calculated from the total weight of prey found in stomachs, corrected for digestion. (a) and (b) show diet composition in north and south zones, respectively. (c) shows diet in both zones, weighted by the proportion of catch (CPUE) of each weight category caught in each zone.

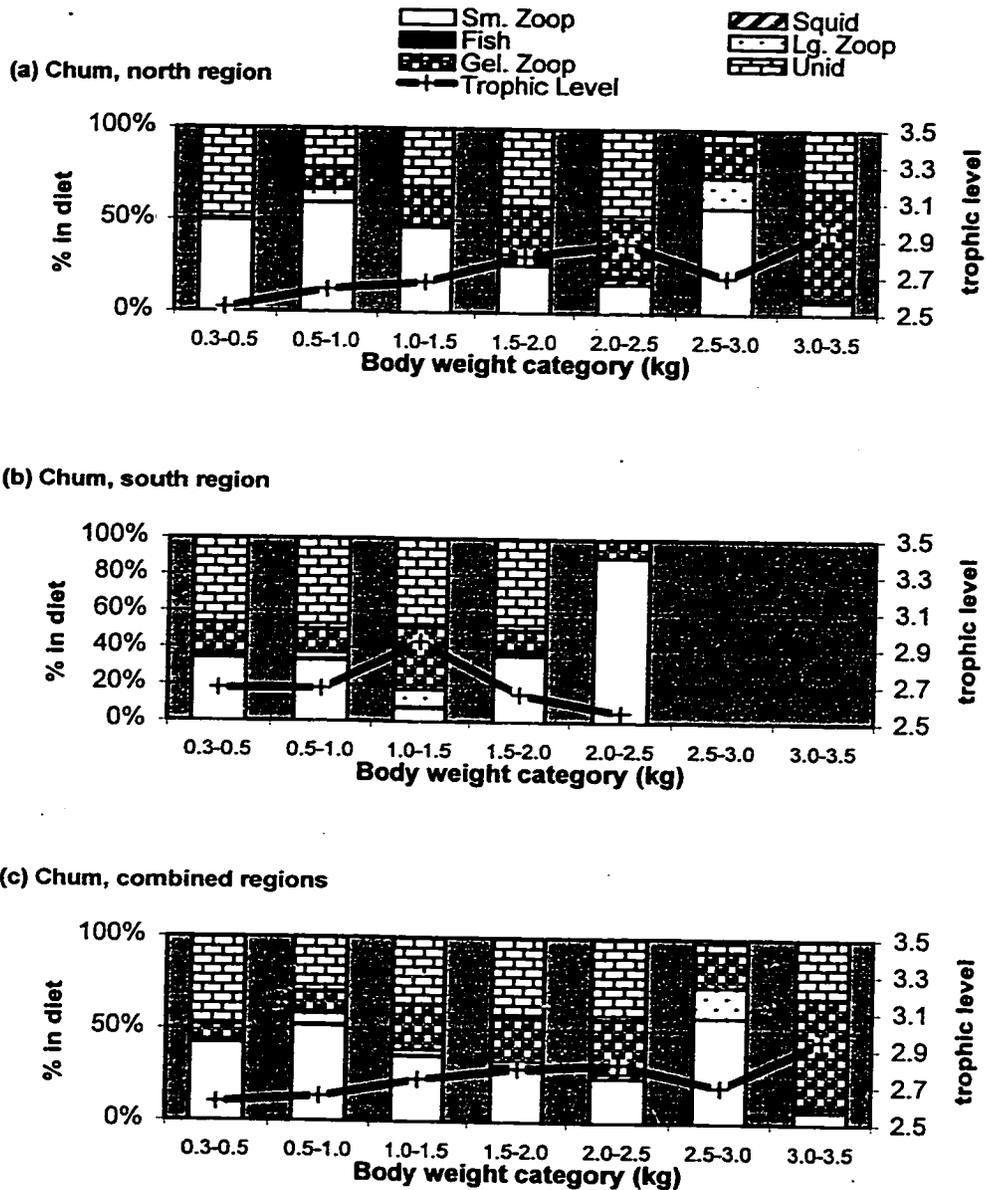


Figure 4.19. Diet composition of chum salmon by body weight, calculated from the total weight of prey found in stomachs, corrected for digestion. (a) and (b) show diet composition in north and south zones, respectively. (c) shows diet in both zones, weighted by the proportion of catch (CPUE of research gillnet) of each weight category caught in each zone.

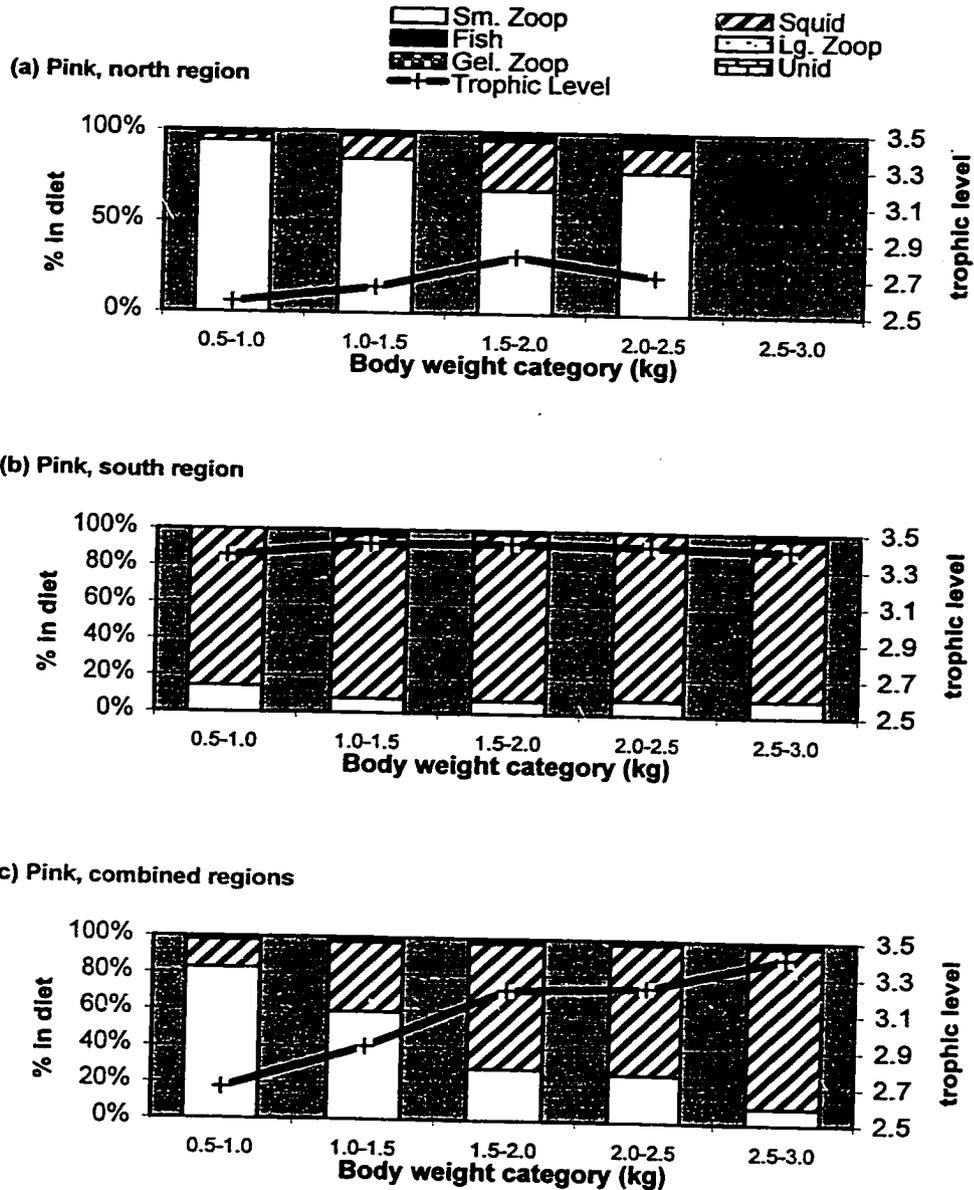


Figure 4.20. Diet composition of pink salmon by body weight, calculated from the total weight of prey found in stomachs, corrected for digestion. (a) and (b) show diet composition in north and south zones, respectively. (c) shows diet in both zones, weighted by the proportion of catch (CPUE of research gillnet) of each weight category caught in each zone.

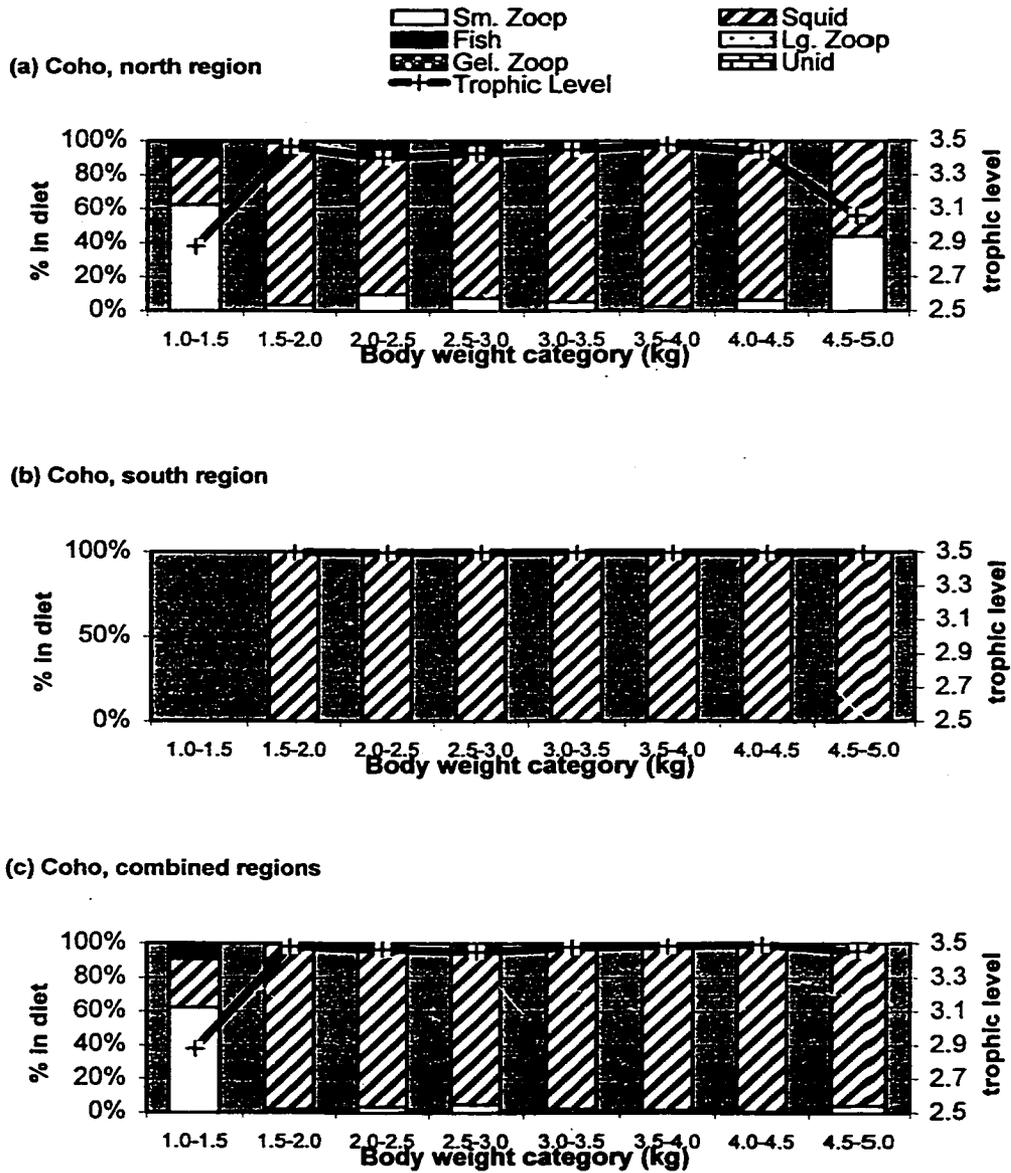


Figure 4.21. Diet composition of coho salmon by body weight, calculated from the total weight of prey found in stomachs, corrected for digestion. (a) and (b) show diet composition in north and south zones, respectively. (c) shows diet in both zones, weighted by the proportion of catch (CPUE of research gillnet) of each weight category caught in each zone.

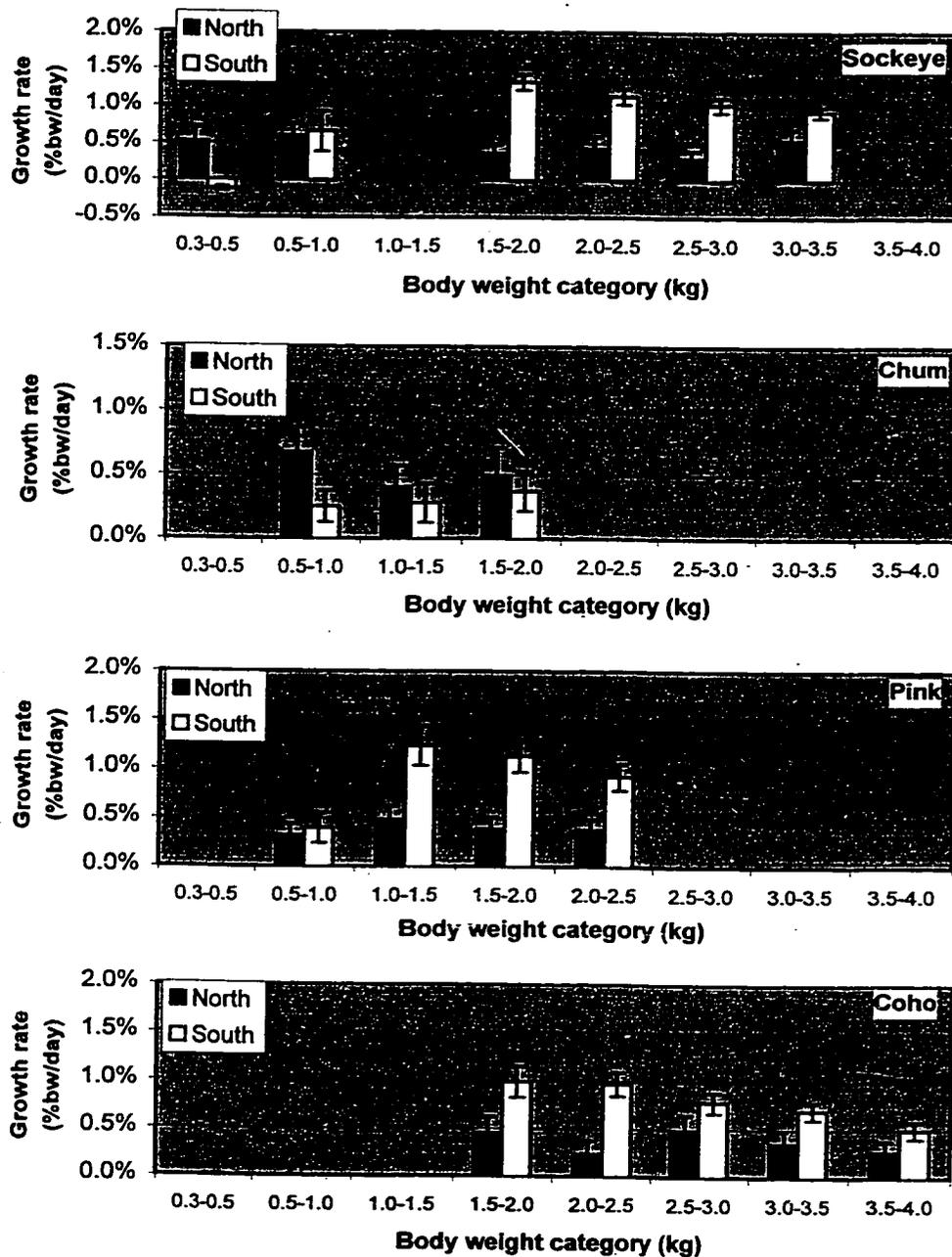


Figure 4.22. Simulated growth rates (% body weight/day) of salmon, by species and body weight, in north and south zones, assuming squid caloric density=1000 cal/g wet weight. Error bars show standard deviation of growth rate based on 10,000 replicate samples of 30 fish, drawn from the original data set.

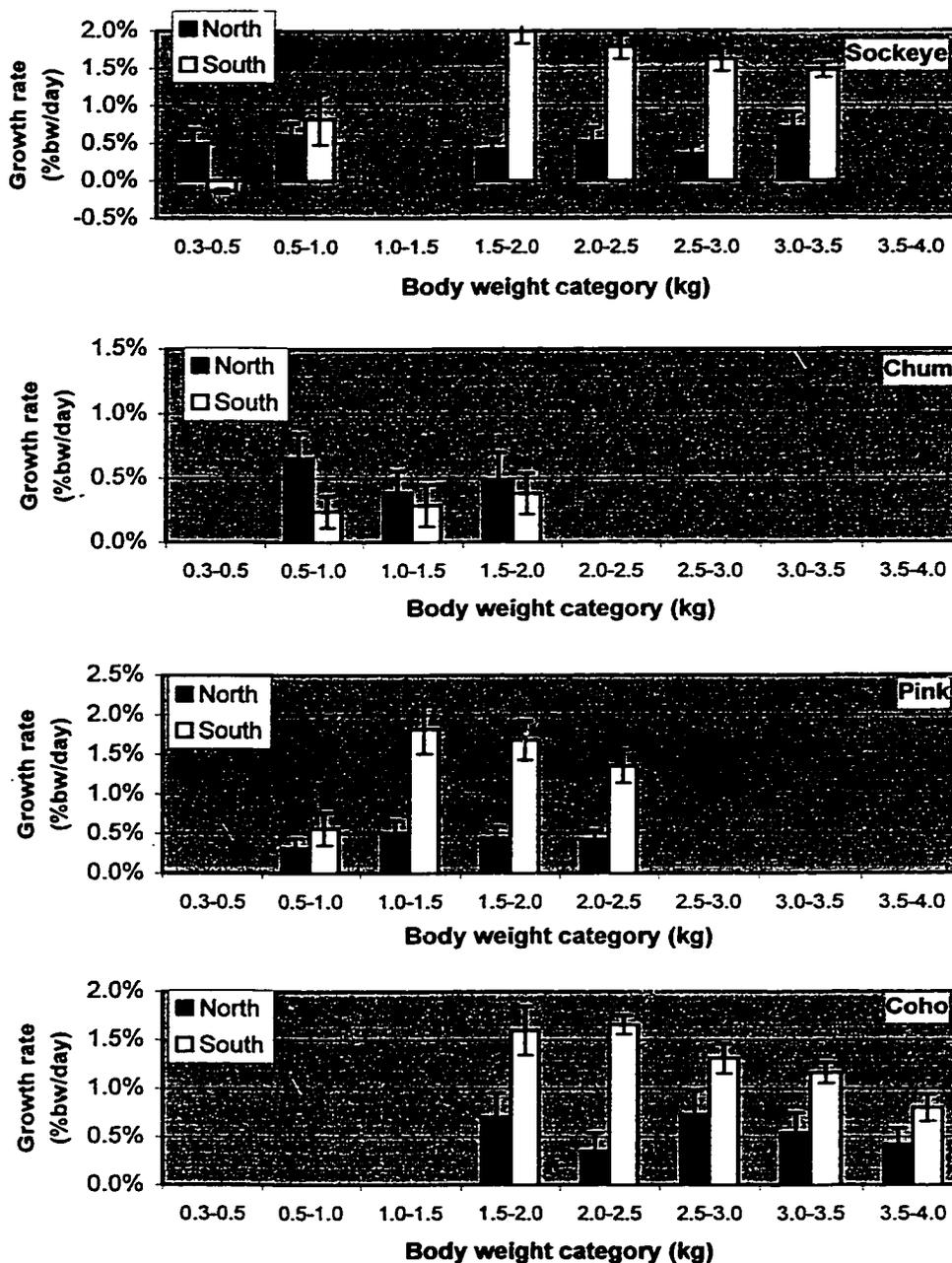


Figure 4.23. Simulated growth rates (% body weight/day) of salmon as in Figure 4.22, assuming squid caloric density=1500 cal/g wet weight.

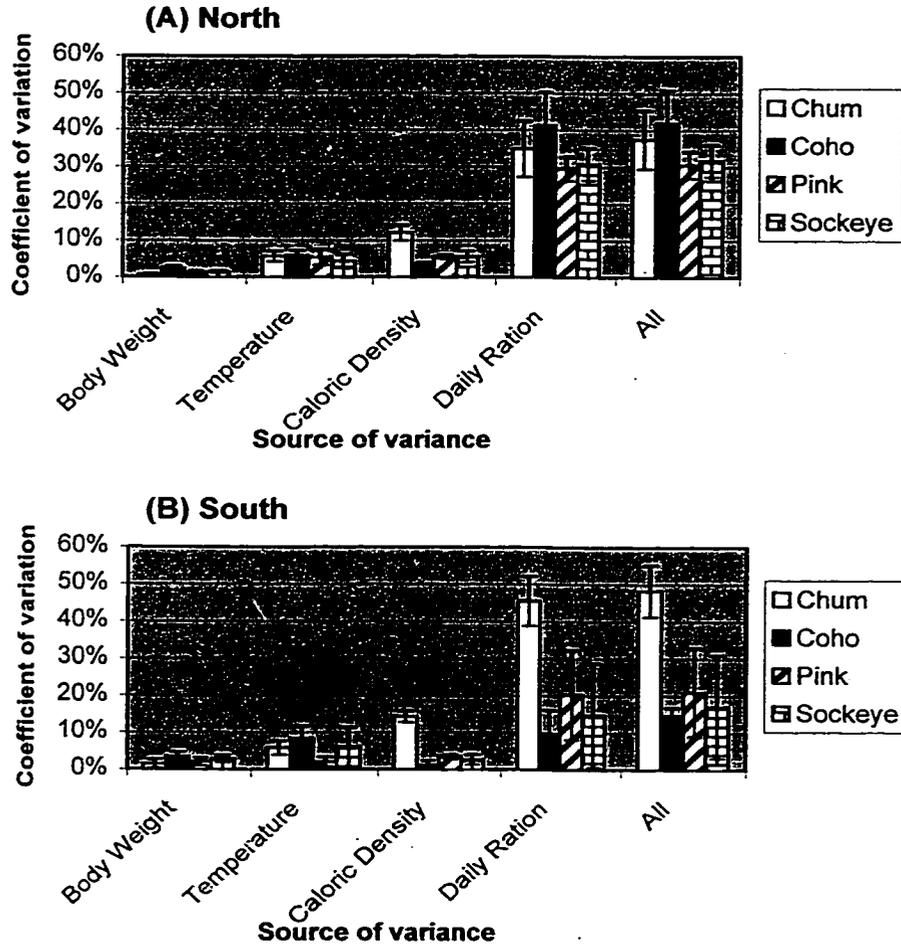


Figure 4.24. Coefficient of variation of growth rates shown in Table 4.16, calculated for each factor (body weight, water temperature, daily ration, and prey caloric density) separately. See text for calculation method.

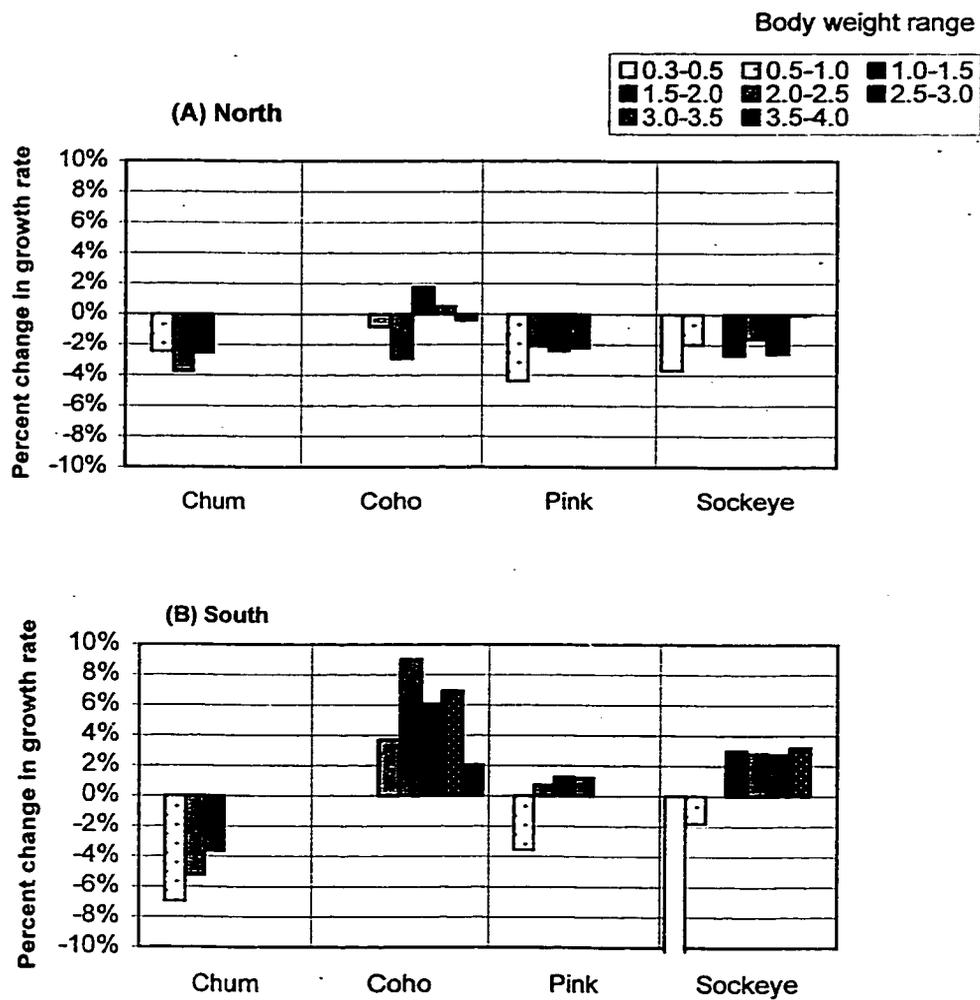


Figure 4.25. Estimated percent change of the growth rates reported in Table 4.16 with a 10% increase in 0-40m water temperature. Estimates assume that fish physiological temperature is equal to the 0-40m average.

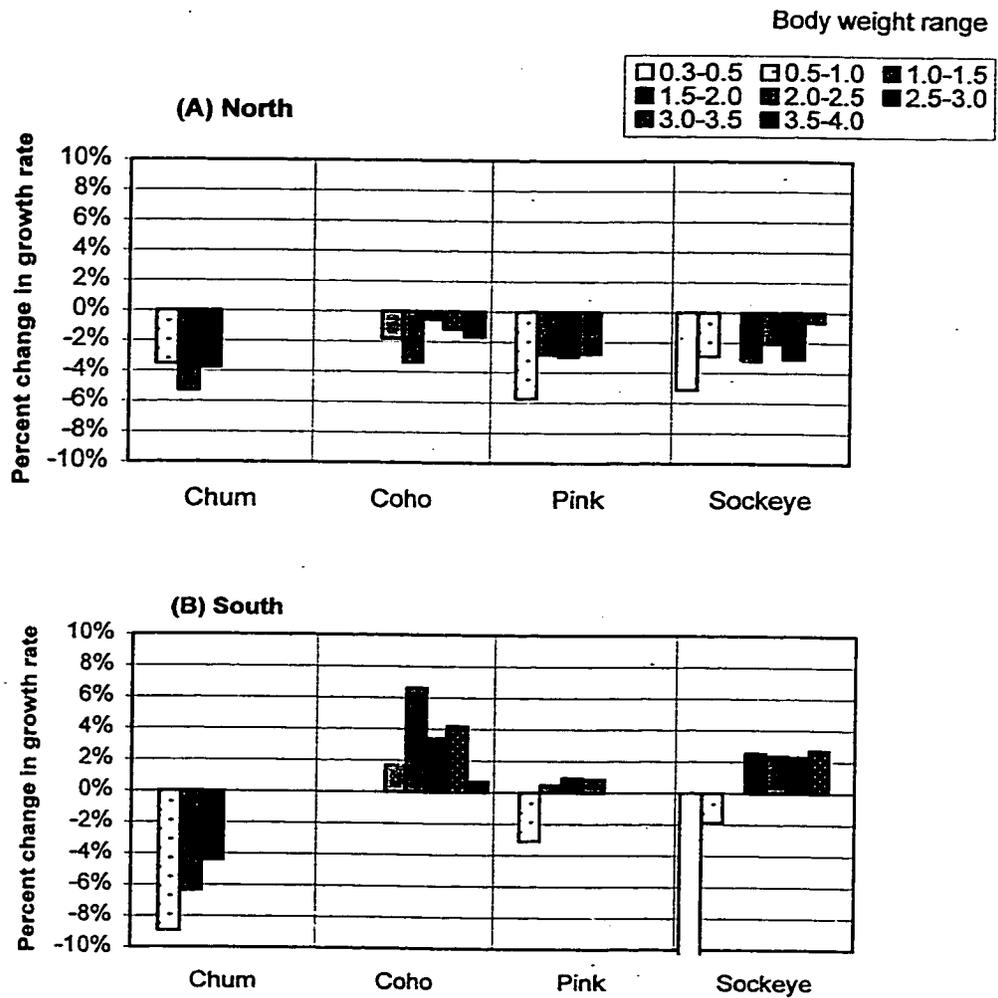


Figure 4.26. Estimated percent change of the growth rates with a 10% increase in sea surface temperature. Estimates assume that fish physiological temperature is equal to the sea surface temperature average

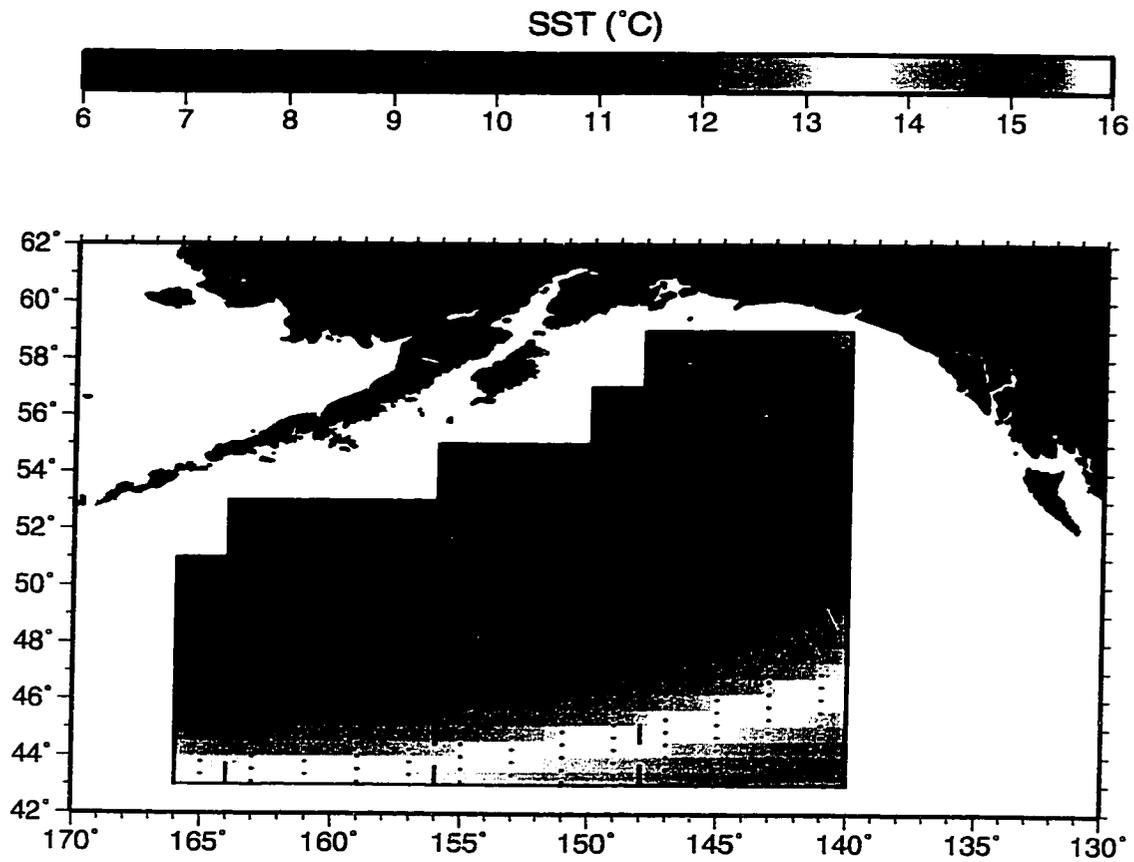


Figure 4.27. Long-term (1982-98) averaged $1^{\circ}\times 1^{\circ}$ July sea surface temperatures (IGOSS 1994), north/south transects used for fitting oceanographic parameters (dotted lines), and dividing lines for east, mid, and west gyre areas (dashed lines).

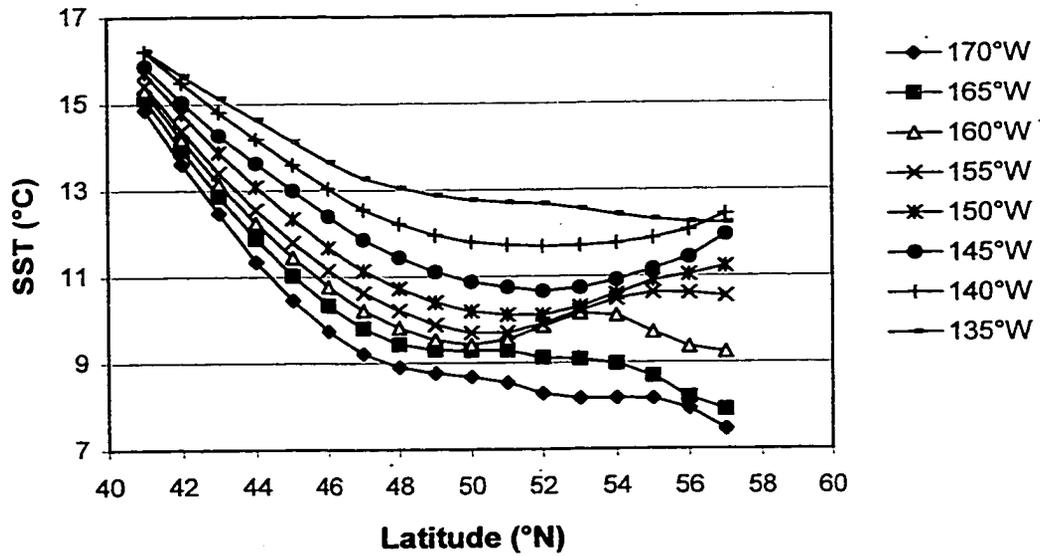


Figure 4.28. Long-term (1982-98) averaged $1^{\circ} \times 1^{\circ}$ July sea surface temperatures (IGOSS 1994) shown as north/south transects across the Gulf of Alaska. Transects from western longitudes include Bering Sea data.

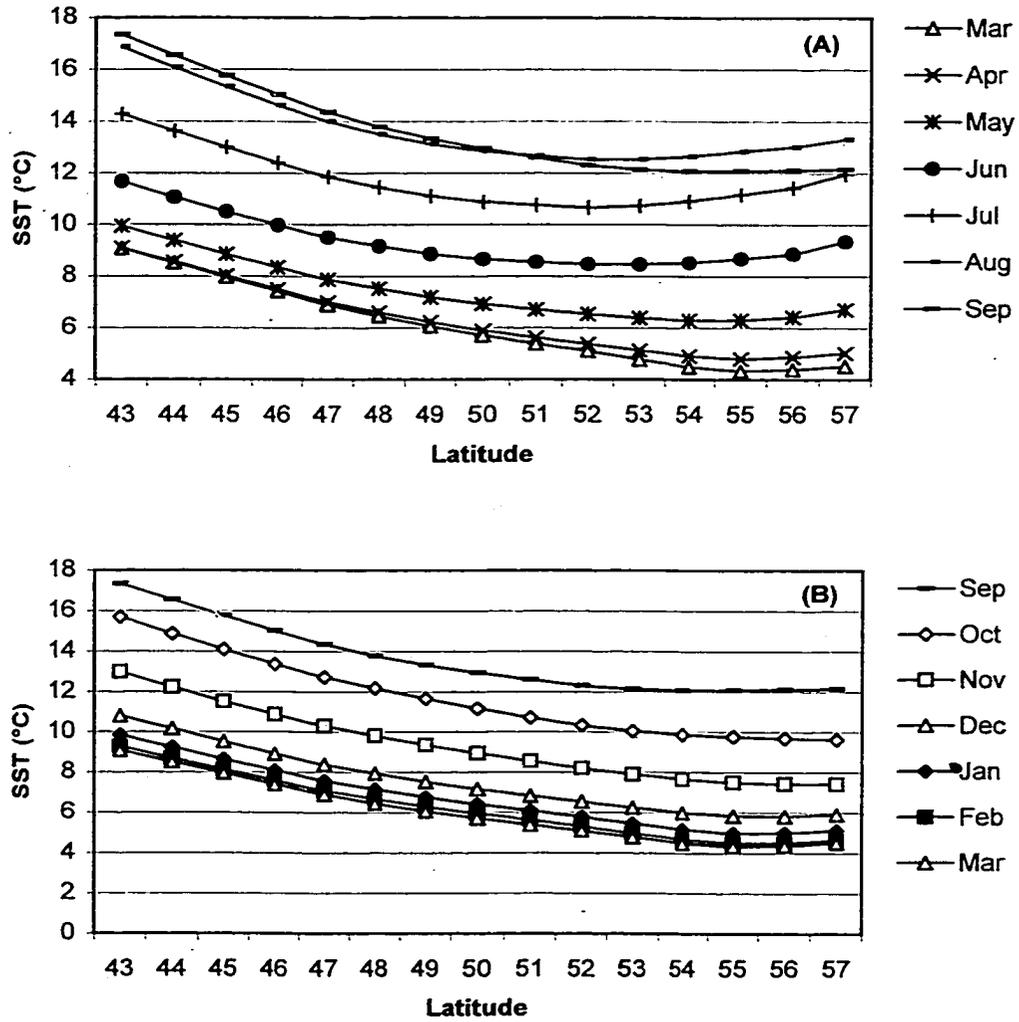


Figure 4.29. Long-term (1982-98) averaged 1°x1° sea surface temperatures along 145°W, shown by month: (A) spring and summer transects; (B) fall and winter transects.

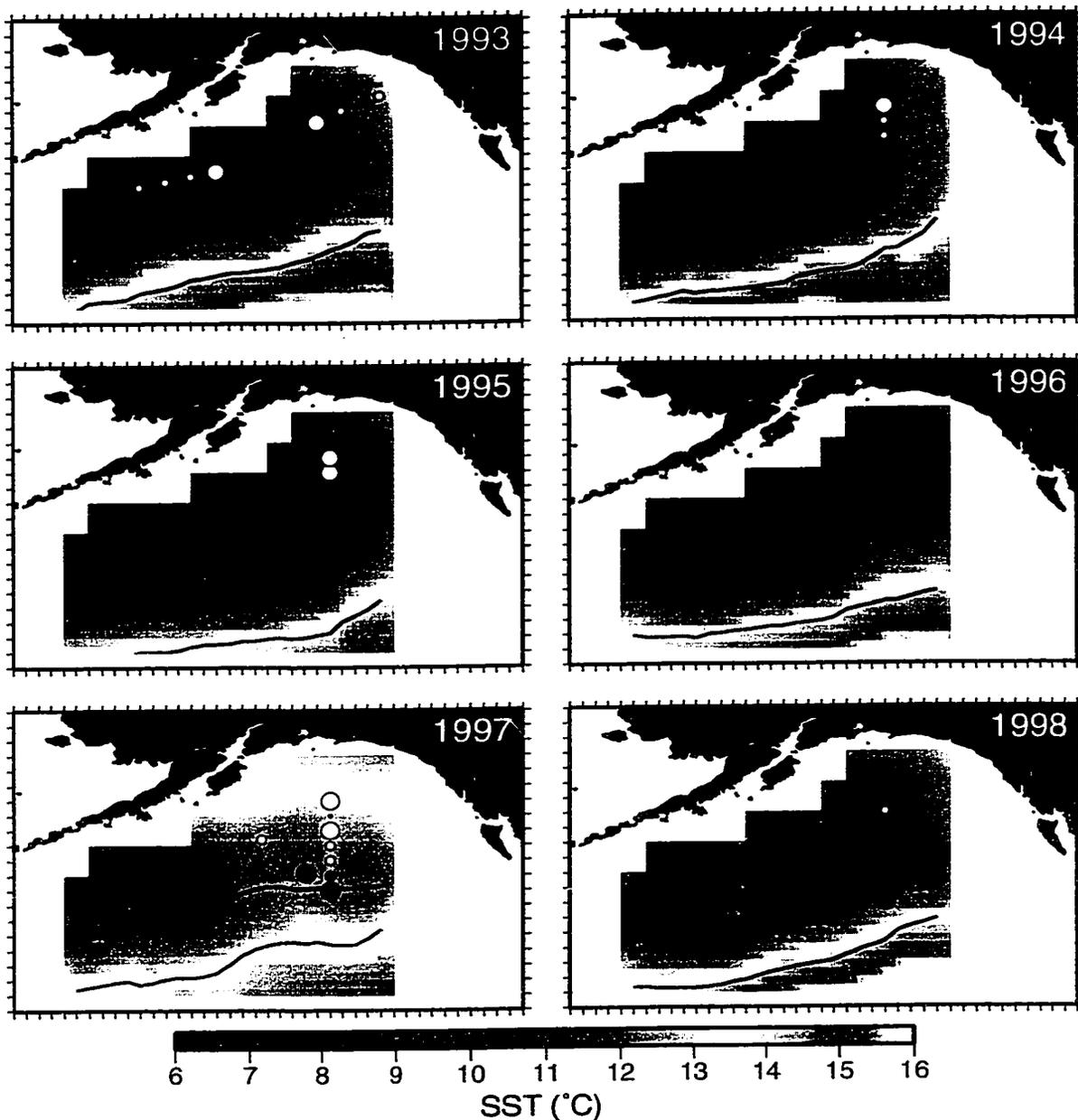


Figure 4.30. July sea surface temperatures from IGOSS data 1993-98, latitude of minimum temperature (MinLat) fitted at every degree of longitude (northern solid line), 13°C SST isotherm fitted at every degree of longitude (southern solid line) and squid index values calculated from salmon stomach contents as described in Section 4.2. Circles show squid index values, scaled as in Figure 4.13. The shown MinLat does not correspond exactly with the latitudinal minimums suggested by the temperature field in this figure due to differences in the smoothing procedure used to draw the SST field.

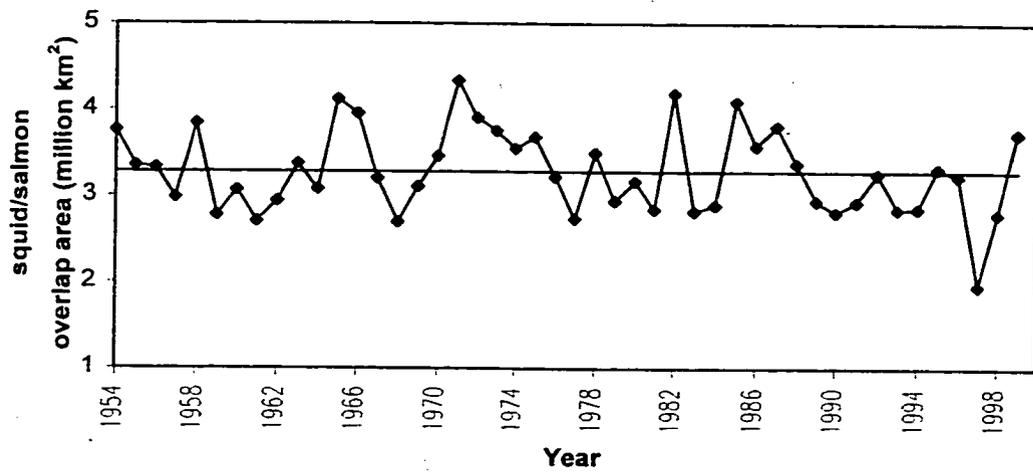


Figure 4.31. Total ocean surface area of hypothesized squid/salmon overlap between 140°-164°W, 1954-99. Horizontal line indicates the average overlap area over all years 1954-99 (3.28 million km²).

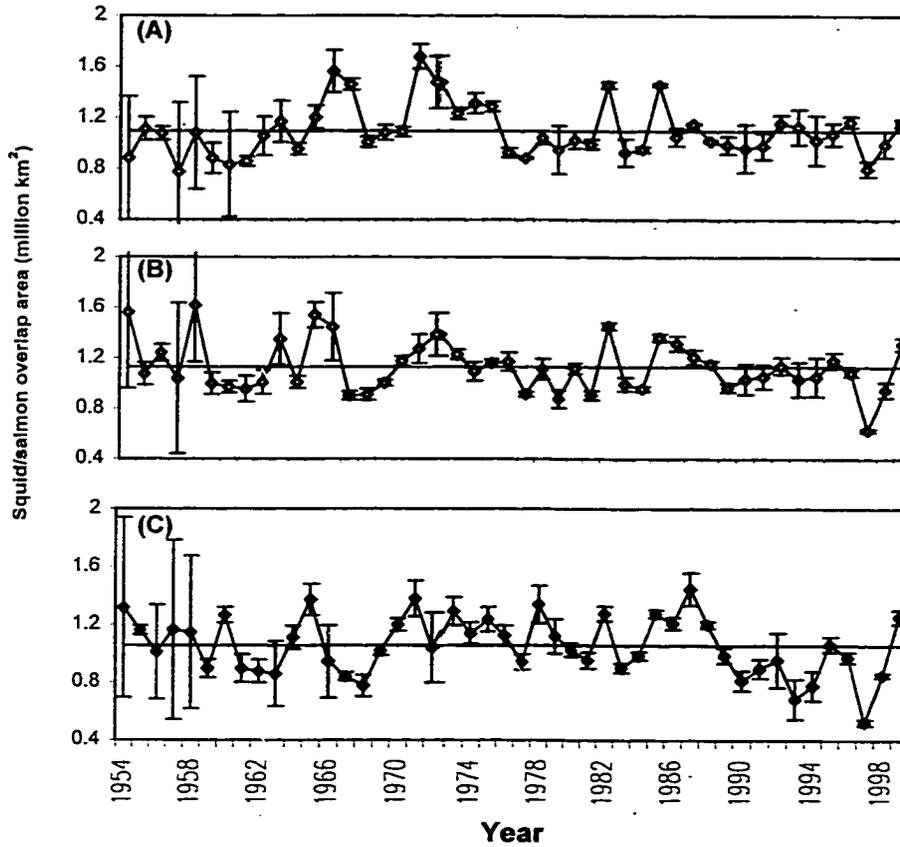


Figure 4.32 Ocean surface area of hypothesized squid/salmon overlap, 1954-99 for western, middle, and eastern gyre regions as defined in the text. Horizontal line indicates long-term average values. (A) western region, 156-165°W, average 1.10 million km²; (B) middle region, 148-156°W, average 1.13 million km²; (C) eastern region, 140-148°W, average 1.05 million km². Error bars are the standard error of the estimates when averaged from individual transect lines.

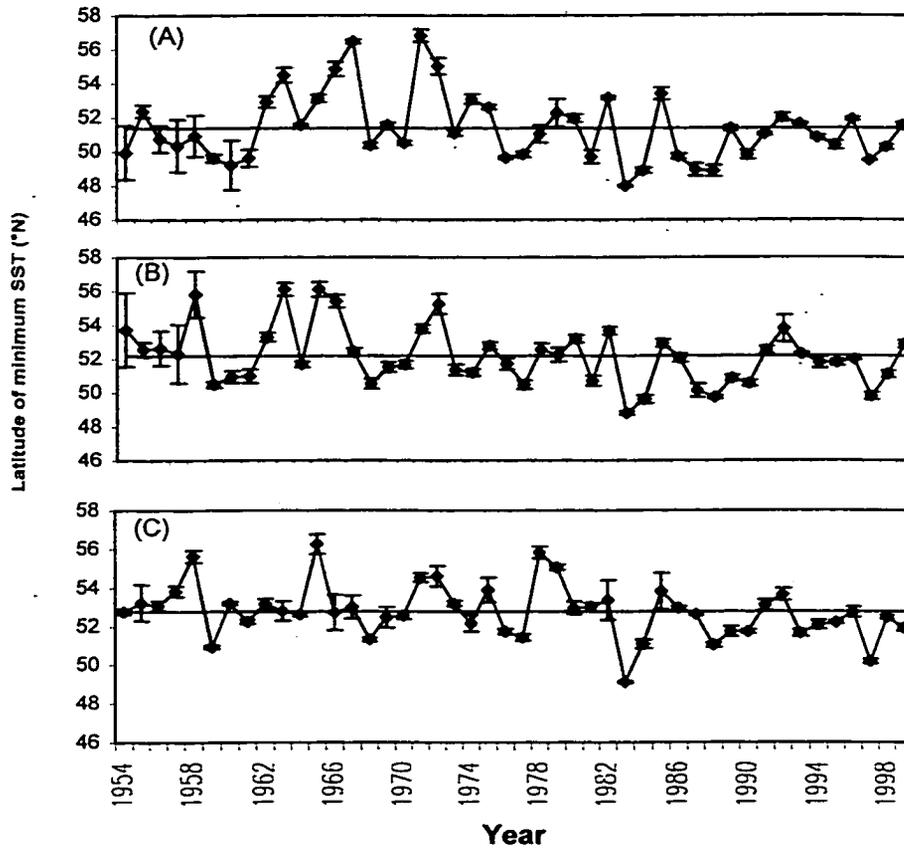


Figure 4.33. Latitude of July minimum temperature (MinLat), 1954-99, for western, middle, and eastern gyre regions as defined in the text. Horizontal line indicates long-term average values. (A) western region, 156-165°W, average 51.4°N; (B) middle region, 148-156°W, average 52.2°N; (C) eastern region, 140-148°W, average 52.8°N. Error bars are the standard error of the estimates when averaged from individual transect lines.

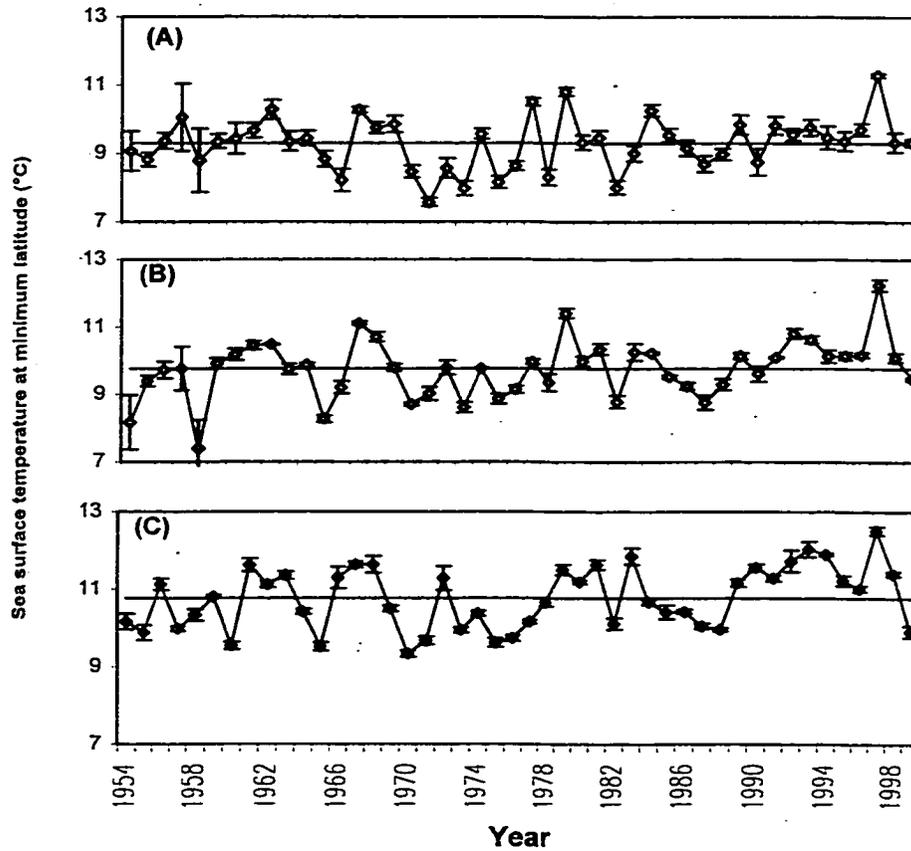


Figure 4.34. July sea surface temperature at the latitudinal temperature minimum (T_{min}), 1954-99, for western, middle, and eastern gyre regions as defined in the text. Horizontal line indicates long-term average values. (A) western region, 156-165°W, average 9.3°C; (B) middle region, 148-156°W, average 9.8°C; (C) eastern region, 140-148°W, average 10.8°C. Error bars are the standard error of the estimates when averaged from individual transect lines.

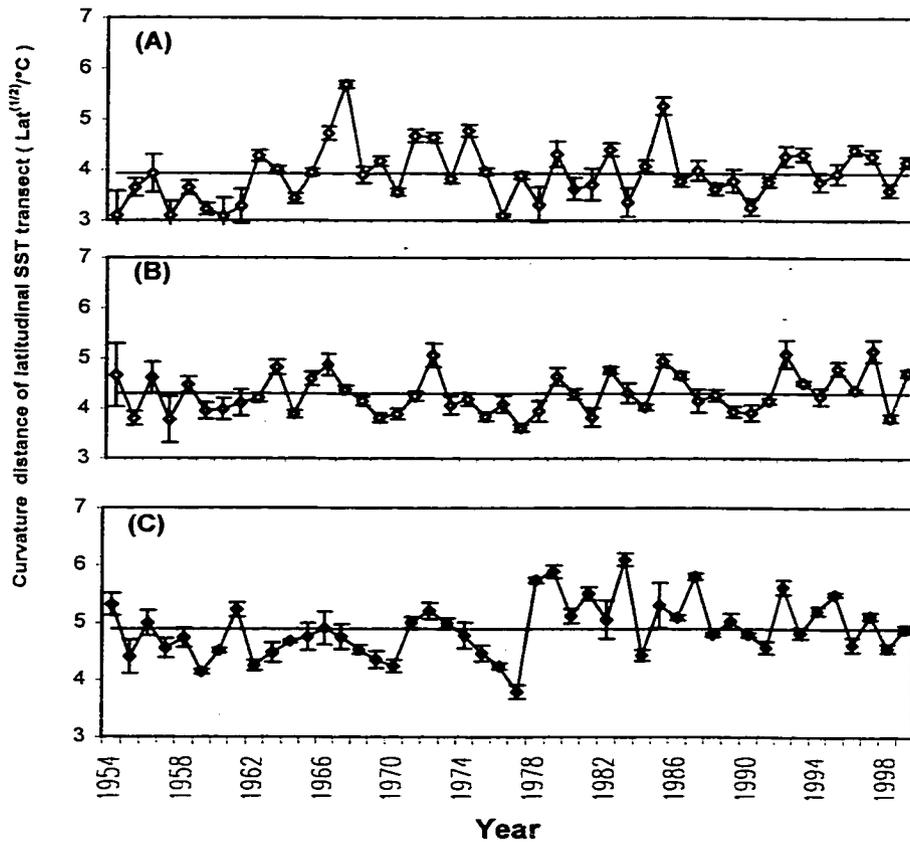


Figure 4.35. Curvature distance of temperature as a function of latitude ($D1^\circ$), 1954-99, for western, middle, and eastern gyre regions as defined in the text. Horizontal line indicates long-term average values. (A) western region, 156-165°W, average $3.9^\circ\text{lat}^{1/2}/^\circ\text{C}$; (B) middle region, 148-156°W, average $4.3^\circ\text{lat}^{1/2}/^\circ\text{C}$; (C) eastern region, 140-148°W, average $4.9^\circ\text{lat}^{1/2}/^\circ\text{C}$. Error bars are the standard error of the estimates when averaged from individual transect lines.

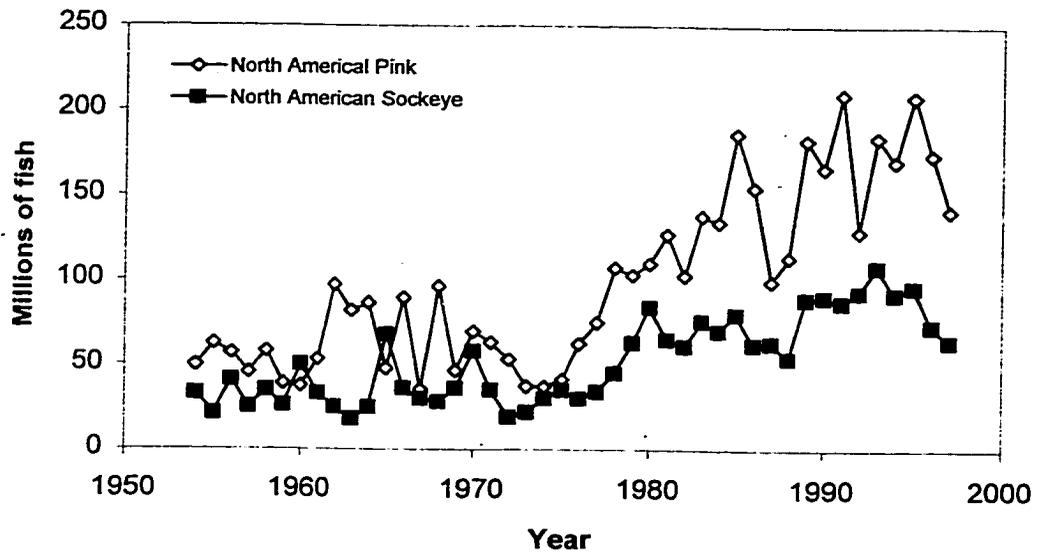


Figure 4.36. Total run size (catch + escapement) of North American sockeye and pink salmon, 1954-97. Data are from Rogers (1999).

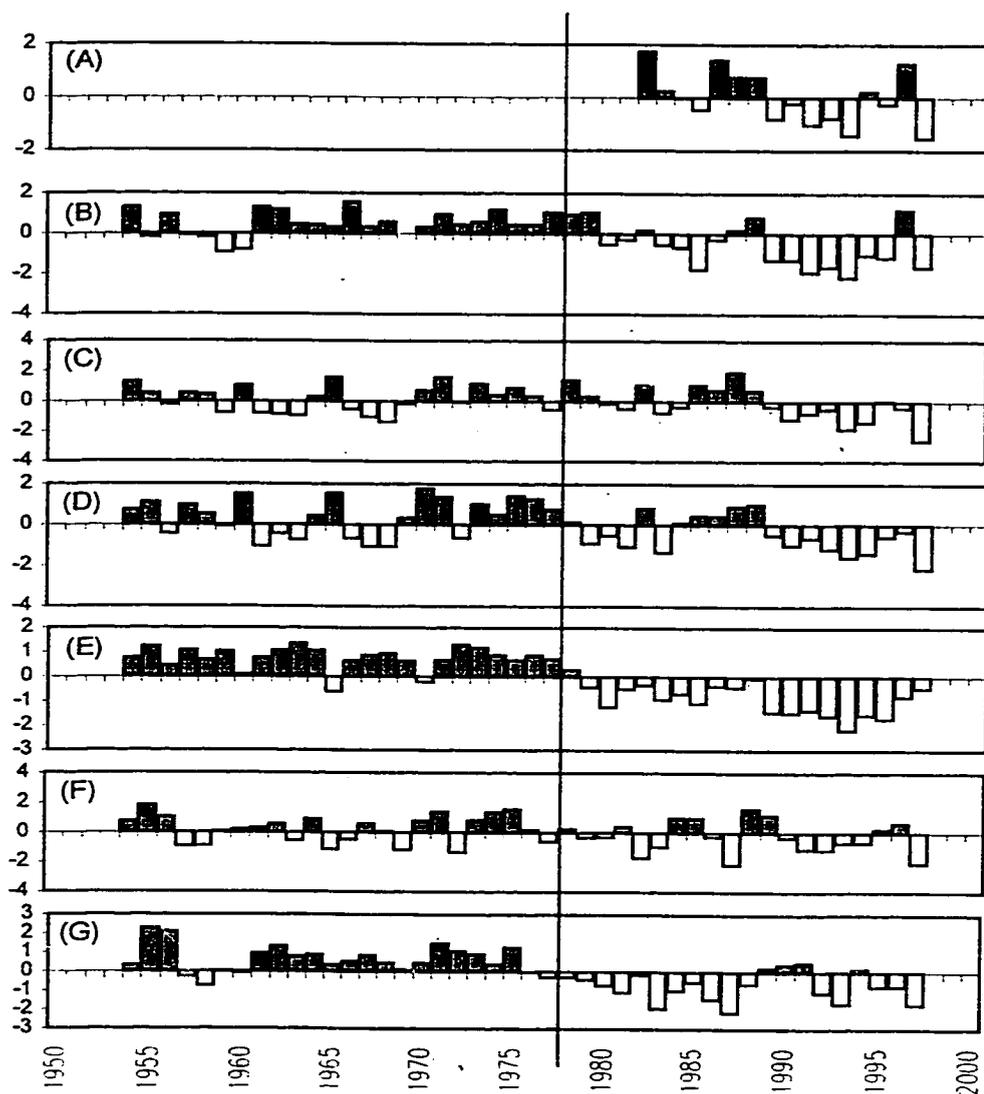


Figure 4.37. Standardized anomalies from long term mean values for (A) body weight of commercial seine-caught sockeye salmon in British Columbia statistical areas 12, 13, and 20, 1982-97; (B) eye-fork length of Fraser River age 1.2 sockeye 1954-97; (C) eastern squid/salmon overlap area (AreaEast), 1954-97; (D) negative anomalies of SST at eastern latitude of minimum temperature (TminEast) 1954-97; (E) negative anomalies of run sizes of North American sockeye salmon run sizes, 1954-97; (F) negative anomalies of PDO index, 1954-97; (G) negative anomalies of ENSO 3.4 index, 1954-97. Solid line shows "regime shift" break between 1977 and 1978.

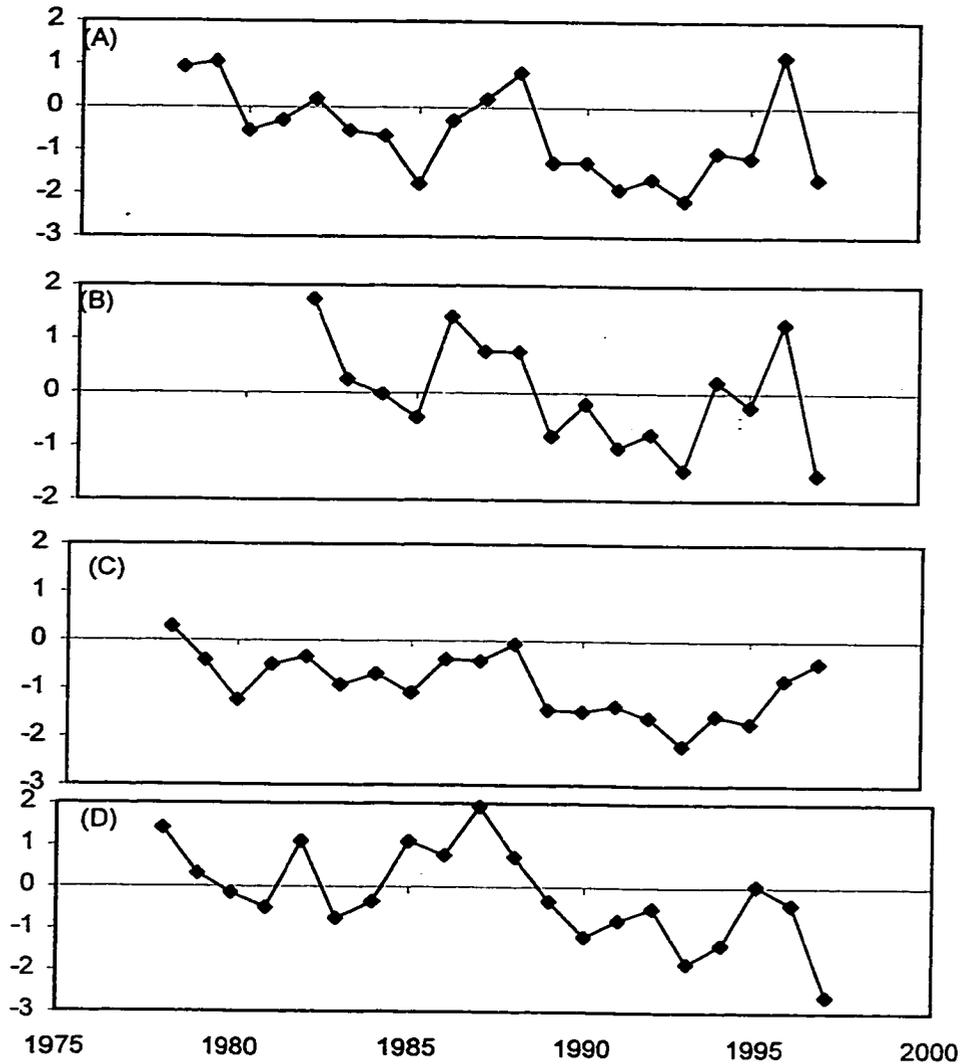


Figure 4.38. Normalized anomalies from long term mean values for (A) eye-fork length of Fraser River age 1.2 sockeye 1978-97; (B) body weight of commercial seine-caught sockeye salmon in British Columbia statistical areas 12, 13, and 20, 1982-97; (C) negative anomalies of run sizes of North American sockeye salmon run sizes, 1978-97; (D) eastern squid/salmon overlap area (AreaEast), 1978-97.

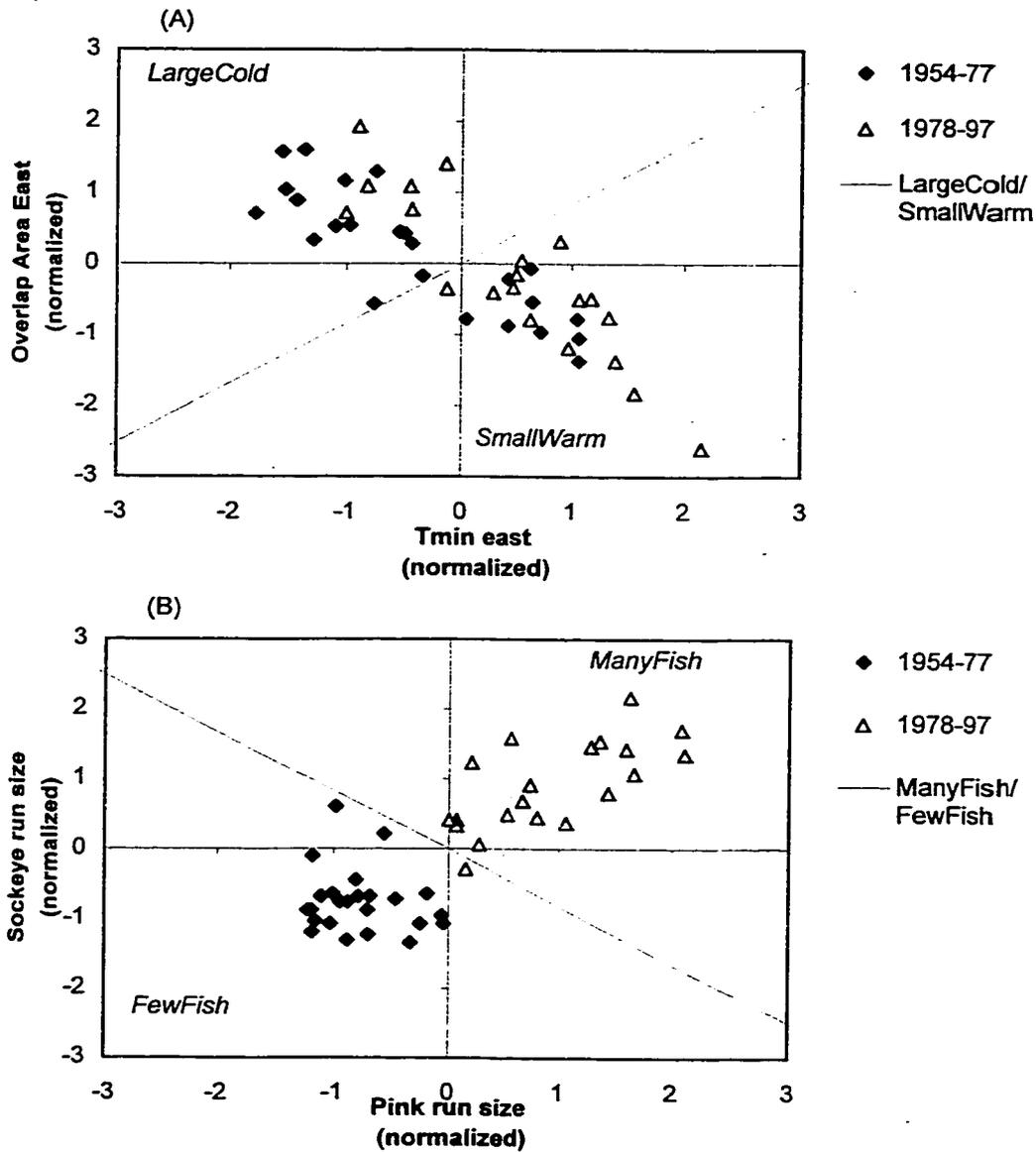


Figure 4.39. (A) Relationship between TminEast and Overlap area east, used to divide years into "LargeCold" or "SmallWarm" categories. (B) Relationship between North American pink and sockeye salmon run sizes, used to divide years into "ManyFish" or "FewFish" categories. Two time periods are distinguished, 1954-77 and 1978-97. The dividing for the categories is perpendicular to the slope of the regression between the time series. Because the time series are normalized (mean value=0 over all years) the slope of the regression passes through 0,0.

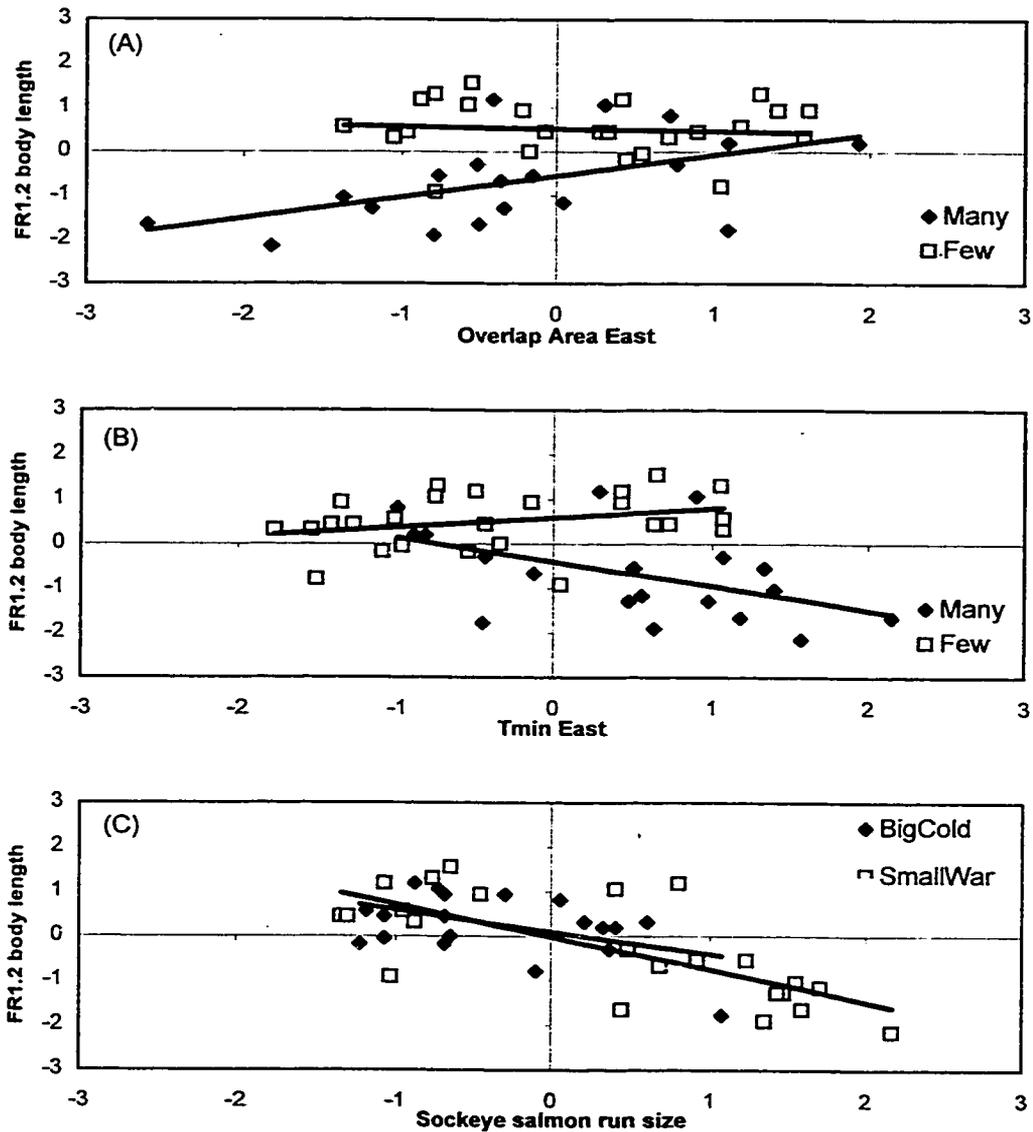


Figure 4.40. Normalized anomalies and regression relationships of Fraser River 1.2 eye-fork lengths with (A) overlap area east in years of "Many" and "Few" salmon; (B) TminEast in years of "Many" and "Few" salmon; (C) sockeye salmon run size in "LargeCold" and "SmallWarm" years. Definitions of year categories and regression relationships and significance are found in the text.

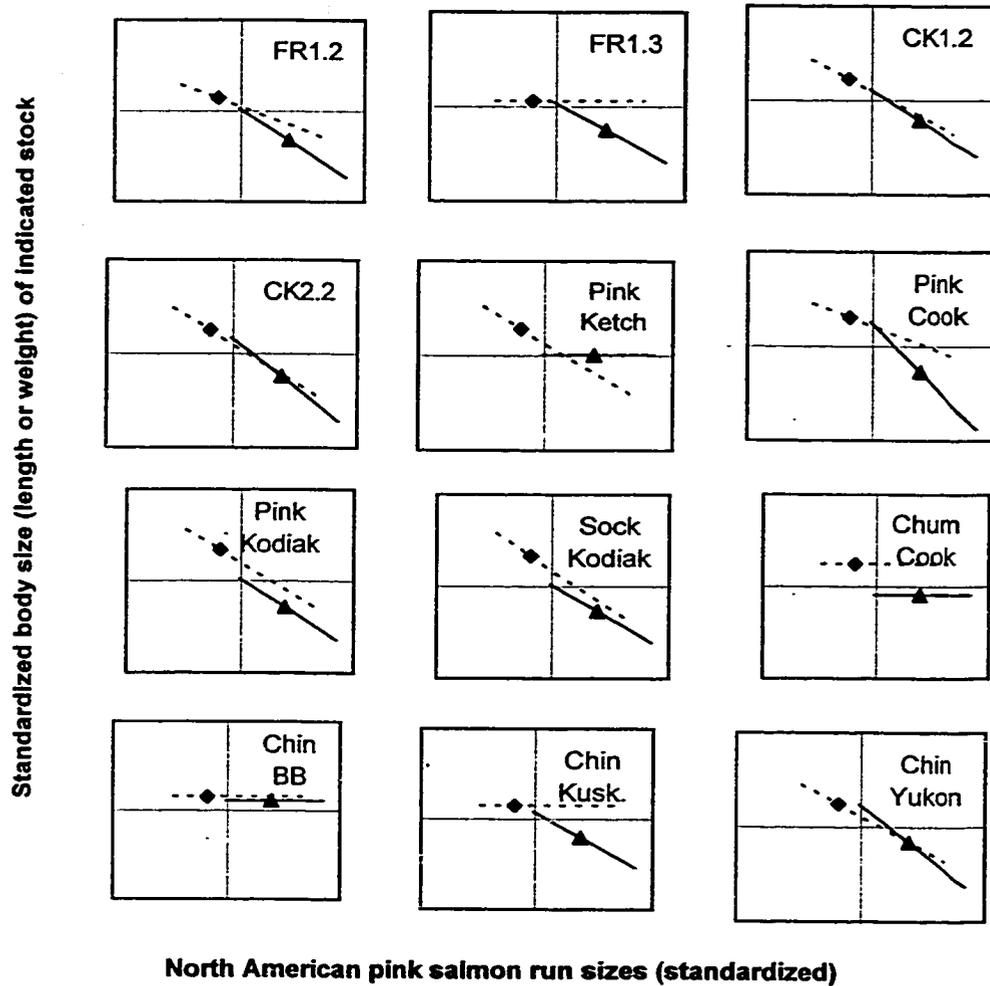


Figure 4.41. Mean values and slopes of regressions between normalized North American pink salmon run size (X-axis of all graphs) and body size (length or weight) index of selected stocks (Y-axis, stock time series name shown in graph label). Diamond and dotted line indicates mean and slope of "LargeCold" years, while triangle and solid line indicates mean and slope of "SmallWarm" years. Ends of lines indicate minimum and maximum values. Stock names are shown in Table 4.23, and significance of regressions is shown in Table 4.34. Regressions with slopes not significantly different from 0 are shown by horizontal lines.

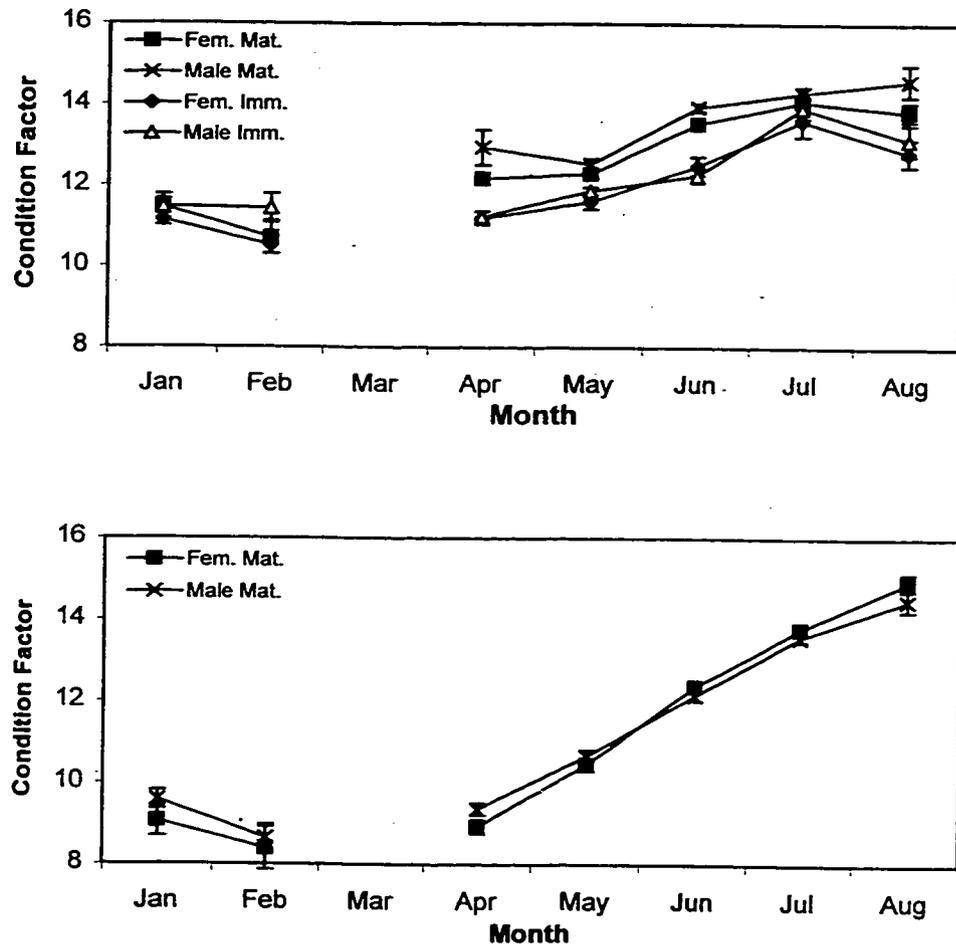


Figure 4.42. Condition factor $(\text{Body Weight}(\text{g}) \cdot 10^6) / (\text{Fork Length}(\text{mm}))^3$ of 6,223 pink and sockeye salmon sampled in the Gulf of Alaska, averaged by month, sex, and maturity status (immature or maturing). Salmon were collected between 1956-1965 as described in Chapter 3.

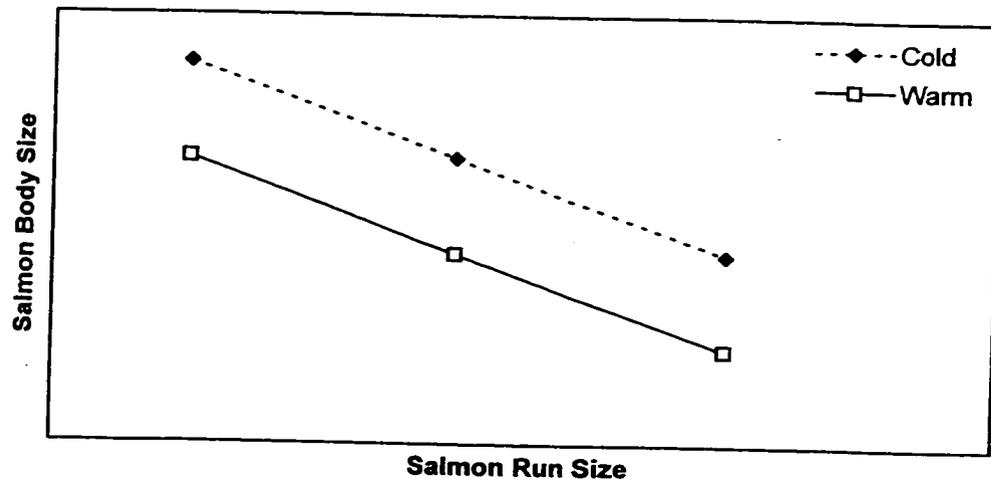


Figure 4.43. Relationship between salmon numbers and body size with environmental conditions of warm and cold water temperatures hypothesized by Peterman (1987).

5 Trophic implications of seasonal prey supply and size-based ontogenetic diet shifts in adult Pacific salmon

5.1 Introduction

5.1.1 Foraging theory and density-dependence

A maturing salmon places a high evolutionary premium on achieving a large body weight at sea (Healey 1987; Beacham and Murray 1987). Its day-to-day behavior, especially in the months immediately prior to spawning, reflects the necessity of maintaining high growth rates as it migrates back towards coastal waters. In order to maintain high growth rates, it must balance the energy spent in searching for food with the energy obtained by that search.

The body of theory used by researchers to calculate this moment-to-moment balance is called *foraging theory*, and the theory has been substantially developed (Stephens and Krebs 1986). Combined with the laboratory-calibrated bioenergetics models discussed in Section 4.3, a modeler can make excellent predictions of the maximum feeding rates and resulting growth rates that a salmon may achieve at any given instant in time.

However, the dynamic nature of ocean conditions makes predicting salmon behavior difficult, especially if a modeler is attempting to capture density-dependent (competitive) effects. A predator that maximizes its growth rate at every given instant in time does not necessarily end up as the largest fish. A fish may forgo food at one point to travel to richer feeding grounds, and a salmon, in particular, must balance foraging and migration. Moreover, as a salmon grows, the conditions which provide the best growth opportunities may change. Specifically, ontogenetic changes in a salmon's diet from zooplanktivory to piscivory (or "teuthivory") may change its ideal behavior as it grows.

Sections 4.2 and 4.3 suggest that in the Gulf of Alaska, the distribution of summer prey, particularly micronektonic squid, may be the largest source of variation in instantaneous growth rates for adult salmon. However, measuring instantaneous growth rates during the season in which prey is the most plentiful does not necessarily address salmon density-dependence or intra- and inter-species competition. Feedback may occur between predator and prey, as salmon deplete local prey populations, thereby limiting their future food resources (Figure 5.1).

Predators may move to and from areas of prey concentrations, and the detection of food depletion on a small scale may be next to impossible. Competitive interactions can occur at multiple scales. On short ("instantaneous") time scales, a dense concentration of fish may deplete prey in their immediate vicinity, temporarily limiting their own growth. Due to the patchy distribution of prey in the ocean, such local competitive depletion may be enough to slow individual salmon growth, even if prey is not depleted over a larger area.

Thus density-dependence may not result from continual competition for food throughout a salmon's life, but from a relatively small number of "growth bottlenecks" amplified by feedback. Short-term limitations in instantaneous growth rates during critical development periods may cause cascading effects later in a salmon's life cycle (Thorpe et al. 1998).

In general, it is almost impossible to measure local prey depletion in the field, especially over an area the size of the Alaska Gyre. The time scales of the patchiness, in comparison with the overall scale of the ocean, are too disparate. However, it is possible to use currently available data in conjunction with growth models to pinpoint periods in a salmon's life cycle when density dependence is most likely to occur.

Two approaches may be taken to find such bottlenecks. The first method is to construct an extremely detailed model of a salmon's life history, following a single fish through a succession of its habitats. This type of modeling, individual-based modeling (IBM), has been successfully used to follow maturing Fraser River sockeye salmon (Rand et al. 1997). However, this type of model requires an extremely large amount of data, and may not be easily adaptable as knowledge of salmon foraging grows to include, for example, details such as the ontogenetic shift in diet discussed in this dissertation.

The second approach is to examine a series of more general growth and foraging models, to paint the Pacific with broad brushes before focusing on details. While this approach will never give an exact number for the "carrying capacity" of salmon, it may help to pinpoint the bottlenecks which might create density-dependent growth, and to determine if such bottlenecks are limiting enough to give rise to the trends seen in data the in Section 4.4. An advantage of this method is that separate models may be used to isolate particular aspects of the growth process, and to determine their relative importance to the overall production of a population.

In this chapter, I combine bioenergetics and foraging models in three distinct ways, each one focusing on a different extreme of a salmon's possible behavioral choices, in the hope that even a broad brush can reveal some of the details of production bottlenecks that have occurred on the high seas in recent years.

5.1.2 Outline of the three methods used

The balance between predator and prey is an issue of supply and demand. In an evolutionary sense, a predator has many choices when faced with a shortfall in food. It may increase its foraging effort in order to make up the shortfall, or it may maintain, or even decrease, its foraging effort and accept

a lower level of growth. In reality, a fish will follow more complicated, mixed strategies, but these two extremes provide a guide for examining possibilities.

The three models in Chapter 5 are listed in Table 5.1. The details of each model are contained in the methods sections of 5.2-5.4, but the primary difference between the models can be summarized by describing the difference in the way consumption rate is set for the three models.

Model 1 is a *fixed demand* approach. Using historical body weight records, I ask the question: how much food is required for an individual salmon to match its population's historical rate of growth? In terms of density-dependence, I ask: during what periods in the salmon's life history is there the greatest disparity between the amount of food required for growth and the amount of food available in the environment?

Model 2 examines the other end of the spectrum of strategies: the *fixed supply* approach. Consumption rate is set as a fixed proportion of a salmon's body weight, and I ask the question: if the salmon makes no effort to adjust its feeding rate as a response to external conditions, what environments will cause the salmon's growth to depend on minor changes in growth conditions? In this model, the effect of the ontogenetic diet shift from zooplankton to squid is more fully explored.

Finally, Model 3 balances the supply/demand issue as a question of *foraging effort*. Rather than using a fixed supply or demand, it models the foraging effort that will achieve the maximum growth rate at any given instant in time. This model adds density-dependent effects directly, by asking how this optimization changes as food availability decreases in the ecosystem due to competition.

Each of these models should be considered a "sub-model" for the examination of a particular aspect of density-dependent growth arising from specific strategies that a salmon may use in determining its foraging behavior.

Taken together, they may clarify the issue of density-dependence and aid in the development of more complex models.

The three models combine data from across the high seas of the Gulf of Alaska, and thus represent an amalgam of conditions which may exist for salmon. Much of the data used for these models was collected along the 145°W transect line: fish foraging along this line in the spring and summer prior to maturation return to shore areas along much of the North American west coast (Figure 5.2 and Table 5.2). While the models do not follow fish from any particular stock, they offer a baseline for comparison which may apply across many North American populations of salmon.

These models are not spatially explicit. Hypothesized July-August trajectories of returning salmon, based on archival tagging (Walker et al. in press) are shown in Figure 5.2, but the model only roughly corresponds to these trajectories. This is because there is little available data on salmon behavioral responses to high or low prey abundance and other environmental conditions. Murphy (1995) finds that salmon may travel long distances to congregate at oceanographic features rich in food such as the upwelling region around the Emperor Seamounts, while Brandt (1993) uses bioenergetics models to show that prey congregation at thermal fronts may provide the same function. Such fronts may or may not result in the thermal limits to salmon distribution observed by Welch et al. (1998). This model does not explore migratory movement to and from areas of differing prey density.

5.2 Experiment 1: ocean area required for a fixed demand

5.2.1 Methods

The "fixed demand" approach asks two questions: 1. Given the average growth (in body weight) of an individual salmon as a fixed quantity, what is the ingestion energy required from the ecosystem to meet this growth; and 2. How

does this demand, calculated on a monthly basis, compare to the amount of food available in the ecosystem?

This approach assumes that:

1. The growth of an individual salmon is represented by the month-to-month increase in average salmon body weights measured across the North Pacific, stratified by salmon species, age, and maturity condition.
2. Salmon swimming activity (swim speed) is close to the "optimum" swimming speed calculated by Ware (1978).
3. The available food at a given location is represented by the density ($\text{g}/1000\text{m}^3$) of mesozooplankton in the upper 150m of the water column. This final assumption provides the bare minimum biomass of mesozooplankton required to supply the measured salmon growth, as a portion of the food actually eaten by salmon may pass through micronekton, at a cost of conversion efficiency, before being incorporated into salmon body weight.

Salmon were stratified by species, age, and maturity status into 14 groups (Table 5.3). The salmon were followed over 13 monthly time-steps, from July through August of the following year. For a pink or coho salmon, the period begins in July in its first year at sea (ocean age .0) and ends in August of its maturation year (age .1). For maturing sockeye and chum, this period begins with the July prior to the maturation year and proceeds through the August of the maturation year.

For each age class, monthly average at-sea body weights were taken from Ishida et al. (1998). This data source summarizes catch data from research fishing over the entire North Pacific between 1972 and 1995 (Figure 5.4). This data set represents a rough baseline: sampling was not geographically uniform over all areas. Moreover, little sampling has been conducted on the high seas in winter and early spring. Therefore, while this set

of body weights gives a starting point, the data cannot be considered to be specific of fish in a given geographical region or stock.

For water temperatures throughout the year, I used weekly 1° lat. X 1° lon. averaged sea surface temperatures on the N/S transect line 48-56°N along 145°, between 1982-1998 from the IGOSS data set. There were significant annual variations of up to +/-1°C from the mean weekly temperature at any given week of this cycle (Figure 5.3C); this variation was similar in magnitude to the latitudinal variation shown in Figure 5.3B. Because the scale of interannual variation is similar to the scale of latitudinal variation, I fitted a single sine function using all available Ocean Station P data shown in Figure 5.3A. The resulting function was $SST(^{\circ}C) = 4.03 \cdot \sin(0.02 \cdot (\text{Julian Day}) + 2.53) + 8.86$, where the quantity $0.02 \cdot (\text{Julian Day}) + 2.53$ is in radians.

While salmon are generally surface-oriented, evidence from archival tags in the Gulf of Alaska suggests that they spend a substantial portion of their daylight hours in subsurface waters which may be 1-3°C cooler than surface waters, while feeding in surface waters at night (Walker et al. 2000). To account for the effects of daily vertical migrations, geographic variation, and interannual variations in water temperature, model runs were repeated using values of the temperature offset between +/-3°C of the mean.

For the purposes of matching monthly growth rates with daily water temperatures, the reported weight of salmon in a given category and month, as reported by Ishida et al. (1998), was assumed to be the average weight of salmon on the first day of that month. The total growth of a salmon in month t was calculated as $W_{t+1} - W_t$. Between some of the months, especially between December and March, the reported average body weights decreased (Figure 5.4). It is not clear if this is due to actual body weight decreases in salmon over the winter or due to the difference in the location and methods of sampling in different months. The raw data was fitted with a simple exponential

growth curve so the growth increment between months would be positive in all cases (solid lines in Figure 5.4).

The bioenergetics model in Appendix B was used to calculate the daily consumption rate C_{tot} required for a single salmon to achieve the change in average body weight observed between each month. For the purposes of this model, each month was assumed to have 30 days. The daily consumption rate was calculated by iteratively determining a single P-Value (body-weight dependent proportion of maximum growth rate) for each month that best fitted the starting and ending body weights.

The units of consumption rate C_{tot} were calculated as calories required per day averaged over a single month: leaving C_{tot} in terms of calories rather than prey weight made the results relatively insensitive to prey caloric density. The prey caloric density used for all results was 700cal/g with 10% of prey considered indigestible, a similar density to many zooplankton species (see Chapter 4). The sensitivity of C_{tot} was tested by re-running the model with a +/- 10% change in body weight increment, water temperature, prey caloric value, and indigestible proportion of prey.

The total prey calories required per month were compared with the monthly averaged 0-150m standing stock of zooplankton biomass at Ocean Station P, measured continuously by Canadian weather ships during the years 1956-80 (data provided by R. Brodeur). By converting the zooplankton density (g/m^3) to an estimate of calories available per m^3 of water, using a prey caloric density of 700cal/g, it is possible to use the results of the bioenergetics model to calculate volume of water near Ocean Station P required to support a salmon of a given species, age, and maturity class in a given month.

The zooplankton density (mg/m^3) are averaged across 0-150m depth; however, the main concentrations of zooplankton would be expected to exist across a narrower vertical distribution. The majority of zooplankton will be

concentrated into more dense patches, especially during the summer when a shallow summer thermocline exists between 20-50m depth (Figure 2.8). To account for this, the 0-150m density/volume of zooplankton was multiplied by 150m to obtain biomass of mesozooplankton, between 0-150m depth, per m² of ocean surface area. The results thus indicate the minimum surface area of ocean needed to support a single salmon's food requirements in a given day. As this food may be "filtered" through multiple trophic levels resulting in greater energy loss, this estimate of surface area should be treated as a minimum.

5.2.2 Results

5.2.2.1 Energy requirements of Pacific salmon by month

The daily energy requirement (kcal/day), calculated by month for each modeled salmon group, is shown in Figure 5.5 and Table 5.4. For all species, age and maturity classes, the total energy requirements were highest when they were largest, during the summer months. Coho salmon had the largest demand for food during summer months, requiring a maximum of 125 kcal/day during July. During the summer, maturing sockeye and chum required 50-100% more energy than immature fish of the same age class (Table 5.4).

The caloric content and percent of indigestible prey does affect the respirative costs of digestion for salmon, and an initial sensitivity analysis showed that a +/- 10% change in these two variables changed the total calories required for growth by less than 1%.

For several sockeye and chum salmon age classes, daily consumption rate requirements were lowest during winter months (December-February). For pink and coho salmon, rates were lowest when they were at their smallest size, at the beginning of the simulation. Pink and coho show less slow-down during the winter high growth rates as they must maintain their rate to achieve all of their growth during their single ocean year. Energy requirements in the final

July were 1.7-6.9 times higher than energy requirements in December (Table 5.4).

5.2.2.2 Sensitivity of calculated energy requirements to input variables

Table 5.5 shows the sensitivity of the calculated energy requirements to a +/- 10% change in input variables. Only pink salmon are shown as an example: the sensitivity of other species to each input variable was similar. Energy requirements were most sensitive to changes in the reported growth (grams) for each month: a 10% change in total monthly growth changed the energy requirements by 20-50% (Table 5.5A). The difference was greatest in the summer months: in order to increase its final body weight by 10% over its baseline during the final July, a pink salmon would need to consume 46% more calories every day during that month.

Summer water temperatures had a lesser, but noticeable, effect: if water temperature increased by 10% in July, the energy required for the pink salmon to maintain its baseline growth increased by 8%. In all cases, an increased water temperature led to increased energy requirements. Changes in winter water temperatures were considerably less important, as a 10% increase in winter water temperatures led to an increase in energy requirements of less than 2% (Table 5.5B). Total energy requirements were relatively insensitive to changes in the cost of prey digestion, changing less than 2% when the caloric value or indigestible proportion of the prey changed by 10% (Table 5.5 C-D).

5.2.2.3 Zooplankton required to satisfy demand

The average wet weight of "small" zooplankton per m³ of water between 0-150m depth, and per 0-150m-integrated surface area of ocean (g/m² or tons/km²) at Ocean Station P between 1956-1980, is shown averaged by month in Table 5.6 and Figure 5.6. The geometric mean is used due to the log-normal distribution of zooplankton in the ocean: the geometric mean is approximately

25% less than the arithmetic mean in any given month. The monthly mean zooplankton standing stock peaked in June (23 g/m^2), about 22 times higher than February, which had the lowest standing stock of zooplankton (1.0 g/m^2).

If the average zooplankton caloric density is assumed to be 700 cal/g wet weight, the results of Figures 5.5 and 5.6 may be combined to calculate the amount of surface area of ocean (near Station P) that must be "emptied" of mesozooplankton in a single day to support a single salmon's growth. The results, by salmon species, age and maturity class are shown in Figure 5.7 and Table 5.7.

The minimum level of demand for all individual salmon occurs at the beginning of the simulation, when zooplankton density is high (summer) but salmon size is small. At this time, the surface area required per salmon is between 0.2 and 2.4 m^2 , depending on the salmon group. As caloric requirements increase slightly between summer and winter, while zooplankton concentration decreases dramatically, the surface area per salmon increases from fall until February, when each maturing salmon requires between 20 m^2 (pink salmon) and 51 m^2 (coho salmon) of ocean area per day (Table 5.7; Figure 5.7).

While the total calories required continues to increase from winter to summer, the zooplankton concentration also increases during this time. By the end of the summer, while energy requirements have increased for all salmon as shown in Figure 5.5, the surface area required to supply this energy has dropped again, to a low of between 1 and 6 m^2 per salmon in May and June (Table 5.7, Figure 5.7).

Figure 5.8 shows the difference in the area required to support baseline pink salmon growth in a "good" year and a "bad" year, where a "good" (or "bad") year is defined as zooplankton concentrations 1 standard deviation above (or below) the geometric mean for all months, with the standard deviations taken

from Table 5.6. During all months, a bad year requires approximately twice the surface area of ocean that a "normal" year does, while a good year requires approximately half the surface area. In absolute terms, this difference is greatest in February and least in May and June.

5.2.3 Discussion

Density-dependent salmon growth may occur as a result of local depletion of prey standing stock on a time scale of hours, whether or not this standing stock is replenished by new zooplankton production on a time scale of days or weeks. This is especially true if both salmon foraging and zooplankton replenishment occurs on a diel cycle, whereby a limitation on available food during a night of foraging may be enough to slow a salmon's growth rate.

An examination of Figure 5.7 reveals an important result: the ocean surface area required to support a salmon. Even though the highest growth rates occur in salmon during the summer, the magnitude of difference between supply and demand means that winter is when density dependence is most likely to occur. The surface area of ocean required to be emptied of mesozooplankton to support a salmon achieving "average" growth near Station P is 8-16 times higher in the winter than in the summer, depending on salmon species, age and maturity status (Table 5.7). This is in spite of the fact that salmon growth during the winter is relatively low. Therefore, the likelihood of local food depletion occurring is greatest during the winter months.

Trends in annual averages of zooplankton biomass tend to emphasize summer standing stocks, as the biomass of zooplankton in surface waters is considerably higher during this season. However, winter zooplankton may show distinctly different long-term trends (Figure 5.9). For example OSP winter zooplankton biomass shows a marked increasing trend between 1968 and 1972, and a decreasing trend between 1972 and 1980, a period during which many Gulf of Alaska salmon body weights decreased (see Section 4.4).

Unfortunately, winter zooplankton data was not collected in this region during the 1980s and 1990s, so it is not possible to examine the relationship between winter zooplankton standing stocks and salmon growth during this time period.

The “ocean surface area required to be emptied of zooplankton” should be taken as a conceptual guide rather than as a prediction of actual feeding/foraging areas for salmon over time. Several dynamic mechanisms may act to modify the link between zooplankton standing stock and salmon consumption rates in any given month:

- Both feeding and zooplankton replenishment (production) are continual processes, and the standing stock of zooplankton measured on any given day may represent a balance of energy entering and leaving the zooplankton pool. However, on the scale of local depletion, the standing stock of zooplankton biomass is an important consideration.
- The vertical concentration of zooplankton in the surface layer will change from the summer to the winter as the mixed-layer deepens. The 0-150 integrated zooplankton samples do not capture this dilution of zooplankton in the winter, which would be expected to make foraging in the winter even more difficult than suggested by these results.
- Energy which passes through secondary trophic levels, such as squid, does not pass instantaneously. While the presence of micronekton may increase the demand on zooplankton, micronekton may also serve as “storage” for energy, if they consume zooplankton in the summer, and are not themselves eaten by salmon until the winter.
- The zooplankton data used in this study was taken from a single geographic point. The “required ocean area” of salmon, on the other hand, may be mitigated by their migratory behavior: it is not clear whether they spread out or concentrate their distribution in the winter (Nagasawa in press).

- Finally, this model assumes that the measured growth in salmon occurs at “average” levels of temperature-specific swimming speed: changes in the activity level of the salmon may alter their overall demands, although this will not eliminate their need to grow.

Any attempt to tackle these points brings about a simple conclusion: there is very little data concerning salmon distribution or feeding on the high seas in the winter. The limited amount of data that has accumulated for this stage of the salmon’s life cycle represents a major gap in the understanding of salmon growth.

It is tempting, of course, to suggest that the overall importance of winter growth is minimal for a maturing salmon. After all, a relatively small percentage of actual growth occurs in the winter, and summer food availability may be enough to make up for low winter food supplies. However, this suggestion does not take two factors into account. First, maturation and fecundity may be set by growth processes occurring early in the winter and spring prior to maturation (Thorpe et al. 1998). Secondly, it is possible that a small discrepancy in growth early in the season may, through the damping of growth feedback, greatly limit later growth. This latter hypothesis is explored in the next experiment.

5.3 Experiment 2: trophic feedback and seasonal growth

5.3.1 Methods

As shown in Table 5.5, if the starting and ending body weights of a salmon are determined for a single period of growth, the caloric density of prey, and therefore the type of prey, does not affect the amount of calories required to obtain the growth. However, this assumes that the starting and ending body weights are fit as specific goals, and that the salmon will be able to feed as much as necessary to achieve these goals. The other extreme is to assume the consumption rate C_{tot} is fixed over a given time period (i.e., fixed supply), either

as an absolute quantity or as a percentage of salmon body weight. If the fixed C_{tot} is measured in grams of prey rather than calories, the caloric density of the prey becomes critical: a gram of squid has approximately twice the calories and therefore twice the growth potential of a gram of zooplankton (Table 3.2).

The purpose of this model is to determine the effect of an ontogenetic diet shift on modeling the link between salmon and salmon prey on the high seas. Does the addition of a diet shift change the critical factors which may determine salmon growth?

As shown in Chapter 3, pink and sockeye salmon undergo a diet switch between the body weights of 600 and 1200 g, from zooplankton to squid. Pink salmon cross this size range during the spring and summer of their maturation year: sockeye salmon cross this range during the spring and summer of their ocean age .2 year (Figure 5.4). Other species do not undergo this switch during any dietary period measured in this dissertation, and are not included in this model. Bioenergetics models for pink and sockeye salmon use identical parameters (Table B.1), so the results in this section are presented for a single "fish" which may be either a pink or a sockeye.

The model covers the growth period between April 15 (Julian day 105) and September 15 (Julian day 255). Fish are started at 585 g body weight, the average April high seas pink salmon body weight from Figure 5.4. Daily water temperature was set as described in Section 5.2.1 and represents water conditions in the eastern portions of the Alaska Gyre. While many of the North American pink and sockeye stocks will mature and returned to spawn within the time period in this model, using September as an endpoint allows this model to extrapolate conditions for almost all stocks, as well as for both immature and maturing sockeye.

Prey quantity and composition is set as a function of salmon body weight, and changed during each day of the simulation. Prey is divided into two

types: zooplankton (700 cal/g wet weight) and squid (1500 cal/g wet weight; Table 3.2). The model is run for four scenarios of prey density in the environment that roughly correspond to the range of variation seen in zooplankton and squid consumption in Section 4.3. The scenarios are referred to as: (1) zooplankton low, squid low; (2) zooplankton high, squid low; (3) zooplankton low, squid high; and (4) zooplankton high, squid high.

Each of these cases is represented by a distinct relationship between salmon body weight and prey consumption (Figure 5.10). Prey consumption is measured by the bioenergetic P-Value: the body-weight dependent proportion of maximum physiological consumption (between 0 and 1). Using a constant P-Value during a simulation is similar to using a fixed proportion of a salmon's body weight as its ration.

In all scenarios, fish between 300-600g body weight feed exclusively on zooplankton. When zooplankton are "low", fish of this size feed on zooplankton at a P-Value of 0.5 (Figure 5.10a,b). The value of 0.5 is similar to the P-Value seen for small sockeye in northern regions in July (Table 4.14). When zooplankton are "high", fish between 300-600g body weight feed on zooplankton at their maximum consumption rate (P-Value=1.0; Figure 5.10c,d). This high P-Value is not matched for pink or sockeye in the "north" region of Table 4.14, where they feed on zooplankton. This may be due to the lower zooplankton abundance in the gyre in late summer: it is not unrealistic to assume that this level of consumption may be reached in the spring by salmon feeding on zooplankton alone (LeBrasseur 1966).

Between 600-1200g body weight, the proportion of squid in the salmon's diet increases linearly in this model. If squid availability is "high", squid increases until it replaces zooplankton entirely in the salmon's diet, at a P-Value of 1.0 (Figure 5.10b,d). If squid is "low", squid increases until it reaches a P-Value of 0.5, with the rest of the diet (up to a P-Value of 1.0) consisting of

zooplankton (Figure 5.10a,c). Above 1200g body weight, the diet of the modeled fish remains constant.

This overall diet pattern should be considered as a rough schematic of diet changes which might take place. The July diet data in the north and south zones in Section 4.3 suggests that the pattern for squid high/squid low is reasonable for the "south" and "north" zones for the larger fish. However, it is impossible to know if zooplankton should be considered to be low or high during the 1980s and 90s, as spring data is not available during that time period.

It should be noted that the terms squid- or zooplankton- "specialization" or "switching" are not meant to indicate behavioral preference. In fact, as squid are uniformly a higher energy food source, it should be expected that salmon would prefer squid, and would only be limited by their ability to catch squid, which may increase with body size. However, without having measurements of the energetic costs of squid capture versus zooplankton capture, it is not possible to define patterns of optimal foraging behavior.

With the dietary and temperature regime set, the salmon growth model was run from April to September, to determine the final adult body weight of the fish under each of the four prey scenarios, above. These results were then tested for sensitivity by varying the starting body weight and water temperature by +/-20%. Prey was not tested for sensitivity as the four scenarios take into account varying levels of prey.

Finally, these results were placed on the scale of population growth by following the growth and mortality of a "cohort" of a single (starting) metric ton of salmon, from April to September. The ecosystem consequences of variation in salmon starting body size were calculated, by running the model assuming that the single ton of fish was made up of "many small fish" or "fewer large fish" (defined below). The ecosystem consequences reported include the amount of

salmon biomass produced and the amount of prey consumed to achieve this biomass.

5.3.2 Results

With a starting body weight of 585g, the projected growth trajectory for each of the different scenarios is shown in Figure 5.11. When both zooplankton and squid were low, overall growth was low, and the final (September) body weight of the fish was 1077g (Table 5.8). For zooplankton high / squid low or zooplankton low / squid high, the final body weights were similar at 1831g and 1948g respectively. However, the growth trajectories differed (Figure 5.11). With zooplankton low and squid high, growth began fairly slow and accelerated rapidly at about Julian Day 200 (July), while for zooplankton high and squid low, growth was higher early, but did not accelerate. With both zooplankton and squid high, growth rates were high throughout the simulation, and the final body weight was 2667g.

When the starting body weight was varied by +/-20%, the effects on final body weight differed for each scenario (Figure 5.12 and Table 5.8). In both cases in which zooplankton were low, the 20% change in starting weight caused a change far greater than 20% in final weight (Figure 5.12a,b). When squid and zooplankton were both low, a decrease (increase) of 20% in beginning body weight led to a decrease (increase) of 44% (79%) in the final weight. When squid were high and zooplankton were low, final body weights changed by 60-70% for a 20% change in starting weight. On the other hand, when zooplankton abundance was high, a variation of 20% in the beginning weight led to a change in ending weight that remained close to 20% (Figure 5.12c,d).

The cause of this amplification of a slight variation in April body weight, when zooplankton abundance is low, can be seen in Figure 5.13. The two trajectories shown in Figure 5.13 are both for the zooplankton low / squid high

case. When the starting body weight is 585g (Figure 5.13b), the salmon grows large enough to begin consuming squid by May, whereas the fish beginning at 526g (10% smaller) does not begin consuming squid until June.

As the first, larger fish begins to consume squid, its growth rate increases due to the higher ration and increased caloric content of its diet. This in turn allows it to feed even more heavily on squid, which further accelerates growth, initiating a positive feedback which greatly amplifies this small difference in starting body size. Hence, if zooplankton is limiting to salmon in the winter and spring, the resulting small (10-20%) difference in spring body weight may be amplified to a difference in final weight of over 70%, even if food is not limiting later in the year.

Variations of +/- 10% in water temperature or prey indigestibility throughout resulted in less than a 2% change in final body size: these results are not shown.

Five "populations" of fish, each starting in April with 1 mt of biomass, were modeled for each of the 4 scenarios. Each starting population was assumed to consist of fish of identical starting body weights, and this weight was varied by +/-20% to create the five populations. The number of fish starting each simulation were calculated by dividing the 1mt of total biomass by the starting body weight in each population (Table 5.9).

Throughout the simulation, each individual fish in the population was assumed to follow one of the growth trajectories shown in Figure 5.12, depending on its starting body weight and the prey scenario. In addition, the number of fish in the population was reduced every 15 days by 0.8%, or 8% over the course of the simulation, representing an annual instantaneous mortality rate of 0.2.

The final (September) biomass of each population, the overall percent increase in biomass, and the total biomass of both types of prey consumed, is

presented in Table 5.9 and in Figures 5.14-5.17 for the combination of the 5 populations and 4 scenarios. In addition, the total mesozooplankton required to supply the salmon increase was calculated by assuming that each unit of squid biomass represented 5 units of zooplankton biomass: a rough zooplankton to squid conversion efficiency of 0.2 was estimated by Pauly and Christensen (1996). The overall conversion efficiency of mesozooplankton biomass to salmon biomass, including the passage of biomass through squid, was therefore calculated as

$$\text{Conversion efficiency (percent)} = \frac{100 * (\text{Sept. salmon biomass} - \text{April salmon biomass})}{(\text{zooplankton consumed} + 5 * \text{squid consumed})}$$

When both zooplankton and squid are low, the increase in biomass between April and August was 18% for the larger numbers of the smallest fish and 252% for the smallest numbers of the largest fish. The final biomass for 1 ton of initial biomass ranged from 1.18-2.52 mt (Figure 5.14a). Zooplankton consumption increased slightly for larger fish, from 3.8 to 4.5 mt (Figure 5.14b). Squid consumption was low overall: the smallest fish did not eat squid, while the largest fish ate 3.6 mt. The total zooplankton required ranged from 3.8 to 22.4 mt for the smallest to the largest fish, and the conversion efficiency ranged from 4.8 to 6.8%.

When zooplankton is low and squid is high, the largest difference exists between the populations with the smallest and the largest fish (Figure 5.15). The final biomass ranges from 1.18 to 3.16 mt, or from an 18% increase to a 316% increase in biomass. Squid consumption increases dramatically, from 0mt for the smallest fish to 10.6mt for the largest fish (Figure 5.15c). As each mt of squid requires 5 mt of zooplankton, the largest fish require the most zooplankton overall (Figure 5.15d). Conversion efficiency is lower for both smallest and largest fish than for fish of medium sizes (Figure 5.15e).

When zooplankton is high, the difference in growth and consumption between smaller and larger fish is minimal. If squid are low, final biomass ranges from 2.78mt to 2.89t for the smallest and the largest fish, respectively. The overall change in all of the consumption totals is fairly low (Figure 5.16). This ecosystem condition, with zooplankton high and squid low, is the most insensitive to the effects of changing the starting body weight of the salmon.

Finally, when both zooplankton and squid are high, the total increase in biomass is highest, between 3.82-4.31mt total final biomass of salmon (Figure 5.17). The populations consisting of larger fish consume very little zooplankton, as they are able to feed on squid early in the simulation period.

These population experiments were repeated with normally distributed starting weights with a varying mean for each population, rather than with identical starting body weights for each population. The results did not differ appreciably, and depended on the mean body weight in the population, with results similar to those reported in Table 5.9. These experiments were also repeated for a doubled yearly mortality rate (0.4), which changed the total amount of squid consumed as more fish died earlier, but did not affect the general pattern of the results reported above.

5.3.3 Discussion

The population scenario which was most sensitive to changes in April salmon body weight was the one in which zooplankton was low, and squid was high. In this scenario, an increase in the April body weight from 468 to 701g resulted in an increase in September body weight from 601 to 3172g (Table 5.9; Figure 5.12b).

A portion of Table 5.9 for the zooplankton low/squid high scenario is shown in Figure 5.18, scaled so that the results for the population in which April body weight=585g are scaled to 1. If one mt of salmon at 468g April body

weight each enter the simulation (2139 fish), the final September biomass is 58% of the case in which one mt of 585g salmon enter the simulation (1711 fish). The amount of squid consumed is 80% less for the smallest fish, but the amount of zooplankton consumed is 60% more, despite the lower biomass at the end of the simulation. Conversely, one mt of the largest fish in beginning the simulation (1426 fish at 701g body weight each) produces 25% more biomass than the population of average-sized fish, while consuming 40% more squid and 40% less zooplankton.

These results have two important implications. First, they confirm that under a range of growth conditions, a small difference in pink or sockeye salmon body weight in April may lead to a considerably larger difference in late summer, due to the effect of trophic (positive) feedback amplifying the growth rates of larger fish through the ontogenetic shift in diet between zooplankton and squid. Therefore, the difficulty of finding food in winter may have a strong effect on a salmon's final body weight, run timing, and maturation rates, even if the majority of its weight is put on in the summer.

Second, the results suggest that under certain conditions, a population with large numbers of small fish may produce considerably less biomass than a population with small numbers of large fish, even if the populations start with the same initial biomass. Note that this situation may be even more dramatic than Figure 5.18 suggests. The smaller fish not only eat more zooplankton and grow less: they do *not* eat squid. This may release squid from top-down control, increasing the demand for zooplankton even further. This suggests that the release of large numbers of hatchery fish may be self-defeating, if they are produced to increase the biomass of returning fish.

It is impossible, from current data, to know whether the ecosystem in any given year was in a "high" or "low" state for squid or zooplankton. Clearly, there are more squid and fewer zooplankton south of the July SST boundary than

north of it (Chapter 4), but not enough is known about these species to further refine these general patterns. One additional problem in this model is that it does not correct for differing energy expenditures required to catch squid vs. zooplankton, although bioenergetics models do account for the cost of increased swimming speed as a function of body weight. It is not known if additional energetic costs are required for capturing squid.

It is also impossible to know, in this trophic triangle, which species, if any, is the keystone. An increase in smaller salmon may lead to a decrease in predation on squid (Figure 5.18), which may lead to a population explosion of squid, further decreasing the size of salmon. Conversely, the increase in squid may be climate-related and not subject to top-down control from salmon.

The trophic position of the highly productive *Beryteuthis anonychus* means it may be in a controlling position in the ecosystem, and its life cycle, reviewed in Chapter 3, may make it prone to substantial population increases and declines, as have been seen in forage fish around the world (Bakun 1996). Clearly, if salmon carrying capacity is to be estimated, the population dynamics of this little-understood species must be further researched.

The results presented here are accurate for pink and ocean age .2 sockeye. Older sockeye and coho feed very little on zooplankton and would be more sensitive to changes in squid, while younger sockeye and chum might be expected to be more sensitive to zooplankton changes: in either case, the lack of an ontogenetic shift in diet may make them more resistant to changes in winter body size.

Finally, it is important to know that these models do not take into account biogeography. The presence of high and low squid zones in a single year, reported in Chapter 4, means that salmon may move back and forth to the most advantageous zone for their body size, at least within the limits of their migration pattern. Spatially explicit models of salmon foraging may be

expanded to take into account the biogeography of salmon movement with respect to their size and foraging mode.

5.4 Experiment 3: mixed effects of density-dependence and water temperature

5.4.1 Methods

The preceding two models are not dynamic in terms of salmon foraging behavior. The first model assumes that the measured growth of a salmon is fixed, while the second model assumes that a certain fixed amount of food is obtainable each day. However, obtaining food requires energy expenditure. A fish may choose to expend an amount of energy on foraging which depends on the amount of prey present in the environment, in an attempt to achieve the optimal growth over a given time period.

Model 3, in some senses, is more abstract than the previous two models. It measures growth on an instantaneous scale only. Predator size, water temperature, and prey caloric values are direct inputs to the model and do not reflect a seasonal progression of conditions. However, performing this instantaneous calculation provides insights on the relationship between density-dependence and water temperature found in Section 4.4.

Dynamic optimization on any time scale longer than instantaneous requires substantial knowledge of the biogeography of predator and prey which is not available at this time. However, even at the instantaneous time scale, it is possible to model the effects of predator competition on salmon rates of growth. This model determines the maximum rate of growth possible for a given fish in a given water temperature, assuming that both the amount of food eaten and the amount of energy spent on foraging increase as a function of predator

swimming velocity, the amount of food in the environment, and the number of predators sharing that food.

This model sets daily rations and daily energy expenditure as a function of predator swimming velocity, water temperature, and available prey. The relationship between swimming velocity and energy expenditure (respiration) may be found in Appendix B. Model results are reported for a single pink salmon, 1,500g in body weight, feeding on prey of 1000cal/g wet weight (indigestibility 0.1). While changes in these input parameters change the actual rates of growth, they do not change the patterns of density-dependence reported in the results.

The number of (salmon) foraging competitors ($N_{\text{predators}}$) is set with an arbitrary index of salmon abundance: the value of 1 is used as the base case. The model was calibrated so that when $N_{\text{predators}}=1$ (base case), the salmon had a maximum consumption rate ($P=1$) at a water temperature of 12°C: this required the salmon to consume 54.8 g prey/day in the base case (Table 5.10).

The relationship between prey capture and swimming velocity is given in the search rate equation C.2 (Appendix C) which requires an estimate of the available prey in the environment. Values for Reaction Distance=20 cm and probability of capture = 0.5 (assuming turbid water), and assuming in the base case that swimming velocity = $V_{\text{opt}}=41.6$ cm/sec (eq. B. 3). Use of these values resulted in an estimate of the prey available (D_{avail}) required to supply 54.8 g prey/day at the swimming velocity V_{opt} as 25.2 g prey /m³ water.

Available prey, in turn, is a function of both the total amount of prey in the environment and the number of predators (salmon) that must share that prey. This model uses the "mixed" equation C.8., so called because it can model density-dependence or density-independence by setting the Density Dependence Index (DD_{index}) as a function of the prey available to salmon and the total prey in the environment (eq. C.10).

Water temperature and N_{predator} were varied for each of three levels of density-dependence: weak ($DD_{\text{index}}=-1$); medium ($DD_{\text{index}}=0$); and strong ($DD_{\text{index}}=1$). For each value of water temperature, N_{predator} , and DD_{index} , the swimming velocity of the salmon was set to maximize growth rate ΔB (Appendix B).

5.4.2 Results

For all three levels of density-dependence (weak, medium and strong; $DD_{\text{index}} = -1, 0, \text{ and } +1$), the model was calibrated so that when $N_{\text{predators}}$ was equal to 1, the density of available prey was equal to 25.2g, enough to result in a high physiological growth rate ($P_{\text{value}}=1.0$) when the water temperature was 12°C. As $N_{\text{predators}}$ changed, the amount of prey available in the environment changed depending on the level of density dependence (Figure 5.19).

Figure 5.20 shows growth rate as a function of swimming velocity for three values of N_{predator} , when density dependence is strong (+1) and water temperature is 12°C. At lower predator densities, the maximum growth rate is highest (point A), and occurs at a lower swimming speed than at high predator densities.

Figure 5.21 shows the complete results of the maximization of instantaneous growth rates as a function of N_{predator} and water temperature, for three levels of density dependence: weak (Figure 5.21A), medium (Figure 5.21B) and strong (Figure 5.21C). The lines in each figure represent the different density-dependent response curves (growth rate as a function of N_{predator}) for varying temperatures. Each point along the lines is the maximization of a growth curve for the given temperature and N_{predator} level, as shown by point A in Figure 5.20.

For weak density-dependence, the slope of the line is low for all water temperatures. The slope of the line changes very little with water temperature, but the y-intercept of the lines change. Growth rates are highest for any given N_{predator} level at 8°C and lower at 4°C and 16°C. The slope at 16° is slightly steeper than at other temperatures (Figure 5.21A).

As density dependence increases to medium and strong, the temperature shows a strong effect on both the y-intercept and slope of the response (Figure 5.21B and C). In addition, when density-dependence is strong, the response becomes increasingly nonlinear (Figure 5.21C for the 16°C temperature line).

This nonlinearity comes from the interaction of temperature and digestion. When density-dependence is strong, a small decrease in the predator population leads to a large increase in available prey. As prey becomes more available, warmer temperatures become more beneficial as the metabolic rate of the salmon increases. However, as the predator population increases, the growth rate drops off extremely quickly at higher temperatures, as the metabolic costs of respiration are prohibitive at high temperatures, if food is limiting.

Finally at the lowest temperature used in the experiment (4°C), the height and slope of the response changes very little between weak and strong density-dependent cases (Figure 5.21A-C).

5.4.3 Discussion

Section 4.3 suggests that temperature is second in importance to prey availability for determining salmon growth, while Section 4.4 suggests that an interaction occurred between the adult body weight of salmon, salmon numbers, and water temperature over the last 20 years. The model proposed by Peterman (1987) and shown in Figure 4.43 suggests that the effects of

temperature are independent of population density. However, the model of instantaneous growth rate limitation in Figure 5.21 suggests a more complicated interaction between temperature and density-dependence. This interaction is seen in actual data in the increasing slopes of the body size/salmon abundance regressions shown in Figure 4.41.

If the bioenergetics models are accurate, an increase in environmental temperature will magnify density-dependent growth and increase the sensitivity of salmon stocks to competition. At low salmon numbers, salmon growth rates will be positively correlated with temperature, while at high salmon numbers, salmon growth rates will be negatively correlated with temperature. These results offer a partial explanation for the interaction between temperature, prey availability (overlap area), salmon numbers, and salmon size.

This model has an important implication for how we view both the environment and anthropogenic change, either on the scale of salmon hatchery management or on the scale of global warming. The results suggest that large numbers of salmon alone, or increases in water temperature alone, may have no effect on the growth rate of salmon. However, a critical combination of the two, as has occurred in the northeastern Pacific between 1989-98, may create a dramatic change even when the individual effects are negligible. Even if we are safe with either change occurring separately, in conjunction, the non-additive nature of these effects may take salmon populations far outside the range of any predictions.

5.5 Conceptual model of salmon carrying capacity

Overall, the approach of this dissertation was to focus on simple models, and to isolate individual elements of density-dependent growth in adult Pacific salmon in the high seas of the Gulf of Alaska. Chapter 3 explored the food habits of post-juvenile salmon in this region, and pointed out the importance of the micronektonic squid *Berryteuthis anonychus* in salmon diets. Section 4.2

examined the biogeography of this species, and Section 4.3 modeled salmon growth rates resulting from this variation in prey. Section 4.4 suggested that some of the previous models of interaction between climatic trends in sea surface temperature and salmon growth could be explained by the changing area of overlap between squid and salmon. This emphasizes the importance of oceanographic and climate-driven interpretation of biogeography and the importance of the interannual variability of habitat fronts discussed in Chapter 2.

Moreover, the results suggest a nonlinear interaction between the overlap area, temperature, and density-dependent growth. A mechanism for this nonlinear interaction was presented in Section 5.4. Little is known about the interannual variation in micronektonic squid, and measuring its population fluctuations is an area of important future study.

The results of Sections 5.2 and 5.3 suggest that the search for bottlenecks in ocean growth should focus on salmon in their winters at sea. Combining the models allows the creation of a new conceptual model of salmon carrying capacity (Figure 5.22). For chum and ocean age .1 sockeye, which are zooplankton specialists, variation in zooplankton density may be a strong determinant of total growth during winter and spring, with water temperature playing an equal role later in the season. Coho and ocean age .3 and older sockeye would be expected to respond most to variations in squid populations as indexed by changes in sea surface temperature, and may be less prone to density-dependent effects.

However, the most numerous species of salmon, pink salmon, are probably controlled strongly by density-dependent competition for zooplankton in the winter months. Pink, along with ocean age .2 sockeye, undergo their ontogenetic shift in diet at a time when small differences in early growth may be greatly magnified. The strongest single controller of growth may be zooplankton during this period. Combined with the results in Section 5.3,

density-dependence in salmon occurs as a function not only of salmon numbers and prey quantity, but also of prey trophic position, the relative abundance of each prey type, and interactions with prey biogeography and temperature, which may amplify the density-dependent response (Table 5.11).

This response may be further modified by detailed food web interactions, the physiology of salmon development and maturation timing, stock-specific migration patterns, and the distribution and abundance of salmon predators, such as sharks.

Two important conclusions should be drawn from this work, in terms of the human management of salmon populations. First of all, producing large numbers of salmon in hatcheries may not be the most efficient way of obtaining desirable or healthy stocks. Secondly, density-dependent effects of growth, and thus salmon carrying capacity, may arise through a non-linear combination of factors, even if each individual factor has little influence on salmon growth. Pumping up the production of the North Pacific ecosystem through the release of high numbers of small fish may have cascading effects that, while producing large numbers of salmon in the short term, may be deleterious to the health of the ecosystem overall.

Table 5.1. Experimental methods used in the bioenergetics models in Chapter 5.

	Experiment 1 (Section 5.2)	Experiment 2 (Section 5.3)	Experiment 3 (Section 5.4)
Model type	Fixed growth at average activity	Fixed consumption at average activity	Activity modified to maximize growth
Salmon species	All species shown in Table 5.2	Pink and ocean age .2 sockeye	Pink and sockeye
Time period	Throughout ocean life	April-August of maturation	"Instantaneous"
Water temperature	SST at OSP ¹	SST at OSP	Varied over range
Prey type	Zooplankton at OSP ²	Ontogenetic switch between zooplankton and squid determined by body weight	Results calculated for multiple prey types
Consumption rate	Food required to fit measured high seas body weights	Fixed amount of prey available per salmon	Swimming velocity
Salmon swimming velocity	Cruising optimum for body weight	Cruising optimum for body weight	Varied to obtain maximum growth rate at set prey densities
Output of model	Food requirements per month to fit observed growth, amount of zooplankton and ocean area required to satisfy this demand	Body weight obtained at each simulation day, April through August	Maximum possible "instantaneous" (daily) growth rate for a range of input variables
Sensitivity tests	Temperature, body weight, prey caloric value, indigestibility	Available prey, starting body weight, temperature	Output measured over range of conditions
Density-dependent growth implication	Winter is the time during which the greatest ocean area is required to support a single salmon's growth.	The ontogenetic switch causes a feedback by which a small difference in initial (winter) body size may be amplified greatly by the summer.	If catch-per-unit-effort of foraging is inversely related to salmon density (numbers), the relationship between maximum growth rate and numbers will be affected by water temperature.

¹Ocean Station P, 50°N, 145°W.²'Prey type' in Model 1 is not directly consumed, but used to calculate the amount of ocean area required to satisfy caloric requirements of the fish.

Table 5.2. A selection of pink and sockeye salmon tagged on the high seas and recovered with archival (temperature or depth) tags in North American nearshore fisheries. See Walker et al. (2000) for a description of tagging methodology. Minimum speed is the velocity required to travel the great circle distance between release and recovery locations (Figure 5.2) in the time indicated.

	Release				Recovery			Days Out	Dist. (km)	Min Vel. (cm/sec)
	Date	Lat (°N)	Long. (°W)	FL (mm) Age	Date	Lat (°N)	Long. (°W)			
A. Sockeye Salmon										
S1	5/20/99	54.8	145.0	615 2.2	8/14	55.3	128.9	86	1024	13.8
S2	5/20/99	54.8	145.0	520 2.2	7/13	58.2	156.6	54	808	17.3
S3	5/20/99	54.8	145.0	490 2.2	7/11	56.5	158.1	52	845	18.8
S4	5/21/99	56.7	145.0	555 2.3	7/9	61.5	143.6	49	542	12.8
S5	5/22/99	58.4	145.0	640 1.3	6/16	56.3	157.5	25	785	36.3
S6	5/22/99	59.0	145.0	635 1.3	7/4	58.2	133.9	43	648	17.5
S7	7/14/99	56.2	144.9	635 1.3	8/3	58.1	133.9	20	697	40.4
B. Pink salmon										
P1	7/12/99	54.0	143.0	475 0.1	8/26	55.3	130.1	45	844	21.7
P2	7/13/99	56.0	145.0	468 0.1	8/5	57.6	151.9	23	455	22.9

Table 5.3. Species, ocean ages, and maturity status of salmon modeled in Section 5.2. The model follows the 14 groups from July, through winter, to a second July and August: "Imm" and "Mat" refers to immature and maturing, respectively in the *final* months of the simulation. Number indicated is ocean age in the final months: groups begin the model one year prior to the shown age. For a given age class, immature and maturing fish are indistinguishable in the model prior to March.

Pink	Coho
Age .1 Maturing	Age .1 Maturing
Sockeye	Chum
Age .1 Immature	Age .1 Immature
Age .2 Immature	Age .2 Immature
Age .2 Maturing	Age .2 Maturing
Age .3 Immature	Age .3 Immature
Age .3 Maturing	Age .3 Maturing
Age .4 Maturing	Age .4 Maturing

Table 5.4. Kilocalories required per salmon per day (averaged by month) to match observed growth patterns in high seas Pacific salmon. Jul/Dec is the ratio between July and December requirements.

	Sock.1imm	Sock.2imm	Sock.2mat	Sock.3imm	Sock.3mat	Sock.4mat
Prior Jul	1.7	7.1	7.2	17.3	17.2	25.9
Prior Aug	2.2	9.4	10.2	21.5	21.5	30.6
Sep	2.5	10.6	12.8	21.7	22.7	29.2
Oct	2.7	11.1	15.2	19.5	22.7	25.7
Nov	3.1	11.9	18.0	17.8	23.9	24.2
Dec	3.8	13.0	21.5	17.1	26.9	25.4
Jan	4.6	14.2	25.2	16.8	30.8	28.3
Feb	5.4	15.2	28.8	16.5	34.8	31.8
Mar	6.4	16.2	32.2	16.4	39.1	36.1
Apr	7.5	17.5	36.0	17.0	44.2	41.9
May	9.0	19.5	40.8	18.8	51.0	50.1
Jun	11.1	22.9	48.1	22.6	61.1	62.2
Jul	14.0	27.7	58.3	28.2	75.1	78.8
Jul/Dec	3.7	2.1	2.7	1.7	2.8	3.1

	Chum.1imm	Chum.2imm	Chum.2mat	Chum.3imm	Chum.3mat	Chum.4mat
Prior Jul	0.8	6.4	6.8	14.1	14.2	18.9
Prior Aug	1.0	7.5	9.8	16.3	17.1	22.5
Sep	1.3	7.4	12.4	15.2	17.3	21.9
Oct	1.6	6.8	14.4	13.0	16.4	19.8
Nov	2.2	6.9	16.4	11.8	16.7	19.3
Dec	2.9	7.8	18.5	12.1	18.4	20.8
Jan	3.9	9.3	20.6	13.3	21.1	23.4
Feb	5.0	11.2	22.3	14.9	24.0	26.6
Mar	6.4	13.6	23.8	17.0	27.3	30.4
Apr	8.0	16.6	25.7	20.0	31.6	35.3
May	10.2	20.9	28.8	24.5	37.6	42.5
Jun	13.3	27.1	34.1	31.4	46.8	53.4
Jul	17.7	35.9	42.1	41.0	59.9	69.0
Jul/Dec	6.0	4.6	2.3	3.4	3.2	3.3

	Pink	Coho
Prior Jul	0.8	3.7
Prior Aug	1.6	5.1
Sep	2.9	6.9
Oct	4.5	9.3
Nov	6.5	12.9
Dec	8.9	18.3
Jan	11.6	25.8
Feb	14.4	36.3
Mar	17.4	49.0
Apr	20.9	59.4
May	25.2	73.1
Jun	31.2	94.6
Jul	39.5	125.7
Jul/Dec	4.4	6.9

Table 5.5. Percentage change in kilocalories required per day for a pink salmon (from Table 5.4) with a +/-10% change in the indicated input variable.

(A) Total body growth (g)			(B) Water temperature (°C)		
	-10%	+10%		-10%	+10%
P. Jul	-18%	43%	P. Jul	-11%	13%
P. Aug	-27%	27%	P. Aug	-8%	9%
Sep	-22%	23%	Sep	-5%	5%
Oct	-23%	23%	Oct	-3%	3%
Nov	-25%	27%	Nov	-1%	2%
Dec	-28%	31%	Dec	-1%	1%
Jan	-31%	36%	Jan	-1%	1%
Feb	-34%	40%	Feb	-1%	1%
Mar	-37%	45%	Mar	-1%	1%
Apr	-40%	47%	Apr	-1%	2%
May	-41%	47%	May	-2%	3%
Jun	-41%	47%	Jun	-4%	5%
Jul	-41%	46%	Jul	-6%	8%

(C) Prey caloric value (cal/g)			(D) Prop. prey indigestible		
	-10%	+10%		-10%	+10%
P. Jul	0%	0%	P. Jul	-1%	1%
P. Aug	0%	0%	P. Aug	-1%	1%
Sep	1%	0%	Sep	-1%	1%
Oct	1%	-1%	Oct	-1%	1%
Nov	2%	-1%	Nov	-1%	1%
Dec	2%	-1%	Dec	-1%	1%
Jan	2%	-1%	Jan	-1%	1%
Feb	2%	-2%	Feb	-1%	1%
Mar	2%	-1%	Mar	-1%	1%
Apr	2%	-1%	Apr	-1%	1%
May	2%	-1%	May	-1%	1%
Jun	1%	-1%	Jun	-1%	1%
Jul	1%	-1%	Jul	-1%	1%

Table 5.6. Mesozooplankton density by month, averaged over the time period 1964-1980 for Ocean Station P (50°N, 145°W). (A) Average wet weight per unit volume (mg/m³), 0-150m depth. (B) Integrated total wet weight from 0-150m depth (g/m² surface area of ocean).

(A) Mesozooplankton per 0-150m depth volume (mg/m³)

Month	N	Minimum	Maximum	Geometric		
				mean	-1sd	+1sd
Jan	134	0.20	42.0	8.5	4.2	17.2
Feb	94	0.60	50.7	6.8	-3.2	14.3
Mar	173	2.50	180.6	18.1	7.7	42.5
Apr	191	2.67	597.3	49.4	21.2	115.2
May	360	2.67	1026.7	126.2	50.9	312.4
Jun	386	2.67	1400.0	153.3	69.8	336.5
Jul	348	2.67	1008.0	103.5	42.1	254.1
Aug	292	8.00	610.7	81.3	38.1	173.6
Sep	243	2.00	780.1	34.8	11.5	105.2
Oct	133	2.58	362.7	16.4	7.4	36.5
Nov	108	1.17	101.3	13.8	6.7	28.5
Dec	120	2.10	80.1	10.0	5.0	20.1

(B) Total mesozooplankton in 0-150 surface layer (g/m²)

Month	N	Minimum	Maximum	Geometric		
				mean	-1sd	+1sd
Jan	134	0.03	6.3	1.3	0.6	2.6
Feb	94	0.09	7.6	1.0	0.5	2.1
Mar	173	0.38	27.1	2.7	1.2	6.4
Apr	191	0.40	89.6	7.4	3.2	17.3
May	360	0.40	154.0	18.9	7.6	46.9
Jun	386	0.40	210.0	23.0	10.5	50.5
Jul	348	0.40	151.2	15.5	6.3	38.1
Aug	292	1.20	91.6	12.2	5.7	26.0
Sep	243	0.30	117.0	5.2	1.7	15.8
Oct	133	0.39	54.4	2.5	1.1	5.5
Nov	108	0.18	15.2	2.1	1.0	4.3
Dec	120	0.32	12.0	1.5	0.7	3.0

Table 5.7. Ocean surface area (m²) required to be "emptied" of 0-150m zooplankton to satisfy caloric demands of salmon, by species, age, and maturity status.

	Sock.1imm	Sock.2imm	Sock.2mat	Sock.3imm	Sock.3mat	Sock.4mat
Prior Jul	0.2	0.7	0.7	1.6	1.6	2.4
Prior Aug	0.3	1.1	1.2	2.5	2.5	3.6
Sep	0.7	2.9	3.5	5.9	6.2	8.0
Oct	1.6	6.4	8.8	11.3	13.2	14.9
Nov	2.2	8.2	12.4	12.3	16.5	16.7
Dec	3.6	12.4	20.5	16.3	25.7	24.3
Jan	5.1	15.9	28.2	18.8	34.4	31.6
Feb	7.6	21.4	40.5	23.2	48.9	44.7
Mar	3.4	8.5	17.0	8.6	20.6	19.0
Apr	1.4	3.4	6.9	3.3	8.5	8.1
May	0.7	1.5	3.1	1.4	3.9	3.8
Jun	0.7	1.4	3.0	1.4	3.8	3.9
Jul	1.3	2.6	5.4	2.6	6.9	7.3

	Chum.1imm	Chum.2imm	Chum.2mat	Chum.3imm	Chum.3mat	Chum.4mat
Prior Jul	0.1	0.6	0.6	1.3	1.3	1.7
Prior Aug	0.1	0.9	1.2	1.9	2.0	2.6
Sep	0.4	2.0	3.4	4.2	4.7	6.0
Oct	1.0	4.0	8.3	7.5	9.5	11.5
Nov	1.5	4.8	11.3	8.2	11.5	13.3
Dec	2.8	7.5	17.7	11.6	17.6	19.8
Jan	4.4	10.5	23.1	14.9	23.6	26.2
Feb	7.1	15.8	31.3	21.0	33.7	37.4
Mar	3.4	7.2	12.5	9.0	14.4	16.0
Apr	1.5	3.2	5.0	3.9	6.1	6.8
May	0.8	1.6	2.2	1.8	2.8	3.2
Jun	0.8	1.7	2.1	1.9	2.9	3.3
Jul	1.6	3.3	3.9	3.8	5.5	6.3

	Pink	Coho
Prior Jul	0.1	0.3
Prior Aug	0.2	0.6
Sep	0.8	1.9
Oct	2.6	5.4
Nov	4.5	8.9
Dec	8.5	17.4
Jan	12.9	28.9
Feb	20.3	51.1
Mar	9.2	25.8
Apr	4.0	11.4
May	1.9	5.5
Jun	1.9	5.9
Jul	3.6	11.6

Table 5.8. Final (Sept. 15) body weight of a pink or ocean age .2 sockeye with a starting body weight of 585g on April 15, under 4 scenarios of prey availability, and percent change in final body weight for a +/- 10 and 20% change in starting body weight.

Prey Availability Squid · Zoop.		September body weight for starting April weight of 585 g	Percent change in Sept. weight for percent change in April weight of:			
			-20%	-10%	+10%	+20%
Low	Low	1077 g	-44%	-31%	+46%	+79%
Low	High	1831 g	-23%	-11%	+11%	+20%
High	Low	1948 g	-69%	-49%	+40%	+63%
High	High	2667 g	-27%	-13%	+13%	+23%

Table 5.9. Change in biomass and consumption of prey of five populations of salmon (1 tonne of biomass each in April). Each population differs in the body weight of salmon, and thus the number of salmon required to make up 1 tonne of starting weight.

Apr. Body Weight (g)		468	526	585	643	701
Apr. Salmon Numbers		2139	1901	1711	1555	1426
Apr. Biomass (t)		1.0	1.0	1.0	1.0	1.0
Yearly Mortality				0.2		
Percent Lost (Sept-April)				8.0%		
Sept. Salmon Numbers		1967	1749	1574	1431	1312
Zoop. LOW	Sept. Body Weight (g)	601	747	1077	1572	1923
Squid LOW	Sept. Biomass (t)	1.18	1.31	1.70	2.25	2.52
	Percent Increase	18%	31%	70%	125%	152%
	Squid Consumed (t)	0.00	0.34	1.36	2.81	3.60
	Zoop. Consumed (t)	3.80	3.74	3.90	4.24	4.45
	Total Zoop Req. (t)	3.80	5.45	10.71	18.30	22.43
	Efficiency	4.8%	5.6%	6.5%	6.8%	6.8%
Zoop. LOW	Sept. Body Weight (g)	601	987	1948	2717	3172
Squid HIGH	Sept. Biomass (t)	1.18	1.73	3.07	3.89	4.16
	Percent Increase	18%	73%	207%	289%	316%
	Squid Consumed (t)	0.00	1.54	6.05	9.22	10.55
	Zoop. Consumed (t)	3.80	3.80	2.28	1.35	0.84
	Total Zoop Req. (t)	3.81	11.48	32.55	47.43	53.61
	Efficiency	4.8%	6.3%	6.3%	6.1%	5.9%
Zoop. HIGH	Sept. Body Weight (g)	1414	1626	1831	2027	2204
Squid LOW	Sept. Biomass (t)	2.78	2.84	2.88	2.90	2.89
	Percent Increase	178%	184%	188%	190%	189%
	Squid Consumed (t)	2.84	3.38	3.82	4.14	4.34
	Zoop. Consumed (t)	7.68	6.92	6.34	5.88	5.52
	Total Zoop Req. (t)	21.87	23.85	25.43	26.58	27.23
	Efficiency	8.2%	7.7%	7.4%	7.1%	6.9%
Zoop. HIGH	Sept. Body Weight (g)	1941	2309	2667	3002	3287
Squid HIGH	Sept. Biomass (t)	3.82	4.04	4.20	4.30	4.31
	Percent Increase	282%	304%	320%	330%	331%
	Squid Consumed (t)	7.37	8.70	9.79	10.60	11.05
	Zoop. Consumed (t)	4.26	3.05	2.10	1.40	0.90
	Total Zoop Req. (t)	41.10	46.53	51.04	54.39	56.16
	Efficiency	6.9%	6.5%	6.3%	6.1%	5.9%

Table 5.10. Parameters used for the density dependent model in Section 5.4. See Appendix C for definitions of terms. Bold values are direct inputs, while non-bold values are calculated from inputs. Reaction distance is based on a study by Beauchamp et al. (1999) while other bold values are taken from "typical" salmon sampled in other sections of this dissertation.

Salmon numbers (index)	1
Body weight (g)	1500
Prey caloric density (cal/g)	1000
Prey indigestibility	0.1
Temperature (°C)	12
P Value	1
Vopt (cm/sec)	41.6
Food consumed(g/day)	54.8
ReactDist(cm)	20
Vprey (cm/sec)	0
Pc	0.5
SR (m ³ /day)	4343
Davail(mg/m ³)/salmon	25.2
Density Dependence Index	
DD High	1
DD Medium	0
DD Low	-1

Table 5.11. Predicted differences in instantaneous ocean growth rates of maturing pink and ocean age .2 sockeye as the result of changing environmental conditions. "Low" and "High" represent values used in Section 5.3.

		Summer squid density	
		Low	High
Winter-Spring zooplankton density	Low	Poor overall growth, density-dependence weak	Poor overall growth, density dependence strong
	High	Medium overall growth, density-dependence weak	High overall growth, density dependence strong
Effect of spring/ summer ambient water temperature (upper 50m)		A steeper density-dependent growth slope will occur at higher water temperatures. At low salmon densities, fish may be larger at higher water temperatures than at lower water temperatures, while at high salmon densities, fish may be smaller at higher water temperatures and larger at lower water temperatures.	

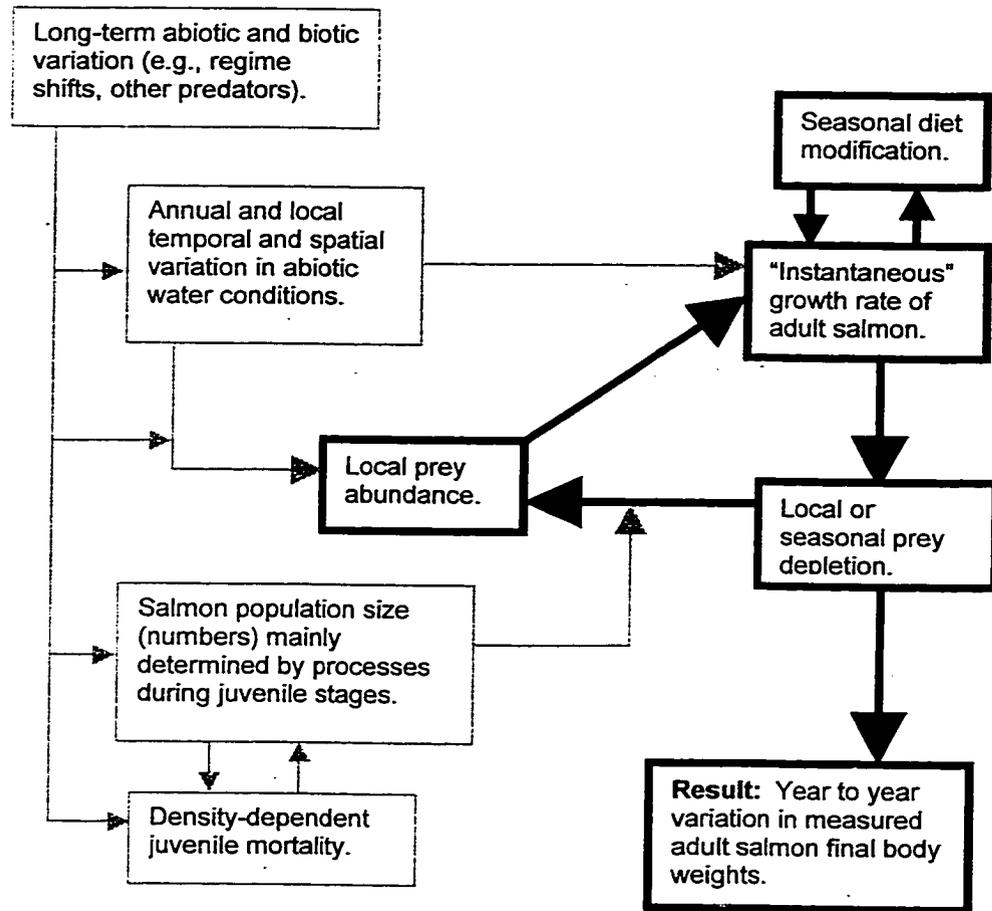


Figure 5.1. A conceptual model of salmon carrying capacity, emphasizing the portions of the model discussed in Chapter 5.

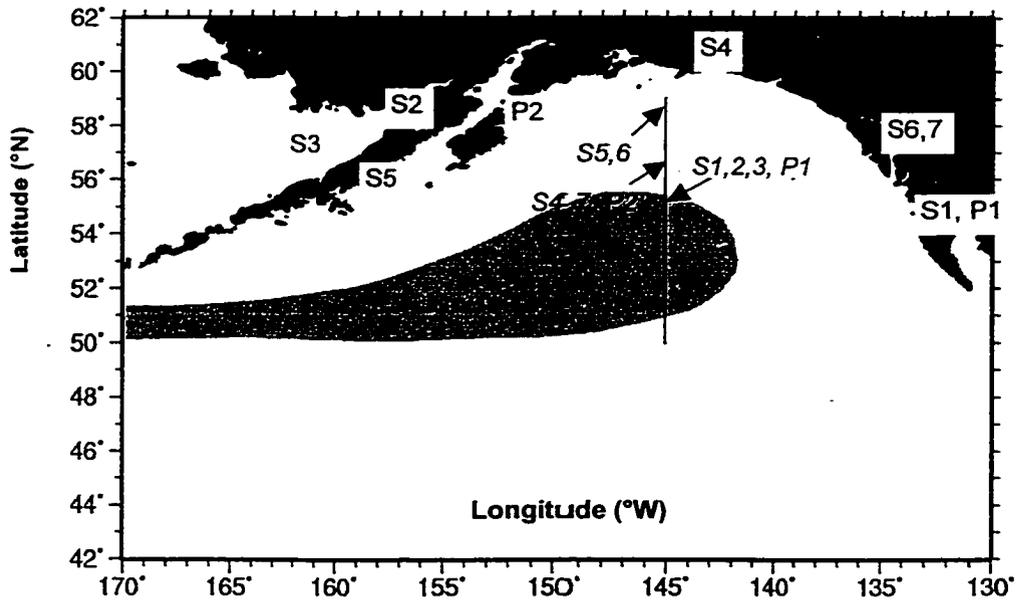


Figure 5.2. Release and recovery locations for a selection of pink (p) and sockeye (s) salmon tagged in the Gulf of Alaska along 145°W in May and July. Italicized letters are tagging locations (see Table 5.2).

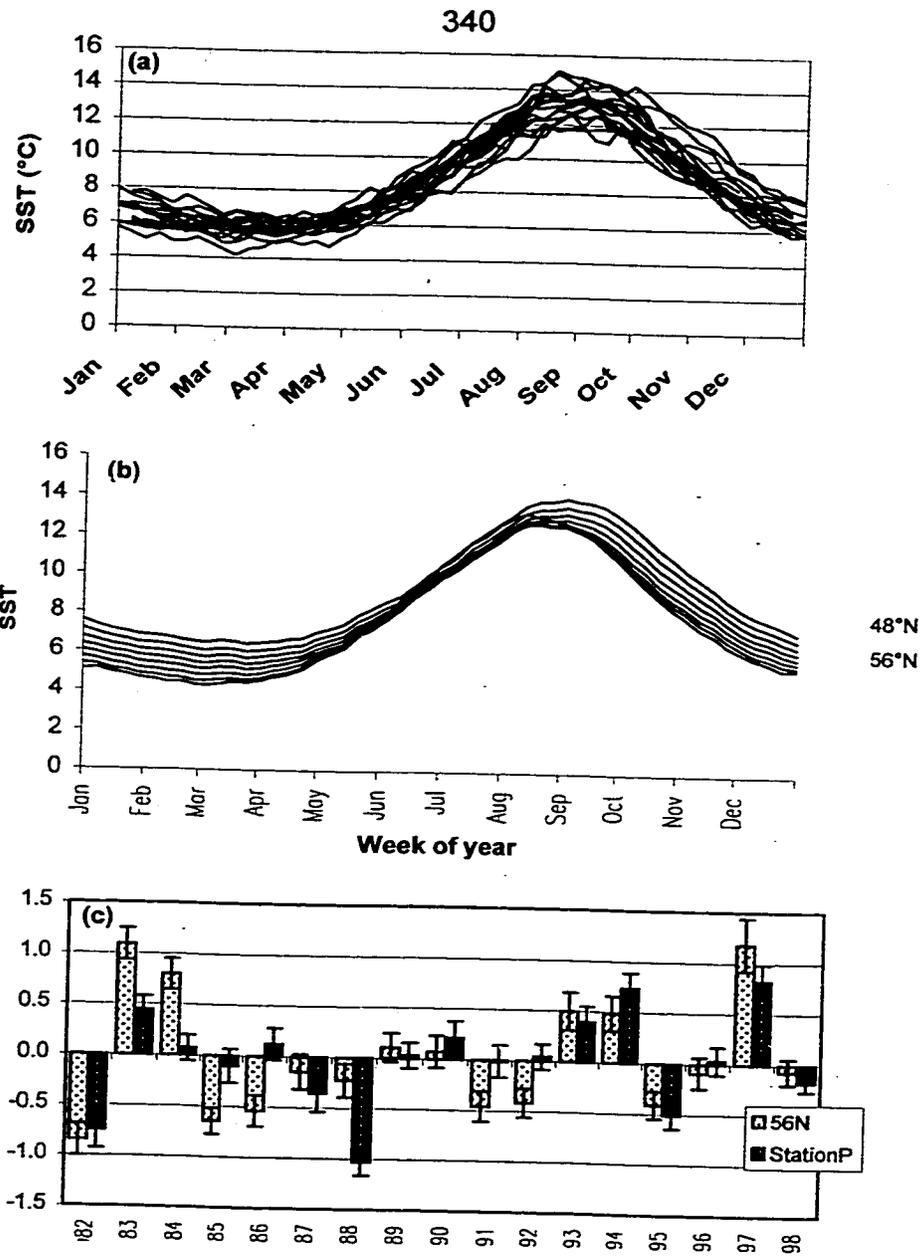


Figure 5.3. Weekly 1°x1° sea surface temperature (SST) along 145°W, 1982-98 (IGOSS). (A). Each line represents a single year between 1982-98 at Ocean Station P, 50°N, 145°W. (B). Weekly SSTs for all years 1982-98, averaged for each degree of latitude along 145°W, between 48-56°N. (C). Yearly anomalies from weekly averaged SSTs for Ocean Station P (50°N, 145°W) and 56°N, 145°W. Error bars show 95% confidence intervals for anomalies.

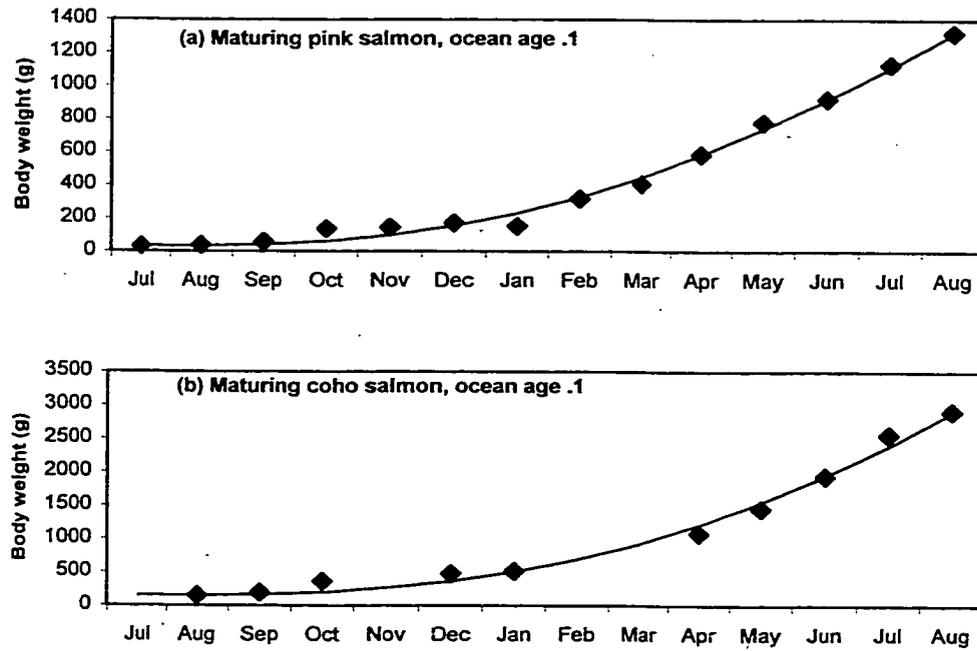


Figure 5.4. Monthly mean (points) of body weight for salmon caught in the high seas of the North Pacific (Ishida et al. 1998). Weights are stratified by species, ocean age, and maturity status. Age and maturity status indicate condition in the final July shown on the graph. Lines show a least-squares fit of a simple exponential growth curve (Figure continued on next 4 pages).

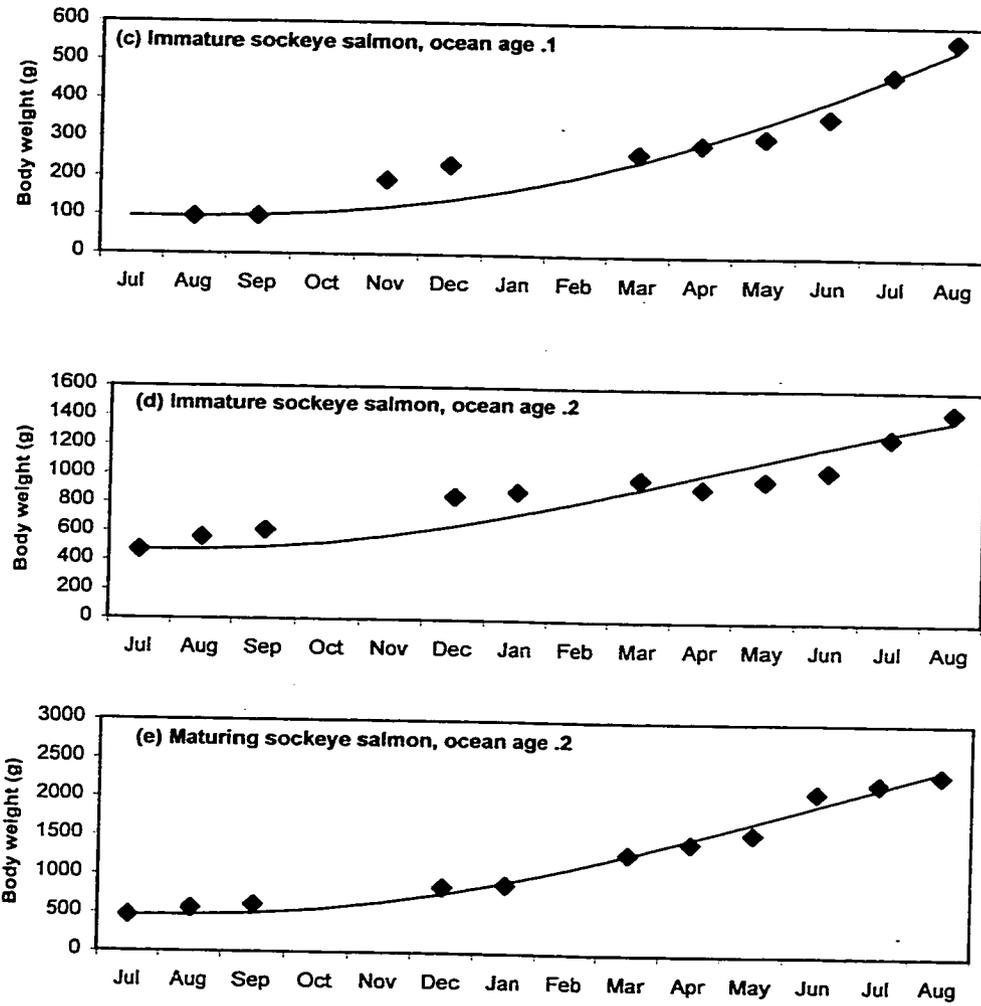


Figure 5.4. (continued).

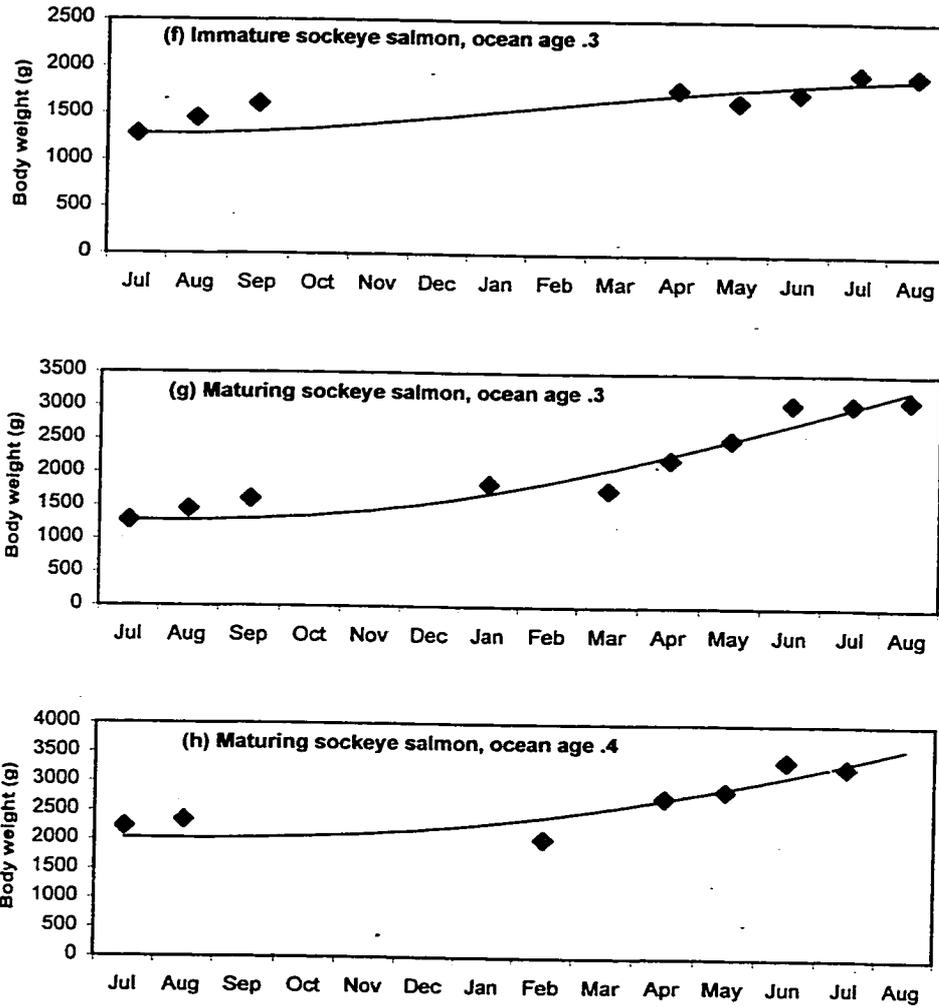


Figure 5.4. (continued).

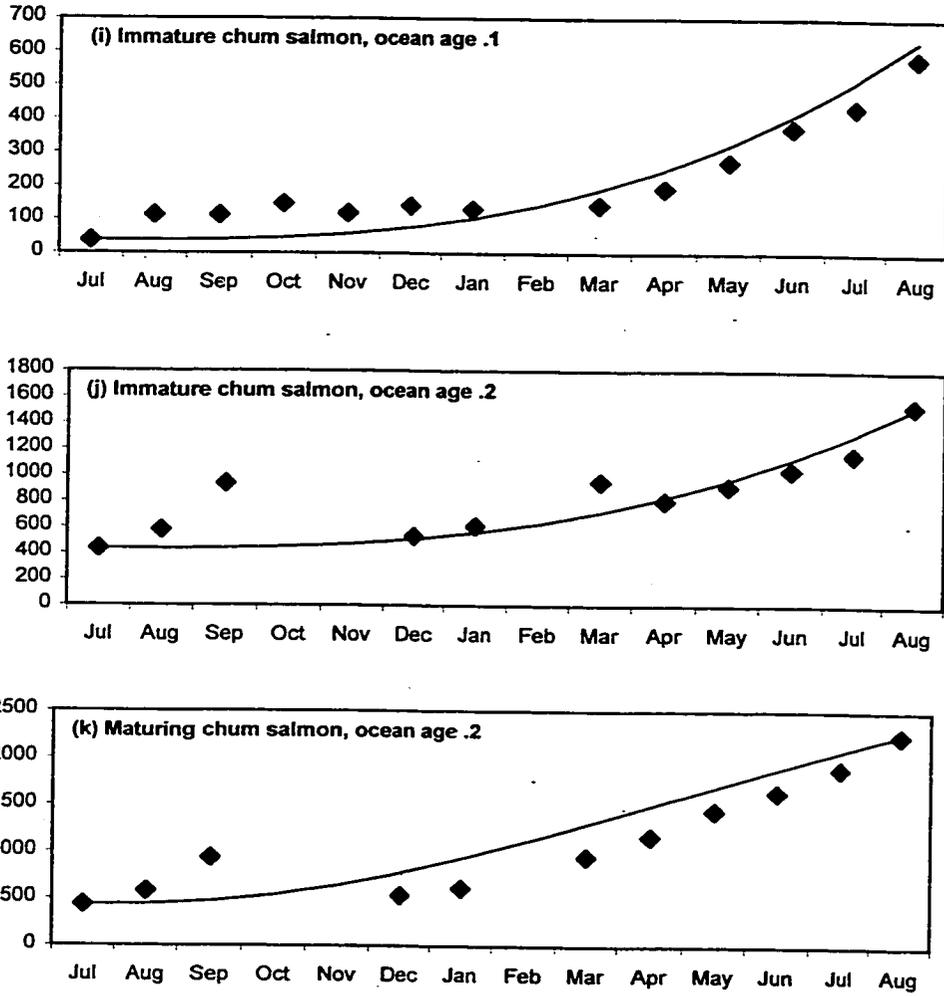


Figure 5.4. (continued).

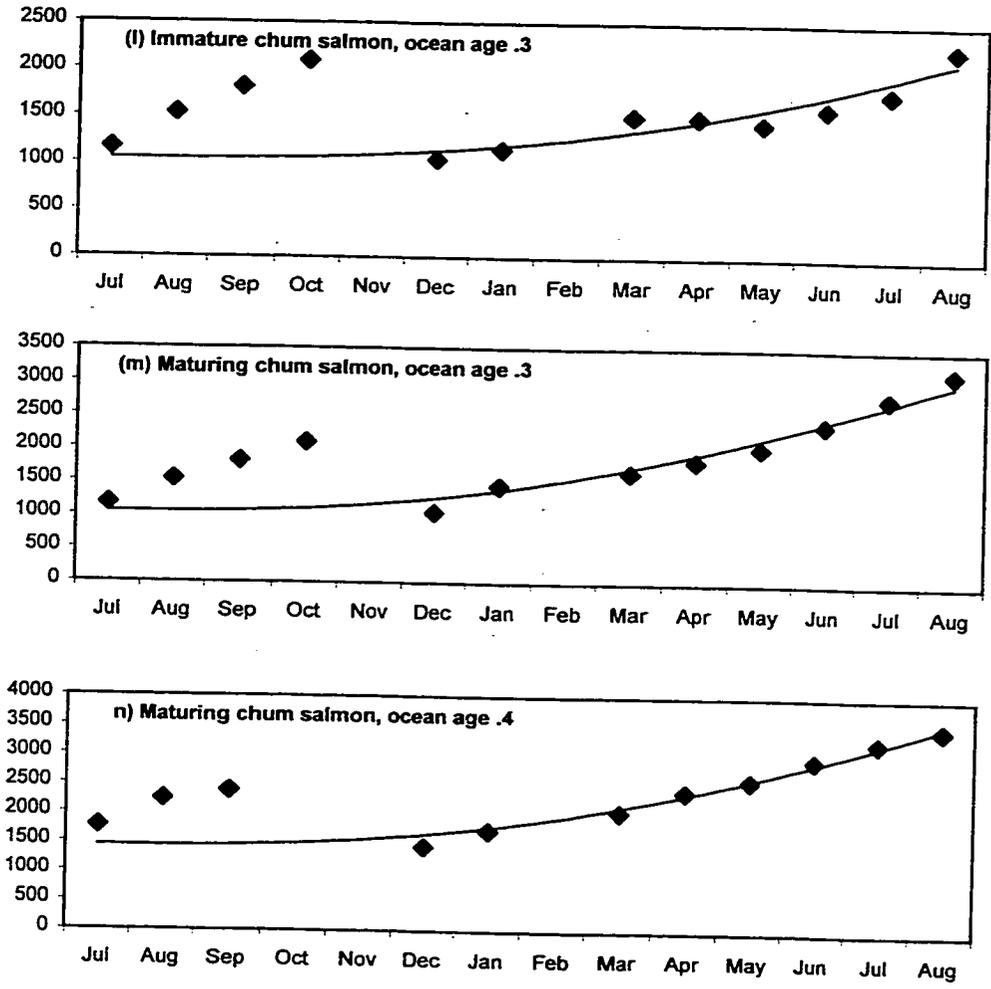


Figure 5.4. (continued).

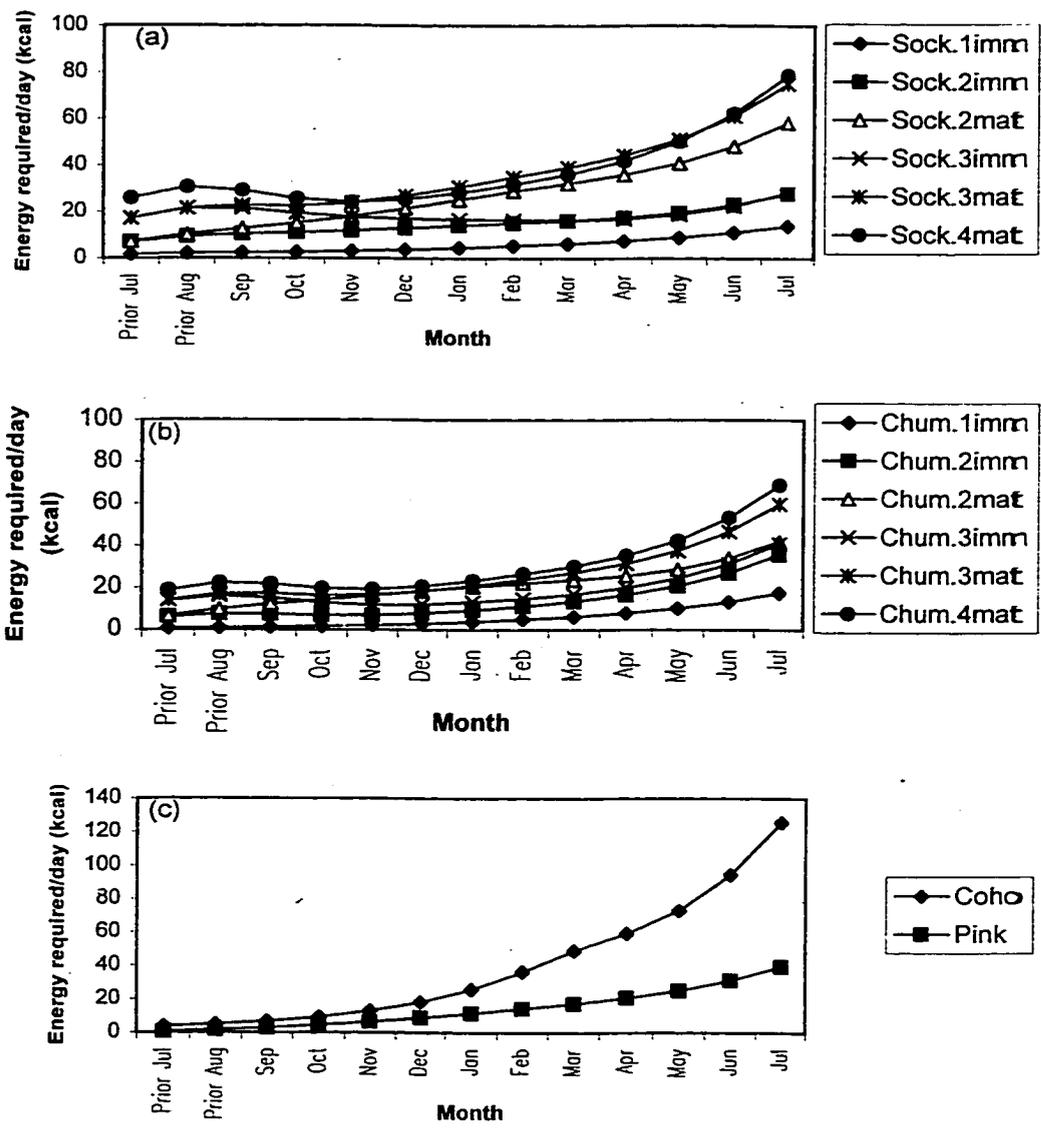


Figure 5.5. Kilocalories of prey required per day, calculated by month and by species group, to maintain growth levels implied by measured increases in body weight.

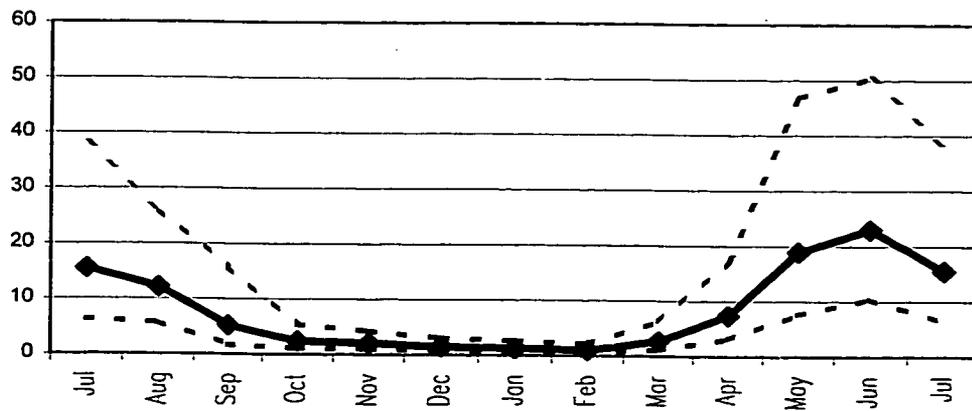


Figure 5.6. Monthly geometric mean of total mesozooplankton biomass per unit ocean surface area (g/m^2) between 0-150m depth, measured at Ocean Station P between 1956-80 . Dotted lines show ± 1 standard deviation of lognormal distribution.

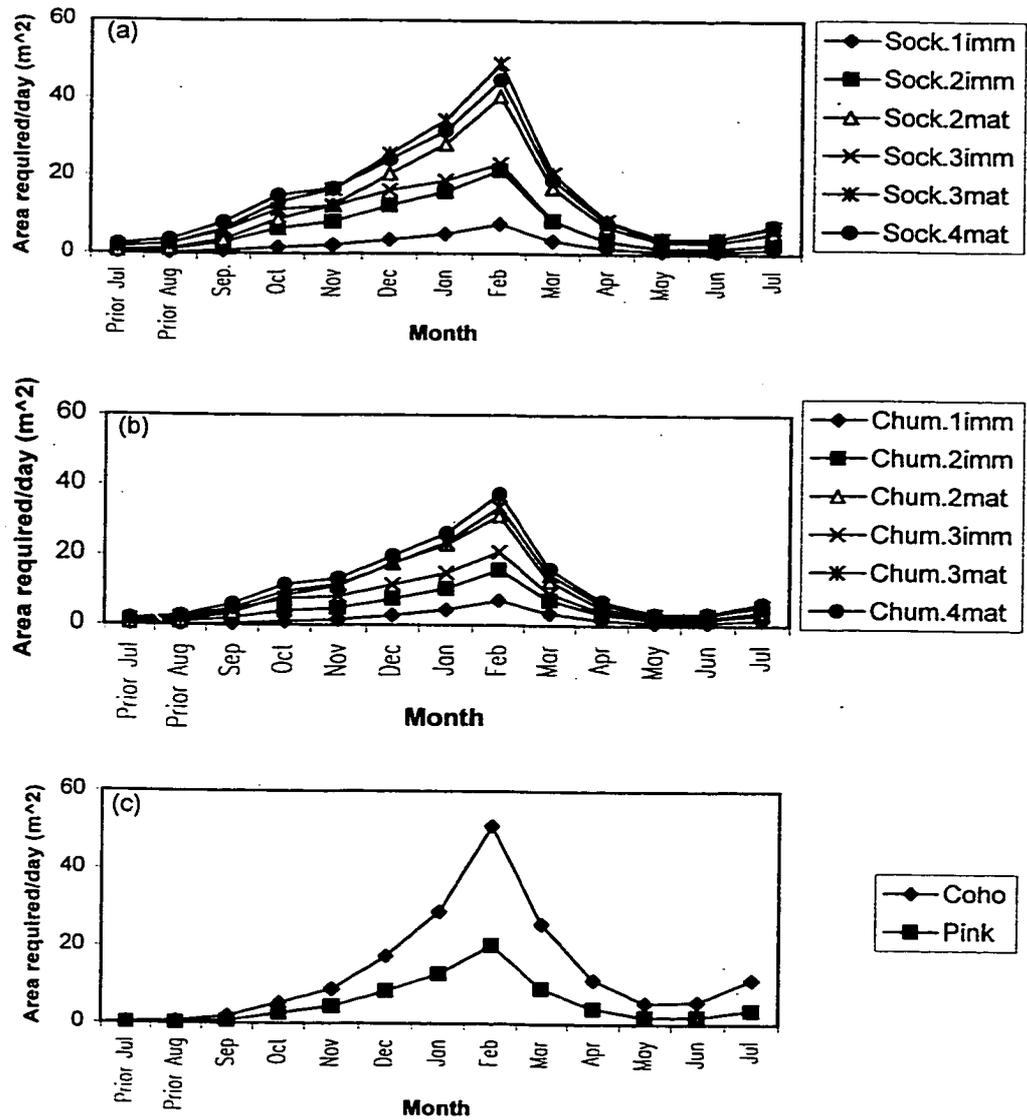


Figure 5.7. Total surface area required to be “emptied” of zooplankton biomass between 0-150m in a single day, to satisfy the dietary requirements of one salmon of each modeled species and age class, by month.

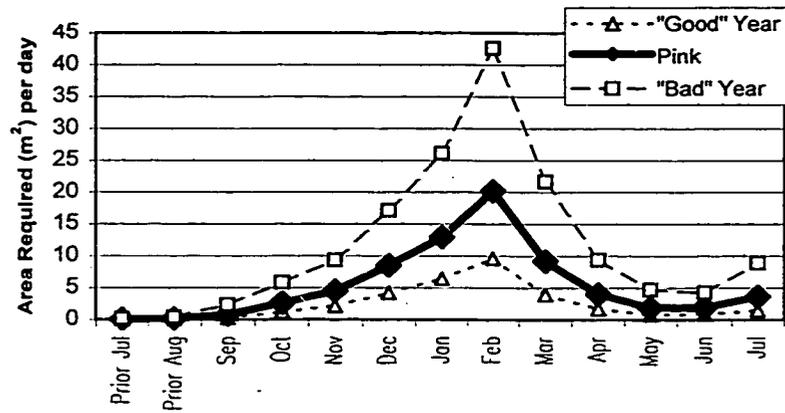


Figure 5.8. Total surface area required to be "emptied" of zooplankton biomass in a single day, to satisfy the dietary requirements of one pink salmon, given that zooplankton density is equal to: (solid line) the long-term monthly geometric mean; (triangles) 1 lognormal standard deviation more than the long-term mean; (squares) 1 lognormal standard deviation less than the long-term-mean.

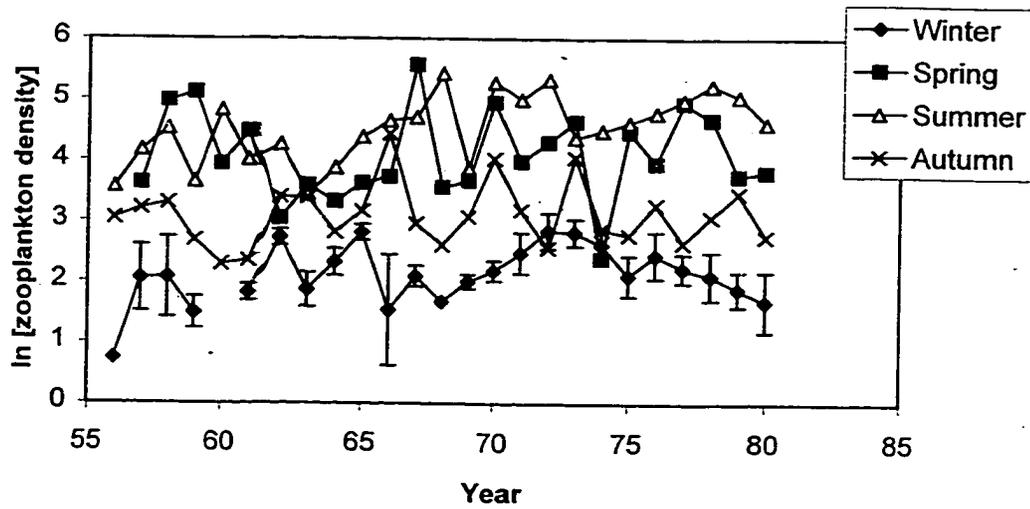


Figure 5.9. $\text{Log}[\text{Zooplankton density (mg/m}^3\text{)}]$, averaged by season and year, 1956-80. Winter = December-February.; Spring = March-May; Summer = June.-August; Autumn = September-November. Error bars show ± 1 standard error of the mean for winter values.

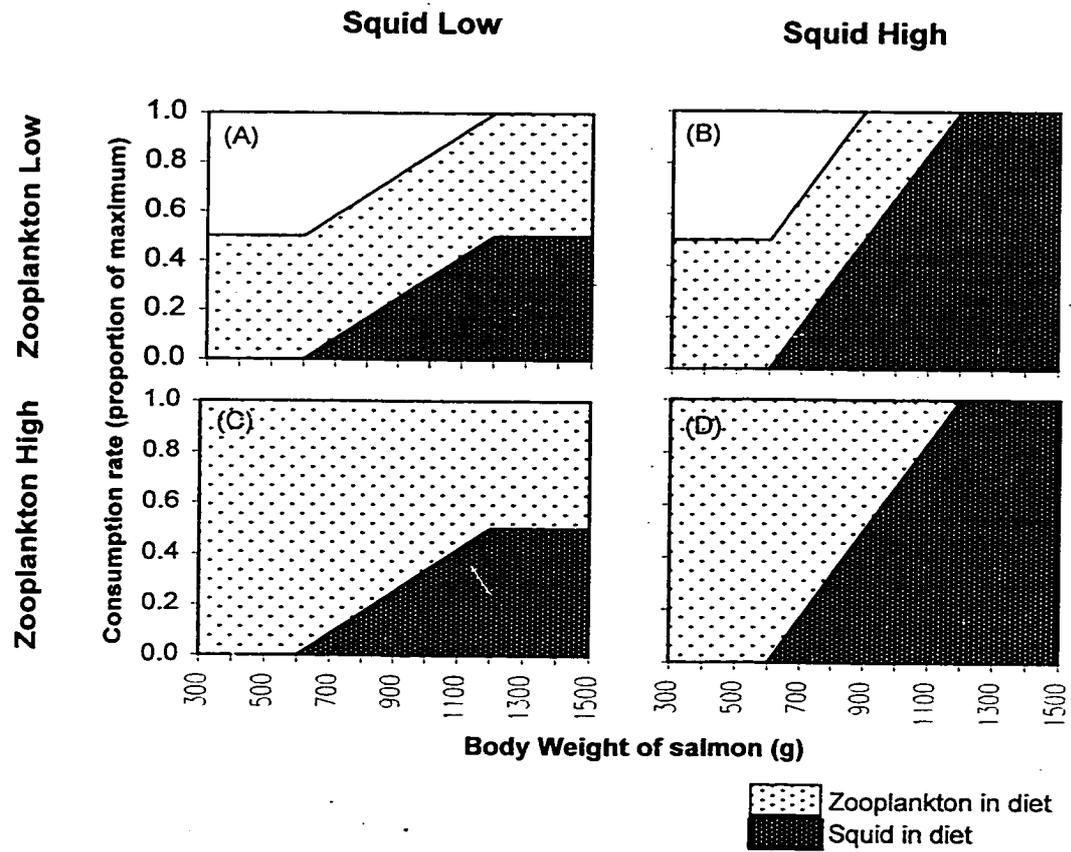


Figure 5.10. Pink salmon diet (proportion of maximum physiological consumption rate) as a function of body weight for four scenarios of differing availability of zooplankton and squid.

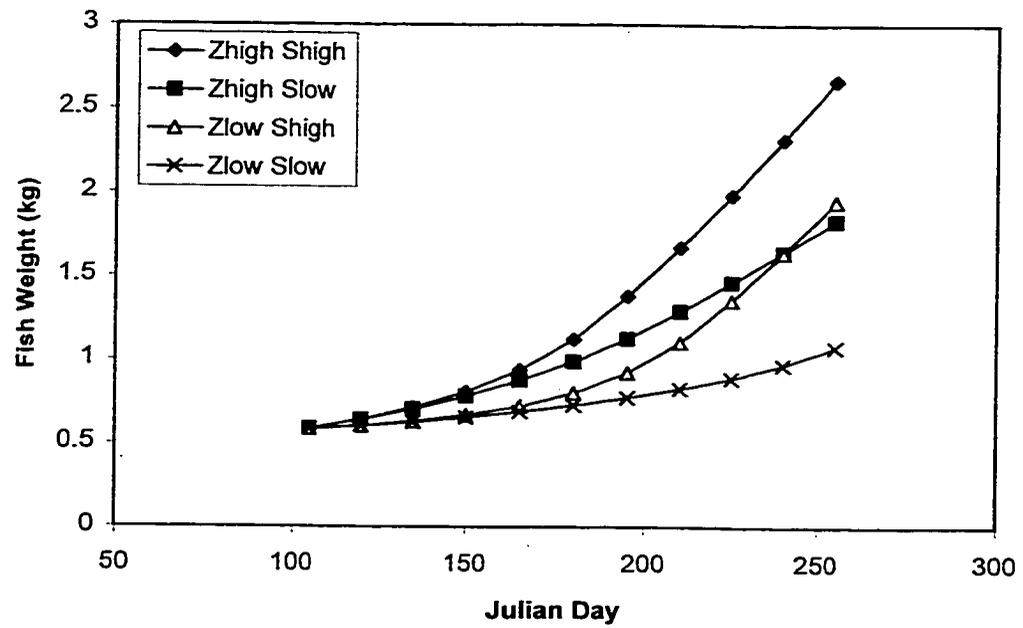


Figure 5.11. Pink salmon body weight, April-August, for a starting April (Julian day 100) body weight of 585 grams, under 4 scenarios of prey availability. Zhigh/low indicates zooplankton availability, while Shigh/low indicates squid availability.

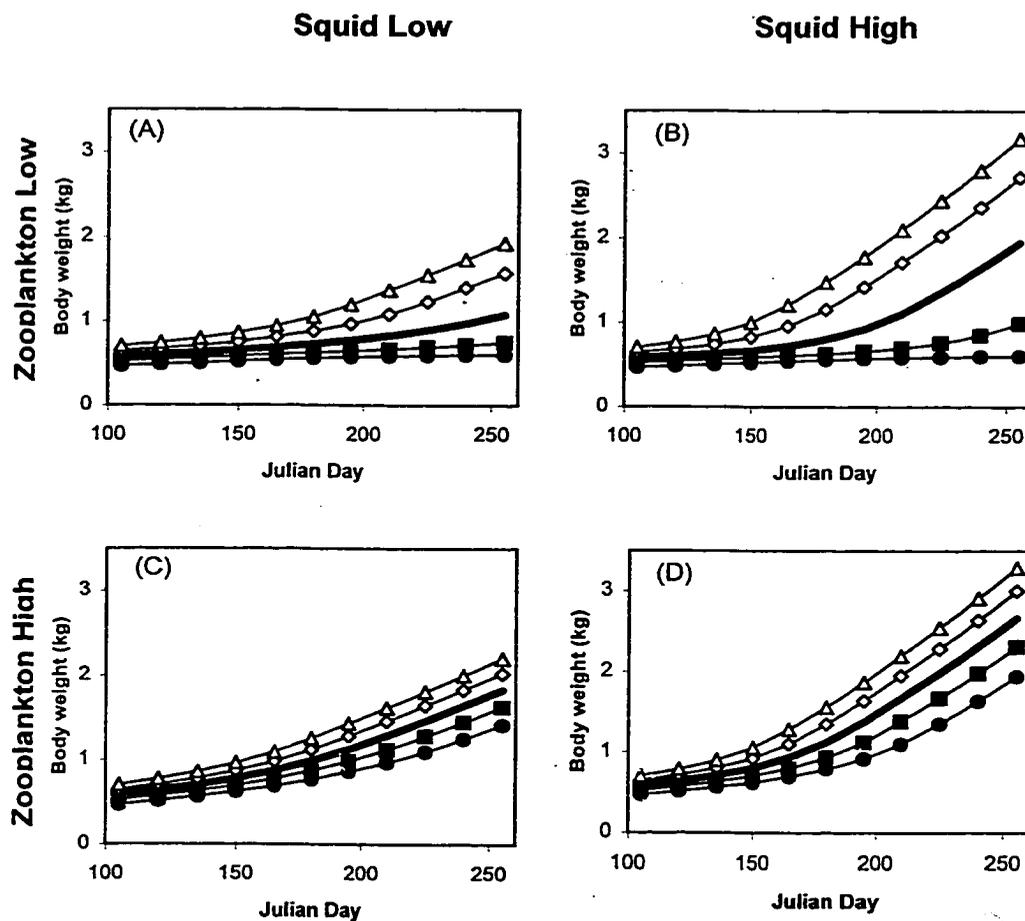


Figure 5.12. Pink salmon body weight, April-August, under 4 scenarios of prey availability, for a starting April (Julian day 100) body weight of: 468g (solid circles); 526g (solid squares); 585g (heavy line); 643g (open diamonds); and 701g (open triangles). Range of starting body weights is +/- 10 and 20 % of base 585g April body weight.

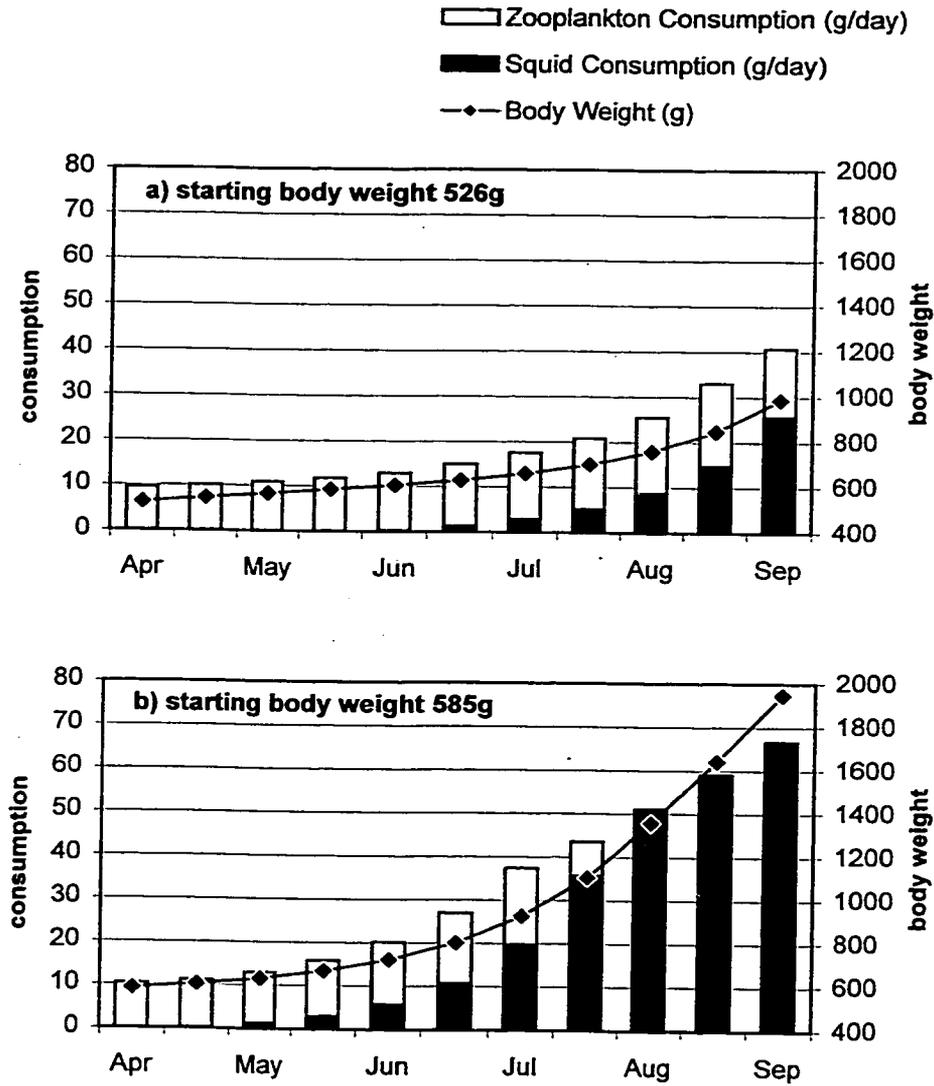


Figure 5.13. Body weight (g) and consumption rate (g/day) of pink salmon of two different starting weights under conditions of low zooplankton, high squid availability.

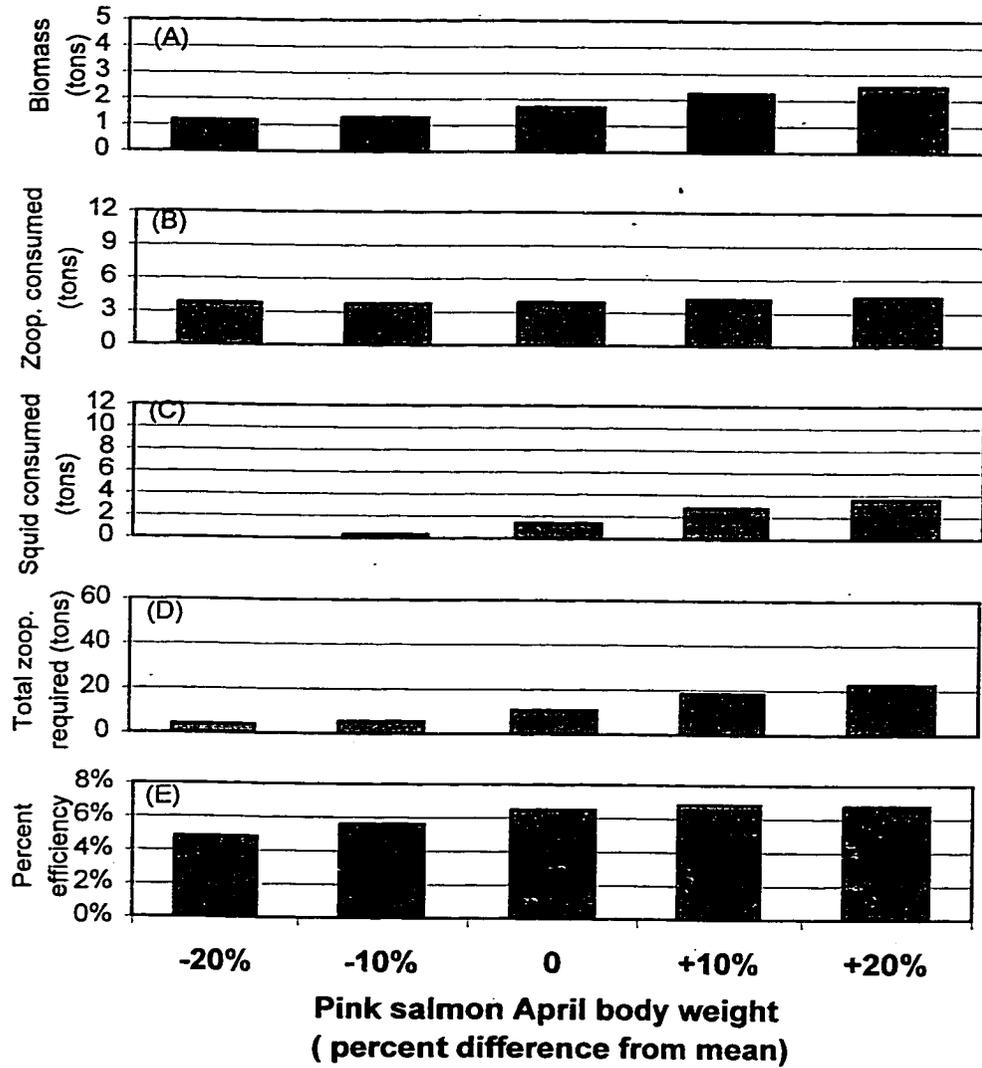


Figure 5.14. Difference in ecosystem effects of changing the starting individual body weight of 1 ton of pink salmon in conditions of low zooplankton/low squid. (A) total August biomass of salmon; (B) total zooplankton consumed; (C) total squid consumed; (D) total zooplankton required by salmon and squid combined; (E) percent efficiency (tons biomass of salmon in August/total zooplankton required).

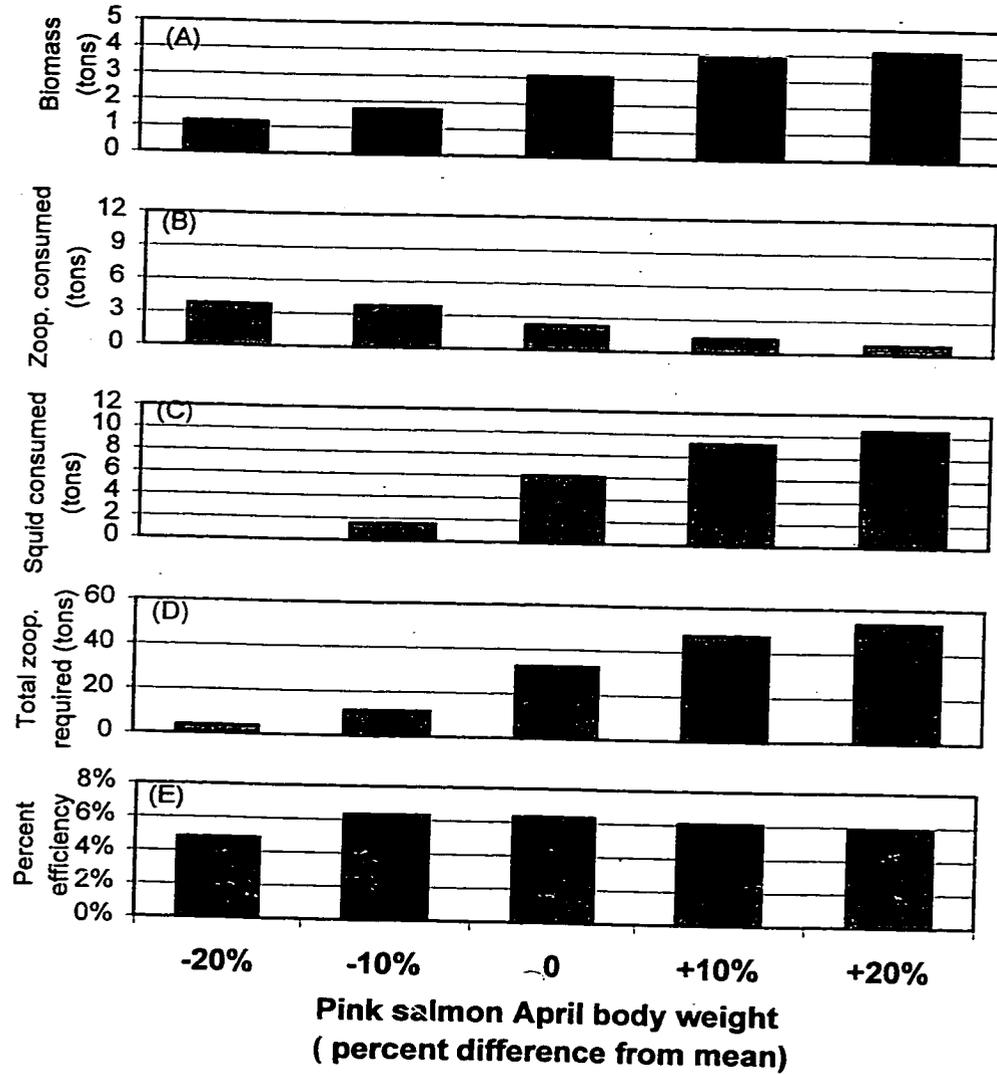


Figure 5.15. Difference in ecosystem effects of changing the starting individual body weight of 1 ton of pink salmon in conditions of low zooplankton/high squid. (A) total August biomass of salmon; (B) total zooplankton consumed; (C) total squid consumed; (D) total zooplankton required by salmon and squid combined; (E) percent efficiency (tons biomass of salmon in August/total zooplankton required).

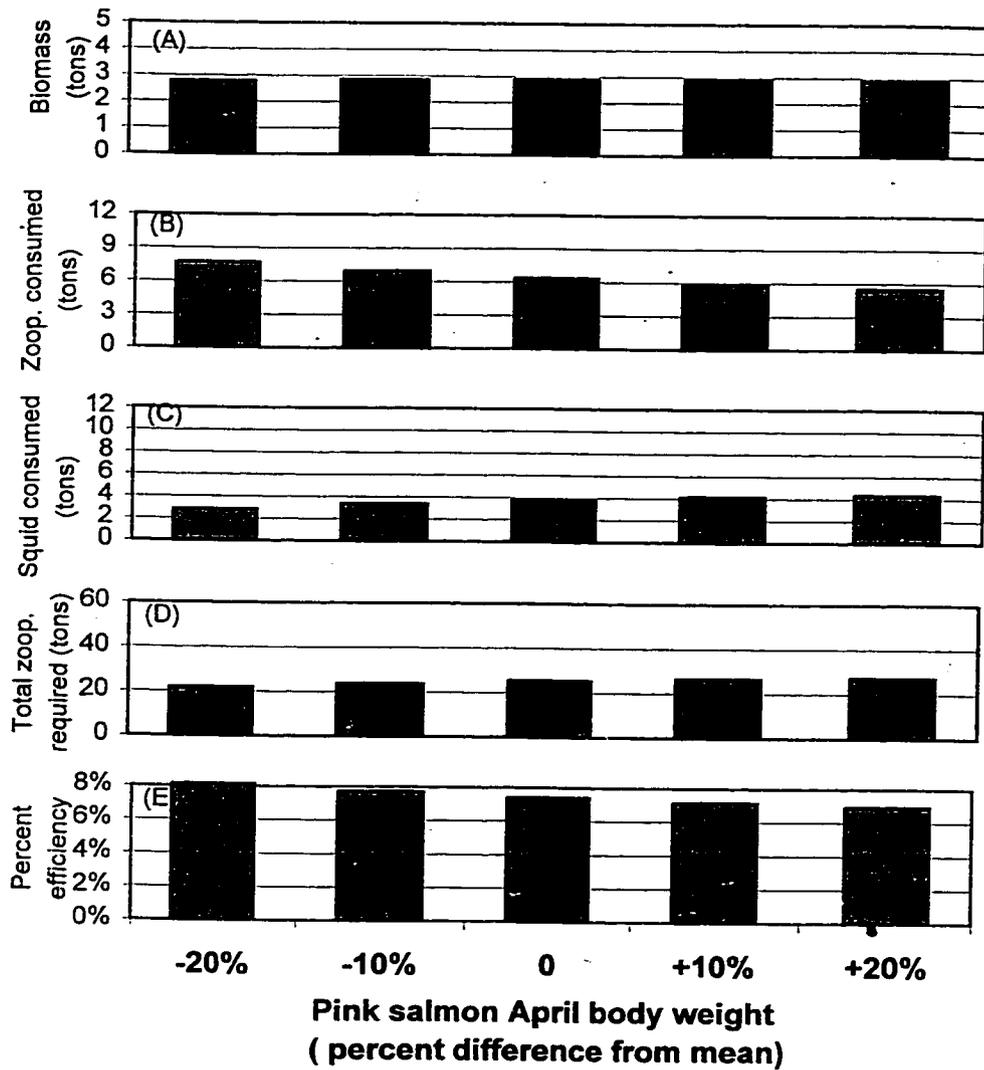


Figure 5.16. Difference in ecosystem effects of changing the starting individual body weight of 1 ton of pink salmon in conditions of high zooplankton/low squid. (A) total August biomass of salmon; (B) total zooplankton consumed; (C) total squid consumed; (D) total zooplankton required by salmon and squid combined; (E) percent efficiency (tons biomass of salmon in August/total zooplankton required).

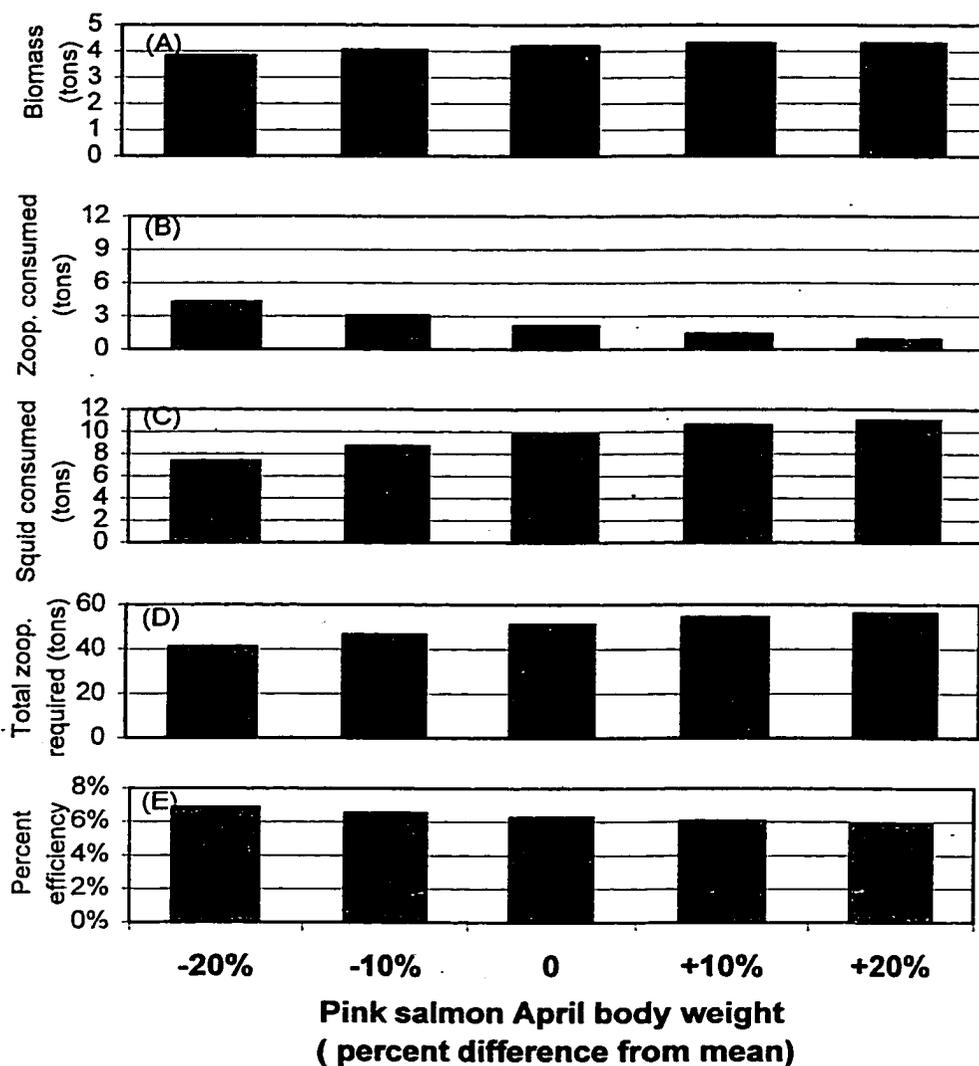


Figure 5.17. Difference in ecosystem effects of changing the starting individual body weight of 1 ton of pink salmon in conditions of high zooplankton/high squid. (A) total August biomass of salmon; (B) total zooplankton consumed; (C) total squid consumed; (D) total zooplankton required by salmon and squid combined; (E) percent efficiency (tons biomass of salmon in August/total zooplankton required).

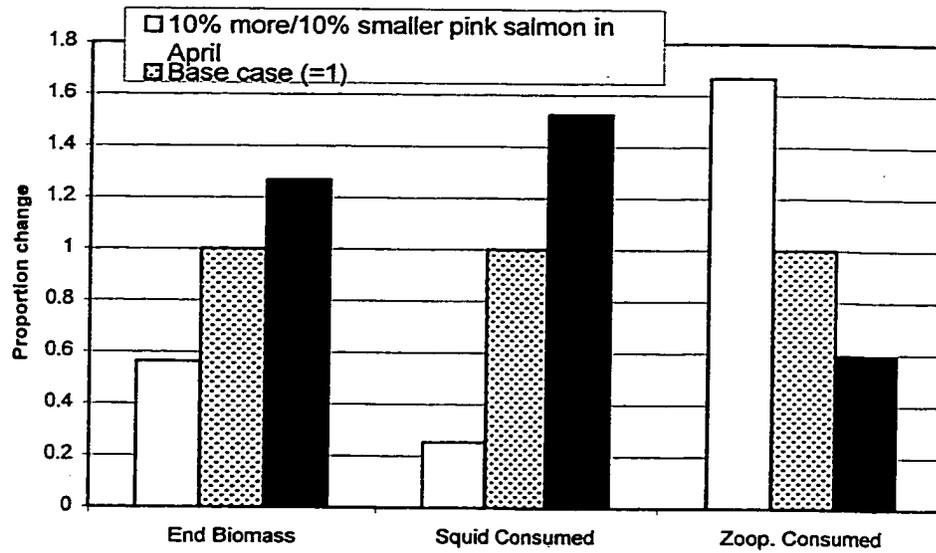


Figure 5.18. Change in final maturing salmon biomass, zooplankton consumed, and squid consumed, resulting from a +/- 10% change in the number of salmon in April of the maturation, if a 10% increase (decrease) in salmon numbers results in a 10% decrease (increase) in April body weight from winter density-dependent processes.

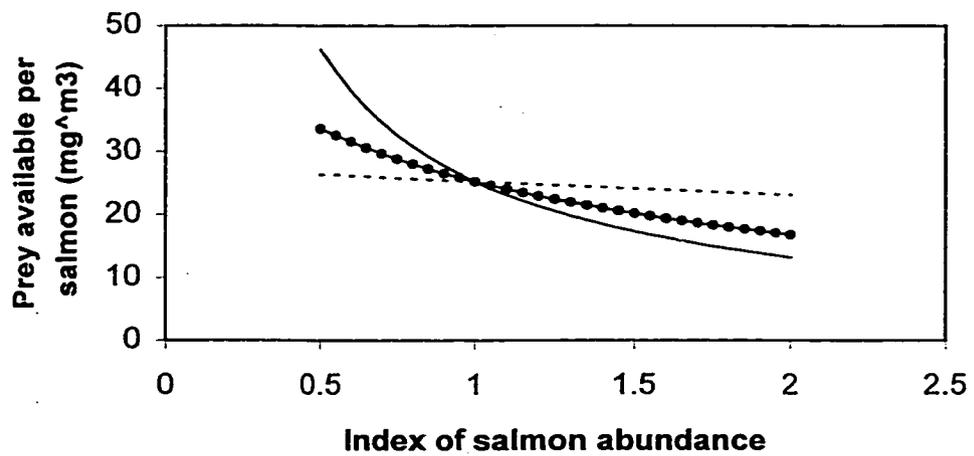


Figure 5.19. Relationship between index of salmon abundance ($N_{\text{predators}}$) and prey available per salmon (D_{avail}) for weak density-dependence ($DD_{\text{index}} = -1$; dashed line), medium density-dependence ($DD_{\text{index}} = 0$; circles) and strong density-dependence ($DD_{\text{index}} = 1$; solid line).

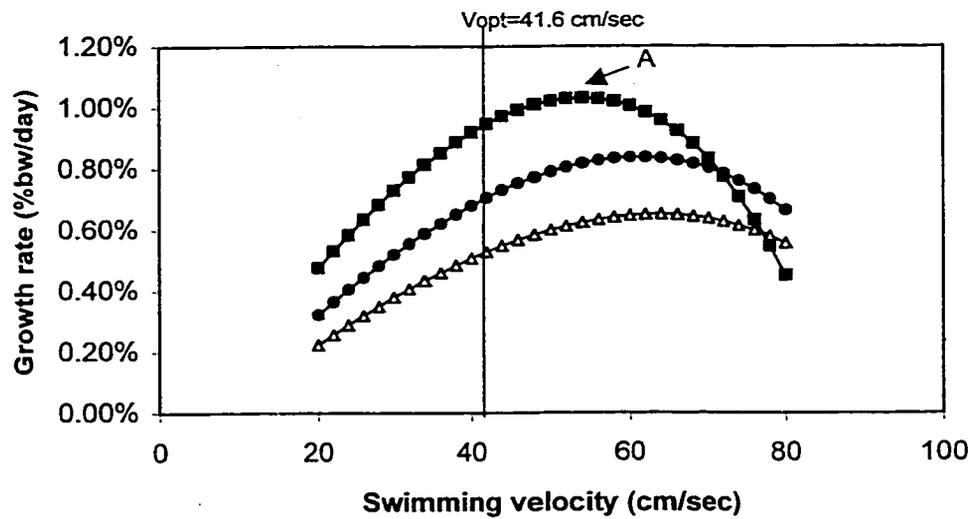


Figure 5.20. Swimming velocity vs. growth rate for strong density dependence ($DD_{index} = 1$) for $N_{predator}$ values of 0.75 (squares), 1.0 (circles) and 1.25 (open triangles). 'A' shows point at which swimming velocity maximizes growth rate for $N_{predator} = 0.75$. c

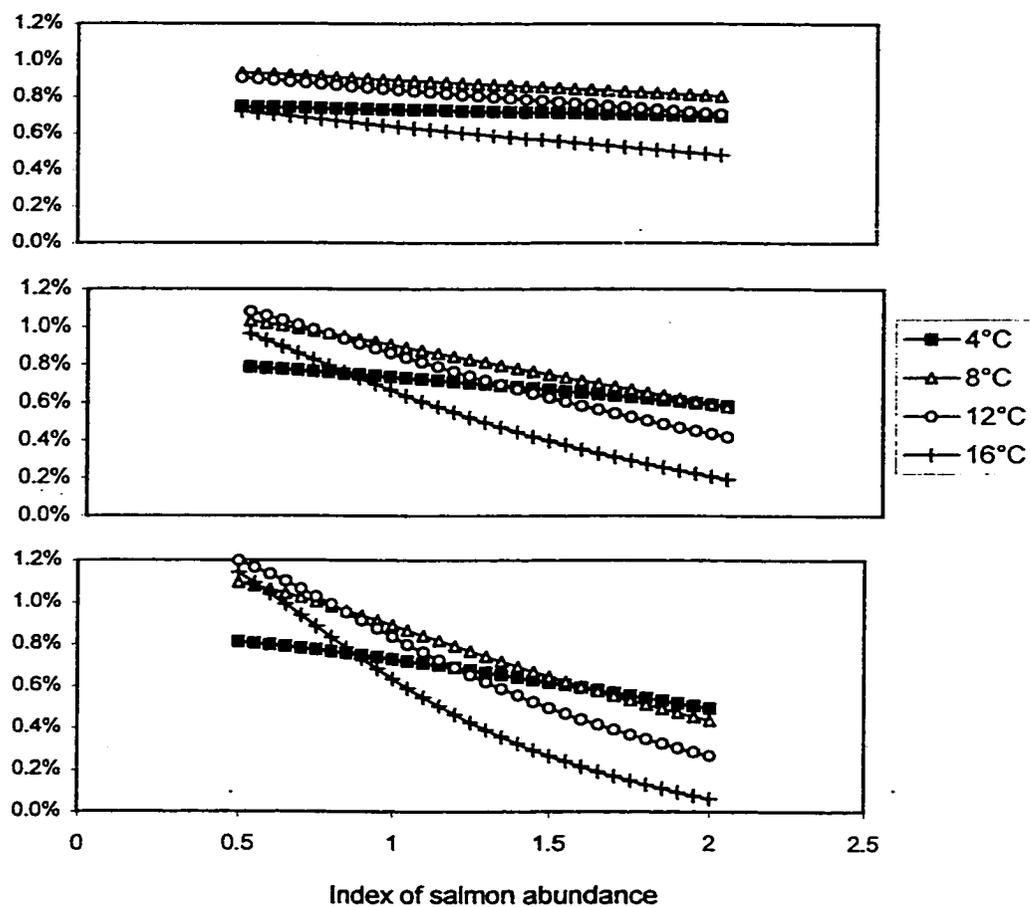


Figure 5.21. Maximum temperature-specific instantaneous growth rate vs. predator abundance for three levels of density-dependence: weak (top graph), medium (middle graph) and strong (bottom graph). Density-dependent curves are shown for 4 different levels of water temperature.

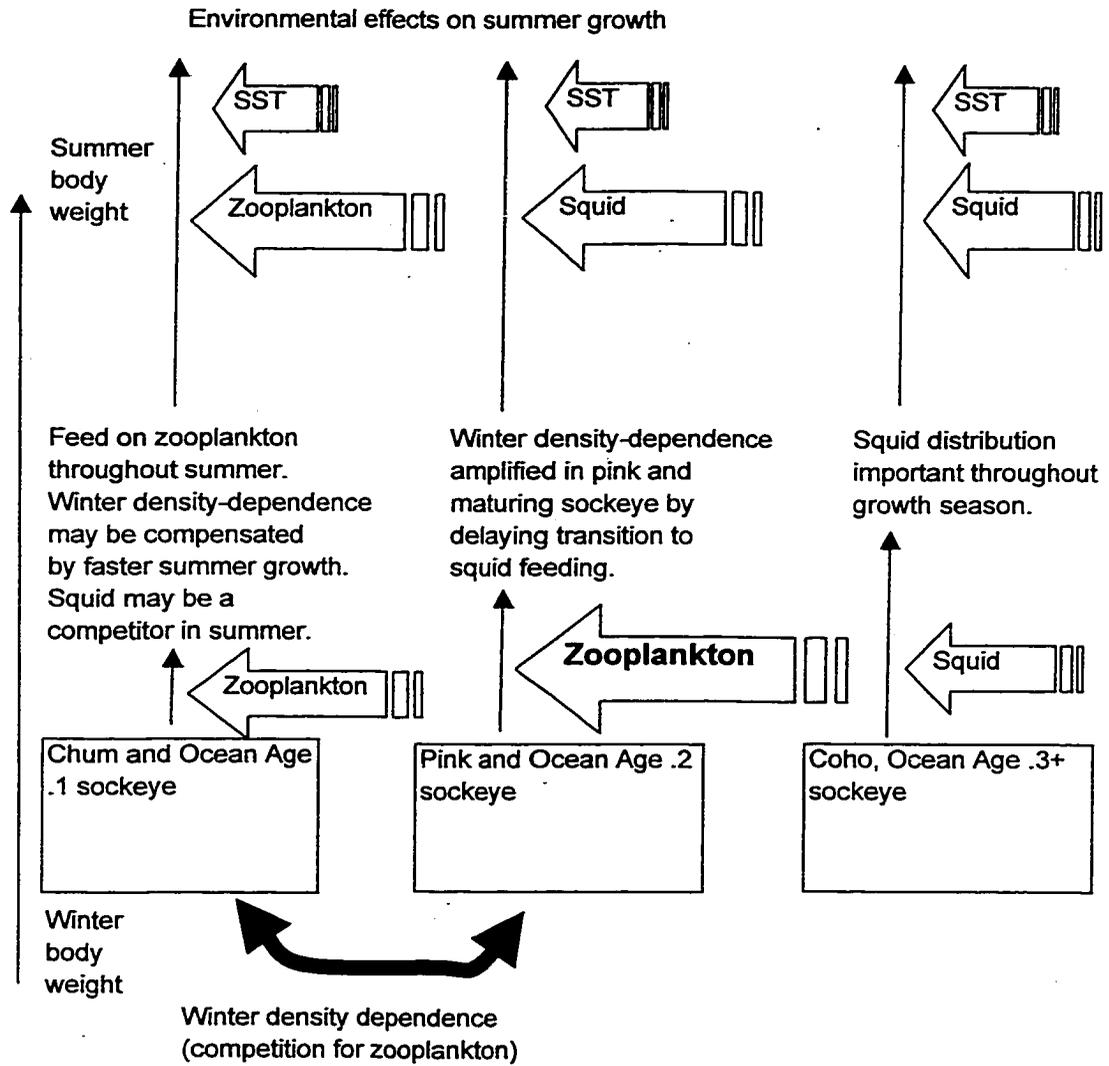


Figure 5.22. A species-specific conceptual model of the factors controlling the ocean growth of salmon, with the size of arrows indicating the relative importance of each factor. See text for details.

Literature Cited

- Adkison, M.D., R.M. Peterman, M.F. Lapointe, D.M. Gillis, and J. Korman. 1996. Alternative models of climatic effects on sockeye salmon, *Oncorhynchus nerka*, productivity in Bristol Bay, Alaska, and the Fraser River, British Columbia. *Fish. Oceanogr.* 5: 137-152.
- Allen, G. H., and W. Aron. 1958. Food of salmonid fishes of the western North Pacific Ocean. Scientific Special Report – Fisheries No. 237, United States Dept. of the Interior, Fish and Wildlife Service, Washington DC. 11 p.
- Allen, T.F.H., and T.W. Hoekstra. 1992. Toward a unified ecology. Columbia University Press, New York. 384 p.
- Allen, T.F.H., and T.B. Starr. 1982. Hierarchy: perspectives for biological Complexity. University of Chicago Press, Chicago.
- Aydin, M., Z. Top, R.A. Fine, and D.B. Olson. 1998. Modification of the intermediate waters in the northeastern subpolar Pacific. *J. Geophys. Res. (C Oceans)* 103: 923-930.
- Bakun, A. 1996. Patterns in the ocean. California Sea Grant Press. 323 p.
- Baumgartner, T.R., A. Soutar, and W. Riedel. 1996. Natural time scales of variability in coastal pelagic fish populations of the California Current over the past 1500 years: response to global climate change and biological interaction. California Sea Grant Biennial Report of Completed Projects, 1992-94: 31-37.
- Beacham, T.D., and C.B. Murray. 1987. Adaptive variation in body size, age, morphology, egg size, and developmental biology of chum salmon (*Oncorhynchus keta*) in British Columbia. *Can. J. Fish. Aquat. Sci.* 44: 244-261.
- Beamish, R.J. 1993. Climate and exceptional fish production off the west coast of North America. *Can. J. Fish. Aquat. Sci.* 50: 2270-2291.
- Beamish, R.J. [ed.]. 1995. Climate change and northern fish populations. *Can. Spec. Publ. Fish Aquat. Sci.* 121.
- Beamish, R.J. 1999. An introduction to the PICES symposium on the ecosystem dynamics in the eastern and western gyres of the subarctic Pacific. *Prog. Oceanogr.* 43: 157-161.
- Beamish, R.J. and C. Mahnken. 1999. Taking the next step in fisheries management. p. 1-22 *in* Ecosystem approaches for fisheries management. University of Alaska Sea Grant AK-SG-99-01.

- Beamish, R.J., D.J. Noakes, G.A. McFarlane, L. Klyashtorin, V.V. Ivanov, and V. Kurashov. 1999. The regime concept and natural trends in the production of Pacific salmon. *Can. J. Fish. Aquat. Sci.* 56: 516-526.
- Beauchamp, D.A., C.M. Baldwin, J.L. Vogel, and C.P. Gubala. 1999. Effects of light, prey size, and turbidity on reaction distances of lake trout (*Salvelinus namaycush*) to salmonid prey. *Can. J. Fish. Aquat. Sci.* 56: 1293-1297.
- Berryman A.A., J. Michalski, A.P. Gutierrez, and R. Arditi. 1995. Logistic theory of food web dynamics. *Ecology* 76: 336-343.
- Bhaskaran, S., F.S.E. Lagerloef, G.H. Born, W.J. Emery, and R.R. Leben. 1993. Variability in the Gulf of Alaska from Geosat altimetry data. *J. Geophys. Res.* 98: 16311-16330.
- Bigler, B.S., D.W. Welch, and J.H. Helle. 1996. A review of size trends among North Pacific salmon (*Oncorhynchus* spp.). *Can. J. Fish. Aquat. Sci.* 53: 455-465.
- Bisbal, G.A. and W.E. McConnaha. 1998. Consideration of ocean conditions in the management of salmon. *Can. J. Fish. Aquat. Sci.* 55: 2178-2186.
- Boyd, P.W., S. Strom, F.A. Whitney, S. Doherty, M.E. Wen, P.J. Harrison, C.S. Wong, and D.E. Varela. 1995a. The NE Subarctic Pacific in winter: 1. Biological standing stocks. *Mar. Ecol. Prog. Ser.* 128: 11-24.
- Boyd, P.W., F.A. Whitney, P.J. Harrison, and C.S. Wong, CS. 1995b. The NE Subarctic Pacific in winter: 2. Biological rate processes. *Mar. Ecol. Prog. Ser.* 128: 25-34.
- Brandt, S.B. 1993. The effect of thermal fronts on fish growth: A bioenergetics evaluation of food and temperature. *Estuaries* 16: 142-159.
- Breck, J.E. 1993. Foraging theory and piscivorous fish: are forage fish just big zooplankton? *Trans. Am. Fish. Soc.* 122: 902-911.
- Brodeur, R.D. 1990. A synthesis of the food habits and feeding ecology of salmonids in marine waters of the North Pacific. Fisheries Research Institute, University of Washington, Seattle, WA. 38 p.
- Brodeur, R.D., and D.M. Ware. 1992. Long-term variability in zooplankton biomass in the subarctic Pacific Ocean. *Fish. Oceanogr.* 1: 32-39.
- Brodeur, R.D., and D.M. Ware. 1995. Interdecadal variability in distribution and catch rates of epipelagic nekton in the Northeast Pacific Ocean. p. 329-356 *in*: R.J. Beamish [ed.] *Climate change and northern fish populations*, National Research Council of Canada, Ottawa.
- Brodeur, R.D., B.W. Frost, S.R. Hare, R.C. Francis, and W.J. Ingraham, Jr. 1996. Interannual variations in zooplankton biomass in the Gulf of

- Alaska, and covariation with California Current zooplankton biomass
CALCOFI Rep. 37: 80-99.
- Brodeur, R., S. McKinnell, K. Nagasawa, W. Pearcy, V. Radchenko, and S. Takagi. 1999. Epipelagic nekton of the North Pacific Subarctic and Transition Zones. *Prog. Oceanogr.* 43: 365-398.
- Burgner, R.L. 1991. Life history of sockeye salmon (*Oncorhynchus nerka*). p. 1-118 *in*: C. Groot and L. Margolis [eds.] *Pacific Salmon Life Histories*. University of British Columbia Press, Vancouver, BC.
- Carlson, H.R., E.V. Farley, K.W. Myers, E.C. Martinson, J.E. Pohl, and N.M. Weemes. 1998. Survey of salmon in the southeastern Bering Sea, Gulf of Alaska, and northeastern Pacific Ocean, April-May 1998. Auke Bay Laboratory, Alaska Fisheries Science Center, National Marine Fisheries Service, NOAA, Juneau, AK. 33 p.
- Casella, G., and R.L. Berger. 1990. *Statistical inference*. Duxbury Press, Belmont, CA. 650 p.
- Chelton, D.B., and R.E. Davis. 1982. Monthly mean sea-level variability along the west coast of North America. *J. Phys. Oceanogr.* 12: 757-784.
- COADS (Comprehensive Ocean-Atmosphere Data Set). 1994. Climate Research Program, Boulder, Colorado.
- Conversi, A., and S. Hameed. 1997. Evidence for quasi-biennial oscillations in zooplankton biomass in the subarctic Pacific. *J. Geophys. Res. (C Oceans)*: 102: 15659-15665.
- Conversi, A., and S. Hameed. 1998. Common signals between physical and atmospheric variables and zooplankton biomass in the subarctic Pacific. *ICES Journal of Marine Science* 55: 739-747.
- Cooney, R.T. 1993. A theoretical evaluation of the carrying capacity of Prince William Sound, Alaska, for juvenile Pacific salmon. *Fish. Res.* 18: 77-87.
- Cooney, R.T., and R.D. Brodeur. 1998. Carrying capacity and North Pacific salmon production: Stock-enhancement implications. *Bull. Mar. Sci.* 62: 443-464.
- Cooney, R.T., T.M. Willette, S. Sharr, D. Sharp, and J. Olsen. 1995. The effect of climate on North Pacific pink salmon (*Oncorhynchus gorbuscha*) production: examining some details of a natural experiment. p. 475-482 *in*: R.J. Beamish [ed.] *Climate change and northern fish populations*. National Research Council of Canada, Ottawa.
- Cox, S.P., and S.G. Hinch. 1997. Changes in size at maturity of Fraser River sockeye salmon (*Oncorhynchus nerka*) and associations with temperature. *Can. J. Fish. Aquat. Sci.* 54: 1159-1165.

- Cox, D.R., and E.J. Snell. 1989. Analysis of binary data. Chapman and Hall, London. 236 p.
- Davis, N.D., K.Y. Aydin, and Y. Ishida. 1998a. Diel feeding habits and estimates of prey consumption of sockeye, chum and pink salmon in the Bering Sea in 1997. (N. Pac. Andr. Fish. Comm. Doc. 363). FRI-UW-9816. Fish. Res. Inst., Univ. of Washington, Seattle. 24 p.
- Davis, N.D., K.W. Myers, and Y. Ishida. 1998b. Caloric value of high-seas salmon prey organisms and simulated salmon ocean growth and prey consumption. N. Pac. Anadr. Fish. Comm. Bull. 1: 146-162.
- Davis, N.D., K.Y. Aydin, and Y. Ishida. In Press. Diel feeding habits of sockeye, pink and chum salmon in the central Bering Sea. N. Pac. Andr. Fish. Comm. Bull 2.
- DFO Circular. Commercial catch statistics as prepared by the Department of Fisheries and Oceans (DFO), Canada. Data provided by the British Columbia Salmon Marketing Council, Vancouver, British Columbia.
- Didenko, V.D. 1990. Prospects of fishery for the squid *Beryteuthis anonychus* in the north-eastern Pacific. p. 82-83 in: Vth All-USSR Conference on Commercial Invertebrates, Abstract of Communications, Minsk-Naroch.
- Dinniman, M.S., and M.M. Rienecker. 1999. Frontogenesis in the North Pacific oceanic frontal zones—a numerical simulation. J. Phys. Oceanogr. 29: 537-559.
- Dodimead, A.J., F. Favorite, and T. Hirano. 1963. Salmon of the North Pacific Ocean—Part II. Review of oceanography of the Subarctic Pacific Region. Int. N. Pac. Fish. Comm. Bull. 13. 195 p.
- Dunback, R.LeB., and D.M. Ware. 1987. Energy constraints and reproductive trade-offs determining body size in fishes. p. 191-218 in: P. Calow [ed.] Evolutionary Physiological Ecology. Cambridge Univ. Press, Cambridge, UK.
- Evans, G.T., and J.S. Parslow. 1985. A model of annual plankton cycles. Biol. Oceanogr. 3: 327-347.
- Faculty of Fisheries, Hokkaido University. 1998. Data Record of Oceanographic Observations and Exploratory Fishing 41.
- Favorite, F., A.J. Dodimead, and K. Nasu. 1976. Oceanography of the Subarctic Pacific Region, 1960-71. Int. N. Pac. Fish. Comm. Bull. 33. 187 p.
- Favorite, F., and J.F. Hebard. 1961. Oceanography. Int. N. Pac. Fish. Comm. Annual Report 1960: 81-88.
- Favorite, F. and T. Laevastu. 1979. A study of the ocean migrations of sockeye salmon and estimation of the carrying-capacity of the North Pacific

- Ocean using a dynamical salmon ecosystem model (NOPASA). Northwest and Alaska Fisheries Center, NMFS, Seattle, WA. 47 p.
- Francis, R.C., K.Y. Aydin, R.L. Merrick, and S. Bollens. 1999. Modeling and management of the Bering Sea ecosystem. p. 409-434 *in* T.R. Loughlin and K. Ohtani [eds.] Dynamics of the Bering Sea. University of Alaska Seagrant, Fairbanks, Alaska.
- Francis, R.C., and S.R. Hare. 1994. Decadal-scale regime shifts in the large marine ecosystems of the North-east Pacific: A case for historical science. *Fish. Oceanogr.* 3: 279-291.
- Francis, R.C., S.R. Hare, A.B. Hollowed, and W.S. Wooster. 1998. Effects of interdecadal climate variability on the oceanic ecosystems of the NE Pacific. *Fish. Oceanogr.* 7: 1-21.
- Freeland, H., K. Denman, C.S. Wong, F. Whitney, and R. Jacques. 1998. Evidence of change in the winter mixed layer in the northeast Pacific Ocean. *Deep-sea Res. I.* 44: 2117-2129.
- Frost, B.W. 1987. Grazing control of phytoplankton stock in the open subarctic Pacific Ocean: A model assessing the role of mesozooplankton, particularly the large calanoid copepods *Neocalanus* spp. *Mar. Ecol. (Prog. Ser.)* 39: 49-68.
- Frost, B.W. 1993. A modelling study of processes regulating plankton standing stock and production in the open subarctic Pacific Ocean. *Prog. Oceanogr.* 32: 17-56.
- Gargett, A.E. 1997. The optimal stability 'window': A mechanism underlying decadal fluctuations in North Pacific salmon stocks? *Fish. Oceanogr.* 6: 109-117.
- Grimm, V., and C. Wissel. 1997. Babel, or the ecological stability discussions: an inventory and analysis of terminology and a guide for avoiding confusion. *Oecologia* 109: 323-334.
- Groot, C., and L. Margolis [eds.] 1991. Pacific salmon life histories. University of British Columbia Press, Vancouver, BC. 564 p.
- Hameed, S., and A. Conversi. 1995. Signals in the interannual variations of zooplankton biomass in the Gulf of Alaska. p. 21-27 *in* Holocene cycles: climate, sea levels, and sedimentation. Coastal Education and Research Foundation, Charlottesville.
- Hare, S.R. and N.J. Mantua. 2000. Empirical evidence for North Pacific regime shifts in 1977 and 1989. *Prog. Oceanogr.* 47: 103-146.
- Hare, S.R., N.J. Mantua, and R.C. Francis. 1999. Inverse production regimes: Alaska and West Coast Pacific salmon. *Fisheries* 24: 6-15.

- Hartt, A.C., and M.B. Dell. 1986. Early oceanic migrations and growth of juvenile Pacific salmon and steelhead trout. *Int. N. Pac. Fish. Comm. Bull.* 46: 109 p.
- Hastie, T.J. 1993. Generalized additive models. p. 249-307. *in*: J.M. Chambers and T.J. Hastie [eds.] *Statistical Models in S*, Chapman and Hall, London.
- Hastie, T., and R. Tibshirani. 1990. *General additive models*. Chapman and Hall, London.
- Healey, M.C. 1987. The adaptive significance of age and size at maturity in female sockeye salmon (*Oncorhynchus nerka*). p. 110-117 *in* H.D. Smith, L. Margolis and C.C. Wood [eds.] *Sockeye salmon (Oncorhynchus nerka) population biology and future management*. *Can. Spec. Publ. Fish. Aquat. Sci.* 96.
- Healey, M.C., and W.R. Heard. 1984. Inter- and intra-population variation in the fecundity of chinook salmon (*Oncorhynchus tshawytscha*) and its relevance to life history theory. *Can. J. Fish. Aquat. Sci.* 41: 476-483.
- Hewett, S.W., and T.B. Johnson. 1992. *Fish Bionergetics*. University of Wisconsin Sea Grant.
- Higgs, D.A., J.S. Macdonald, C.D. Levings, and B.S. Dosanjh. 1995. Nutrition and feeding habits in relation to life history stage. p. 159-315 *in*: C. Groot, L. Margolis & W.C. Clarke (ed.) *Physiological ecology of Pacific salmon*, Univ. British Columbia Press, Vancouver, BC.
- Hinch, S.G., M.C. Healey, R.E. Diewert, K.A. Thomson, R. Hourston, M.A. Henderson, and F. Juanes. 1995. Potential effects of climate change on the marine growth and survival of Fraser River sockeye salmon. *Can. J. Fish. Aquat. Sci.* 52: 2651-2659.
- Hollowed, A.B., S.R. Hare, and W.S. Wooster. 1998. Pacific - basin climate variability and patterns of northeast Pacific marine fish production. p. 89-104 *in* G. Holloway, P. Muller, and D. Henderson, [eds.] *Proceedings of the 10th 'Aha Huliko'a Hawaiian winter workshop on biotic impacts of extratropical climate variability in the Pacific, January 26-29, 1998*. SOEST Special Publication.
- Hollowed, A.B., and W.S. Wooster. 1992. Variability of winter ocean conditions and strong year classes of northeast Pacific groundfish. *ICES Mar. Sci. Symp.* 195: 433-444.
- IGOSS (Integrated Global Ocean Services System Products Bulletin). 2000. *Joint WMO/IOC Technical Commission for Oceanography and Marine Meteorology*.

- Ikeda, T. 1972. Chemical composition and nutrition of zooplankton in the Bering Sea. p. 433-442 in A.Y. Takenouti [ed.] Biological Oceanography of the northern Pacific Ocean. Idemitsu Shoten, Tokyo.
- Ingraham, W.J. Jr., C.C. Ebbesmeyer, and R.A. Hinrichsen. 1998. Imminent climate and circulation shift in northeast Pacific Ocean could have major impact on marine resources. *Eos Trans. Am. Geophys. Union.* 79: 16.
- Ishida, T. 1966. Salmon of the North Pacific Ocean—Part III. A review of the life history of North Pacific salmon 2. Pink salmon in the far east. *Int. N. Pac. Fish. Comm. Bull.* 18: 29-38.
- Ishida, Y., S. Ito, M. Kaeriyama, S. McKinnell, and K. Nagasawa. 1993. Recent changes in age and size of chum salmon (*Oncorhynchus keta*) in the North Pacific Ocean and possible causes. *Can. J. Fish. Aquat. Sci.* 50: 290-295.
- Ishida, Y., S. Ito, Y. Ueno, and J. Sakai. 1998. Seasonal growth patterns of Pacific salmon (*Oncorhynchus* spp.) in offshore waters of the North Pacific Ocean. *N. Pac. Anadr. Fish. Comm. Bull.* 1: 66-80.
- Ito, J. 1964. Food and feeding habit of Pacific salmon (Genus *Oncorhynchus*) in their oceanic life. *Bull. Hokkaido. Reg. Fish. Res. Lab.* 29: 85-97. Translated as *Fish. Res. Bd. Canada Translation Series No. 1309* (1969).
- Jefferts, K. 1988. Zoogeography of cephalopods in the north-eastern Pacific Ocean. *Bull. Ocean Res. Inst. Univ. Tokyo* 26: 123-157.
- Jobling, M. 1987. Influences of food particle size and dietary energy content on patterns of gastric evacuation in fish: test of a physiological model of gastric emptying. *J. Fish. Biol.* 30: 299-314.
- Kaeriyama, M. 1996a. Changes in body size and age at maturity of a chum salmon, *Oncorhynchus keta*, population released from Hokkaido in Japan. National Salmon Hatchery, 2-2 Nakonoshima, Toyohira-ku, Sapporo, 062 Japan. (*N. Pac. Anadr. Fish. Comm. Doc* 208). 9 p.
- Kaeriyama, M. 1996b. Effects of population density and habitat environment on life history strategy and migration of juvenile (*Oncorhynchus nerka*) and chum salmon (*O. keta*). *Sci. Rep. Hokkaido Salm. Hatch.* 50: 101-111.
- Kaeriyama, M. 1996c. Population dynamics and stock management of hatchery-reared salmon in Japan. *Bull. Natl. Res. Inst. Aquacult. Suppl.* 2: 11-15.
- Kaeriyama, M., M. Nakamura, M. Yamaguchi, H. Ueda, G. Anma, S. Takagi, K.Y. Aydin, R.V. Walker, and K.W. Myers. In Press. Feeding ecology of sockeye and pink salmon in the Gulf of Alaska. *N. Pac. Anadr. Fish. Comm. Bull.* 2.

- Kaeriyama, M, S. Urawa, and M. Fukuwaka. 1995. Variation in body size, fecundity, and egg size of sockeye and kokanee salmon, *Oncorhynchus nerka*, released from hatchery. Sci. Rep. Hokkaido Salm. Hatch. 49: 1-9.
- Kashiwai, M. 1995 History of carrying capacity concept as an index of ecosystem productivity (review) Bull. Hokkaido Natl. Fish. Res. Inst. 59: 81-101.
- Kelly, K.A., M.J. Caruso, and J.A. Austin. 1993. Wind-forced variations in sea surface height in the northeast Pacific Ocean. J. Phys. Oceanogr. 23: 2390-2411.
- Kruse, G.H. 1998. Salmon run failures in 1997-1998: a link to anomalous ocean conditions? Alaska Fish. Res. Bull. 5: 55-63.
- Kubodera, T., W.G. Pearcy, K. Murakami, T. Kobayashi, J. Nakata, and S. Mishima. 1983. Distribution and abundance of squids caught in surface gillnets in the subarctic Pacific, 1977-1981. Memoirs of the Faculty of Fisheries, Hokkaido University 30: 1-49.
- Kubodera, T., and K. Shimazaki. 1989. Cephalopods from the stomach contents of the pomfret (*Brama japonica* Hilgendorf) caught in surface gillnets in the northern North Pacific. Journal of Cephalopod Biology 1: 71-83.
- Lagerloef, G.S.E. 1995. Interdecadal variations in the Alaska Gyre. J. Phys. Oceanogr. 25: 2242-2258.
- Lapashina, V.I. 1988. On the feeding of the squid *Berryteuthis anonychus* Pearcy and Voss from the area of the north-eastern Pacific. pp. 1-5, Deposited MS, Dep VINITI 25.10.88.
- LeBrasseur, R.J. 1966. Stomach contents of salmon and steelhead trout in the northeastern Pacific Ocean. J. Fish. Res. Bd. Canada 23: 85-100.
- LeBrasseur, R.J. 1972. Utilization of herbivore zooplankton by maturing salmon. p. 581-588 in A.Y. Takenouti [ed.] Biological Oceanography of the Northern Pacific Ocean, Idemitsu Shoten, Tokyo.
- Levins, R., and B.B. Schultz. 1996. Effects of density dependence, feedback and environmental sensitivity on correlations among predators, prey and plant resources: models and practical implications. J. Anim. Ecol. 65: 802-812.
- Longhurst, A. 1998. Ecological geography of the sea. Academic Press, San Diego, CA. 398 p.
- Mackas, D.L., R. Goldblatt, and A.G. Lewis. 1998. Interdecadal variation in developmental timing of *Neocalanus plumchrus* populations at Ocean Station P in the subarctic North Pacific. Can. J. Fish. Aquat. Sci. 55: 1878-1893.

- Mann, K.H., and J.R.N. Lazier. 1996. Dynamics of marine ecosystems biological-physical interactions in the oceans, 2nd edition. Blackwell Science, Cambridge, Mass.
- Mantua, N.J., S.R. Hare, Y. Zhang, J.M. Wallace, and R.C. Francis. 1997. A Pacific interdecadal climate oscillation with impacts on salmon production. *Bull. Am. Meteorol. Soc.* 78: 1069-1080.
- Martin, J.H., R.M. Gordon, S. Fitzwater, and W.W. Broenkow. 1989. VERTEX: phytoplankton/iron studies in the Gulf of Alaska. *Deep-Sea Res. (A Oceanogr. Res. Pap.)* 36: 649-680.
- Mason, D.M., T. B. Johnson, and J. F. Kitchell. 1998. Consequences of prey fish community dynamics on lake trout (*Salvelinus namaycush*) foraging efficiency in Lake Superior. *Can. J. Fish. Aquat. Sci.* 1273-1284.
- Mathsoft. 1995. Guide to Statistical and Mathematical Analysis. Mathsoft, Inc., Seattle WA.
- McCann, K; and B. Shuter. 1997. Bioenergetics of life history strategies and the comparative allometry of reproduction. *Can. J. Fish. Aquat. Sci.* 54: 1289-1298.
- McClain, C.R., K. Arrigo, K. Tai, and D. Turk. 1996. Observations and simulations of physical and biological processes at Ocean Weather Station P, 1951-1980. *J. Geophys. Res. (C Oceans)* 101: 3697-3713.
- McCullagh, P., and J.A. Nelder. 1989. Generalized linear models, 2nd edition, Chapman & Hall, London.
- McKinnell, S. 1994. Age-specific effects of sockeye abundance on adult body size of selected British Columbia sockeye stocks. *Can. J. Fish. Aquat. Sci.* 52: 1050-1063.
- McKinnell, S, H.J. Freeland, and S.D. Groulx. 1999. Assessing the northern diversion of sockeye salmon returning to the Fraser River, BC. *Fish. Oceanogr.* 8: 104-114.
- Meyers, S.D., A. Melsom, and J.J. O'Brien. 1998. Ocean variations along the eastern Gulf of Alaska due to ENSO. *Tech. Rep. North Pac. Anadr. Fish Comm.* 1998: 47-48.
- Miller, C.B. 1993. Pelagic production processes in the Subarctic Pacific. *Prog. Oceanogr.* 32: 1-15.
- Miller, C.B., B.W. Frost, P.A. Wheeler, M.R. Landry, N. Welschmeyer, and T.M. Powell. 1991. Ecological dynamics in the subarctic Pacific, a possibly iron-limited ecosystem. *Limnol. Oceanogr.* 36: 1600-1615.

- Miller, C.B., J. Fulton, and B.W. Frost. 1992. Size variation of *Neocalanus plumchrus* and *Neocalanus flemingeri* in a 20-yr sample series from the Gulf of Alaska. *Can. J. Fish. Aquat. Sci.* 49:389-399.
- Mobrand, L.E., J.A. Lichatowich, L.C. Lestelle, and T.S. Vogel. 1997. An approach to describing ecosystem performance 'through the eyes of salmon.' *Can. J. Fish. Aquat. Sci.* 54: 2954-2973.
- Mori, J. 1995. Small squids caught by the surface trawl net in the North Pacific Ocean in December 1992. *Natl. Res. Inst. Far Seas Fisheries Salmon Rep. Ser.* 39: 216-223.
- Murphy, J. 1995. Patterns in the spatial distribution of salmon (*Oncorhynchus* spp.) captured in the Pacific driftnet fishery for flying squid (*Ommastrephes bartrami*). MS Thesis, University of Alaska Fairbanks, Fairbanks, AK. 110 p.
- Musgrave, D.L., T.J. Weingartner, and T.C. Royer. 1992. Circulation and hydrography in the northwestern Gulf of Alaska. *Deep-Sea Res.* 39: 1499-1519.
- Myers, K.W., K.Y. Aydin, R.V. Walker, S. Fowler, and M.L. Dahlberg. 1996. Known ocean ranges of stocks of Pacific salmon and steelhead as shown by tagging experiments, 1956-1995. (NPAFC Doc. 192.). Univ. Washington, Fish. Res. Inst., Seattle.
- Myers, K.W., R.V. Walker, N.D. Davis, K.Y. Aydin, S.-Y. Hyun, R.W. Hilborn, and R.L. Burgner. 1998a. Migrations, abundance, and origins of salmonids in offshore waters of the North Pacific-1998. Fisheries Research Institute, Seattle, WA. 72 p.
- Myers, R.A., G. Mertz, J.M. Bridson, and M.J. Bradford. 1998b. Simple dynamics underlie sockeye salmon (*Oncorhynchus nerka*) cycles. *Can. J. Fish. Aquat. Sci.* 55: 2355-2364.
- Mysak, L.A., W.W. Hsieh, and T.R. Parsons. 1982. On the relationship between interannual baroclinic waves and fish populations in the Northeast Pacific. *Biol. Oceanogr.* 2: 63-103.
- Nagasawa, K. In Press. Winter zooplankton biomass in the subarctic North Pacific, with a discussion on the overwintering survival strategy of Pacific salmon (*Oncorhynchus* spp.) *N. Pac. Andr. Fish. Comm. Bull.* 2.
- Nesis, K.N. 1997. Gonitid squids in the subarctic North Pacific: ecology, biogeography, niche diversity and role in the ecosystem. *Advances in Marine Biology* 32: 243-324.
- Nishiyama, T. 1977. Food-energy requirements of Bristol Bay sockeye salmon *Oncorhynchus nerka* (Walbaum) during the last marine life stage. *Res. Inst. N. Pac. Fish. Spec. Vol.*: 289-320.

- Onishi, H., S. Ohtsuka, and G. Anma. 2000. Anticyclonic, baroclinic eddies along 145°W in the Gulf of Alaska, 1994-1999. *Bull. Fac. Fish. Hokkaido Univ.* 51: 31-43.
- Pauly, D., and V. Christensen [eds.]. 1996. Mass-balance models of north-eastern Pacific ecosystems. Fisheries Centre, University of British Columbia. Research Reports 4. 131 p.
- Pearcy, W.G. 1992. Ocean ecology of North Pacific salmonids. Washington Sea Grant Press, Seattle, WA. 179 p.
- Pearcy, W.G., R.D. Brodeur, J.M. Shenker, W.W. Smoker, and Y. Endo. 1988. Food habits of Pacific salmon and steelhead trout, midwater trawl catches and oceanographic conditions in the Gulf of Alaska, 1980-85. *Bull. Ocean. Res. Inst.* 26: 29-78.
- Pearcy, W.G., T. Nishiyama, T. Fuji, and K. Masuda. 1984. Diel variations in the feeding habits of Pacific salmon caught in gillnets during a 24-hour period in the Gulf of Alaska. *Fish. Bull.* 82: 391-399.
- Peterman, R.M. 1987. Interactions among sockeye salmon in the Gulf of Alaska. p. 187-199 in H.D. Smith, L. Margolis and C.C. Wood [eds.] Sockeye salmon (*Oncorhynchus nerka*) population biology and future management. Dept. of Fisheries and Oceans, Canada.
- Peterman, R.M., B.J. Pyper, M.F. LaPointe, M.D. Adkison, and C.J. Walters. 1999. Patterns of covariation in survival rates of British Columbian and Alaskan sockeye salmon (*Oncorhynchus nerka*) stocks. *Can. J. Fish. Aquat. Sci.* 55: 2503-2517.
- Polovina, J.J., G.T. Mitchum, and G.T. Evans. 1995. Decadal and basin-scale variation in mixed layer depth and the impact on biological production in the Central and North Pacific, 1960-88. *Deep-Sea Res. I.* 42: 1701-1716.
- Pyper, B.J., and R.M. Peterman. 1999. Relationship among adult body length, abundance, and ocean temperature for British Columbia and Alaska sockeye salmon (*Oncorhynchus nerka*), 1967-1997. *Can. J. Fish. Aquat. Sci.* 56: 1716-1720.
- Pyper, B.J., R.M. Peterman, M.F. LaPointe, and C.J. Walters. 1999. Patterns of covariation in length and age at maturity of British Columbia and Alaska sockeye salmon (*Oncorhynchus nerka*) stocks. *Can. J. Fish. Aquat. Sci.* 56: 1046-1057.
- Rand, P.S., and S.G. Hinch. 1998. Spatial patterns of zooplankton biomass in the northeast Pacific Ocean. *Mar. Ecol. Prog. Ser.* 171: 181-186.
- Rand, P.S., J.P. Scandol, and E.E. Walter. 1997. NerkaSim: a research and educational tool to emulate the marine life history of Pacific salmon in a dynamic environment. *Fisheries* 22: 6-13.

- Reynolds, R.W., and T. M. Smith. 1994. Improved global sea surface temperature analyses. *J. Climate* 7: 929-948.
- Rice, J. 1995. Food web theory, marine food webs, and what climate change may do to northern marine fish populations. p. 357-372 *in*: R.J. Beamish [ed.] climate change and northern fish populations, National Research Council of Canada, Ottawa.
- Ricker, W.E. 1981. Changes in the average size and average age of Pacific salmon. *Can. J. Fish. Aquat. Sci.* 38: 1636-1656.
- Ricker, W.E. 1995. Trends in the average size of Pacific salmon in Canadian catches. p. 593-602 *in*: R.J. Beamish [ed.] climate change and northern fish populations, National Research Council of Canada, Ottawa.
- Roden, G.I. 1991. Subarctic-subtropical transition zone of the North Pacific: large-scale aspects and mesoscale structure. NOAA Tech. Rep. NMFS 105: 1-38.
- Rogers, D.E. 1980. Density-dependent growth of Bristol Bay sockeye salmon. p. 267-283 *in* Proceedings of a symposium on salmonid ecosystems of the North Pacific Ocean. Oregon Sea Grant College Program.
- Rogers, D.E. 1984. Trends in abundance of northeastern Pacific stocks of salmon. p. 100-127 *in* W.G. Percy [ed.] The influence of ocean conditions on the production of salmonids in the North Pacific. Oregon State Univ. Sea Grant College Program, Corvallis (ORES-U-83-001).
- Rogers, D.E. 1986. Pacific salmon. p. 461-476 *in* D.W. Hood and S.T. Zimmerman [eds.] The Gulf of Alaska Physical Environment and Biological Resources. U.S. Dept. of Commerce.
- Rogers, D.E. 1999. Estimates of annual salmon runs from the North Pacific, 1951-1998. Fisheries Research Institute, Seattle, WA. 11 p.
- Rogers, D.E., and G.T. Ruggerone. 1993. Factors affecting marine growth of Bristol Bay sockeye salmon. *Fish. Res.* 18: 89-103.
- Roper, C.F.E., M.J. Sweeney, and C.E. Nauen. 1984. Cephalopods of the World. 277 p.
- Royer, T.C. 1981. Baroclinic transport in the Gulf of Alaska Part I. seasonal variations in the Alaska Current. *J. Mar. Res.* 39: 219-250.
- Royer, T.C., and J.W. Emery. 1987. Circulation in the Gulf of Alaska, 1981. *Deep Sea Res.* 34: 1361-1377.
- Sanger, G.A. 1972. Fishery potentials and estimated biological productivity of the subarctic Pacific region. p. 561-574 *in*: A.Y. Takenouti [ed.] Biological oceanography of the northern Pacific Ocean, Idemitsu Shoten, Tokyo.

- Schwing, F.B. 1998. Patterns and mechanisms for climate change in the North Pacific: the wind did it. p. 29-36 in G. Holloway, P. Muller, and D. Henderson, [eds.] Proceedings of the 10th 'Aha Huliko'a Hawaiian winter workshop on biotic impacts of extratropical climate variability in the Pacific, January 26-29, 1998. SOEST Special Publication.
- Smith, W.H.F., and P. Wessel. 1990. Gridding with continuous curvature splines in tension. *Geophysics* 55: 293-305.
- Solow, A.R., and J.H. Steele 1990. On sample size, statistical power, and the detection of density dependence. *J. Anim. Ecol.* 59: 1073-1076.
- Steele, J.H. 1991. Marine ecosystem dynamics—comparison of scales. *Ecol. Res.* 6: 175-183.
- Steele, J.H. 1998. Regime shifts in marine ecosystems. *Ecol. Appl.* 8 (suppl. S): 33-36.
- Stewart, D.J., and M. Ibarra. 1991. Predation and production by salmonine fishes in Lake Michigan, 1978-88. *Can. J. Fish. Aquat. Sci.* 48: 909-922.
- Stewart, D.J., D. Weininger, D.V. Rottiers and T.A. Edsall. 1983. An energetic model for lake trout, *Salvelinus namaycush*: Application to the Lake Michigan population. *Can. J. Fish. Aquat. Sci.* 40: 681-698.
- Stephens, D.W., and J.R. Krebs. 1986. Foraging Theory. Princeton University Press, Princeton, New Jersey. 247 p.
- Sugimoto, T., and K. Tadokoro. 1997. Interannual-interdecadal variations in zooplankton biomass, chlorophyll concentration and physical environment in the subarctic Pacific and Bering Sea. *Fish. Oceanogr.* 6: 74-93.
- Tabata, S. 1982. The anticyclonic, baroclinic eddy off Sitka, Alaska, in the Northeast Pacific Ocean. *J. Phys. Oceanogr.* 12: 1260-1282
- Tadokoro, K., Y. Ishida, N.D. Davis, S. Ueyanagi, and T. Sugimoto. 1996. Changes in chum salmon (*Oncorhynchus keta*) stomach contents associated with fluctuation of pink salmon (*O. gorbuscha*) abundance in the central subarctic Pacific and Bering Sea. *Fish. Oceanogr.* 5: 89-99.
- Takagi, K. 1961. The seasonal change of gonad weight of sockeye and chum salmon in the North Pacific Ocean, especially with reference to mature and immature fish. *Bull. Hokkaido Reg. Fish. Res. Lab.* 23: 17-34.
- Thomson, R.E., and J.F.R. Gower. 1998. A basin-scale oceanic instability event in the Gulf of Alaska. *J. Geophys. Res. (C-Oceans).* 103: 3033-3040.
- Thorpe, J.E., M. Magel, N.B. Metcalfe, and F.A. Huntingford. 1998. Modelling the proximate basis of salmonid life-history variation, with application to Atlantic salmon, *Salmo salar* L. *Evol. Ecol.* 12: 581-599.

- Trenberth, K.E. 1990. Recent observed interdecadal climate changes in the Northern Hemisphere. *Bull. Am. Meteorol. Soc.* 71: 988-993.
- Trenberth, K.E., and J.W. Hurrell. 1995. Decadal coupled atmosphere-ocean variations in the North Pacific Ocean. p. 15-24 *in* R.J. Beamish [ed.] *Climate change and northern fish populations*, National Research Council of Canada, Ottawa.
- Tully, J.P. 1965. Time series in oceanography. *Trans. Royal Soc. Can., III, Ser. 4, Sec. 3*: 337-366.
- Uda, M. 1963. Oceanography of the subarctic Pacific Ocean. *J. Fish. Res. Board Can.* 20: 119-179.
- Ueno, Y., Y. Ishida, K. Nagasawa, and T. Watanabe. 1997. Winter distribution and migration of Pacific salmon. National Research Institute of Far Seas Fisheries, 7-1, Orido 5-chome, Shimizu, Shizoka, 424, Japan. 22 p.
- Urawa, S., M. Kawana, G. Anma, Y. Kamei, T. Shoji, M. Fukuwaka, K. Munk, K.W. Myers, and E.V. Farley, Jr. In Press. Geographical origin of high-seas chum salmon determined by genetic and thermal otolith markers. *N. Pac. Anadr. Fish. Comm. Bull.* 2.
- US Bureau of Commercial Fisheries Biological Laboratory (USBCFBL) 1969. Investigations by the United States for the International North Pacific Fisheries Commission—1967. *Int. N. Pac. Fish. Comm. Annu. Rep.* 1967: 78-123.
- US GLOBEC. 1996 Report on climate change and carrying capacity of the North Pacific ecosystem. *Rep. No. 15*: 95 p.
- Van Scoy, K.A., D.B. Olson, and R.A. Fine. 1991. Ventilation of North Pacific intermediate waters: The role of the Alaskan Gyre. *J. Geophys. Res. (C Oceans)* 96: 16,801-810.
- Venables, W.N., and B.D. Ripley. 1997. *Modern applied statistics with S-Plus*. Springer, New York. 548 p.
- Walker, R.V., K.W. Myers, N.D. Davis, K.Y. Aydin, K.D. Friedland, H.R. Carlson, G.W. Boehlert, S. Urawa, Y. Ueno, and G. Anma. 2000. Ambient temperatures and diurnal behavior as indicated by data storage tags on salmonids in the North Pacific. *Fish. Oceanogr.* 9: 171-186.
- Walters, C, V. Christensen, and D. Pauly. 1997. Structuring dynamic models of exploited ecosystems from trophic mass-balance assessments. *Rev. Fish. Biol. Fish.* 7: 139-172.
- Ware, D.M. 1978. Bioenergetics of a pelagic fish: theoretical change in swimming speed and ration with body size. *J. Fish. Res. Board. Can.* 35: 220-228.

- Ware, D.M. 1995. A century and a half of change in the climate of the NE Pacific. *Fish. Oceanogr.* 4: 267-277.
- Welch, D.W. 1997. Anatomical specialization in the gut of Pacific salmon (*Oncorhynchus*): evidence for oceanic limits to salmon production? *Can. J. Zool.* 75: 936-942.
- Welch, D.W., and Y. Ishida. 1994. On the statistical distribution of salmon in the sea: Application of the negative binomial distribution, and the influence of sampling effort. *Can. J. Fish. Aquat. Sci.* 50: 1029-1038.
- Welch, D.W., Y. Ishida, and K. Nagasawa. 1998. Thermal limits and ocean migrations of sockeye salmon (*Oncorhynchus nerka*): long-term consequences of global warming. *Can. J. Fish. Aquat. Sci.* 55: 937-948.
- Welch, D.W., and T.R. Parsons. 1993. ^{13}C - and ^{15}N values as indicators of trophic position and competitive overlap for Pacific salmon (*Oncorhynchus* spp.). *Fish. Oceanogr.* 2: 11-23.
- Wheeler, P.A., and S.A. Kokkinakis. 1990. Ammonium recycling limits nitrate use in the oceanic subarctic Pacific. *Limnol. Oceanogr.* 35: 1267-1278.
- Whitney, FA, C.S. Wong, and P.W. Boyd. 1998. Interannual variability in nitrate supply to surface waters of the Northeast Pacific Ocean. *Mar. Ecol. Prog. Ser.* 170: 15-23.
- Winemiller, K.O., and K.A. Rose. 1992. Patterns of life-history diversification in North American fishes: implications for population regulation. *Can. J. Fish. Aquat. Sci.* 49: 2196-2218.
- Wessel, P., and W.H.F. Smith. 1995. New version of the Generic Mapping Tools released. *EOS Trans. Amer. Geophys. U.* 76: 329.
- Wu, J.Q., and W. W. Hsieh. 1999. A modeling study of the 1976 climate regime shift in the North Pacific Ocean. *Can. J. Fish. Aquat. Sci.* 56: 2450-2462.
- Yuan, X., and L.D. Talley. 1996. The subarctic frontal zone in the North Pacific: Characteristics of frontal structure from climatological data and synoptic surveys. *J. Geophys. Res. (C Oceans)*. 101: 16491-16508.
- Zar, J.H. 1984. *Biostatistical analysis*. Prentice Hall, New Jersey. 718 p.
- Zhang, R.C, and K. Hanawa. 1993. Features of the water-mass front in the northwestern North Pacific. *J. Geophys. Res. (C Oceans)* 98: 967-975.

A Calibrating the logistic response

A.1 Estimating prey density with the logistic model

If the probability of capturing a single prey type in a single short time unit ΔT is constant, then foraging may be considered to be a Poisson process with mean λ , where $\lambda = T * P$. P is the probability of capture in the short time unit ΔT , where ΔT is small enough that two captures cannot occur, and T is the number of time units in a foraging period (or length of feeding bout).

λ is related to the density of prey available in the environment (D_{avail}) by $\lambda = SR * Pc * D_{avail}$, where SR and Pc are the search rate and probability of capturing a prey item given that an encounter occurs. Here, SR and Pc are considered to be functions of the predator, dependent on predator body weight and species. Therefore λ is a linear estimator of the density of prey available in the environment.

To estimate λ using predator food habits, rather than use the total it is possible to use the presence/absence of prey items rather than the total number of successes. This removes the problem of predator satiation or handling time, as the first item of prey will be captured when the foraging rate is high. In this case $\lambda = -\ln(1-P1)$ where $P1$ is the probability of a stomach containing *at least* 1 prey item. Thus $D_{avail} = -\ln(1-p1) / (SR * Pc)$.

$P1$ can be estimated as a function of explanatory variables using logistic regression to create an appropriate error structure. In logistic regression, $P1$ is assumed to be a function of appropriate explanatory variables using:

$$P1 = \frac{\exp(f(x1) + f(x2) + f(x3) + E)}{1 + \exp(f(x1) + f(x2) + f(x3) + E)}$$

where $x1, x2, \dots$ are explanatory variables and E is normally distributed error.

In Chapter 3, an index of squid abundance is calculated by assuming that all of the explanatory variables $x_1..x_2$ etc. are either predator- and size-specific or related to prey density, so $SQI = f(D_{avail}) - \alpha$.

This SQI is the squid index value used in Chapters 3 and 4, and can range between $\pm \infty$. An estimate of SQI and its variance can be made directly from stomach contents data at a single sampling location, using the empirical logistic transformation in Chapter 3 and a predator-specific α . α , in this dissertation, was estimated empirically for pink, sockeye and coho salmon in a specific size range, by examining a general additive model of stomach contents data of over 10,000 salmon (Table 3.8). Working backwards gives

$P1 = \exp(SQI / (1 + \exp(SQI)))$ and

$$(A.1) \quad D_{avail} = -\ln \left[1 - \frac{\exp[SQI]}{1 + \exp[SQI]} \right] \cdot C$$

C is considered to be a constant of proportionality which takes into account SR and Pc .

The Squid Index SQI , while having the useful properties of an approximately normal distribution when estimated from empirical data, is not linearly proportional to D_{avail} . If the transformation of equation A.1 is used to directly estimate D_{avail} from point estimates of SQI , the resulting error structure of D_{avail} may not have useful properties. However, using a Taylor Series expansion, if the values of SQI are >0 , $D_{avail} \approx C * SQI$ can be used, while for values of $SQI < 0$, $D_{avail} \approx C * \exp(SQI)$.

The values calculated for SQI in Chapter 3 are between -3 and $+3$. If it is assumed that $D_{avail} = C * \exp(SQI)$ for all values in this range, estimates of D_{avail} will have a lognormal distribution since SQI has a normal distribution, although the estimates D_{avail} estimates will be lower than actual densities for SQI when $SQI > 0$, with increasing error for $SQI > 1$.

This overall approach assumes that prey encounters follow a Poisson distribution: evidence suggests that in many cases that the increased variance a negative binomial distribution may better describe foraging encounters. Also note that method works best for large prey such as squid, where encounters involve a single prey item rather than a large patch. Finally, if other prey types are taken in large numbers in the same location as the sampling, biases due to prey selection may occur.

If a predator's stomach does not empty completely (on average) between foraging periods, or if the foraging period is continuous for longer than it takes for a prey item to digest completely T is proportional to T_d , the time it takes a captured prey to be fully digested (this is the "time window" which a single stomach sample can view).

A.2 Correcting for the effect of temperature on digestion

The above discussion assumes that the time of a foraging bout T is constant: in other words, when a stomach is examined, the amount of time over which the prey inside it was caught does not vary. The "time" window for examining past foraging is related to the digestion rate of prey. Assuming exponential digestion of stomach contents (see Jobling 1987 for a review), a captured prey goes from its size at capture to a minimum detectable size in

$$T_f = \frac{\ln\left(\frac{W_{consumed}}{W_{min}}\right)}{d}$$

where d is the digestion rate, $W_{consumed}$ is the weight of a prey when first consumed, and W_{min} is the minimum detectable size for a prey item. Therefore, if the prey weight, detectable size, and predator digestion rate are constant over time and between sampling periods, then T_f can be taken to be constant.

In the case of Pacific salmon feeding on pelagic squid, prey weight at capture and minimum detection is taken to be constant while d varies with exponentially with water temperature. The feeding period is taken to be an average over Td . Thus,

$$T_f \propto \frac{1}{d} = a \cdot e^{-bT_{\text{water}}}$$

If a predator feeds at the same rate on the same density of squid, the digestion rate will increase with temperature, and the estimate of the squid index will decrease. This decrease will be proportional to the exponential of temperature: however, this becomes approximately linearly proportional to temperature when the logistic transformation is used. Based on published digestion rates for pink, sockeye, and coho salmon, the Squid index **SQI** for pink, sockeye and coho salmon would be expected to decrease by approximately 0.05 for every 1°C increase in ambient water temperature. Any relationship with temperature which differs from this rate of decrease could be explained by the relationship between temperature and prey abundance.

Appendix B. Equations used to calculate consumption, respiration, egestion, and excretion rates of salmon. Symbols and equations similar to those of Hewett and Johnson (1992). Parameter values are shown in Table B1.

Required input parameters

<i>T</i>	=	Water Temperature (°C)
<i>W</i>	=	Predator starting body weight (grams)
<i>PC</i>	=	Prey caloric density (calories/g prey)
<i>PFF</i>	=	Proportion of prey indigestible
<i>VEL</i>	=	Predator swimming velocity (cm/sec)

Solution variables

ΔB	=	Specific assimilation rate (calories/g pred./day)
C_{tot}	=	Specific gross consumption rate (calories/g pred./ day)

Equations

(B.1) Predator specific growth rate ΔB

$$\Delta B = \text{Direct model input (calories/g pred./day)}$$

OR

$$\Delta B = C_{tot} - (F + U + S) - R$$

(B.2) Specific gross consumption rate C_{tot}

$$C_{tot} = \text{Direct model input (calories/g pred./day)}$$

OR

$$C_{tot} = \Delta B + (F + U + S) + R$$

(B.3) Respiration R

$$R = (RA * W^{RB} * f(T) * \text{Activity}) * OXY$$

$$\text{where } f(T) = e^{(RQ * T)}$$

$$\text{Activity} = e^{((RTO - (RTM * T)) * VEL)}$$

$$VEL = \text{Direct model input (cm/sec.)}$$

OR

$$VEL = V_{opt} = ACT * (WRK^4) * e^{(BACT * T)}, T \leq RTL$$

(B.4) Egestion F

$$F = PF * C_{tot} * PC$$

$$\text{where } PF = ((PE - 0.1) / (1 - 0.1)) * (1 - PFF) + PFF$$

$$PE = FA * T_{FB} * e^{(FG * P)}$$

$$P = C_{tot} / C_{max}$$

(B.5) Excretion U

$$U = UA * T_{(UB)} * e^{(UG * P)} * (C_{tot} - F) * PC$$

$$\text{where } P = C_{tot} / C_{max}$$

(B.6) Specific Dynamic Action S

$$S = (SDA * (C_{tot} - F)) * PC$$

(B.7) Maximum specific consumption rate C_{max}

$$C_{max} = CA * W^{CB} * f(T) * PC$$

$$\text{where } f(T) = K_A * K_B$$

$$K_A = (CK1 * L1) / (1 + CK1 * (L1 - 1))$$

$$L1 = e^{(G1 * (T - CQ))}$$

$$G1 = (1 / (CTO - CQ)) * LN((0.98 * (1 - CK1)) / (CK1 * 0.02))$$

$$K_B = (CK4 * L2) / (1 + CK4 * (L2 - 1))$$

$$L2 = e^{(G2 * (CTL - T))}$$

$$G2 = (1 / (CTL - CTM)) * LN((0.98 * (1 - CK4)) / (CK4 * 0.02))$$

Note on units:

The energy units of each of the 6 terms listed above are often calculated differently to emphasize their origins in laboratory experiments and give a biological meaning to empirical parameters. C_{tot} , C_{max} , F, U, and S were originally measured as grams of prey, and are converted to calories in this model formulation by multiplying by the measured prey caloric density PC. Respiration, on the other hand, was originally calculated by measuring the grams of oxygen (O₂) respired, and that value is converted to calories using the conversion factor OXY.

If predator energy density is considered constant, calories of growth may be converted to grams of predator body weight by dividing by the predator energy density (calories/g. predator). However, if predator energy density increases with body weight, as with salmonids, the quadratic conversion method described in Stewart et al. (pg. 688) and parameterized with terms QA and QB in Hewett and Johnson (1992) should be used.

Appendix Table B1. Fish bioenergetics parameter values used to estimate growth and prey consumption by sockeye, chum, pink, and coho salmon (Hewett and Johnson, 1992; except for * from Davis et al. 1998b).

Symbol	Physiological Parameter Value	Nominal Value		
		Pink/ Sockeye	Chum	Coho
MAIN TERMS and UNITS				
C_{tot}	Specific feeding rate (cal/g pred/day)			
R	Specific respiration rate (cal/g pred/day)			
F	Specific egestion rate (cal/g pred/day)			
U	Specific excretion rate (cal/g pred/day)			
S	Specific cost of digestion (cal/g pred/day)			
C_{max}	Maximum feeding rate (cal/g pred/day)			
P	Constant proportion of maximum feeding rate (C_{tot}/C_{max})			
V_{opt}	Optimal cruising velocity for body weight and temperature (cm/sec)			
PARAMETERS				
CA	Intercept for weight dependence of CON	0.303	0.394*	0.303
CB	Slope for weight dependence of CON	-0.275	-0.275	-0.275
CQ	Lower temperature where dependence is CK1	3	3	5
CTO	Higher temperature where dependence is 0.98 of max	20	20	15
CTM	Temp CTO where dependence is still .98 of max	20	20	18
CTL	Temperature where dependence is CK4	24	24	24
CK1	Temperature dependence at CQ	0.58	0.58	0.36
CK4	Temperature dependence at CTL	0.50	0.50	0.01
OXY	Conversion factor for respiration (g-O ₂ to calories)	3240	3240	3240
RA	Intercept for std. Metabolism vs. weight, temperature, and swimming speed	1.43x 10 ⁻³	1.43x 10 ⁻³	2.64x 10 ⁻³
RB	Slope for weight dependence of standard metabolism	-0.209	-0.209	-0.217
RQ	Coefficient for temperature dependence of metabolism	0.086	0.086	0.06818
RTO	Coefficient for swimming speed dependence of metabolism	0.0234	0.0234	0.0234
RTM	Coefficient for swim speed dependence of temperature	0	0	0
RTL	Cut-off temp	25	25	25
RK1	Intercept for weight dependence of optimal swimming speed when temperatures >RTL	1	1	1
RK4	Slope for weight dependence of optimal swimming speed	0.13	0.13	0.13
ACT	Intercept for optimal swimming speed vs. temperature and weight (cm/sec/1-g fish at 0°), when temperature <RTL	9.9	9.9	9.7
BACT	Coefficient for temperature dependence of optimal swimming speed when temperature <RTL	0.0405	0.0405	0.0405
SDA	Proportion of assimilated energy lost to specific dynamic action	0.172	0.172	0.172
FA	Intercept for proportion of C _{tot} egested vs. temperature and ration	0.212	0.212	0.212
FB	Slope for temperature dependence of	-0.222	-0.222	-0.222
FG	Coefficient for feeding level dependence of F	0.631	0.631	0.631
UA	Intercept for proportion of assimilated consumption excreted vs. temperature and ration	0.0314	0.0314	0.0314
UB	Slope for temperature dependence of excreted	0.58	0.58	0.58
UG	Coefficient for feeding level dependence of excreted	-0.299	-0.299	-0.299

C Combining salmon foraging and bioenergetics models with density-dependence

C.1 Optimizing instantaneous growth

From Appendix B (equation B.1), the equation for the daily growth increment of salmon body weight ΔB is:

$$(C.1) \quad \Delta B = C_{tot} - (F + U + S) - R$$

Thus, ΔB can be maximized by maximizing the difference between C_{tot} and the digestive loss terms $(F + U + S)$ and respiration rate R . The exact growth rate of this optimum will vary with the input variables shown in Appendix B: all of the terms on the right of equation C.1 are dependent on water temperature, prey type, body weight, swimming velocity, and consumption rate (equations B.2-B.7).

If water temperature, prey type, and body weight are beyond the behavioral control of a salmon at any given instant, a salmon's only method of modifying growth rate is to modify consumption rate C_{tot} or respiration R by changing swimming velocity **VEL**.

Two factors must be taken into account in this optimization. F , U , S are functions of C_{tot} , as shown in equations B.4-B.6. If no feeding occurs in a day, $C_{tot}=0$, $(F+U+S) = 0$, and all losses are respirative. As C_{tot} increases, $(F + U + S)$ increases as an exponential function of C_{tot} . The slope of this increase is initially less than 1, so that C_{tot} initially increases more rapidly than $(F + U + S)$ and net positive growth occurs. However as consumption rate increases above a salmon's ability to digest it, $(F + U + S)$ catches up with C_{tot} . This introduces an optimum level for C_{tot} which exists even if swimming velocity is independent of consumption rate.

The equations in Appendix B do not relate swimming velocity **VEL** directly to C_{tot} . The model assumes that overall, a salmon maintains an optimal cruising speed (V_{opt} in Appendix B) which minimizes energy expenditure per unit distance traveled, taking into account hydrodynamic aspects of drag and water viscosity. The temperature and body-weight dependence of V_{opt} is derived in Ware (1978) and agrees well with the measured sustained swimming rates of adult sockeye salmon.

In order to determine the relationship between C_{tot} and swimming velocity **VEL**, equations from foraging theory must be introduced into C_{tot} . One possible formulation is:

$$(C.2) \quad C_{tot} = SR * P_c * D_{avail}$$

where **SR** is the search rate of the predator (volume of water searched per unit time), P_c is the probability of capture given an encounter between predator and prey, and D_{avail} is the density of available prey. Each of the three terms on the right hand side of equation C.2 has important implications for predator foraging.

C.2 Search Rate SR

Given the velocities of predator and prey, an equation for search rate **SR** derived by ref and in common use in many foraging models is:

$$(C.3) \quad SR \text{ (volume/time)} = (\pi * RD^2 / 3) * (3 * VEL + VPR^2 / VEL)$$

RD is the reaction distance, or the maximum distance at which a predator may see and capture a prey item, and **VPR** is the velocity of the prey. Note that if $VPR \ll VEL$, as might be expected for a salmon feeding on zooplankton VPR^2 / VEL becomes very small with respect to **VEL**, and C_{tot} becomes a linear function of predator swimming velocity **VEL**, given a constant P_c and D_{avail} .

From equation B.3, respiration R is an exponential function of VEL . Substituting the right hand side of equation C.3 for the SR term in equation C.2, and substituting the resulting right hand side of equation C.2 for the C_{tot} term in equation C.1 makes all of the terms on the right hand side of equation C.1 functions of swimming velocity VEL .

If $P_c * D_{avail}$ are constant on a given day, and high enough that starvation does not occur at all swimming velocities, and if water temperature, prey type, reaction distance and predator starting body weight are also constant, an optimum swimming velocity VEL will exist which maximizes a salmon's growth ΔB . The actual swimming velocity of the optimum, and the resulting growth rate ΔB , will vary with all of the listed input variables.

The model experiments investigated in Chapter 5 are investigated are subjected to sensitivity tests for all of the above parameters with the exception of prey swimming speed VPR (taken to be low for zooplankton), probability of prey capture P_c (discussed below) and reaction distance RD . The last item may be the most troublesome— RD depends on the light level in the water and the size or contrast level of the prey item, which may vary with time of day, weather conditions, or water turbidity. For this model, it is taken to be 20cm and corresponds to reaction distance expected in waters high turbidity.

One of the possible problems with equations C.2 and C.3 is that they do not allow for foraging rate limitation through handling time (the required time that a predator must take from searching to handle and swallow prey). If handling time is large in relation to search time, net search rate becomes a Holling Type-II functional response, dependent on P_c and D_{avail} . However, as reviewed in Chapter 3 and Breck 1993, handling time is not likely to be an important issue for many large fish, especially if they are piscivorous. Handling time is not included in the models here.

C.3 P_c

P_c may change with swimming speed, predator body weight, or water visibility, and a change in P_c with respect to squid may be an important part of the body weight response seen in Chapter 3. For the zooplankton-driven models in Chapter 5, it is taken as a scaling constant.

C.4 Available prey – Density Dependence.

The fundamental problem with measuring density-dependence is determining the scale on which it takes place. If, at any given instant, all of the prey are available to all of the predators, then the available prey is directly proportional to the total prey in the environment:

$$(C.4) \quad D_{avail} = Vul * D_{tot}$$

The parameter **Vul** is a measure of the prey's vulnerability to the predator, discussed below. If equation C.4. is used for prey availability, the consumption rate C_{tot} in equation C.2 becomes:

$$(C.5) \quad C_{tot} = \text{Food}/_{\text{predator*time}} = SR * P_c * Vul * D_{tot}$$

This is the most traditional type of predator/prey equation, the Lotka-Volterra model. Lotka-Volterra models tend to be unstable, and lead to predator/prey oscillations which may or may not occur in nature. In a heterogeneous environment, this type of model is most useful on a short, "local" scale, where prey in a single region may be completely consumed by a predator population in a short time. If this model is scaled up to a longer time scale, the only density-dependence that occurs would occur as prey was depleted, requiring a description of prey replenishment which may lead to unstable dynamics overall.

A second approach, the opposite extreme, is to assume that the available prey is divided equally among all of the predators ($N_{\text{predators}}$) in the system. In this case,

$$(C.6) \quad D_{\text{avail}} = \text{Vul} * D_{\text{tot}} / N_{\text{predators}}$$

And thus:

$$(C.7) \quad C_{\text{tot}} = \text{Food} / \text{predator} * \text{time} = \text{SR} * P_c * \text{Vul} * D_{\text{tot}} / N_{\text{predators}}$$

As the number of predators in a system increases, the amount of food available for each decreases, “gently” putting the brakes on the growth of the predator. Equation C.7 may be a good approximation of predator/prey interactions on a longer time scale, when the amount of prey produced over an entire season must be divided by the predators existing over that season. However, on short time scales it is inadequate, as if the predator population is low, the amount of food consumed by each predator goes up to infinity, requiring the addition of satiation or handling time limitations to control predator growth.

A hybrid model may be the best combination of short and long time scales into a single model. One such hybrid equation is:

$$(C.8) \quad D_{\text{avail}} = \left[\frac{\text{Vul}}{\text{Vul} + \text{SR} * P_c * N_{\text{predators}}} \right] * D_{\text{tot}}$$

which results in a consumption per predator equation of:

(C.9)

$$C_{\text{tot}} = \text{Food} / \text{predator} * \text{time} = \left[\frac{\text{Vul}}{\text{Vul} + \text{SR} * P_c * N_{\text{predators}}} \right] * \text{SR} * P_c * D_{\text{tot}}$$

This equation may be derived by a “combined” assumption of predator and prey: assuming that prey exists in “vulnerable” and “invulnerable” states, and

may move in and out of these states rapidly with respect to their own growth or the consumption rates of predators (Walters et al. 1997). This type of switching between vulnerable and invulnerable states in the case of prey may be a more realistic overall approach to capturing prey dynamics. Note that with this model, if $SR * P_c * N_{predators} \ll Vul$ or identically if $SR * P_c * N_{predators} / Vul$ is close to 0, then

$$C_{tot} \approx SR * P_c * D_{tot},$$

resembling the Lotka-Volterra case in equation C.5. Adding a single predator increases the amount of prey consumed (top-down control of prey) but doesn't change the amount of food eaten by each predator (density-independent growth). On the other hand if $SR * P_c * N_{predators} \gg Vul$ or identically if $SR * P_c * N_{predators} / Vul \gg 1$ then

$$C_{tot} \approx Vul * D_{tot} / N_{predators}$$

resembling equation C.7. In this case, adding a single predator does not increase the amount of prey consumed (no top-down control of prey) but decreases the amount of food eaten by each predator (density-dependent growth).

Finally, if $SR * P_c * N_{predators} / Vul = 1$, then the available prey D_{avail} is equal to half of the total prey: the strength of the density-dependent relationship might be considered "half saturated in this case."

Since $SR * P_c * N_{predators} / Vul$ completely describes the slope of the density-dependent curve, ranging from 0 (no density-dependence) to high values (strong density-dependence) it is useful to define the following index:

$$(C.10) \quad DDindex = \log \left[\frac{SR * P_c * N_{predators}}{Vul} \right] = \log \left[\frac{D_{tot} - D_{avail}}{D_{avail}} \right]$$

This density dependent index equal 0 at the "half-saturation" of density dependence, and have increasingly positive values for strong density-dependence and increasingly negative values for weak density dependence.

The fact that equation C.9 resembles both equations C.5 and C.9 depending on parameter values reduces the fundamental question of scale to a parameter issue rather than an issue of selecting the proper equation. Thus, equation C.9 may allow the most flexibility for modeling predator/prey interactions. SR and P_c may be measured through foraging studies of individual fish. Deciding whether prey consumption is density-dependent or density-independent becomes a question of figuring out the appropriate value of Vul .

Of course, while using equation C.9. allows a single predator/prey equation to be used in both density-independent and density-dependent growth, Vul is a parameter which may be extremely difficult to measure in the field (Walters et al. 1997). For the predator/prey models in Chapter 5, several values of Vul are used, to estimate the ideal swimming velocity for salmon for a range of Vul values: in other words, for cases with "high" and "low" density dependence. Determining "true" values for vulnerabilities in any ecosystem is perhaps the largest challenge facing predator/prey models and is beyond the scope of this dissertation. At least, by using this hybrid equation, a single functional form can be used to explore the effect of density-dependence on predator growth.

CURRICULUM VITAE

Kerim Yunus Aydin

EDUCATION

- 1994-2000** Doctoral candidate, School of Aquatic and Fishery Sciences, University of Washington, Seattle, WA
- 1993-1994** Thomas J. Watson Fellow, Istanbul, Turkey
- 1988-1992** B.S. in Mathematical Biology, Harvey Mudd College, Claremont, CA

AREAS OF EXPERTISE

- Analysis of the effects of fishing and fisheries management on ecosystem resources, and the development of multi-species ecological models for fisheries investigations.
- Investigation of marine ecosystem dynamics across multiple scales of time and space, including ecosystem processes and evolution, and human- or climate-driven change across multiple decades.
- Statistical, programming, ecosystem modeling, and biological field and laboratory skills appropriate to examining large-scale questions.
- Written and oral communication for a professional audience.

RESEARCH EXPERIENCE

1997-present: *Marine Ecosystems Modeling Consultant/Contractor*

Consulted on multiple ecosystem modeling projects, including a current long-term contract with U.S. National Marine Fisheries Service to develop North Pacific marine ecosystem management approaches.

Skills and Experience

- Software development of ECOPATH and other food web modeling software.
- Adapting previously-collected fisheries survey and assessment data into appropriate multi-species model parameters. Work includes combining data from multiple surveys and single-species stock assessments into multi-species trophic fisheries models.
- Realistic assessment of data quality based on several years of field experience in fisheries data collection techniques.
- Facilitating and leading workshops enabling scientists from multiple institutions and countries to create functioning models.
- Presentations to scientists and local, national and international decision-making organizations to achieve buy-in on using food web models for ecosystem management.
- Creating software tools for presentation of results, including visual tools for sharing model results through the World Wide Web.

CURRICULUM VITAE

Kerim Yunus Aydin

Contract History

- U.S. National Marine Fisheries Service* *1999-present*
 Comparison of multi-species and single-species approaches to fisheries management in the **Eastern Bering Sea**, including ECOPATH, ECOSIM, and ECOSPACE.
 Facilitation and development of a **Western Bering Sea** ECOPATH model in conjunction with Russian researchers.
- Inter-American Tropical Tuna Commission* *1998-present*
 Consultation and development of ECOPATH and ECOSIM models of bycatch and predator removal in **Eastern Tropical Pacific** tuna fisheries (international forum).
- Great Lakes Management Council* *1997*
 Development of a multi-species **Lake Superior** ECOPATH model for use in Great Lakes management efforts.
- National Center for Ecological Analysis and Synthesis (NCEAS)* *1997-98*
 Development and comparison of ECOPATH models of the **Central North Pacific** and **Subarctic North Pacific** to examine the effects of the removal of apex predators from multiple ecosystems.

1994-2000: *Doctoral candidate, School of Aquatic and Fishery Sciences, University of Washington, Seattle, WA*

Dissertation title: "Trophic Feedback and Carrying Capacity of Pacific Salmon (*Oncorhynchus* spp.) on the High Seas of the Gulf of Alaska."

Dissertation completed at University of Washington, Seattle: October 2000.

- Tied together salmon population and growth models in multiple scales of time and space.
- Models created include: predator-prey interaction (foraging) models; bioenergetics models; multi-species stock assessment models (ECOPATH and ECOSIM); single-species fishery (VPA) models; dynamic programming; large-scale oceanographic process data to examine the effects of climate change on marine ecosystems.
- Coursework included: study of fisheries stock assessment; fisheries management; fish ecology and behavior; biological modeling; ecosystem processes; advanced statistical inference. Statistical techniques include: Bayesian analysis, bootstrapping and other Monte-Carlo approaches.
- Designed and participated in field work aboard international high seas research vessels, including fish tagging operations for 4 years.

1991-1993: *Research Assistant for Dr. Catherine McFadden, Harvey Mudd College, Claremont, CA*

- Performed SCUBA and shore-based sampling of intertidal animals.
- Conducted Scanning Electron Microscope (SEM) taxonomic identification of samples.
- Adapted spatial statistical methods analyzing genetic flow in intertidal animal communities.
- Developed and maintained DOS-based statistical software, and provided user-support for software use at multiple academic institutions.

CURRICULUM VITAE

Kerim Yunus Aydin

COMPUTER EXPERIENCE

Programming languages	C and C++ (Unix and DOS environments) Perl (Unix and Windows environments) Visual Basic (Windows environment) SQL HTML, CGI and VRML (World-Wide Web database programming and visualization languages)
Software	MathSoft S-Plus (PC and Unix) Math Works Matlab and Simulink Microsoft Excel, Access, Word, PowerPoint Wolfram Research Mathematica Ecopath, Ecosim (Ecosystem Modeling) GMT (Unix Mapping Analysis Tools)
Operating systems	Linux: programming and system administration PC-based DOS, Windows 95, 98, NT Some Macintosh experience

SELECTED PUBLICATIONS

Refereed

- Aydin, K.Y., K.W. Myers and R.V. Walker. In Press. Variation in summer distribution of the prey of Pacific salmon (*Oncorhynchus* spp.) in the offshore Gulf of Alaska in relation to oceanographic conditions, 1994-98. North Pacific Anadromous Fish Commission Bulletin 2.
- Kitchell, J.F., S.P. Cox, C.J. Harvey, T.B. Johnson, D.M. Mason, K.K. Schoen, K.Y. Aydin, C. Bronte, M. Ebener, M. Hansen, M. Hoff, S. Schram, D. Schreiner, and C.J. Walters. In Press. Sustainability of the Lake Superior fish community: interactions in a food web context. Ecosystems 1.
- Walker, R.V., K.W. Myers, N.D. Davis, K.Y. Aydin, K.D. Friedland, H.R. Carlson, G.W. Boehlert, S. Urawa, Y. Ueno, and G. Anna. In Press. Diurnal variation in thermal environment experienced by salmonids in the North Pacific as indicated by data storage tags. Fish. Oceanogr. 9.
- Davis, N.D., K.Y. Aydin and Y. Ishida. In Press. Diel catches and food habits of sockeye, pink, and chum salmon in the central Bering Sea in summer. North Pacific Anadromous Fish Commission Bulletin 2.
- McFadden, C.S. and K.Y. Aydin. 1996. Spatial autocorrelation analysis of small-scale genetic structure in a clonal soft coral with limited larval dispersal. Marine Biology 126: 215-224.

CURRICULUM VITAE Kerim Yunus Aydin

Non-Refereed (Recent Selection)

- Pearcy, W.G., **K.Y. Aydin** and R.D. Brodeur. 1999. What is the carrying capacity of the North Pacific Ocean for salmonids? PICES Press 7(2): 17-23. PICES c/o Institute of Ocean Sciences, Box 6000, Sidney, B.C., Canada.
- Aydin, K.Y.** 1998. Abiotic and biotic factors influencing food habits of Pacific salmon in the Gulf of Alaska. Workshop and Climate Change and Salmon Production, North Pacific Anadromous Fish Commission (NPAFC) Technical Report: 39-40.
- Francis, R.C., **K. Y. Aydin**, R. Merrick and S. M. Bollens. 1998. Modeling and management of the Bering Sea ecosystem. In [R.C. Francis, ed.] Dynamics of the Bering Sea. Alaska Sea Grant Publications, Fairbanks, AK.
- Davis, N.D., **K.Y. Aydin**, and Y. Ishida. 1998. Diel feeding habits and estimates of prey consumption of sockeye, chum, and pink salmon in the Bering Sea in 1997. (NPAFC Doc. 363) FRI-UW-9816. Univ. Washington, Fish. Res. Inst., Seattle. 24 pp.
- Myers, K.W., R.V. Walker, N.D. Davis, **K.Y. Aydin**, W.S. Patton, and R.L. Burgner. 1997. Migrations, abundance, and origins of salmonids in offshore waters of the North Pacific - 1997. Annual report to U.S. National Marine Fisheries Service, contr. no. 50ABNF700003. FRI-UW-9708. Univ. Washington, Fish. Res. Inst., Seattle. 46 pp.
- Myers, K.W., **K.Y. Aydin**, G. Anma, H. Ueda, M. Kaeriyama, T. Norgard, and T. Sands. 1997. The 1997 international cooperative salmon research cruise of the Oshoro maru. (NPAFC Doc. 253.) FRI-UW-9706. Fish. Res. Inst., Univ. Washington, Seattle. 17 pp.
- Myers, K.W., **K.Y. Aydin**, R.V. Walker, S. Fowler, and M.L. Dahlberg. 1996. Known ocean ranges of stocks of Pacific salmon and steelhead as shown by tagging experiments, 1956-1995. (NPAFC Doc. 192.) FRI-UW-9614. Univ. Washington, Fish. Res. Inst., Seattle. 4pp. + 155 figs. and 63 append. figs.

Full list available upon request

SELECTED RECENT PROFESSIONAL PRESENTATIONS

- | | |
|----------|--|
| Apr 1999 | Invited participant and modeling consultant in the Inter-American Tropical Tuna Commission (IATTC) international Bycatch Working Group meeting. |
| Apr 1999 | Sixth Annual U.S. NFMS National Stock Assessment Symposium. Presented workshop entitled "Straying from the ECOPATH: a critique and demo of the ECOPATH/ECOSIM/ECOSPACE programs." |
| Mar 1999 | Beyond El Niño Symposium, La Jolla, CA. Presented paper entitled: "Top-down, bottom-up, ENSO-PDO-fishing? Figuring the frequency of variation in marine ecosystems." |
| Nov 1999 | North Pacific Anadromous Fish Commission Annual Meeting, Juneau, Alaska. Presented paper entitled "ENSO- and regime-scale variation in Gulf of Alaska micronekton as a mechanism driving the observed growth trends in Pacific salmon (<i>Oncorhynchus</i> spp.)" |
| Oct 1999 | Eighth Annual North Pacific Marine Science Organization (PICES) Meeting, Vladivostok, Russia. Facilitated development of ECOPATH model of the Western Bering Sea. |

CURRICULUM VITAE

Kerim Yunus Aydin

-
- | | |
|----------|---|
| Oct 1998 | Seventh Annual North Pacific Marine Science Organization (PICES) Meeting, Fairbanks, Alaska. Presented paper entitled "Pacific salmon carrying capacity, ecosystem structure, and density dependent predator-prey interactions on the high seas." |
| Sep 1998 | Ecosystem Considerations in Fisheries Management—16 th Lowell Wakefield Fisheries Symposium, Anchorage, Alaska. Presented paper entitled "Managing for Biological Feedback and Carrying Capacity in the Alaskan Gyre." |
| Apr 1998 | FAO Workshop on Climate Change and Salmon Production, Vancouver, Canada. Presented paper entitled "Abiotic and biotic factors influencing food habits of Pacific salmon in the Gulf of Alaska." |
| Apr 1998 | Invited participant in workshop entitled "Use of Ecopath with Ecosim to Evaluate Strategies for Sustainable Exploitation of Multi-Species Resources," Vancouver, Canada. |
| Mar 1998 | First GLOBEC Open Science Meeting, Paris, France. Presented paper entitled "Modeling and measuring the effects of biological feedback on carrying capacity and ecosystem structure in the Alaskan Gyre." |
| May 1997 | Invited participant in workshop entitled "Apex Predators in Marine Ecosystems," National Center for Ecological Analysis and Synthesis (NCEAS), Santa Barbara, CA. |

AWARDS AND SCHOLARSHIPS

- | | |
|----------|--|
| Sep 1994 | Egtvedt Graduate Scholarship, University of Washington |
| Jun 1993 | Thomas G. Watson Fellow, Thomas G. Watson Foundation, Providence, RI |
| Jun 1991 | Dean's List, Harvey Mudd College |

LANGUAGES

- English (Native Speaker)
 Turkish (Fluent oral, Intermediate Written)